



# Università degli Studi di Ferrara

DOTTORATO DI RICERCA IN

'SCIENZE e TECNOLOGIE per l'ARCHEOLOGIA e i BENI CULTURALI'

CICLO XXV

COORDINATORE Prof. Carlo Peretto

**Technological study of the seventeenth century *haft rang* tiles in Iran**  
with a comparative view to the *cuerda seca* tiles in Spain

Settore Scientifico Disciplinare GEO/09

## Dottorando

Dott. Holakooei, Parviz

## Tutori

Prof. Petrucci, Ferruccio Carlo

Prof.ssa Vaccaro, Carmela

Anni 2010/2012

---

Corso di Dottorato in convenzione con



UNIVERSITA'  
DEGLI STUDI  
DI  
SIENA



UNIVERSITÀ DEGLI STUDI  
DI MODENA E REGGIO EMILIA



*To*

*Moslem Mishmastnehi*



## Abstract

The history of polychrome glazed objects in Iran is synchronised with the history of the first known examples of polychrome glazed artifacts. The polychrome glazed bricks of Chughā Zanbīl, dated back to the thirteenth century BC, might be the first evidences of such a claim. This tradition was followed until the fall of the Achaemenids in the fourth century BC, when glazed bricks objects were vastly used to cover the friezes of palaces and important edifices at Persepolis and Susa. Making polychrome glazes on ceramic materials, however, seems to be abandoned until the Islamic period, when polychrome underglaze objects were widely in use in Iran from the tenth century onwards. The first evidences of creating overglaze polychrome decoration was nevertheless achieved on *mīnā'ī* glazed objects in the thirteenth century AD, which as Abu'l Qasim stated used be originally called *haft rang*, e.g. 'seven colours.' This technique was slightly modified and used throughout the fifteenth and sixteen centuries in Iran, and then was extensively used in the seventeenth century over the Safavid period (1501-1736). In all these types of polychromies, a dark colour line (mostly black) is used to separate various coloured glazes. This technique is still alive and is widely used in decorating the architectural facades of scholastic buildings in Iran. In the twentieth century, art historians attributed this type of polychrome technique to a Spanish style of making polychrome glazed objects called  *cuerda seca*. The only feature by which such an attribution is established is a 'black line,' which is used in both techniques of *haft rang* and  *cuerda seca* for separating coloured glazes.

This thesis provides firsthand information about the seventeenth century *haft rang* tiles in Iran using various analytical approaches, including optical microscopy, wavelength dispersive x-ray fluorescence (WDXRF), x-ray diffraction (XRD), densitometry, ultraviolet visible spectroscopy (UV-Vis spectroscopy), micro-Raman spectroscopy, and energy dispersive x-ray spectroscopy (EDS). Here, optical microscopy was mainly used to have a general idea about the stratigraphy and various layers of the *haft rang* tiles. WDXRF was however used to respond to the question of the provenance of the tiles as this subject has always been of interest to frame the archaeological context of *haft rang* tiles. Another issue emphasised in this thesis is the thermal history of the tiles, which was studied by XRD and measuring the density of the bodies' tiles. This subject was particularly was interesting for me to delve into because multi layer structure of *haft rang* tiles makes the study of thermal behaviour of the bodies much complicated. On the other hand, the study of the coloured glazes was firstly achieved by UV-Vis spectroscopy, where the possible colourants and network modifiers of the glazes were studied. Micro-Raman spectroscopy, however, presented very notable results about the opacifiers and un-dissolved particles suspended in the glazes' matrixes. EDS microanalyses were nonetheless carried out to have a general idea about the chemical composition of the glazes and their fluxes, opacifiers, and network formers.

The results of the aforementioned studies showed that, regardless where they are found, the bodies of the seventeenth century *haft rang* tiles are local products and are not imported from other centres of tile-making. Moreover, under the optical microscope three layers of a terracotta body, a white glaze, and coloured glazes could be observed in a single *haft rang* tile from the bottom up to the top of the tile. In addition, the thermal history of the tiles' bodies showed that the tiles were not fired most probably at temperatures higher than 1000°C. In fact, the equivalent firing temperature (EFT) of the majority of these tiles was estimated to be between 800 and 1000°C. As far as the white glaze is concerned, it was achieved by dispersing tin oxide particle in an alkali glaze as opacifier. The lead content of the white glazes can be technically associated with the manufacturing white glazes in medieval Iran, where tin and lead was roasted to make an opacifier for alkali glazes. Another issue concerning the white glaze was its maturing temperature, which was estimated to be at about 850°C. The yellow glazes were however achieved by dispersing lead tin yellow particles in a lead-based glaze. The green and brown glazes were practically the yellow glazes in which copper(II) and iron(III) respectively used. The maturing temperature of the yellow, green, and brown glazes was calculated to be roughly placed at 615°C. The blue, violet, and turquoise glazes showed however different behaviour by an alkali matrix in which cobalt(II), manganese(III), and copper(II) had yielded the blue, violet, and turquoise tones. The maturing temperature of these glazes was assessed to be at about 700°C. The black lines did not show to be true glazes due to the high alumina and manganese oxide contents in their composition. The high maturing temperature of about 1150°C of the black glazes revealed very interesting results. This property has certainly been of interest in manufacturing *haft rang* tiles; that is, when the low temperature glazes were runny enough to be mixed together, the black line was resistant enough to keep separated the glazes in order not to run together. The relatively higher maturing temperature of the white glaze has also been desirable since it does not softened in low temperatures at which the upper coloured glazes were runny and the chance of mixing the white glaze and the upper glazes was substantially lessened.

Another subject on which this thesis shed light is the attribution of *haft rang* technique to the Spanish technique of  *cuerda seca*. In the discussion and final chapters of the thesis, an attempt is made to put together the technological features of these two techniques. What can be at least understood on the evidences exist about these two techniques is that there is no technological reason by which *haft rang* technique can be attributed to  *cuerda seca*. The use of black line for separating coloured glazes in Iran, as showed in this thesis, has a history much longer the history of  *cuerda seca*. Hence, I have finally suggested that  *cuerda seca* is an inappropriate term to cover the seventeenth century Persian polychrome tiles. The term '*haft rang*,' which is used for nominating the antecedents of the seventeenth century polychrome tiles, is preferred in this thesis as this term is also widely used in today's Iran to address this type of polychrome tiles.

Parviz Holakooei  
Ferrara, Italy  
March 2013

## Riassunto

La storia degli oggetti smaltati policromi ritrovati in Iran nasce dai primi artefatti vetrati policromi, di cui i mattoni vetrati policromi di Chughā Zānbīl, risalenti al XIII secolo a.C., potrebbero costituire una prima testimonianza. Questa tradizione è stata portata avanti fino al declino degli Achemenidi nel IV secolo a.C., quando i mattoni vetrati sono stati ampiamente utilizzati per i fregi dei palazzi e degli edifici più importanti di Persepoli e Susa. In seguito, l'uso degli smalti policromi sui materiali ceramici sembrerebbe essere stato abbandonato fino al X secolo d.C., durante il periodo islamico in Iran, quando oggetti policromi *underglaze* tornarono ampiamente in uso. Le prime evidenze di decorazioni policrome smaltate sono state ritrovate nei casi dei *mīnā'ī* iraniani nel XIII secolo d.C. che, come Abu'l Qasim ha dichiarato, venivano originariamente chiamate *haft rang* ('sette colori'). Questa tecnica è stata leggermente modificata nel corso del XV e XVI secolo d.C. ed ampiamente utilizzata anche nel XVII secolo d.C. durante il periodo safavide (1501-1736). Attualmente, in Iran, le piastrelle *haft rang* sono ancora largamente impiegate nella decorazione delle facciate architettoniche degli edifici scolastici.

Nel XX secolo, gli storici dell'arte hanno correlato questa tecnica ad un stile spagnolo chiamato *cuerva seca*, sebbene l'unica caratteristica comune di queste due tecniche sia una 'linea nera' che separa gli smalti colorati. Questo lavoro di tesi, al fine di fornire maggiori informazioni riguardo le piastrelle iraniane *haft rang* del XVII secolo, utilizza diversi approcci analitici tra cui la microscopia ottica, la fluorescenza a raggi X (WDXRF), la diffrazione a raggi X (XRD), la densitometria, la spettroscopia ultravioletta visibile (UV-Vis spettroscopia), la micro-spettroscopia di Raman e la spettroscopia di dispersione di energia a raggi X (EDS). La microscopia ottica è stata utilizzata principalmente per avere un'idea generale sulla stratigrafia delle piastrelle. La WDXRF è stata utilizzata, invece, per effettuare un'analisi di provenienza, fondamentale nell'inquadramento del contesto archeologico. Un'altra problematica trattata nel presente lavoro riguarda la storia termica delle piastrelle, studiata attraverso le analisi di XRD e densitometria. Questo tema è risultato particolarmente interessante e complesso in considerazione della struttura multistrato delle piastrelle *haft rang*. Riguardo, invece, lo studio degli smalti colorati, questo è stato inizialmente ottenuto grazie alla spettroscopia UV-Vis che ha permesso di analizzare i diversi coloranti. Infine, la micro-spettroscopia Raman ha presentato risultati molto importanti riguardo gli opacificanti e le particelle sospese nelle matrici degli smalti e grazie alle microanalisi EDS sono state effettuate le analisi sulla composizione chimica degli smalti e dei loro fondenti, opacificanti, e dei *network formers* della matrice vetrosa.

I risultati di tutte queste analisi hanno dimostrato che gli impasti delle piastrelle, indipendentemente dal luogo da cui originano, sono costituiti da prodotti locali e non di altri centri di produzione delle piastrelle

*haft rang*. Al microscopio ottico è stato possibile evidenziare tre strati ossia, dal basso verso l'alto, un impasto di terracotta, uno smalto bianco e gli smalti colorati. Lo studio della storia termica degli impasti delle piastrelle ha mostrato che la 'temperatura di cottura equivalente' (EFT) della maggior parte di queste piastrelle è compresa tra 800 e 1000°C, per cui verosimilmente non sono state utilizzate temperature superiori ai 1000°C. Per quanto riguarda lo smalto bianco, si è visto che questo deriva dalla dispersione delle particelle di ossido di stagno (utilizzate come opacificante) in una matrice vetrosa alcalina. Il piombo ritrovato negli smalti bianchi è, invece, proveniente dal procedimento tecnico in cui lo stagno ed il piombo sono arrostiti per ottenere gli opacificanti degli smalti alcalini. Un altro problema relativo allo smalto bianco è stato la sua temperatura di maturazione, stimata a circa 850°C. Infine, riguardo agli smalti colorati, quelli gialli sono stati ottenuti dalla dispersione di particelle di giallo costituite da stagno-piombo in uno smalto a base di piombo; gli smalti verdi e marroni sono risultati essere gli smalti gialli in cui, rispettivamente, sono stati utilizzati, il rame(II) ed il ferro(III). La temperatura di maturazione degli smalti gialli, verdi e marroni è stata calcolata a circa 615°C. Gli smalti blu, viola e turchese, invece, hanno mostrato un comportamento diverso; infatti, il cobalto(II), il manganese(III) ed il rame(II) sono stati utilizzati in una matrice alcalina per creare, rispettivamente, il blu, il viola ed il turchese. La temperatura di maturazione di questi smalti è stata considerata a circa 700°C. Le "linee nere" non possono essere considerati smalti veri a causa dell'alta quantità di allumina e di ossido di manganese. Inoltre, l'elevata temperatura di maturazione (circa 1150°C) degli smalti neri ha rivelato risultati molto interessanti, di sicuro interesse per la produzione delle piastrelle *haft rang*. Infatti, a basse temperature, gli smalti colorati sono abbastanza liquidi da permettere di essere ben mescolati, mentre la "linea nera" è sufficientemente resistente da mantenere questi smalti separati tra loro. Anche l'alta temperatura di maturazione dello smalto bianco è importante perché questo smalto non si ammorbidisce alle basse temperature, quando gli altri smalti colorati sono, invece, liquidi così da ridurre la possibilità di mescolare lo smalto bianco e gli smalti colorati.

Per concludere questa tesi si è occupata anche della problematica di attribuzione della tecnica *haft rang* alla tecnica spagnola della *cuerda seca*. Nei capitoli *Discussion*, *Final Remarks* e *Conclusions* sono state messe in relazione insieme le caratteristiche tecnologiche di queste due tecniche e, sulla base delle evidenze esistenti, non è stata trovata alcuna prova o motivazione per cui la tecnica *haft rang* possa essere attribuita a quella della *cuerda seca*. L'uso della 'linea nera' utilizzata per separare gli smalti colorati, come dimostrato da questo lavoro di tesi, ha una storia molto più lunga nella tecnica *haft rang* rispetto alla spagnola *cuerda seca*. *Cuerda seca* è, quindi, da considerare un termine improprio se riferito alle piastrelle persiane policrome del XVII secolo, la cui corretta denominazione è *haft rang*, termine oggi ampiamente utilizzato in Iran.

Parviz Holakoei  
Ferrara, Italia  
Marzo 2013

## Acknowledgements

This work could not have been achieved without contributing many people who helped me over the past three years of my study in Italy. First of all, I am grateful to my tutors, Prof. Carmela Vaccaro and Prof. Feruccio Carlo Petrucci, who supported me during the past three years with their patience and knowledge. They were always helping me for any discussion and provided me a good ambient of working. I would like also to express my gratitude to Prof. Ahmad Salehi-Kakhki and Prof. Hossein Ahmadi at the Art University of Isfahan who stood by me throughout Bachelor and Master Degrees and were always available for any help. Furthermore, two tutors of mine, Prof. Abbas Abed-Esfahani and Prof. Hesam Aslani at the Art University of Isfahan who have always been encouraging me to look for new and interesting perspectives. I would also like to thank Prof. Samad Samanian at the Art University of Tehran whose support was never stopped. I also thank Prof. Micheal Tite at the Research Laboratory for Archaeology and the History of Art, Oxford University, for his comments on the *Eight Chapter* of the thesis. Finally, my gratitude goes to Prof. Carlo Peretto and Dr. Ursula Thun for their warm and encouraging support and I especially thank Lena Fabbri at the doctorate office of the University for her useful helps regarding bureaucratic affairs.

I am also grateful to many people who supported me in the laboratory work and other affaires concerning this thesis. I express my gratitude to Renzo Tassinari for WDXRF analyses who was always available for any help, Massimo Verde for XRD analyses, Umberto Tessari for density measurements, Flavia Tisato for UV-Vis measurements, Mehri Qobadi for microchemical tests, and Dr. Daniela Palmeri of SEM micrographs and EDS microanalyses. I express also my sincere thanks to Amir-Hossein Karimy, Masoud Nikoubayan, Yaser Hamzavi, M. Enayati, Iman Peymani, Moein Eslami, M. Rahi, and Hamed Sayyadshahri who helped me for collecting samples from various regions of Iran. I would also like to appreciate the Iranian Ministry of Science and Technology and Italian Ministry of Foreign Affairs for their financial supports during these three years and of course the University of Ferrara is especially thanked for giving me the opportunity to carry out my research in a suitable scientific ambient.

Emotional and moral supports were never stopped over the three year sojourn in Italy. First of all, my parents and siblings who were always cheering me up to carry on my work in the difficult moments I faced with at the very beginning of my arrival in Italy. Also, my colleagues at the University of Ferrara, Lisa Volpe, Sabrina Russo, Salvatore Peppi, Andrea Savo, and Hamed Sayyadshari who were kindly helped me during my studies for describing the complicated situation that foreign students usually face with entering in another country. My friends, as always, were stood by me during these three years whose aids were priceless. Moslem Mishmastnehi, Ali Bahabadi, Amir Hossein Karimy, Ali Astaneh, Mohsen Charehsaz, Maryam Ahmadi, and Morteza Fotouhi are my good friends from Iran, as well as my new good friends who I had the pleasure to meet in the residential college of the University, Theneshkumar

Sathiyaseelan, Ahmed Rjoob, Sotiris Sboras, Chiran Pokharel, Abdul Haseeb, and many others. Finally, I would like to thank the Marcati's family whose kindness cheered me up over the past two years.

# Contents

<i>Abstract</i>	<i>i</i>
<i>Riassunto</i>	<i>iii</i>
<i>Acknowledgements</i>	<i>v</i>
<i>List of figures</i>	<i>xi</i>
<i>List of tables</i>	<i>xiii</i>
<i>Guidelines for the readers</i>	<i>xv</i>
<b>Chapter One: From haft rang to cuerda seca</b>	<b>1</b>
Who and where were the Safavids	1
Safavid art of tile-making	2
Haft rang technique	4
Terminology of cuerda seca	7
Origin of cuerda seca	7
<i>Production of cuerda seca in the Caliphate era</i>	8
<i>Spanish cuerda seca in the first Taifa and Almoravid eras</i>	8
<i>Almohad period</i>	9
<i>Nasrid dynasty onwards</i>	9
Cuerda seca tiles	9
Technological features of cuerda seca	10
<i>Cuerda seca total</i>	10
<i>Cuerda seca partial</i>	10
<i>Incised cuerda seca</i>	11
<i>Firing process</i>	11
<b>Chapter Two: Studied area and the samples</b>	<b>13</b>
<i>Ardabīl</i>	13
<i>Qazvīn</i>	14

<i>Mashhad</i>	14
<i>Māzandarān</i>	15
<i>Isfahan</i>	16
Introduction to the samples	18
<i>Masjid-i Jāme‘-i ‘Abbāsī</i>	18
<i>‘Ālī-Qāpū palace</i>	19
<i>Bethlehem Church</i>	20
<i>Other samples of Isfahan</i>	21
<i>Masjid-i Jāme‘ of Qazvīn</i>	22
<i>Muṣallā in Mashhad</i>	22
<i>‘Abbās-qulī Khān madrasa in Mashhad</i>	22
<i>Chishma Imārat in Bihshahr, Māzandarān</i>	23
<i>Mīr-Buzurg tomb in Āmul, Māzandarān</i>	23
Preliminary microscopic observations towards the analytical studies	24
<b>Chapter Three: WDXRF quantitative analysis and the question of the provenance</b>	<b>27</b>
3.1 Introduction	27
3.2 Data handling	31
3.2.1 <i>Problems associated with provenance studies</i>	31
3.2.2 <i>An introduction about PCA</i>	32
3.2.3 <i>Interpretation of the data by PCA</i>	33
3.3 Interpretation of the dataset by bivariate plots	38
3.4 Concluding remarks	38
<b>Chapter Four: X-ray diffraction on assessing firing temperature</b>	<b>41</b>
4.1 Introduction	41
4.2 Materials and method	42
4.2.1 <i>Instrumentation</i>	42
4.2.2 <i>Statistical treatment</i>	43
4.2.3 <i>Density measurement</i>	43
4.3 On the potential phases composing the bodies	43
4.4 Estimation of EFT of the bodies	44
4.5 Principal component analysis on the XRD data	49
4.6 Density measurement	53
4.7 Concluding remarks and future perspective	55
<b>Chapter Five: Optical spectroscopy and colourimetry</b>	<b>57</b>

5.1 Introduction	57
5.2 Instrumentation and the optical dataset	58
5.3 Interpretation of the dataset	59
5.3.1 Whites	61
5.3.2 Yellows	62
5.3.3 Blues	63
5.3.4 Violets	64
5.3.5 Browns	65
5.3.6 Greens	66
5.3.7 Turquoises	67
5.3.8 Final discussion	68
<b>Chapter Six: Micro-Raman spectroscopy on glaze characterisation</b>	<b>69</b>
6.1 Introduction	69
6.2 Sample preparation and the instrumentation	70
6.3 Interpretation of the Raman spectra of various coloured glazes	70
6.3.1 General facts about Raman spectra of amorphous glazes	71
6.4 Coloured glazes and micro-Raman spectroscopy	73
6.4.1 Turquoise glazes	73
6.4.2 Blue glazes	74
6.4.3 Violet glazes	75
6.4.4 White glazes	76
6.4.5 Yellow glazes	76
6.4.6 Green glazes	77
6.4.7 Brown glazes	77
6.4.8 Black lines	78
<b>Chapter Seven: SEM observations and EDS microanalyses</b>	<b>79</b>
7.1 Introduction	79
7.2 Samples and experimental	80
7.3 Results	80
7.3.1 Whites	82
7.3.2 Yellows	83
7.3.3 Green glazes	83
7.3.4 Brown glazes	84
7.3.4 Turquoise glazes	84

7.3.5 <i>Blue glazes</i>	85
7.3.6 <i>Violet glazes</i>	85
7.3.7 <i>Black lines</i>	86
7.4 Estimation of maturing temperature of the glazes	86
<b>Chapter Eight: Discussion</b>	<b>89</b>
8.1 Bodies	89
8.2 Glazes	92
8.2.1 <i>Network formers</i>	92
8.2.2 <i>Fluxes</i>	93
8.2.3 <i>Intermediates</i>	94
8.2.4 <i>The transparent frit</i>	95
8.2.5 <i>The opaque frit (white glaze)</i>	95
8.2.6 <i>Blue glazes</i>	97
8.2.7 <i>Violet glazes and black lines</i>	98
8.2.8 <i>Turquoise glazes</i>	99
8.2.9 <i>Yellow glazes</i>	99
8.2.10 <i>Green glazes</i>	100
8.2.11 <i>Brown glazes</i>	101
<b>Final Remarks and Conclusions</b>	<b>103</b>
<b>References</b>	<b>109</b>
<b>Appendices</b>	<b>141</b>

## List of figures

Figure 1.1 Mosaic tilework (cut-tile) in the porch of ‘Alī Mosque in Isfahan (photo: the author)	2
Figure 1.2 Vast application of haft rang tilework at Masjid-i Jāme‘-i ‘Abbāsī of Isfahan (left) (photo: the author) and details of the polychrome tiles (right) (photo: courtesy of A.H. Karimy)	3
Figure 1.3 A fifteenth century haft rang Timurid tile (c. 1440. The David Collection, Copenhagen, Inv. no. 27/1967)	5
Figure 2.1 Details of inappropriate restorations on haft rang tiles of Shaykh Şafī-al-Dīn’s shrine in Ardabīl (photo: the author)	13
Figure 2.2 Details of haft rang tiles in a spandrel at Masjid-i Jāme‘ of Qazvīn (photo: the author)	14
Figure 2.3 Detail of Safavid haft rang tiles in a spandrel of ‘Abbās-qulī madrasa (photo: the author)	15
Figure 2.4(left) Few monochrome cut-tiles still attached on a vault of Chishma Imārat of Bihshahr and (right) severely deteriorated rectangular haft rang pieces closed by monochrome glazes at ‘Abbāsābād palace in Bihshahr (photo: the author)	16
Figure 2.5 Haft rang tiled dado of Mīr-Buzurg tomb in Āmul (photo: the author)	16
Figure 2.6(left) Vast haft rang tile revetment on the dado of Bethlehem Church (photo: courtesy of A.H. Karimy) and (right) in the entrance of Luţfallāh Mosque (photo: the author)	17
Figure 2.7 Ten collected samples of Masjid-i Jāme‘-i ‘Abbāsī	19
Figure 2.8 Seven collected samples of ‘Ālī-Qāpū	20
Figure 2.9 Two collected samples of Bethlehem Church	21
Figure 2.10 Seven samples of Işfahānak (I.E. serie) and seven samples of ICHHTO collection storages (I.C. serie)	21
Figure 2.11 Three haft rang samples of Masjid-i Jāme‘ of Qazvīn	22
Figure 2.12 The single sample of Muşallā of Mashhad	22
Figure 2.13 Two samples of ‘Abbās-qulī Khān madrasa in Mashhad	23
Figure 2.14 Three fragmentary haft rang tiles collected as samples from Chishma Imārat palace	23
Figure 2.15 The single haft rang tile detached from the dado of Mīr-Buzurg tomb	24
Figure 2.16 The area under study with Safavid haft rang tile on Iran’s today map	24
Figure 2.17 (left) Surface observation on sample I.S.7 and (right) the cross section of the same point of the sample	25
Figure 2.18 Schematic stratigraphy from different layers of haft rang tiles	25
Figure 3.1 PCA biplots derived from first two principal components of a) major, minor, b) trace elements and c) rare earth and other trace elements of the samples. PCA biplot of Qazvīn and Isfahan’s samples are represented in the biplot d).	35
Figure 3.2 Geological context of the studied areas. (Source: National Geosciences Database of Iran)	36
Figure 3.3 Plane polarised light image of thin sections of a) a Bihshahr tile (no. 40) which shows a crushed shell fragment in the body’s clayey matrix and b) a Qazvīn tile (no. 39) which shows a plagioclase crystal embedded in a volcanic tuff ash particle in the body’s paste.	37
Figure 3.4 Bivariate plots of major, minor, and trace elements obtained from WDXRF data	39
Figure 4.1 Ternary diagrams plotted for the chemical composition of the tiles’ bodies. Legend: An (anorthite), Co (corundum), Cr (cristobalite), Fo (forsterite), Ge (gehlenite), Me (mellilite), Mer (merwinite), Mu (mullite), Py (pyroxene), Sp (spinel), Tr (tridymite), and Wo (wollastonite)	44
Figure 4.2 XRD patterns of the 43 samples in the range of 8–40° in 2θ scale	45

Figure 4.3 PCA score plot on the XRD patterns in 8–40 2θ degree	49
Figure 4.4 PCA biplot on quartz, SiO <sub>2</sub> , alkalis, and amorphous contents of the bodies	50
Figure 4.5 Bivariate plot of quartz versus SiO <sub>2</sub> for FFR and SFR samples	50
Figure 4.6 Quartz versus amorphous contents on the bivariate plot of FFR and SFR samples	51
Figure 4.7 Bivariate plot of SiO <sub>2</sub> versus the alkali contents of both FFR and SFR groups	51
Figure 4.8 EFT of the bodies on Figure 4.6's data (note that in presenting the firing temperature the average values of the EFT are inserted)	52
Figure 4.9 Quartz/alkali ratio versus quartz/amorphous ratio plotted for the FFR and SFR groups (note that nos. 39, 40, and 41 are removed from the SFR group to ease observing the data)	53
Figure 4.10 Quartz versus density contents in FFR and SFR groups	53
Figure 4.11 Amorphous versus density contents in FFR and SFR groups	54
Figure 4.12 Quartz versus density contents in FFR and SFR groups representing average EFT	54
Figure 5.1 Projection of a* and b* SCE values of the coloured glazes on the CIEL*a*b colour plane	60
Figure 5.2 Lightness versus gloss degree for both SCE and SCI values of the various coloured glazes	60
Figure 5.3 Optical spectra of total reflectance (SCI mode) for five white glazes of haft rang tiles	61
Figure 5.4 a) Optical spectral curve of I.C.2 yellow glaze b) and four deteriorated yellow glazes of I.C.7, I.E.1, I.E.7, and Q.J.2	62
Figure 5.5 Optical curve of I.C.5 blue glaze in diffuse reflectance mode	63
Figure 5.6 Reflectance spectra of the altered blue glaze of B.C.3	63
Figure 5.7 Typical reflectance spectra of the violet glazes	64
Figure 5.8 Absorption bands of the dark blue glazes of I.E.3 and I.E.5	64
Figure 5.9 Optical reflectance spectra of some brown glazes	65
Figure 5.10 Optical reflectance spectra of M.A.2 brown glaze with two absorbance at 490 and 650 nm attributable to manganese(III)	65
Figure 5.11 Optical reflectance spectra of the brown glazes of I.E.4 and I.E.2 demonstrate the identical lead-tin yellow type II spectra	66
Figure 5.12 Different optical spectra of the green glazes: a) emerald green hue with the minimum absorbance at around 550 nm; b) dark green hue with the minimum absorbance at around 530 nm; c) light green hue with the minimum absorbance at around 570 nm	66
Figure 5.13 Typical optical spectrum of the turquoise glazes with diffuse reflectance light	67
Figure 5.14 Optical spectra of deteriorated turquoise glazes	68
Figure 5.15 First derivatives of visible spectra of the coloured glazes	68
Figure 6.1 Raman spectra of the turquoise glaze of I.A.2	73
Figure 6.2 Quartz in the turquoise glaze of I.B.1	73
Figure 6.3 a) Copper oxide in the turquoise glaze of I.E.3 b) and its Raman spectrum	74
Figure 6.4 Sharp bands at 590 and 990 cm <sup>-1</sup> in the turquoise glaze of I.A.7	74
Figure 6.5 Raman spectrum of the I.E.5 blue glaze	75
Figure 6.6 a) Raman spectrum of cassiterite in I.A.5 and b) quartz in I.A.1 blue glazes	75
Figure 6.7 Raman spectrum of the violet glaze of I.C.2	75
Figure 6.8 Raman spectrum of I.C.7 yellow glaze	76
Figure 6.9 Raman spectrum of the I.A.4's green glaze	77
Figure 6.10 Raman spectrum of I.C.1 brown glaze	77
Figure 6.11 a) Red spots in the brown glaze of M.A.2 and b) its Raman spectrum	78
Figure 6.12 a) Raman profile of Mn <sub>3</sub> O <sub>4</sub> in the black line of I.C.4 and b) Raman profile of Mn <sub>3</sub> O <sub>4</sub> in the black line of I.E.5	78
Figure 7.1 PCA biplot of the first two principal components resulted from the EDS data on the coloured glazes	82
Figure 7.2 Backscattered image of the white glaze of I.C.7 sample	83
Figure 7.3 Dark iron rich spots in the brown glaze of I.E.2	84
Figure 7.4 Small tin oxide particles in the turquoise glaze of I.A.3	85

## List of tables

Table 3.1 Major and minor elements of the bodies obtained by WDXRF analysis	29
Table 3.2 Trace elements of the samples quantitatively measured by WDXRF (ppm)	30
Table 4.1 Semi-quantitative values of various phases detected by XRD in the bodies. Legend: Qz (quartz), An (Anorthite), Mu (muscovite), Ge (gehlenite), Ca (calcite), Di (diopside), La (laumontite), Wo (wollastonite), He (hematite), Am (amorphous phase), Sa (sanidine), Ab (abundant), EFT (equivalent firing temperature), n.m. (not measured), and n.d. (not detected)	47
Table 4.2 Schematic diagram from behaviour of different phases during firing in the calcareous bodies (Trindade et al., 2009)	49
Table 7.1 The semi-quantitative results of EDS microanalyses on the coloured glazes (normalised to 100%)	81
Table 7.2 Calculated maturing temperature of the coloured glazes	87



## Guidelines for the readers

### Transliterations

This thesis uses British English spelling and punctuation. Technical and local terms, from languages using non-Roman alphabets, have been transliterated with diacritics. Persian, or Farsi, like other languages, comprises of 23 consonants and 6 vowels (Table 1). However, these phonemes vowels and consonants have always been a subject of discussion to transliterate due to their complicity. In this thesis, a system for transliteration of Persian and Arabic terms is suggested based on some other transliteration systems. Here, long vowels are transliterated as **ā** (/ɑ:/), **ī** (/i:/) and **ū** (/u:/) (no macron on **i** or **u**, except for quoted passages and bibliographical data which must retain their original transliterations). Short vowels, however, are transliterated as **a** (/æ/), **i** (/e/) and **u** (/o/).

Table 1 Persian/Arabic characters versus International Phonetic Alphabet (IPA) phonetics Together with their transliterations

Persian/Arabic	Transliteration	IPA
ا	, a, ā	ʔ, æ, ɑ:
ب	b	b
پ	p	p
ت	t	t
ث	t̤	s
ج	j	dʒ
چ	ch	tʃ
ح	h	h
خ	kh	x
د	d	d
ذ	z̤	z
ر	r	r
ز	z	z
ژ	zh	ʒ
س	s	s
ش	sh	ʃ

Persian/Arabic	Transliteration	IPA
ص	ʂ	s
ض	ʒ	z
ط	t̤	t
ظ	z̤	z
ع	ʕ	ʔ, ː
غ	gh	ɣ, ɡ
ف	f	f
ق	q	ɣ, ɡ
ک	k	k
گ	g	ɡ
ل	l	l
م	m	m
ن	n	n
و	v, u	v, u:, o
ه	h, a	h, e, æ
ی	y	j, i:, e

Silent final **-h** in Arabic and Persian is transliterated as **-a**, such as *khāna*, *qit'a*. There are also some compound vowels, such as **ow** (in Persian words like *Firdawsi*), **aw** (in Arabic words like *Majd al-Dawla*), **ay** (in Persian words like *kayhān*) and **ay** (in Arabic words and exceptionally in Persian words: *Husayn*, *ayvān*). Moreover, *kisra* before 'y' is transliterated as **ī** (e.g., *Sīyar al-mulūk* and *adabīyāt*). Also, 'al' before Arabic proper names, except in constructs is dropped, such as *Bīrūnī*, *Hallāj*, but *Ibn al-Aīr*, *Nāṣir al-Dīn*.

Whenever possible, English forms and translations are used instead of Persian or other foreign place names, offices, institutions, *etc.* (a transliteration and/or gloss, if appropriate, might be followed in

parentheses). Moreover, non-Latin author names which have been romanised by the authors themselves have not been transliterated.

#### *Punctuation, etc.*

Italics are used for titles of books and non-Latin materials' and techniques' names. The names which are originally in a non-Latin alphabet names are also transliterated. Double quotation marks are used for titles of articles and dissertations. Single quotes are used for quotations within quotations, and for glosses immediately following foreign words or phrases; a following comma or stop goes outside; e.g., *kutub* 'books.'

#### *Citations and referencing*

Parenthetical referencing, also known as Harvard referencing, is a citation style of this thesis. Here, the citations are enclosed within parentheses (round brackets) and embedded in the text, either within or after a sentence. In fact, author-date style is used recommended by the American Chemical Society. On the other hand, non-Latin books and articles, which are transliterated within the text, are translated to English in the bibliographical section.

#### *Dates*

Dates are given in European style without internal punctuation like **1827**. Centuries are given for the Common Era. Eras are abbreviated as BC and AD. However, years of publication in the citations for non-Gregorian calendar articles and books are transferred to Gregorian calendar in order to unify all the dates.

#### *Capitalization*

Titles and epithets are not capitalised except when appended to a name. Persons' titles or names are hyphenated and capitalised both elements ('*Abd al-Husayn, Fathī 'Alī, Zīnat al-Nisā*). In book titles, institutions, *etc.* the pattern *Nuzhat al-Qulūb, Bayt al-Māl* is used. The first character of each word in books' and articles' titles is capitalised. The names of cities, mines, geographical places are also capitalised.

#### *Units of weight*

The medieval Persian weights and measures are very confusing. In 1926, a law was passed trying to equate Persian measures with the metric system, and at that time the Tabrīz *man* was equivalent to just under three kilograms and there were 640 *miṭqāl* in one *man*. It is thus possible that Kāshānī's *man* and *miṭqāl* correspond to about 3 kilograms and 4.7 grams respectively. According to Qāzān Khān's decree, there were to be 260 *dirhams* in a Tabrīz *man*, which would give a figure for one *dirham* of about 11.5 grams (Allan, 1973; Gignoux and Bates, 2011). However, in Ali Mohamed's scale one Tabrīz *man* equals to forty *seers*, one *seer* equals to sixteen *miṭqāls*, one *miṭqāl* equals to twenty *nukhuds*, and one *seer* is about one kilogram (Ali Mohamed, 1888).

## Chapter One: From *haft rang* to *cuerda seca*

### Who and where were the Safavids

The period of the Safavids, the dynasty that took control of Persia in the early sixteenth century, is often considered the beginning of modern Persian history (Matthee, 2008). The story of the Safavids began when Ismā'il I became the first ruler of the great Shiite dynasty (1501-1732) in the west, while their territories to the east were conquered by the Uzbek Shaybanids, who took Herat in 1507 (Porter, 1995). The origin of the Safavids is obscure. They were at Ardabīl in Azerbaijan, the heartland of the Turkmen. Some historians believe that they are Kurds, while others deem that they are Turkmen (Shapur Shahbazi and Bosworth, 1990). The dynasty was founded by a mystic, the Shaykh Ṣafī whose followers gathered together a sanctuary in the town of Ardabīl in Azerbaijan (DeGeorge and Porter, 2002). In other words, the Safavids began in about 1300 as a mystical order centered in the northwestern town of Ardabīl, the hometown and burial place of the founder, Shaykh Ṣafī al-Dīn (1252-1334) (Matthee, 2008).

In 1501, Ṣafī al-Dīn's descendant, Shah Ismā'il I, forced the Ottomans to leave Tabrīz and went on to seize control of a territory roughly neighboring with the boundaries of modern-day Iran (Savory, 1980). Ismā'il I established Shiism as his official religion, in contrast with the Sunnism of the Ottomans to the West and the Uzbeks to the Northeast (Newman, 2006). Ismā'il I (1501-1524) also established the country under the name of Shah rather than a shaykh (Matthee, 2008). Although Ismā'il I initially gained his control over Azerbaijan, the Safavids ultimately took the control in all of Persia. In fact, a year after his victory in Tabrīz, Ismā'il I claimed most of Persia as part of his territory and, within ten years, established a complete control over all of it (Savory, 1980).

When the Safavids achieved power over the Āq Quyūnlūs in the northwestern Iran during the beginning years of the sixteenth century, they at first made their venue in Tabrīz (Shapur Shahbazi and Bosworth, 1990). As a city which lies near the Ottoman Empire, Tabrīz was occupied many times, to the point that few monuments of importance from this period have handed over to modern times (DeGeorge and Porter, 2002). After Ismā'il I's death his nine-year-old son, Ṭahmāsp I is successor. Shah Ṭahmāsp, the young governor of Herat, succeeded his father Ismā'il in 1524 (Savory, 1980; Newman, 2006). He finally asserted his authority over his rivals, signed a peace treaty with the Ottomans and pulled the Uzbeks back (Newman, 2006). In his time, Persia began to recover from the misery and devastation that accompanied the early Safavid conquests. Shah Ṭahmāsp managed to extend his authority and influence over a number of areas that under his father had been buffer regions (Matthee, 2008). Its main city, Tabrīz, may have had as many as 80,000 inhabitants during his reign. However, he relocated the capital from Tabrīz to Qazvīn (Newman, 2006) in 1555 and hereafter called *dār al-salṭana* (Shapur Shahbazi and Bosworth, 1990). At that time, Qazvīn was an important stage in connecting the vital road of Azerbaijan and Khurāsān, and it also established a strategic situation along the foreign trade route from Anatolia, Russia, and the West into Iran (Shapur Shahbazi and Bosworth, 1990).

The greatest of the Safavid rulers, Shah ‘Abbās I, came to power in 1587 following the ceased Shah Ṭahmāsp. He recognised the weaknesses of his army, which was consistently being defeated by the Ottomans who had captured Georgia and Armenia and by Uzbeks who had captured Mashhad and Sīstān in the east (Savory, 1980). ‘Abbās I (1587-1629) is universally regarded as the greatest Safavid ruler, the embodiment of an ideal monarch (Matthee, 2008). Shah ‘Abbās I, whose reign saw the peak of the Safavid dynasty in political and cultural terms, was an approximate contemporary of Elizabeth I of England, Philip II of Spain, Ivan the Terrible, and Henry IV of France (DeGeorge and Porter, 2002). Qazvīn developed little during forty years reign of ‘Abbās I. However, Isfahan was turned into what became for the first time a genuine metropolis of Iran by the Shah, who for his extensive building and irrigation programs began to attract European merchants and foreign artisans, encourage architecture and the visual arts (Shapur Shahbazi and Bosworth, 1990). The Safavids ultimately succeeded in establishing a new Persian national monarchy (Matthee, 2008).

When Shah ‘Abbās I died of natural causes in early 1629, there were no sons to succeed him. He was therefore succeeded by his grandson Ṣafī, the son of Ṣafī Mīrzā, who had been murdered by Shah ‘Abbās on suspicion of sedition (Matthee, 2008). The accession of Shah Ṣafī II, ‘Abbās II’s successor, in 1666, exposed further signs of the country’s weakening state. The period following his supermacy was followed by famine, causing the court astrologers to declare that the shah had been crowned at a ominous moment (Matthee, 2008). Following the death of Shah ‘Abbās II in 1666, Safavid power gradually waned and the country was overrun in a sequence of Afghan incursions (DeGeorge and Porter, 2002).

### **Safavid art of tile-making**

Shah Ismāīl I established a royal workshop and library for the production of illuminated manuscripts (Matthee, 2008). However, he did not have enough time to be involved in architectural decorations due to his occupancy about political and military affairs. Only a few monuments with mosaic tile decorations are remained from Shah Ismāīl’s reign, from which ‘Alī Mosque in Isfahan is one of the examples (Hunarfar, 1956) (Figure 1.1). The reign of Shah Ṭahmāsp, a ruler of refined taste, however, saw a flourishing of the arts. But, this expressed itself less in architecture, which would only gain celebrity in the seventeenth century, than in the visual arts, most notably painting (Matthee, 2008).



*Figure 1.1 Mosaic tilework (cut-tile) in the porch of ‘Alī Mosque in Isfahan (photo: the author)*

After Shah Ṭahmāsp I, Shah ‘Abbās I was the first Safavid ruler to patronise the arts in a sustained manner (Matthee, 2008). Shah ‘Abbās I’s period not only is the most flourishing era in the Safavid art, but also is considered as one of the most eminent periods of Persian art and architecture. Shah ‘Abbās I recognised the commercial benefit of promoting the arts products provided much of Iran’s foreign trade. In this period, handicrafts such as tile-making, pottery, and textiles developed (Savory, 1980). ‘Abbās I appears to have been more concerned with the arts of official influence (architecture and city planning)

and economic convenience (exportable ceramics, textiles, and carpets) than with the far more private and personal art of illuminating books (Welch, 1974). Chardin, the famous French traveler who lived in Safavid court, says in this regard: “the ornament is marvelous and unknown in our European architecture. It consists of niches in a thousand shapes where gold and blue are found in abundance with inlay made of enamel squares, and a flat frieze all round of the same material carrying passages of the Koran, the size of the letters depending on the height of the building” (Stevens, 1974). In 1597, Shah ‘Abbās I moved the Safavid capital to Isfahan and, soon after, the country was to European traders from various European companies, particularly the Dutch Vereenigte Oostindische Compagnie, whose trades in Chinese porcelain and celadon were enriched the ceramic technology in Persia (Crowe, 1991).

Safavid art is often recognised with the city planning and architecture, achievements made during the reign of Shah ‘Abbās I (Savory, 1980). The art of tileworking in Isfahan, the capital of Shah ‘Abbās I, is splendid for their delicate designs. This industry was in increasing use for mural decoration furnished with receipts for the several pigments used at the Safavid manufactories (Fortnum, 1873). Safavid mosques and *madrasas* are totally covered with colourful tiles inside and out, the use of tiles even more extensive than the precedent dynasties like Timurids (Porter, 1995). From the techniques widely used for decorating tilework in the Timurid period, tile mosaic and *haft rang*, were most extensively used in Safavid Iran (Figure 1.2). The principal elements of design and the Timurid aesthetic of overall tiling continued without a pause (Porter, 1995). Those architects, who designed the various mosques, palaces, and caravanserais of this era and the masters of tiles, were mostly members of guilds with a spiritual discipline (Nasr, 1974). The tile makers used to participate in the alchemical process not only physically but spiritually. In fact, the choice of colour symbolises a particular state of consciousness in Safavid art of tile-making (Ardalan, 1974). What has remained of the techniques of the traditional arts is of an oral nature preserved within the still existing guilds and transmitted by the way of a master-disciple relationship

which can still be observed in some Persian cities and towns and which is a remnant of the fully active guilds of the Safavid period (Nasr, 1974).



*Figure 1.2 Vast application of haft rang tilework at Masjid-i Jāme‘-i ‘Abbāsī of Isfahan (left) (photo: the author) and details of the polychrome tiles (right) (photo: courtesy of A.H. Karimy)*

The art of Safavid tilework is also exported to beyond the Safavid frontiers. The fifteenth century Ottoman tile revetments can be ascribed to immigrant craftsmen from Iran working with local assistants. Following them there were a group attached to unknown ceramics workshops in Istanbul headed by one of the Tabrīzī master craftsmen (Necipoğlu, 1990). On the other hand, the Safavid ceramic industry was

created by the influence of Persian rulers and the merchant society that controlled and sponsored the work of ceramics, as well as by the products imported from the worlds beyond their frontiers (Crowe, 2004). In fact, it appears that polychrome painted decoration, which was practiced in China only from the thirteenth century onwards, was initiated by Islamic ceramists (Grube, 1965). This influence was reciprocal. Adaptation of Chinese designs was also continued in Islamic ceramic industry. For instance, the lotus scroll became a vine, imitating the arabesque, with which it was often contrasted or intertwined; the two elements in such combinations were called by the fifteenth century authors, *khatā'ī* and *islīmī* respectively and emerged as major features of tile revetments in the Timurid and Safavid periods. In Safavid architecture Sino-Persian vegetal ornaments are clearly evident. Large areas on the surfaces of main religious monuments, including the exteriors of domes, were covered with glazed tiles decorated with intricate networks. Decorative schemes incorporating three or even four systems of interwoven *islīmī* and *khatā'ī* fill the main fields in some sixteenth or seventeenth century carpets (Soucek, 1994).

### **Haft rang technique**

Making polychrome ceramics used to decorate architectural facades has a long history in Iran. The first examples of making polychrome glazes juxtaposed on a single body dates back to the Elamite era in the second millennium BC (Caubet, 1992, 2007). This tradition was also pursued in the Achaemenid era in the mid-first millennium BC at Susa and Persepolis (Caubet and Kaczmarczyk, 1998). In these polychrome glazes, various coloured glazes are separated by a relief black or brown glaze. Making polychrome ceramic objects experienced a long period of absence until the Islamic period when different colours were being applied under a transparent alkali glaze. The first examples of such a technique can be found in the underglaze tableware of Nishapur (Wilkinson, 1973) and Sīrjān (Morgan and Leatherby, 1987) in today Iran. The first evidences of using polychrome glazes as overglaze decorations both on tableware and tiles are those twelve century *mīnā'ī* ware. This technique used to be originally called *haft rang* (literally meaning 'seven colours') however they are recently denominated by some merchants *mīnā'ī* (Fehérvári, 1973). This technique was then modified and used under the name of *lājvardīna* throughout the thirteenth century during Ilkhanid era and, afterwards was spread out with a subtle technical modification in the Transoxiana over the fourteenth century (Figure 1.3). In the Safavid period, throughout the seventeenth century, this technique was turned back to central Iran and rapidly developed and was extensively used to decorate architectural façades (O'Kane, 2011). This style of tile-making is nowadays called *haft rang* in Persian although the Spanish term of '*cuerda seca*' is sometimes used in non-Persian texts to describe this style of tile-making (Porter, 1995; DeGeorge and Porter, 2002; O'Kane, 2011).

*Haft rang* and mosaic tiles have been very common in decorating architectural facades in the Safavid era (Porter, 1995). However, use of *haft rang* in Safavid era was privileged because of impatient and rapid development of architectural constructions. Because of the massive constructions of the early seventeenth century and the consequent expansion in the area of building surfaces to be covered with polychrome tiles, this proved to be the most common technology in Isfahan and practically replaced the mosaic technique (Babaie and Haug, 2007). In mosaic tilework each tile piece was cut in a different shape to fit its designated place. Instead, in the *haft rang* usually a square tile that incorporates various colours in one tile was used. This technique, which is aesthetically less complex than mosaic tile technique, was economical, and fast (Blunt, 1966; Kīyānī *et al.*, 1983). Due to this fact, the new technique allowed a wider range of colours to be used, creating richer patterns and designs (Hattstein and Delius, 2001). Using *haft rang*, a greater variety of colours could be found in tiles on both religious and secular buildings, though not in tile

mosaics, which had become very costly and time-consuming (Degeorge and Porter, 2002). However, *haft rang* appearance was less brilliant and vivid than the mosaic tile (Petersen, 1996).

Figure 1.3 A fifteenth century *haft rang* Timurid tile (c. 1440. The David Collection, Copenhagen, Inv. no. 27/1967)



The term *haft rang* is derived from six colourful glazes; green, brown, turquoise, violet, blue, and yellow, which are applied on a white fired glaze (the seventh colour). All these glazes are separated by a black line (Nīyāzmand, 1964; Bazl, 1965; Kīyānī *et al.*, 1983). *Haft rang* tilework is also called *khishtī*, or according to Ali Mohamed (1888), *kār-rū-rang*. In *haft rang* technique, a set of rectangular tiles are placed next together, and create a whole design. Simply, to create a single *haft rang* tile, a clay body is fired, and then, a white glaze is fired on the body. Third firing, however, is applied to stabilise a second colourful glazed layer on top of the white glaze (Nīyāzmand, 1964; Bazl, 1965; Wulff, 1966). Therefore, each single *haft rang* tile is composed of three separate layers: a body, a white glaze, and layer of coloured glazes. Ustad Ali Mohamed (1888) has provided a description of the method of making the body as follows:

*“To make a brick, the master takes a wooden mould, fills it with potters’ clay, well handled, and mixed with ashes or sand, then with a wire he cuts off the excess paste; he then turns the mould over on the ground and so leaves it for twenty-four hours. Next day he removes the mould, beats and presses the brick on a flat stone to smooth its surface, then places it upright against the wall, so as to dry without warping. When dry he rubs the surface with a damp rag and begins colouring.”*

The raw body was then baked in the kiln. Afterwards, the tile-maker fires an opaque white glaze on the fired body. However, the edges of the tiles are now distorted a bit due to two firing processes. Therefore, the tile-maker bevels the edges in order to make them perpendicular (Bazl, 1965; Wulff, 1966; Zāhidīyān, 2001). Now, the tile-maker transfers a design on the fired white glaze. In this stage, firstly, a design, which is adjusted to the dimensions of want-to-be-tiled area, is designed on a sheet of paper. Then, the tile-maker pins the design on the sheet. Afterwards, he puts the sheet on the white tiles and, then, passes pounced soot or charcoal powder from pined holes. Hence, the design is copied on the white glaze (Māhir al-Naqsh, 2002).<sup>1</sup> The tile-maker should then stabilise the transferred design on the white glaze. It is performed by a paint which is called *maqān* dispersed in the water and Tragacanth gum. This material is

---

<sup>1</sup> Canby (2002) has indicated that this method of copying has been firstly used in Italian paintings.

exactly painted on the powdered charcoal trace and subsequently fixes the unstable design. However, the black line obtained by *maq̄n* has another application in *haft rang* tiles. During the successive firing process this line keeps apart the coloured glazes in order not to run together.<sup>2</sup> After designing, it is the time to paint colourful fritted glazes. The frits are again dispersed in the water. A fine brush is used to paint different coloured frits on the surface of the white glazed tiles. Each coloured frit is obtained by applying metallic oxides mixed with either the transparent or the opaque frit. Ustad Ali Mohamed (1888) recommends that the colours should be tested before their definitive application on the white glaze. He writes:

*“First, take two miṭqāls of essence of the cobalt ore, four miṭqāls of budlike balls of raw cobalt ore, thirty miṭqāls of pounded glass, thirty miṭqāls of pounded flint stone, thirty miṭqāls of tanikār, thirty miṭqāls of the alkaline frit: bray all together, put in an earthenware vessel, and place it in the kiln; heat up, take out, break the vessel, bray the contents, and add water. This is the blue of the haft rang. When you want a green colour, take four miṭqāls of copper, four miṭqāls of the cobalt compound, thirty miṭqāls of glass, thirty miṭqāls of flint stone, thirty miṭqāls of alkaline frit, thirty miṭqāls of saltpeter; mix all in a vessel, put in the kiln, take out, break the earthenware vessel, bray the contents, apply it to a white tile, and it will come out green. For turquoise, you must take four miṭqāls of copper, four of cobalt ore, thirty of miṭqāls of powdered glass, thirty of flint stone, thirty of the alkaline frit, and thirty of saltpeter; put in a vessel and bake. It will come out turquoise paint. For black, take four miṭqāls of maq̄n, thirty of powdered glass, fifty of flint stone, thirty of the alkaline frit, thirty of saltpeter; mix in a vessel, bake, bray, and you will have black paint. For red take half a miṭqāl of gold in aqua regia, also six nukhuds of tin in other aqua regia, fill a bowl with water, and add the gold solution, stirring briskly; next add the tin solution, stirring it with your hand, the froth will set, pour away the water; add half a Tabrīz man or 320 miṭqāls of powdered glass, and 110 miṭqāls of tanikār, and bake in an earthenware vessel. The compound will be red paint. For violet, mix four parts of this red colour and one part of the blue glaze, and you will get violet paint.”*

Finally, the painted tiles were numbered and fired in the kiln. It should be noted that an optimum firing temperature for the coloured glazes should be considered. Normally, different glazes due to their different chemical composition should be fired in their appropriate temperatures. However, in the *haft rang* final firing an average temperature is considered for firing all the glazes. This means that the tile-maker should choose a proper firing temperature for all the glazes. It sometimes ends to some defects in the glazes. Therefore, Ali Mohamed (1888) suggests the following solution:

*“The method of testing is this: paint those seven colours (separately) on a piece of tile, and place it in a portable kiln, which you heat. Taking the brick out, examine it; any colour which is dry, unclear, dull, and must be increased in moisture according to the degree which each requires. After thus regulating the strength of the colours (raising what is too low, lowering what is too high), apply all the seven colours separately, by making a design with each on a brick or vase, and cook it in the kiln.”*

---

<sup>2</sup> This is doubtful that this line can keep separated the different colours. In many cases, the thickness of this layer is not enough to avoid mixing the glazes and, therefore, the glazes are mixed together. It might have the same role as penciling has in traditional illuminated manuscripts.

As mentioned before, *haft rang* technique has been usually attributed to an occidental technique which is called *cuerda seca*. This Spanish term literally means ‘dry cord’<sup>3</sup> and refers to a black line which delineates a design. This attribution is based on the fact that in both techniques a black line is used to keep separated different colours. However, *haft rang* technique is not technically very similar to that of *cuerda seca* (Pickett, 1997). The black line in Spanish *cuerda seca* is composed of manganese oxide and a fatty substance. This substance, due to its hydrophobic properties, keeps apart different glazes’ slurries, which have been immersed in the water (Lane, 1971; Caiger-Smith, 1973; Fehérvári, 1973; O’Kane, 1987; Blair and Bloom, 1994). Then, the fatty substance is burned off the glazes’ composition (Pérez-Arantegui *et al.*, 1999). Nevertheless, there is no concrete reason to accept that this fatty substance have been used in *haft rang* technique (O’Kane, 2011).

### **Terminology of *cuerda seca***

Baron Davillier, in the nineteenth century, described a Spanish technique which ‘looks like Italian sgraffito, but this technique is actually executed without the use of white glaze on the body’. Thereafter, Gestoso and Pérez in 1904, based on a document from the archives of the Cathedral of Seville, proposed the term ‘*cuerda seca*’ which was referred to describe the decorative technique. Although this term was not accepted by most scholars, the fact is that since then, it is used to describe the technique of polychrome glaze making (Fernández, 1988; Motos Guirao, 1994; Suárez, 2007; Zamora, 2007). In any case, Pérez and Gestoso attributed the invention of *cuerda seca* technique to the late fifteenth century, but the history of this technique, in fact, dates back to some centuries later (Martí, 1954). It is mentioned that the first published papers about this technique is in the catalogue that Drury and Frtnum have published in 1873 in London (Hernández, 1992). Translation of the term ‘*cuerda seca*’ from Spanish to other languages caused many misunderstanding. Perhaps everything would have been easier if, according to Aguado, instead of ‘*cuerda*’ the word ‘*línea*’ had been used, without adding the word ‘*seca*’ (Fernández, 1988). Thus, the term *cuerda seca* could be translated as ‘*a linea asciutta*’ (Buscaglia, 1992). In fact, the term *cuerda seca* was created due to the fact that ‘by means of a short taut cord’ would have recorded ‘deep grooves in the clay’ tile, on which, after firing, ‘they remained furrows represented by coloured the incision along the cord’ (Buscaglia, 1992).

### **Origin of *cuerda seca***

*Cuerda seca* has been shown to be produced in Mesopotamia before the Spanish production. Others have suggested that this technique existed before the Mesopotamian productions, from Pharaonic Egypt (Suárez, 2007) or some scholars have suggested that *cuerda seca* was transferred from Iran through the Tunisian coast to the Iberian Peninsula in eighth and ninth centuries (Buscaglia, 1992; Motos Guirao, 1994; Suárez, 2007; Zamora, 2007; Déléry, 2009). As a matter of fact, the Persian provenance of *cuerda seca* is probable since Islamic art in Omayyad and ‘Abbāsīd dynasties is configured based on the art of land occupied by Muslims especially Persian art (Martín *et al.*, 1999; Zamora, 2007). However, Fehérvári (2000) has suggested that *cuerda seca* had been an imitation of Fayyumi pottery which had been producing during Fatimid dynasty in Egypt. Anyhow, *cuerda seca* whether emerged in the Mohammedan Andalusia or arrived from the East, quickly copied or imitated from Spanish potters (Martí, 1954).

---

<sup>3</sup> O’Kane (2011) believes that this signification is misleading and suggests the idiomatic translation as ‘colourless line.’

*Production of cuerda seca in the Caliphate era*

On the contrary to those who believe that *cuerda seca* is an eastern invention, there are some scholars who believe that this technique was an invention of Hispanic Muslims and had been invented in Andalusia in the tenth century (Motos Guirao, 1994; Rodríguez, 2006; Gardner and Kleiner, 2010). Since Caliphate time in the tenth century, the pottery produced in Andalusia has been sometimes covered with glaze for waterproofing, prolong pottery's life, preventing rot and avoiding absorbance of its contents. Passing the time, this coverage became decorative and various techniques applied to ceramic glazes developed in Andalusia, one of which was called *cuerda seca* technique (Déléry, 2004).

The oldest Andalusian *cuerda seca* corresponds to the archaeological sites of Granada and Cordoba, two cities that became totally destroyed in 1010. We do not know if the excavated *cuerda seca* was locally produced or the result of trade with East (Suárez, 2007). On the other hand, Almeria has also been suggested as the origin of *cuerda seca* technique. No wonder, since Almeria was the main center of communication with East Caliphate (Suárez, 2007). Another possible area for producing *cuerda seca* in Alcala de Henares in the end of the Caliphate period is also suggested as the origin place of *cuerda seca*. There are many *cuerda seca* shreds in Castilian deposits, but without any evidence of workshop equipment to prove local manufacture of *cuerda seca* in this city (Suárez, 2007).

*Spanish cuerda seca in the first Taifa and Almoravid eras*

The unity of the Caliphate would allow rapid spread of *cuerda seca* in Taifa period in the eleventh century (Zamora, 2007). During this century, *cuerda seca* technique was very distinguishable in ceramic products in different types of Andalusian exports (Valdés Fernández, 1995). This period is characterised by the development of partial *cuerda seca* technique as well (Déléry, 2004). In this era, production sites were usually located near a strong local power, capital of Taifa, Lorca. It demonstrates the great variety of style and workmanship of the pieces found (Déléry, 2004). Moreover, according to the performed mineralogical analysis, during eleventh century the Andalusian cities in which *cuerda seca* was developed were Malaga and Almeria. Other locations that might have produced *cuerda seca* were Cadiz and Seville. Also, some pieces dated between eleventh and thirteenth centuries have been recovered in Mallorca. In addition, following the trade route to the East, some *cuerda seca* shreds in North Africa have been found. Most of the Taifa's *cuerda seca* productions are probably the products of local potters and many of them were exported outside borders (Suárez, 2007).

The remarkable development of *cuerda seca* is perceptible also in the twelfth century, with other types of closed forms, for liquids, or lids with walls converging curves and single round lip (Déléry, 2004). In fact, twelfth century is marked by the power of the Almoravids in which very rich and luxurious *cuerda seca* wares were produced. This luxury in *cuerda seca*, in addition to a change in financial wealth of the country, led to high technical level of *cuerda seca* production which was associated with a marine export (Déléry, 2004). Another point about the *cuerda seca* production in this period is that, during the reign of Almoravids, previous schemes in ceramic production were continued, but the ceramic industry was more functional than aesthetic (Añón, 2009-2010).

### *Almohad period*

If Taifa is characterised by urban and rural regional broadcasts of partial *cuerva seca*, Almohad era is characterised by a mass distribution of total *cuerva seca* and integration of an entire territory in the same culture. One problem in studying *cuerva seca* ceramic in Almohad period is to distinguish it from Almoravids *cuerva seca* because there is no real break between production of *cuerva seca* in Almoravids and beginning of Almohad era (Déléry, 2004). In this period, we include findings dated from the twelfth to thirteenth centuries. Laboratory experiments confirm that production of *cuerva seca* already existed at this time in Iberian Peninsula, and therefore these productions are not imported objects (Suárez, 2007). Generally, it is believed that the Almohad *cuerva seca* products are rough. Nonetheless, the fact is that these productions are not as rough as it is said about. It is basically accepted that the *cuerva seca* pottery continued to be produced some time in the Almohad period, especially in parts whose shape is linked to the architectural and ritual use (Déléry, 2004). Based on archaeological findings, Almeria, Malaga, Paterna (Suárez, 2007), Lorca (Déléry, 2004), and Seville (Glaire D. Anderson, 2007) are most important centers of the production of *cuerva seca* wares during the Almohad period.

### *Nasrid dynasty onwards*

During the Nasrid dynasty *cuerva seca* pottery was flourished in Malaga (Añón, 2009-2010) and *cuerva seca* shreds in Ceuta (Suárez, 2007) and Seville (Zamora, 2007) show the mastery skill of Nasrid potters in making *cuerva seca* dishes and tiles in Spain. In fact, the production of *cuerva seca* continued from the Nasrid era until the recent times. In historical documents it is indicated that Toledo was a major production center in the early nineteenth century and the second city in which *cuerva seca* has been produced is Seville. Nevertheless, Seville as the most important place of manufacturing *cuerva seca* in Ferdinand and Isabella times has been accepted by most researchers (Suárez, 2007).

### ***Cuerva seca* tiles**

As noted by most scholars, *cuerva seca* technique was first applied on the pieces of tableware and then on tiles. If in eleventh and twelfth centuries industry of tableware was flourished, fifteenth century is associated with development of *cuerva seca* tiles (Suárez, 2007). Between thirteenth to fifteenth century mosaic technique was dominated in revetment of architectural façades in Seville, but after fifteenth century *cuerva seca* technique, due to obtaining several colours in one individual tile, be economic and be fast and easy in designing, was privileged to mosaic technique (Buscaglia, 1992). Although during Almohad period glazed tiles were used on exterior architectural facades, it reached to a high peak in Nasrid period, especially in the interior places for decorating baseboards and floors (Suárez, 2007).

From the chronological point of view, *cuerva seca* production does not go beyond the first third of the sixteenth century. The decline is due to two main reasons: on one hand, the emergence of the technique of ‘*cuenca o arista*’ and the tiles called ‘*pisanos*’ for architectural decoration, and, secondly, to the abundant ceramic arrival import, which will eventually prevail in Spain, as in the rest of Europe, the Renaissance taste in production of ceramics (Suárez, 2007). Details of exportation and importation of *cuerva seca* products in different historic eras of Spain and Al-Andalus can be found in Déléry (2009). Here, we focus on the technological features of this style of polychrome glazed products.

### Technological features of *cuerda seca*

Gestoso is the first person who writes about technical development of this technique. He writes ‘the design is drawn on the fired body with manganese ink and a greasy substance. The slurry of glaze, once is painted on dry pottery’s body quickly absorbs the water and is settled down’ (Suárez, 2007). Surveying more about the technique of *cuerda seca*, it is suggested that in *cuerda seca* technique, different coloured glazes juxtapose on a vitrified glaze. Anyhow, the different colours were separated by a thin line of manganese compound which is not vitrified, achieving an effect similar to *cloisonné* in metal works (Zamora, 2007; Conesa, 2008). In fact, black lines (manganese oxide) in mixture with a fatty substance compose the design of a glazed decoration. Between the black lines, then, was filled by several coloured glazes separated by the black line (cord). Due to repelling character of the fat applied in the composition of black cord, the artist could apply different colour media between the cords easily. If the application of black cord was carried out correctly, a line (cord) with glassy properties, black and apparently baked (dry) was executed around coloured drawings and different coloured glazes were separated due to the dry cord (Palazón, 1990; Buscaglia, 1992; Motos Guirao, 1994; McQuade, 1999; Déléry, 2004; Rodríguez, 2006; Zamora, 2007; Añón, 2009-2010; Gardner and Kleiner, 2010). Afterwards, during firing process, the grease burns away and leaves a thin, sunken, and unglazed line between the slightly raised glazed surfaces (Turner, 1996; Berti, 1997).

Obviously, *cuerda seca* was an economic way to use, because vast surface can be covered with large tiles much quicker than they can with thousands of smaller mosaic tiles. However, when such tiles are used to sheathe curved surfaces, the ceramics must fire the tiles in the exact shape required. It means the *cuerda seca* tiles also have their own drawbacks. Because all glazes are fired at the same temperature, *cuerda seca* tiles are not as brilliant in colour as mosaic tiles and do not reflect light the way the more irregular surfaces of tile mosaics do. In fact, the preparation of the multicoloured tiles also requires greater care (Gardner and Kleiner, 2010). Scholars have distinguished two styles of making *cuerda seca*; *cuerda seca total* and *cuerda seca partial* (Motos Guirao, 1994; Zamora, 2007).

#### *Cuerda seca total*

*Cuerda seca total* was flourished in the Caliphate era and reached to a high level of quality in thirteenth century (Rodríguez, 2006). In total *cuerda seca*, whole the surface of the biscuit (an already fired body) is totally covered by glaze (Palazón, 1990; Zamora, 2007). Here, in fact, the second layer generally appears vitrified with honey-like colour (Palazón, 1990).

#### *Cuerda seca partial*

*Cuerda seca partial* is named by Gómez Moreno and presents partially glazed decoration as well as undecorated biscuit (Rodríguez, 2006). This type is also called false *cuerda seca* pottery, or welt ceramic, on which rough and porous part of pottery’s surface were designed by manganese oxide, and then, between the manganese oxide lines was filled with coloured frits. Generally, applying the frits was done without any respect to line limits. The difference in this method with the true *cuerda seca* is that large areas left undecorated and the natural colour of fired clay was exposed (Palazón, 1990; Motos Guirao, 1994; Zamora, 2007; Añón, 2009-2010). In fact, in *cuerda seca partial* glazed layer is replaced by a grout or very fine slip which gives very well-fired appearance to pottery (Palazón, 1990).

In the ceramic workshops of Seville during eleventh century, potteries were made in  *cuerda seca partial* combined with stamped and incised decoration. Contemporarily, the pottery of Toledo shows a  *cuerda seca partial* technique poorer, in which, only diluted manganese in water was used to draw the picture, was applied to raw clay, reduced the colour to green and honey-like and decorations were simplified (Zamora, 2007).

#### *Incised cuerda seca*

A modified form of the  *cuerda seca* technique consists of imprinting a design in the soft clay with a mould. Then, when the tile has been fired once, the incised lines of the design were filled with the greasy substance. This is a particularly labor-saving device as  *cuerda seca* tiles have complex geometrical Moorish patterns that would be difficult to draw free-hand (Turner, 1996). In this way, the lines guide the designer to find the proper places for painting the glaze slurry. Pressure on the wet clay was sometimes quite enough to avoid any usage of the fat in the composition of black dry cord material (Buscaglia, 1992).

#### *Firing process*

Traditionally, it is confirmed that for achieving a  *cuerda seca* decoration, two oxidant firing process are necessary (Motos Guirao, 1994; Zamora, 2007). The first firing belongs to biscuit firing. Thereafter, the tile is engobed by white clay together with a line of manganese oxide mixed with fat. Then, the interior motifs were generally filled with green and brown glazes. Afterwards, a single firing was applied to fix the colours and matt dark colour of manganese oxide (Martí, 1954; Berti, 1997). By second firing, colour is placed between a groove and a ‘cuerda’ (cord) or uncoloured indent (Martí, 1954). Anyhow, before this system of making  *cuerda seca*, at least in Taifa’s era,  *cuerda seca* was fabricated with one single firing process, by applying frits on raw clay body (Motos Guirao, 1994). On the other hand,  *cuerda seca* tiles need to be stacked horizontally for firing to prevent the glazes from running out of their delineated areas (Turner, 1996).



## Chapter Two: Studied area and the samples

Most of edifices built in the Safavid period have not survived. Many were destroyed, especially during the Afghan conquest of Isfahan in 1722. Others were neglected and left to be demolished, or destroyed by earthquakes. Many of them which survived have been altered in their outward appearance by structural changes (Kleiss, 1993). Hence, it is quite difficult to track Safavid art of tile making in the architectural facades. In this chapter, the main aim is to provide an overview about the samples which have been taken from different Safavid sites. To do so, the main centers of Safavid tilework are firstly introduced and, second, the monuments from which the samples have been collected will be briefly described.

### *Ardabil*

As it is described in the first chapter, the Safavids initiated to rule Iran from Azerbaijan. However, during the first decades of their ruling, The Safavids were mainly involved in seizing lands and developing their supremacy. So that, their first capital was mainly a military state, where the Safavid power was trying to establish one of the most important periods of Persian history. Although the first Safavid Shah, Ismāīl I, erected some edifices decorated with Timurid traditions, during the wars between Safavids and Ottomans these edifices were either demolished or severely damaged. While there is no sample reported from Safavid era in Tabrīz, a collection of Safavid tile working is available in Ardabil, near Tabrīz, from where Safavid kings upraised. Safavid kings were trying to tribute their chieftain, Shaykh Ṣafī al-Dīn Ardabīlī; therefore, the shrine of Shaykh Ṣafī al-Dīn was decorated several times. Among the decorations, mosaic, *haft rang*, and gilded tiles are glomming in the Persian art (Sarre, 1924). The art of tile making in this tomb demonstrates a mastery of Persian tile-makers. The shrine survives today as a complex of buildings arranged around a garden and a paved courtyard. The facade is decorated with glazed polychrome tile mosaic, which has been much repaired and restored often with more enthusiasm than accuracy (Figure



2.1). Many of the inscriptions have been changed in a ‘restoration’ process. The interior decorations, dated to the reign of Shah ‘Abbās I, consist mostly of *haft rang* and gilded tiles (Weaver, 1986). However, Ardabil cannot be mentioned as a center of tile making since no other Safavid monuments with tile revetments is reported in this region.

*Figure 2.1 Details of inappropriate restorations on haft rang tiles of Shaykh Ṣafī-al-Dīn’s shrine in Ardabil (photo: the author)*

### Qazvīn

Qazvīn, unlike Tabrīz, was evolved in the patronage of Safavid rulers, and the examples of authentic Safavid architecture and architectural decoration can be found in this city. This second capital of the Safavids, founded by Shah Ṭahmāsp I, was less in trouble of wars, and many constructions from the Safavid period are known although they also have often been changed by careless restoration work or diverted from their original purpose (DeGeorge and Porter, 2002). However, as mentioned in the first chapter, Shah Ṭahmāsp I's interest in arts was mainly dedicated to illumination and art of the books. Thus, the art of was not evolved sufficiently in Qazvīn. Anyhow, among the Safavid edifices in this city, Masjid-i Jāme' of Qazvīn and Chihil Sutūn palace are the most important ones in where the Safavid tile working is applied (Figure 2.2). In Chihil Sutūn, however, the Safavid art is basically focused on mural painting. The coloured *haft rang* tiles found in Chihil Sutūn belong to the nineteenth century and just a few shreds of Safavids tiles are found in this palace. These pieces convey an impression of the type and quality of ceramic decoration on the walls of the palace pavilion in the early Safavid period (Kleiss, 1990).



Figure 2.2 Details of *haft rang* tiles in a spandrel at Masjid-i Jāme' of Qazvīn (photo: the author)

Qazvīn (36.2667° N, 50.0000° E) is situated in the interface of northern margin of Central Iran and western Alborz zones. In other words, northern heights of this province belong to southern parts of Alborz range and largest territory of this province that is Qazvīn plain and southern heights belong to Central Iran zone. The boundary between these two zones corresponds to north Qazvīn thrust zone. The exact boundary of these zones cannot be correctly defined; therefore, it is preferred to assign the whole province to Alborz-Central Iran zones. According to geological maps of this district and recent geological studies (Asiabanha *et al.*, 2009), this area is covered with clays deposits and volcanic tuffs (Annells *et al.*, 1985) (Figure 3.2).

### Mashhad

The establishment of Shiism in the Safavid era, as the national doctrine, also, encouraged increased respect of the tombs of saints in Mashhad, such as the great Shrine and Khāja Rabī's tomb (Hillenbrand, 1986). The most important ensemble in Mashhad is the holy shrine of Imam Reza, in which Safavid tileworks, together with the tileworks of other historic periods, represent proficiency of glaze tiles in Iranian culture. Except this shrine, the Safavids tried to establish other edifices such as *madrasas* and *imamzadas* to broadcast their Shiite beliefs. 'Abbās-qulī *madrasa* and Muṣallā of Mashhad are good examples of these scholastic edifices. As well as mosaic tiles, *haft rang* tilework in 'Abbās qulī shows specific designs and patterns of Safavid art (Figure 2.3). According to the geological maps of Mashhad, this city is located at northeast of Iran (36°18'N, 59°36'E) where clay deposits are found close to acidic and basic parent rocks (Jalilian *et al.*, 1986) (Figure 3.2).



Figure 2.3 Detail of Safavid *haft rang* tiles in a spandrel of ‘Abbās-qulī madrasa (photo: the author)

### *Māzandarān*

Shah ‘Abbās often spent winters in Māzandarān, north of Iran, where he had the resort towns of Ashraf and Faraḥābād constructed as part of a larger project designed to develop the region (Matthee, 2008). In fact, Māzandarān gained a particular importance during the reign of the Shah ‘Abbās I, where he had created various gardens. Iskandar Munshī, the royal chronicler of Safavid court, among the works of Shah ‘Abbās in Māzandarān mentions the famous gardens at Ashraf, ‘Abbāsābād, and Faraḥābād (Alemi, 1996). Near the Caspian Sea, Faraḥābād, situated on the coast and now in ruins, may be reconstructed in its outward form with the help of nineteenth-century drawings, like those of the Jahān-namā palace (Kleiss, 1993). Faraḥābād was built as a pleasure resort for Shah ‘Abbās I, where he eventually died there (Kleiss, 1999). On the other hand, according to Fraser, who visited Ashraf in the early nineteenth century, five Safavid gardens and their buildings seem to have been surrounded by one wall (Ehlers, 1989). Shah ‘Abbās’s constructions in Māzandarān included many bridges (Blair, 1989). Almost certainly all these palaces were decorated with polychrome *haft rang* tiles however few examples of *haft rang* tiles have survived due to high relative humidity of Māzandarān region such as those found in Chishma Imārat palace (Figure 2.4 left) and ‘Abbāsābād palace in Bihsahr (Figure 2.4 right). The only Safavid monument whose *haft rang* tiles have been survived is Mīr-Buzurg tomb in Āmul (Figure 2.5).

The major part of Māzandarān province is within the northern flanks of Alborz range. They are quite different from other parts of Alborz range. They can be compared with paratethyan marine rocks. Several drilling in Plio-Quaternary sediments have proved that these sediments belong to Caspian basin which has left the ancient coastal plain due to subsidence of the floor. This zone is also covered with spar acidic rocks (Ghandchi *et al.*, 1991; Hossieni and Afsharianzadeh, 1991) (Figure 3.2).



Figure 2.4(left) Few monochrome cut-tiles still attached on a vault of Chishma Imārat of Bihshahr and (right) severely deteriorated rectangular haft rang pieces closed by monochrome glazes at 'Abbāsābād palace in Bihshahr (photo: the author)



Figure 2.5 Haft rang tiled dado of Mīr-Buzurg tomb in Āmul (photo: the author)

### Isfahan

No city received Safavid attention as Isfahan did. Khurāsān and Azerbaijan are neglected and even the earlier Safavid capitals of Tabrīz and Qazvīn saw little major construction. In Iran, only Isfahan, offer the chance to study numerous examples of ambitious Safavid work (Hillenbrand, 1986). Isfahan was in focus of Shah Ismāīl I even as he set out to conquer other parts of the Iranian plateau. Stopping at the city from time to time, he is said to have been keen to restore the city to its pre-Mongol significance and in this regard paid particular attention to the role and function of its squares. Then, Shah Ṭahmāsb I, who was born in a suburb of Isfahan in 1514, added several buildings, mostly mosques, to the city. He incorporated Isfahan into the royal domain in 1534. Although Isfahan made a great contribution to Ṭahmāsb I during its severe resistance, it does not seem to have received any royal favors in return (Haneda and Matthee, 2006).

Shah ‘Abbās I’s attention was focused on the city of Isfahan to where he transferred his capital. “Isfahan could not have been conceived and executed except by kings and architects who spent their days and nights listening to the *Thousand and One Nights*,” wrote Gobineau (Porter, 1995). The focus of Shah ‘Abbās I urban design was a new commercial and administrative area, centering on a magnificent central square known as the *Maydān-i Naqsh-i Jahān*, surrounded by a royal palace, beautiful mosques, and numerous shops. Isfahan at this time became a large, cosmopolitan, and attractive city mixing people of many nationalities who congregated to visit the city (Matthee, 2008). Isfahan was home to many craftsmen who were talented in the decoration of buildings such as plaster molders, mirror makers, and tile-makers (Borjian, 2007). In the course of centuries of urbanization, Isfahan gained a large number of significant monuments. According to the French traveler, Jean Chardin, in the late seventeenth century Isfahan had about 162 mosques, 48 theological colleges (*madrasa*), 1802 caravansaries, and 273 bathhouses (Babaie and Haug, 2007). Isfahan houses the most prominent samples of the Safavid architecture, all constructed in the years after Shah ‘Abbās I permanently moved the capital there in 1598: the *Masjid-i Jāme’-i ‘Abbāsī*, *Masjid-i Imāmī*, *Luṭfallāh Mosque*, and the *Royal Palace of ‘Alī-Qāpū* are only the most important samples (Savory, 1980). The majority of these buildings were extensively decorated with *haft rang* tiles from which *Masjid-i Jāme’-i ‘Abbāsī*, *‘Alī-Qāpū* palace, and *Luṭfallāh Mosque* represent highly elaborated examples of the Safavid art of tilework. The religious buildings of the other religions also received Safavid attentions were gorgeously decorated with various architectural ornaments including tileworks form which *Vānk Cathedral* and *Bethlehem Church* are the most important ones (Figure 2.6).



Figure 2.6(left) *Vast haft rang* tile revetment on the *dado* of Bethlehem Church (photo: courtesy of A.H. Karimy) and (right) in the entrance of Lutfallāh Mosque (photo: the author)

Kirmān was another city that was economically flourished during Safavid era and transformed from a military barracks to an evolved city where many edifices were erected and as a result of Safavid art, many of them were decorated with typical Safavid revetments. Although Kirmān has been one of the most important centres of pottery making in Safavid era (Golombek, 2003; Mason, 2003), Safavid tile-making did not evolve sufficiently in the region as Isfahan did. The only examples of Safavid tileworking can be found in *Ganj-‘Alī Khān Complex* and *Masjid-i Jāme’* of Kirmān. Tileworks of *Ganj-‘Alī Khān*

complex's edifices are mainly based on mosaic and underglaze tileworks. A few examples of *haft rang* tiles in Ganj-ʿAlī Khān complex are dated back to the nineteenth century (Bastani Parizi, 2000; Javādī, 2008). *Haft rang* tiles in Masjid-i Jāmeʿ, which are erected in the twelve and fourteenth centuries whose architectural facades were restored in Safavid, Qajar, and Pahlavi eras. Safavid restorations, however, pertain a replacement of some tileworks among which *haft rang* tiles have also ornamented exterior revetments. These *haft rang* tile panels remind the precedent polychrome *haft rang* tiles in Isfahan (Golombeck, 2003). From a geological standpoint, Isfahan is located in 32.6729° N, 51.6666° E and covered mostly with basic and less acidic rocks (Zahedi *et al.*, 1987) (Figure 3.2).

### Introduction to the samples

Considering the aforementioned remarks, Isfahan, Mashhad, Māzandarān, and Qazvīn were selected as the areas from which samples were collected. Ardabīl and Kirmān were discarded due to the scarcity of authentic Safavid samples from one side and, on the other hand, inaccessibility to samples. Samples were obtained from fragmentary tile shreds in various types of artistic style and visual characteristics. All the samples are dated to the seventeenth century, the period of flourishing Safavid arts and the boom of tile-making craft in Iran. Forty three samples were subjected to our analytical studies: ten samples from Masjid-i Jāmeʿ-i ʿAbbāsī, two samples from Bethlehem Church, seven samples from ʿĀli-Qāpū Palace, seven samples from Safavid tiles preserved in Iṣfahānak collection storage of the Iran's Cultural Heritage, Handicrafts and Tourism Organization (ICHHTO) in Isfahan, seven samples from Safavid *haft rang* tiles preserved in the collection storage of the ICHHTO in Masjid-i Jāmeʿ of Isfahan (all in Isfahan), two samples from *madrasa* of ʿAbbās-qulī Khān, one sample from Muṣallā complex (all in Mashhad), three samples from Chishma Imārat palace in Bihshahr, one sample from Mīr-Buzurg tomb in Āmul (all in Māzandarān province), and three samples from Masjid-i Jāmeʿ of Qazvīn. Due to limitations to have access to samples on the architectural facades and scarcity of authentic samples, the samples were mostly collected from the fragmentary and broken tiles according to their esthetic and visual conditions. In the case of the samples which were detached from the architectural facades, however, the sampling was randomly carried out in a way that all the variety of colours and bodies were included in the selected samples. In fact, limited numbers of tiles pushed us to select random sampling as the main strategy of our sampling process. It has the advantage of making the probability calculations easy to carry out (Reedy and Reedy, 1988). In fact, random sampling, while it does not provide a guarantee, does give us our best chance at a representative sample (Mueller, 1974; Drennan, 2009). The samples were then labeled according to the city and the site from which they were obtained. The first letter in the samples' labels was referred to the city, the second letter to the site of sampling, and the numerical part of the labels shows how many samples were collected from each site. In the forthcoming photos of the samples, red circles show the place where UV-Vis measurements were carried out (see0 Chapter Five, 0p. 57). Here, the details of each site of sampling and samples are provided.

#### *Masjid-i Jāmeʿ-i ʿAbbāsī*

Known also as Masjid-i Jadīd-i ʿAbbāsī, Masjid-i Shāh or Masjid-i Imām after the Revolution of 1978-1979, Shah ʿAbbās I constructed to mark the beginning of a new era of Shiite kingship. This mosque marked the peak of building campaigns that transformed Isfahan into the new Safavid capital city. Built between 1611 and 1630-1631, the massive mosque (some 19,000 square meters in area) was positioned at the southern end of the Maydān-i Naqsh-i Jahān (Babaie and Haug, 2007). The names of two architects

are associated with this mosque; that is, Ustād ‘Alī Akbar Biyg Işfahānī as the mosque’s engineer and architect, whose name appears in the same inscription as that of the royal supervisor, and Ustād Badī‘ al-Zamān Tūnī Yazdī, whose job was to acquire the land and construction resources (Babaie and Haug, 2007). The mosque complex was virtually completed by the end of Shah ‘Abbās I’s reign although additions and repairs continued to be made until 1667 (Haneda and Matthee, 2006).

This mosque’s highly covered with turquoise and blue glazed tiles remain one of the world’s most charming sights. In Masjid-i Jāme‘-i ‘Abbāsī all the outer facades display great inventiveness in tile decoration, with a predilection for *haft rang* polychrome tilework (Figure 1.2). The decorative motifs inside the mosque exhibit a diversity of pattern and design with large panels of polychrome tiles with cut-tile mosaic and *haft rang*. Most of the decor relies on floral arabesque patterns, leaf scrolls, and bouquets. Other motifs are more surprising, incorporating living creatures, such as birds, gazelles, ibex, and panthers (Degeorge and Porter, 2002). Blue is the predominant colour but in this mosque, the blue is contrasted with a brilliant yellow (Porter, 1995). Almost all the vast surfaces of this mosque are decorated in the *haft rang* technique (Babaie and Haug, 2007).

However, most of the tileworks of Masjid-i Jāme‘-i ‘Abbāsī was replaced in the 1930s based on the revetment that remained in situ (Blunt, 1966; Babaie and Haug, 2007). The sampling, however, was carried out on the original fragmentary tiles found in the masques rather than the tiles attached on the architectural façades because, first, the sampling from the tiles placed on high altitude was not possible and, second, the originality of the already attached tiles were to some extent on question. Thus, the original and authenticated Safavid fragmentary tiles were preferred. Figure 2.7 shows the collected samples appearance together with their labels.

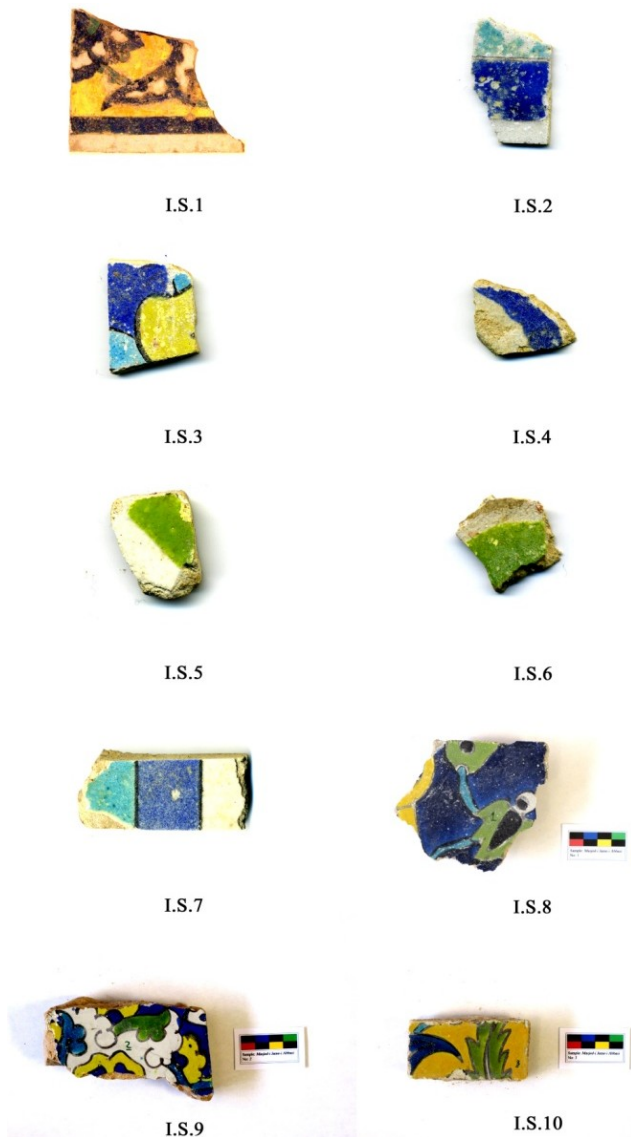


Figure 2.7 Ten collected samples of Masjid-i Jāme‘-i ‘Abbāsī

### ‘Ālī-Qāpū palace

The term palace is frequently used of what we call today the ‘Ālī-Qāpū, the name being reserved for the actual entrance gateway to the palace, which was also a sanctuary (Stevens, 1974). Recent restorations of the ‘Ālī-Qāpū have revealed that it was built in several stages (Soucek, 1985). Unlike many who believe that the initial core of the ‘Ālī-Qāpū was established before Shah ‘Abbās I (Pūrādīrī, 2010), Galdieri

(1974, 1979) suggests that the construction of 'Ālī-Qāpū began by Shah 'Abbās I. The first amongst the urban Safavid palaces in Isfahan was the 'Ālī-Qāpū. Its realisation synchronised with that of the Maydān-i Naqsh-i Jahān project (Babaie and Haug, 2007). From the high terrace of the 'Ālī-Qāpū palace, overlooking the royal square could be achieved (DeGeorge and Porter, 2002). At 'Ālī-Qāpū the open loggia is supported by wooden columns standing above the gateway's monumental ground floor. In contrast to the richly decorated interiors, the outer walls were sparingly decorated (Kleiss, 1993). The outer decorations are generally *haft rang* tileworks which cover arches and portico of the palaces. In the palaces of Isfahan, *haft rang* tiles constitute another of stylistic group of Safavid tiles. These tiles generally form pictures, each tile painted with one element of an overall scene. The subject matter of these tile panels with their scenes of hunting is similar to that of the murals which also adorned the palaces (Porter, 1995). The samples studied in this thesis were obtained from already detached Safavid tiles rather than the tiles in place (Figure 2.8).



Figure 2.8 Seven collected samples of 'Ālī-Qāpū

### Bethlehem Church

A new stylistic group of Safavid tiles is to be found in New Julfa, the Armenian quarter of Isfahan. Shah 'Abbās moved the community in 1604 from old Julfa in Azerbaijan to his capital, needing them for their skills and trading contacts. The churches, of which thirteen survive, were mostly built in the first half of the seventeenth century and in a number of them there are remarkable *haft rang* tile panels. The designs are a fascinating mixture of traditional floral designs with occasional figures (Carswell, 1968; Porter, 1995) (Figure 2.6 left). In the Armenian context the *haft rang* tiles of the walls and pillars not only show inscriptions and geometrical and floral patterns, but their biblical scenes are populated with animals, angels, and mythical creatures such as the phoenix and dragons (Carswell, 1968).

Bethlehem church is one of the thirteen remained Armenian churches in New Julfa, Isfahan. After Vānk cathedral, this church has a significant importance among the Armenian churches in Isfahan. Bethlehem church was built by Khāja Pitrus Valījānīyān, the famous Armenian dealer, in 1628, contemporary with Shah 'Abbās I's reign (der Hovhanian, 2000; Ārākīlīyān, 2001; Haghazarian, 2006). Nowadays, this church is no longer used in its religious context and its touristic and artistic view has more importance. The western exterior portico of this church shows a combination of brick and tilework however internal dados of the church is entirely covered by *haft rang* tiles representing both floral designs and animal figures. These works can be considered as a refined compromise of Iranian and Armenian arts

(Karimy and Holakooei, 2009). For sampling, however, the samples were collected from the fragmentary original Safavid tiles found in the church. Figure 2.9 demonstrates the samples and their labels.



Figure 2.9 Two collected samples of Bethlehem Church

*Other samples of Isfahan*

Other than the mentioned Safavid monuments, there are two collection storages in Isfahan (Işfahānak collection storage in southeast Isfahan and ICHHTO collection storage in Masjid-i Jāme' of Isfahan) where Safavid *haft rang* tiles are preserved. Unfortunately, it is not clear that where they are detached from but it is quite clear that they are collected from the Safavid monuments that were under restoration of Istituto Italiano per il Medio ed Estremo Oriente (IsMEO) during 1960s and 1970s. The designs and patterns used to decorate these tiles are apparently those were being in use during the seventeenth century. For sampling, seven authenticated Safavid tiles preserved in Işfahānak storage and seven original Safavid *haft rang* tiles preserved in the collection storage of the ICHHTO in Masjid-i Jāme' of Isfahan were collected. These samples as well as their labels are represented in Figure 2.10.



Figure 2.10 Seven samples of Işfahānak (I.E. serie) and seven samples of ICHHTO collection storages (I.C. serie)

*Masjid-i Jāme‘ of Qazvīn*

The Masjid-i Jāme‘ of Qazvīn is considered among the oldest mosques in Iran. This mosque is originally built on a Sassanid fire temple; however, it was subsequently developed over several different periods of Safavid and Qajar. Masjid-i Jāme‘ of Qazvīn is constructed of brick, which is covered to some extent with tiles and tiled inscriptions in various areas. The main prayer hall is the most ornamented part of the mosque. The upper part of the walls in the southern and western iwans is ornamented in different floral patterns of polychrome *haft rang* tiles (Godard, 1965). The southern iwan, built by the Shah ‘Abbās II in 1658; however, the western one built by the Safavid ruler Sulaymān in 1670 (Nuṣrafī, 2001). In the northern iwan some interventions were carried out Shah Tahmāsp (Pope, 1965). In this mosque nineteenth century *haft rang* tiles have also been extensively used to decorate the facades nevertheless the samples of this mosque (Figure 2.11) were collected from original fragmentary Safavid tiles which were under restoration.

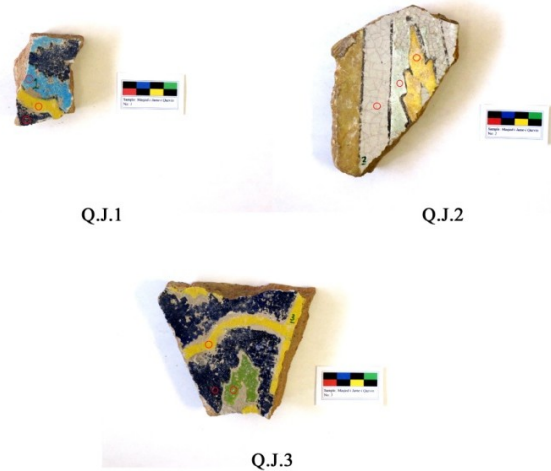


Figure 2.11 Three *haft rang* samples of Masjid-i Jāme‘ of Qazvīn

*Muṣallā in Mashhad*

Muṣallā of Mashhad, according to a survived mosaic tile inscription inside the mihrab, written by Muhammad Ḥusayn Mashhadī, was erected in Shah Sulaymān’s era in the seventeenth century (1877 AD) (Pope *et al.*, 1964). This monument is has a high porch and two porticos on both sides. The building is decorated with glazed *haft rang* and mosaic tiles. Today, the majority of Safavid tiles are either replaced

by recent interventions carried out during the nineteenth century or missing in the monument. Therefore, it was difficult to find original Safavid tile shreds between piles of detached tiles. Hence, the only *haft rang* tile which was to some extent similar to those Safavid tiles was selected (Figure 2.12).



Figure 2.12 The single sample of Muṣallā of Mashhad

*‘Abbās-qulī Khān madrasa in Mashhad*

A mosaic tile inscription of ‘Abbās-qoli *madrasa*, written by Mohammad Raḥīm, shows that this edifice is constructed in 1666-1667 during Shah Sulaymān era (Hājī-qāsimī, 2000). ‘Abbās-qulī Khān was the governor of Herat, who constructed and dedicated this *madrasa* to scholastic ideology of Shiite ideology (Navā’ī and Malikzāda, 2005). In this *madrasa*, niches and arches are decorated by Safavid cut mosaic and *haft rang* tiles (‘Oṭaridī, 2002). The *haft rang* tiles are simply composed of brown, turquoise, black,

blue, yellow, and white as the ground glaze. Two shreds of these tiles were detached and subjected to our subsequent analytical studies (Figure 2.13).



Figure 2.13 Two samples of 'Abbās-qulī Khān madrasa in Mashhad

*Chishma Imārat in Bihshahr, Māzandarān*

Chishma Imārat palace is a seventeenth Safavid palace placed in Bihshahr city, near Sārī in Māzandarān province. Among the Safavid pavilion in the northern Iran, only this pavilion and 'Abbāsābād show the use of *haft rang* tiles for decoration in place. Historical references reveal that other Safavid pavilions, such as that of the Bāq-i Šāhib Zamān, were only decorated with wall paintings. Considering the contemporaneous Safavid precedent of the palace gardens and their pavilions in Isfahan, it is likely that the other pavilions were also ornamented with polychrome *haft rang* tiles however the evidences of the use of this kind of ornament are not easy to find. Today, no single *haft rang* tile can be found pasted on the architectural façades of Chishma Imārat palace. Some fragmentary polychrome *haft rang* tiles, however, are survived in the place which kept in a poor preservation state. Due to the high degree of relative humidity of the region, the tiles were severely deteriorated. Three samples were nonetheless selected from less damaged shreds (Figure 2.14).

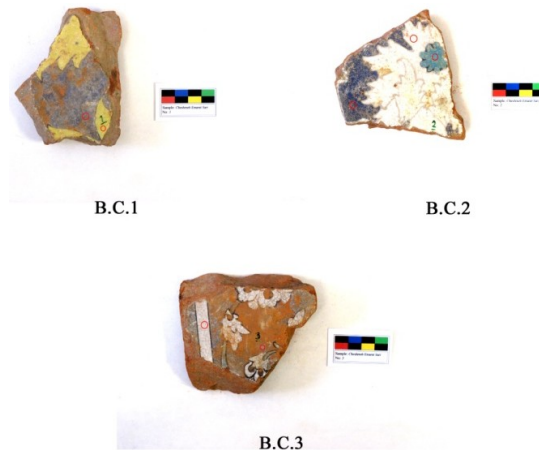


Figure 2.14 Three fragmentary *haft rang* tiles collected as samples from Chishma Imārat palace

*Mīr-Buzurg tomb in Āmul, Māzandarān*

This edifice is located in Āmul city, Māzandarān province, and is in fact an elaborated shrine complex is sometime called the Mashhad-i Mīr-Buzurg, a centrally domed mausoleum with side chambers and prayer

halls. Built under Shah ‘Abbās I, the tomb has a wooden cenotaph dated 1623 and many fine, polychrome *haft rang* tiles covering the interior (Blair, 1989). The variety of glazes colours on *haft rang* tiles can be found on the dado of these building (Figure 2.5). A tile with all variety of colours used in the Safavid *haft rang* tiles (Figure 2.15) was detached from the dado and subjected to the subsequent analytical studies. Prior to close this section, the sites from which the samples were collected are marked in Figure 2.16 showing their geographical position and their relation in terms of commercial trades.



A.M.1

Figure 2.15 The single *haft rang* tile detached from the dado of Mīr-Buzurg tomb



Figure 2.16 The area under study with Safavid *haft rang* tile on Iran’s today map

### Preliminary microscopic observations towards the analytical studies

Prior to any analytical examination on the selected samples, surface characteristics of the samples were observed under an OPTIKA B-600POL-I polarised microscope. These observations were important because they could program the analytical studies carried out throughout this thesis. Moreover, cross sections of the samples should have necessarily been obtained in order to have an overall image from various layers of the samples. As Figure 2.17 left shows, different colours have been separated with a black line in sample I.S.7. Having a look at the cross section of the sample (Figure 2.17 right), it can be seen that each single *haft rang* tile comprises of the following parts, respectively from down to the surface of the tile: a) a terracotta body, b) an intermediate layer between upper layer and the body, c) a white substrate glaze, and d) coloured glazes. Moreover, the black line seen in the surface observations is also present in the cross section showing an intermediate barrier to keep separated different coloured glazes on top. Figure 2.18 shows schematically the relation of these layers one respect another.

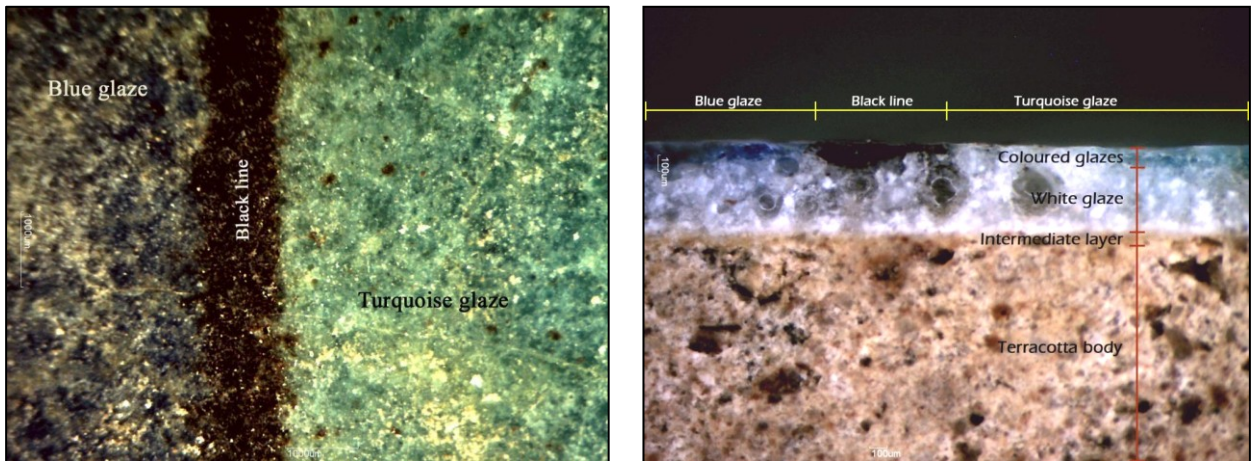


Figure 2.17 (left) Surface observation on sample I.S.7 and (right) the cross section of the same point of the sample

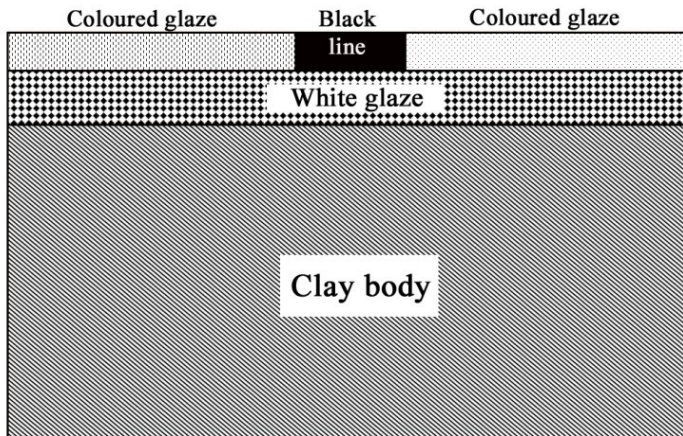


Figure 2.18 Schematic stratigraphy from different layers of haft rang tiles

The subsequent chapters of the thesis are focused on each part of the tiles showed in Figure 2.18. We will try, first of all, to address the question of provenance of tiles by means of WDXRF analyses and petrographic observations. Thereafter, the firing temperature of the bodies will be estimated by XRD analyses. The rest of the analytical studies will be focused on the glazed layers. To do so, UV-Vis measurements were firstly performed on the both white and the coloured glazes. Micro-Raman spectroscopy was however concentrated mainly on the opacifiers and undissolved colourants in the glazes although it was also used to study to distinguish lead-based and alkali glazes. EDS microanalyses and SEM observations, on the other hand, were used to obtain the chemical composition of the glazes.



## Chapter Three: WDXRF quantitative analysis and the question of the provenance

### 3.1 Introduction

One of the most important issues concerning *haft rang* tiles is their provenance which has always been considered as a controversial subject. In fact, scientific data regarding to *haft rang* tiles is rare and the problem of attributing the Safavid *haft rang* tiles to a special centre of tile-making seems to be still unsolved. It can be due to the fact that tileworks might have been manufactured in a region and have been exported to other regions in order to be applied in architectural facades (Mason, 2003). To determine the origin of unknown products, a numerous provenance studies derived from quantitative elemental analysis, such as Neutron Activation Analysis (NAA) (Buko, 1984; Neff *et al.*, 1988; Cogswell *et al.*, 1996, 1998; Mainfort *et al.*, 1997; Arnold *et al.*, 1999, 2000; García-Heras *et al.*, 2001; Neff, 2002; Glascock *et al.*, 2004; Ben-Shlomo, 2008; Descantes *et al.*, 2008; Iñáñez *et al.*, 2008; Partha Sarathi *et al.*, 2008), Particle-Induced X-ray Emission (PIXE) (Zucchiatti *et al.*, 1998, 2003; Ruvalcaba-Sil *et al.*, 1999; Robertson *et al.*, 2002), and various techniques of atomic spectroscopy and spectrometry (ICP-MS, LA-ICP-MS, ICP-AES, *etc.*) (Mallory-Greenough *et al.*, 1998; Kennett *et al.*, 2002; Robertson *et al.*, 2002; Neff, 2003; Zucchiatti *et al.*, 2003; Klein *et al.*, 2004; Li *et al.*, 2005; Tiequan *et al.*, 2010) have been carried out on ceramic bodies. These studies have always been accompanied by statistical methods of data handling to attribute one type of ceramic product to a specific zone. These methods are based on the fact that the quantity of major, minor, and trace elements provides a compositional fingerprint to group together tiles' bodies and to distinguish groups of body made from different raw materials (Tite, 2008). In the present work, wavelength dispersive x-ray fluorescence (WDXRF) is, instead of other methods of quantitative elemental analysis, used to discriminate different workshops and materials of *haft rang* tile-making over the seventeenth century.

A well-established method of quantitative element analysis is x-ray fluorescence (XRF) analysis, which is based on the ionization of atoms of a material being investigated by an energetic beam of primary x-rays (Janssens, 2005). In fact, XRF spectrometry is based on the principle that primary x-rays are incident upon a sample and create inner shell vacancies, and consequently, the unstable ionised atom. These vacancies de-excite by the production of a secondary x-ray whose energy is characteristic of the elements present in the sample. Some of these characteristic x-rays escape from the sample and are counted and their energies measured. Each element produces x-rays with a unique set of energies. Comparison of these energies with known values for each element allows the elements present in the sample to be identified and quantified (Pollard *et al.*, 2007; Artioli, 2010). The secondary x-rays can be analysed in wavelength and intensity and can provide a completely non-destructive method of quantitative chemical analysis (Hall, 1970). XRF analysis allows the concentrations of most elements of the periodic table to be determined. Accurate quantitative analysis may be difficult because XRF suffers from matrix

effects. The concentrations measured with XRF reflect the composition of the outer layers of the material. However, making powder and pressing powder pellets can reduce from the errors and conduct us to more accurate results (Moens *et al.*, 2000). XRF analysis have become very important for classifying the origin of materials because it can simultaneously determine major, minor and several trace elements in the same sample at very low concentrations (LaBrecque *et al.*, 1998). WDXRF is a widely diffused easy and fast to use analytical tool, which is able to measure every element in the periodic table heavier than lithium, with the required accuracy and sensitivity (Falcone *et al.*, 2002). WDXRF systems in the laboratory provide for high-resolution measurements with detection limits down to the ppm level for ideal samples (Stuart, 2007; Artioli, 2010). In WDXRF spectrometry, the sample is irradiated in a vacuum chamber by the primary x-rays of an X-ray source. The secondary x-ray radiation resulting from the sample consists of different wavelengths originating from different elements present in the sample. The secondary radiation is guided through a collimator that allows only x-rays with parallel propagation to pass. The x-rays reach a Bragg crystal where they are reflected according to Bragg's law. In WDXRF, the rotation of the crystal makes it possible to detect x-rays of different wavelength. The radiation selected by the Bragg reflector will pass a second collimator before it reaches a detector. The signal may be converted into a spectrum, or if only some elements are of interest, the intensities of the appropriate wavelengths are recorded (Moens *et al.*, 2000; Pollard *et al.*, 2007).

XRF is a well-established method of quantitative elemental analysis which has been extensively used in archaeological studies (Moens *et al.*, 2000; Janssens, 2005; Pollard *et al.*, 2007). Amongst different types of XRF instrumentation (EDXRF, TXRF, and WDXRF), EDXRF (Energy Dispersive X-ray Fluorescence) have mostly been emphasised in analysing archaeological ceramics (Yap and Tang, 1984a, 1984b; Yap, 1986, 1989; Molera *et al.*, 1996; Yu and Miao, 1996a, 1996b, 1999; Hall *et al.*, 1999; Leung and Luo, 2000; Yu, 2000; Sajo Bohus *et al.*, 2005). However, WDXRF, apart from few exceptions (Falcone *et al.*, 2000; Guilherme *et al.*, 2009; Kibaroglu *et al.*, 2009), has received less attention in investigating archaeological ceramic materials so far despite of the higher resolution which it can offer in comparison with EDXRF (Moens *et al.*, 2000). De Vleeschouwer *et al.* (2011) have recently used WDXRF to analyse small quantities of ceramic samples showing its high accuracy in quantitative analyses of ceramic bodies. We do not go further in theory and instrumentation of WDXRF. Readers may be referred to appropriate literature to find the proper materials (Moens *et al.*, 2000; Janssens, 2005; Artioli, 2010). In our studies, WDXRF was used to determine major, minor, and trace elements of the Safavid *haft rang* tiles' bodies in order to establish a categorical outline of the samples. To do so, the samples were firstly cut by a diamond saw from the bodies and were then powdered in an agate mill. The contaminated surfaces of the bodies were removed to a depth of about three millimetres with a diamond saw to reduce the possibility of contamination. Major, minor, and trace elements were thereafter determined by WDXRF on pressed powder pellets using an ARL Advant-XP spectrometer, following the full matrix correction method suggested by Lachance and Traill (1996). Accuracy was better than 2% for major oxides and better than 5% for trace element determinations, whereas the detection limits for trace elements range from 1 to 2 ppm. Replicate analyses on trace elements gave a precision better than 5%. Here, the accuracy was calculated based on the difference between the measured values and bibliographic values of international standards and precision was calculated as RSD% (Relative Standard Deviation percent) of replicate analyses (10 measurements) in the course of two years. Loss on ignition (LOI) which is a measure of both carbon dioxide and any other volatile components such as organic materials were determined by weighing the samples before and after heating at 1000°C. The results of these analyses are showed in Table 3.1 and Table 3.2.

Table 3.1 Major and minor elements of the bodies obtained by WDXRF analysis

n.	City	Site	Label	SiO <sub>2</sub>	TiO <sub>2</sub>	Al <sub>2</sub> O <sub>3</sub>	Fe <sub>2</sub> O <sub>3</sub>	MnO	MgO	CaO	Na <sub>2</sub> O	K <sub>2</sub> O	P <sub>2</sub> O <sub>5</sub>
1	Isfahan	'Alī-Qāpū	I.A.1	53.38	0.67	11.52	5.45	0.10	4.14	19.85	1.36	2.12	0.22
2	Isfahan	'Alī-Qāpū	I.A.2	52.60	0.64	10.83	4.95	0.10	4.02	21.27	1.49	1.78	0.17
3	Isfahan	'Alī-Qāpū	I.A.3	53.03	0.63	10.40	4.49	0.09	4.09	22.8	2.10	1.29	0.19
4	Isfahan	'Alī-Qāpū	I.A.4	51.95	0.64	10.55	4.81	0.09	3.94	21.56	1.57	1.87	0.18
5	Isfahan	'Alī-Qāpū	I.A.5	52.62	0.64	10.73	4.83	0.09	4.02	21.25	1.52	1.79	0.17
6	Isfahan	'Alī-Qāpū	I.A.6	48.08	0.61	8.75	4.4	0.09	4.35	20.92	1.37	1.60	0.11
7	Isfahan	'Alī-Qāpū	I.A.7	48.62	0.63	9.75	4.74	0.09	4.03	22.66	1.25	1.79	0.13
8	Isfahan	Bethlehem	I.B.1	53.21	0.67	10.98	5.22	0.12	4.05	21.68	1.48	1.7	0.15
9	Isfahan	Bethlehem	I.B.2	50.41	0.66	10.31	5.19	0.12	3.88	21.41	1.36	1.84	0.13
10	Isfahan	ICHHTO	I.C.1	54.02	0.61	9.85	4.54	0.09	3.57	22.95	1.76	1.7	0.14
11	Isfahan	ICHHTO	I.C.2	52.53	0.61	10.28	4.51	0.09	4.23	23.57	1.71	1.59	0.14
12	Isfahan	ICHHTO	I.C.3	51.76	0.63	10.95	4.81	0.10	4.50	23.18	1.62	1.61	0.14
13	Isfahan	ICHHTO	I.C.4	51.85	0.62	10.68	4.71	0.10	4.38	23.80	1.66	1.55	0.14
14	Isfahan	ICHHTO	I.C.5	51.69	0.61	10.30	4.65	0.10	4.35	24.41	1.58	1.63	0.14
15	Isfahan	ICHHTO	I.C.6	51.19	0.63	10.68	4.61	0.10	4.62	24.11	1.90	1.49	0.15
16	Isfahan	ICHHTO	I.C.7	50.93	0.63	11.12	5.14	0.10	4.35	21.43	1.67	1.54	0.14
17	Isfahan	Işfahānak	I.E.1	49.70	0.61	9.68	4.59	0.10	3.72	22.11	1.93	1.12	0.13
18	Isfahan	Işfahānak	I.E.2	54.65	0.67	10.33	5.05	0.10	3.63	20.52	1.49	1.76	0.14
19	Isfahan	Işfahānak	I.E.3	48.84	0.65	11.75	4.67	0.12	5.14	19.17	3.21	1.98	0.19
20	Isfahan	Işfahānak	I.E.4	53.68	0.67	10.27	5.04	0.10	3.71	20.84	1.43	1.76	0.14
21	Isfahan	Işfahānak	I.E.5	47.92	0.65	10.25	4.98	0.13	4.01	19.75	2.19	1.86	0.16
22	Isfahan	Işfahānak	I.E.6	51.10	0.62	10.02	4.37	0.08	4.21	23.83	1.65	1.51	0.14
23	Isfahan	Işfahānak	I.E.7	50.41	0.61	10.25	4.78	0.09	4.12	21.54	1.55	1.59	0.15
24	Isfahan	Jāme' 'Abbāsī	I.S.1	48.95	0.56	8.80	4.02	0.10	3.10	21.41	2.25	1.96	0.14
25	Isfahan	Jāme' 'Abbāsī	I.S.2	51.00	0.60	10.45	4.92	0.10	3.92	21.68	1.50	1.68	0.14
26	Isfahan	Jāme' 'Abbāsī	I.S.3	51.30	0.63	10.63	4.60	0.11	4.41	24.44	1.75	1.45	0.15
27	Isfahan	Jāme' 'Abbāsī	I.S.4	49.46	0.62	8.97	4.77	0.10	4.25	22.32	1.58	1.35	0.13
28	Isfahan	Jāme' 'Abbāsī	I.S.5	47.93	0.61	9.69	5.04	0.13	4.72	21.52	1.83	0.65	0.22
29	Isfahan	Jāme' 'Abbāsī	I.S.6	50.51	0.68	10.86	5.81	0.12	4.44	19.29	1.45	1.38	0.22
30	Isfahan	Jāme' 'Abbāsī	I.S.7	47.39	0.64	9.53	5.16	0.10	4.87	18.11	1.06	1.69	0.18
31	Isfahan	Jāme' 'Abbāsī	I.S.8	49.75	0.64	9.30	4.99	0.11	4.20	20.96	1.34	1.48	0.16
32	Isfahan	Jāme' 'Abbāsī	I.S.9	47.81	0.62	9.62	4.96	0.10	4.30	21.33	1.44	1.65	0.16
33	Isfahan	Jāme' 'Abbāsī	I.S.10	47.41	0.63	9.65	5.37	0.10	4.06	22.42	1.24	1.77	0.16
34	Mashhad	Muṣallā	M.M.1	53.55	0.61	11.26	2.70	0.10	3.25	12.27	8.73	2.24	0.22
35	Mashhad	'Abbās-ḡulī	M.A.2	54.49	0.60	12.80	5.50	0.12	5.71	10.85	2.07	2.92	0.24
36	Mashhad	'Abbās-ḡulī	M.A.1	55.90	0.63	14.59	6.00	0.12	4.95	12.08	2.28	1.94	0.21
37	Qazvīn	Jāme' Mosque	Q.J.1	57.55	0.76	14.57	6.23	0.14	4.14	10.11	2.09	2.74	0.39
38	Qazvīn	Jāme' Mosque	Q.J.2	57.13	0.74	14.19	6.30	0.13	4.65	11.20	1.81	2.59	0.30
39	Qazvīn	Jāme' Mosque	Q.J.3	57.38	0.75	14.38	6.33	0.14	4.23	10.42	2.04	2.8	0.38
40	Bihshahr	Chishma Imārat	B.C.1	63.55	0.81	15.10	7.89	0.13	2.79	3.37	1.46	2.99	0.42
41	Bihshahr	Chishma Imārat	B.C.2	62.48	0.82	15.28	7.99	0.13	2.62	2.89	1.43	3.00	0.21
42	Bihshahr	Chishma Imārat	B.C.3	64.78	0.82	15.67	8.15	0.15	2.77	1.92	1.52	3.16	0.26
43	Āmul	Mīr-Buzurg	A.M.1	57.02	1.11	17.25	7.82	0.13	3.07	8.59	1.54	3.2	0.26

Chapter Three: WDXRF quantitative analysis and the question of the provenance

Table 3.2 Trace elements of the samples quantitatively measured by WDXRF (ppm)

n.	Sample	Ba	Ce	Co	Cr	Cu	Ga	Hf	La	Nb	Nd	Ni	Pb	Rb	S	Sc	Sr	Th	V	Y	Zn	Zr
1	I.A.1	236	69	19	110	28	12	1	17	9	18	88	160	51	1092	18	374	6	125	12	70	113
2	I.A.2	237	59	20	110	33	11	1	11	10	14	86	89	50	652	16	426	6	117	13	68	126
3	I.A.3	240	69	16	120	28	11	n.a.	24	10	14	70	257	37	1606	14	439	5	110	12	58	133
4	I.A.4	236	62	18	104	38	10	1	20	10	14	83	45	48	3347	14	426	6	113	14	65	126
5	I.A.5	231	66	19	108	37	12	1	22	9	12	83	132	48	682	20	419	6	111	13	66	125
6	I.A.6	225	56	18	94	32	10	1	17	9	13	69	68	40	5273	15	498	6	101	15	52	145
7	I.A.7	218	58	17	105	28	10	1	10	8	15	79	93	40	865	15	403	5	109	12	56	130
8	I.B.1	239	66	17	121	34	12	1	15	11	15	81	189	45	932	16	361	6	120	14	59	136
9	I.B.2	236	63	17	104	34	11	1	19	10	12	82	184	45	3552	15	372	5	114	14	58	134
10	I.C.1	258	65	18	104	28	10	n.a.	20	8	16	67	135	41	497	17	472	5	104	12	53	104
11	I.C.2	231	71	19	106	30	10	n.a.	16	9	13	71	240	40	364	16	464	4	114	11	54	107
12	I.C.3	229	67	22	117	27	12	n.a.	15	9	15	82	248	45	541	18	442	5	118	12	62	107
13	I.C.4	231	69	21	107	24	11	n.a.	13	10	11	83	234	43	1343	16	451	4	123	12	58	105
14	I.C.5	225	61	20	103	31	11	n.a.	20	8	12	73	168	40	451	16	488	5	113	12	55	102
15	I.C.6	226	56	20	118	29	11	n.a.	17	10	13	77	155	42	896	16	482	5	117	14	57	116
16	I.C.7	247	68	20	115	32	12	n.a.	14	10	14	92	302	43	1459	17	419	4	126	11	71	106
17	I.E.1	244	84	20	117	27	13	n.a.	21	8	14	80	582	37	1311	17	458	3	98	8	64	102
18	I.E.2	249	65	19	121	28	10	1	12	10	13	74	144	44	695	14	363	5	114	15	56	147
19	I.E.3	308	82	21	149	94	15	1	21	11	15	81	229	57	1589	16	504	7	129	13	92	113
20	I.E.4	242	68	19	114	32	10	1	16	10	14	73	149	42	619	17	357	6	114	15	54	142
21	I.E.5	250	70	20	127	21	12	1	20	11	16	77	116	52	542	16	707	7	113	14	79	129
22	I.E.6	222	75	16	103	23	11	n.a.	19	10	13	67	370	40	435	14	467	4	111	12	53	122
23	I.E.7	245	67	18	118	29	12	n.a.	14	10	16	85	347	35	918	15	499	5	114	12	63	118
24	I.S.1	228	69	19	100	29	10	1	11	8	12	62	238	40	1138	15	439	5	105	11	51	111
25	I.S.2	270	20	23	99	32	9	n.a.	18	7	19	79	61	46	535	13	460	10	113	11	65	92
26	I.S.3	238	70	20	119	28	11	n.a.	20	9	13	85	304	37	1735	16	440	5	118	11	58	104
27	I.S.4	251	9	7	123	41	7	n.a.	9	12	10	81	98	37	277	13	439	4	109	14	52	94
28	I.S.5	265	13	7	130	45	8	n.a.	9	12	7	90	114	23	n.a.	13	504	3	115	12	65	85
29	I.S.6	274	14	11	141	42	10	n.a.	21	14	10	100	157	40	n.a.	16	396	3	134	14	71	94
30	I.S.7	251	17	6	125	43	9	n.a.	6	12	9	82	106	38	1372	11	427	3	106	15	55	107
31	I.S.8	256	13	6	117	47	9	n.a.	9	12	9	83	262	35	434	11	456	2	117	13	57	100
32	I.S.9	282	30	7	117	48	9	n.a.	10	12	7	78	569	34	1106	9	498	n.a.	104	10	62	91
33	I.S.10	237	3	6	108	42	9	n.a.	10	12	13	82	81	43	1909	11	470	4	90	14	53	101
34	M.M.1	402	99	17	258	38	12	3	28	9	15	18	80	75	2880	12	388	11	132	16	74	138
35	M.A.2	355	73	23	171	40	12	3	23	7	20	103	93	73	2321	17	386	9	109	12	87	130
36	M.A.1	396	75	24	156	25	16	2	30	11	21	96	193	81	1565	17	435	8	117	16	82	141
37	Q.J.1	540	76	19	66	40	15	4	25	13	22	40	125	72	990	17	541	8	121	15	87	166
38	Q.J.2	499	76	20	74	32	15	4	24	13	19	44	167	67	627	18	776	7	121	17	83	168
39	Q.J.3	522	73	18	66	25	15	4	19	13	23	40	101	71	916	16	648	8	119	15	84	166
40	B.C.1	485	82	23	103	34	17	6	32	14	34	60	31	117	242	16	172	12	101	22	92	209
41	B.C.2	512	82	23	112	37	17	5	32	13	31	60	84	114	180	16	152	13	104	23	101	185
42	B.C.3	489	79	21	118	41	17	7	32	13	35	62	37	118	n.a.	16	142	14	108	22	102	184
43	A.M.1	463	103	27	114	36	18	3	46	23	39	66	36	108	1141	13	306	15	144	20	108	196

## 3.2 Data handling

The data obtained from the elemental analyses of the samples (Table 3.1 and Table 3.2) were submitted to the multivariate statistical procedure of principal components analysis (PCA). This multivariate analysis technique was used due to the fact that it provides an exceptionally useful tool for grouping samples together and illustrating links between variables. This approach has largely been linked with quantitative elemental analysis in the provenance studies of archaeological ceramics (García-Heras *et al.*, 2001; Iñáñez *et al.*, 2008; Partha Sarathi *et al.*, 2008; Tite, 2008). There are two approaches in handling data by the multivariate statistical analyses which use a) non log-transformed data or b) log-transformed data. Both approaches have frequently been used in data analysing of archaeological ceramics (Bieber, 1976; Aitchison, 1994; Neff, 2002; Glascock *et al.*, 2004; Descantes *et al.*, 2008; Iñáñez *et al.*, 2008). There is no general agreement showing which approach works more properly. However, analysing five datasets of glass composition data, Tangri and Wright (1993) have discussed that the log-transformation approach can sometimes introduce spurious structure into a dataset. Therefore, in this paper, the first approach (non-log-transformed data) was preferred to handle the datasets showed in Table 3.1 and Table 3.2 and, instead of log-transforming, the datasets were standardised<sup>1</sup> to give an equal weight in the analyses (Baxter, 1995, 2004; Baxter and Buck, 2000; Tangri and Wright, 2003; Baxter *et al.*, 2005). Statistical analyses of the samples were developed using IBM SPSS Statistics 20 package.

### 3.2.1 Problems associated with provenance studies

It must be also remembered that the result of such an analysis of the same samples might be differ significantly from one laboratory to another (Buko, 1984). Moreover, in real world almost it is not easy to simply interpret data without some considerations. The bodies almost address some challenges. For instance, although chemistry of the clay and temper used to manufacture the bodies is a reflection of the local geologic environment, the addition of tempers may alter the chemical signature and preclude sourcing it to a specific clay deposit (Hall *et al.*, 1999). Even though this temper is usually believed to consist purely of nonplastics, it may also consist of a mixture of plastic and nonplastic materials. The use of tempers thus dilutes the proportions of some chemical elements and enhancing others (Baxter and Buck, 2000). Moreover, water, which is a necessary ingredient for all ceramics, contains soluble salts of such elements as sodium, potassium, magnesium, calcium, and iron, and the concentrations of these elements may thus become enriched when water is added to clay to achieve plasticity. Other factors that have been suspected to cause the compositional profile of pottery to diverge from the chemical profile of the source clay include: levigation, firing, use, post-discard processes (Arnold *et al.*, 1991), the use of clays from more than one source, poor mixing of raw materials, contamination of the samples due to insufficient care and inappropriate sampling are the factors other than site of production that can affect the interpretation of data (Cogswell *et al.*, 1998; Baxter and Buck, 2000). Removal by soil water leaching or contrariwise deposition from soil water into the ceramic body of elements such as sodium, barium and calcium,

---

<sup>1</sup> Standardisation is done with the mean and standard deviation. That is, for each variable, the mean of the batch for that variable is subtracted from each number in the batch, and the remainder is divided by the standard deviation. Standardization does tend to equalise the impact of the different variables, and in most cases this is desirable (Drennan, 2009). Standardization gives all variables equal weight in an analysis (Baxter and Buck, 2000). Standardization tends to inflate variables whose variance is small and reduce the influence of variables whose variance is large (Davis, 2002).

especially when the latter two are present as the carbonates is another issue which should be considered (Bieber *et al.*, 1976).<sup>2</sup>

### 3.2.2 An introduction about PCA

Principal component analysis is used to display chemically distinct groups suggested by cluster analysis (Baxter, 1995). The idea behind principal components analysis is to reduce a large number of variables to a much smaller number of variables that still reflects reasonably accurately (although not perfectly) the major patterns in the original dataset. This approach, however, does not begin by measuring the similarities between all pairs of cases. It begins instead by looking at relationships between variables (Drennan, 2009). PCA reveals similarities and differences between cases (Moropoulou and Polikreti, 2009).

The point of departure for principal components analysis is a matrix of correlations between all pairs of variables in the original dataset. This matrix tells us about relationships between cases. If two variables show a strong correlation that means they behave quite similarly. The broad thought behind principal components analysis is that a set of variables that all show strong correlations with each other are all responding to the same underlying thing and that these variables could, in some sense, be replaced in the dataset by a single variable with little damage to the overall patterning of relationships between cases or variables that characterises the original dataset. The dataset would thus, in some sense, be re-expressed with fewer variables. Principal components are extracted mathematically by working with the matrix of correlations between variables. The goal is to produce a set consisting of as few components as possible that show strong correlations with the original variables (Drennan, 2009).

Principal components analysis can be visualised as beginning with a scatter plot in as many dimensions as there are variables in the initial dataset. Something akin to a single best-fit straight line is determined for this multidimensional scatter plot, and this becomes the first component. This component will align relatively closely with one or more of the original variables, which is the same as saying that it will show a strong correlation with one or more of the original variables. To the extent that several of the original variables are strongly correlated with each other, then this first component can simultaneously show strong correlations with all of them. If many of the variables are strongly correlated with each other, then the first few components will be able to account for a very large proportion of the variation in the original dataset (Drennan, 2009). Once the components have been extracted, they can be thought of as coordinate axes in a space of multiple dimensions. Whole set of extracted axes can be rotated around in the space to maximise various different criteria of relationships with the original variables. They can be subjected to orthogonal rotation in which the axes are rotated as a set and all are kept at right angles to each other (*i.e.*, they are uncorrelated with each other). Or they can be rotated individually in oblique rotation, in which they lose the property of being uncorrelated with each other (Drennan, 2009). As a commonsense, the first PC is the direction through the data that explains the most variability in the data. The second PC is orthogonal to the previous one and describes the maximum amount of the remaining variability (Moropoulou and Polikreti, 2009). The results of PCA are often displayed through loading and score

---

<sup>2</sup> On the other hand, it is suggested that temper characteristics had little effect on the practical separability of clay source-related groups when clay and tempers were mixed in proportions which approximate real world proportions. This suggests that there is no need to exclude tempered ceramics from analysis. Even the highest variability temper does not seriously affect the separability of the groups (Neff *et al.*, 1988). Moreover, it is safe to assume that pottery-firing temperature does not affect analyses of the raw and fired clays. However, sulphur, bromine and chlorine, two elements suspected to be affected by firing (Cogswell *et al.*, 1996).

scatter plots. The scores are basically the projection of the data to the new coordinate system. But, the loadings define the size of the contribution of each original variable to the PCs. Loadings plot, in fact, will give an overview of the importance of your original variables. Baxter (1994, 2004), Shennan (1997), and Baxter and Buck (2000) have provided the mathematics behind principal component analysis.

There is an option in presentation of PCA results which offers score and loading plot simultaneously in one plot so called biplot. Here, we have used this option since its capacity of data interpretation is much easier and more efficient. Biplots have been used increasingly in archaeometry over the last decade (Baxter and Buck, 2000; Baxter *et al.*, 2005). Biplots facilitate quick identification of the elements most responsible for differences between specimen groups (Glascock *et al.*, 2004). Displaying objects and variables on the same plots makes it possible to observe the contributions of specific elements to group separation and to the distinctive shapes of the various groups (Descantes *et al.*, 2008). An acute angle between vectors is indicative of a high positive correlation; an oblique angle is indicative of high negative correlation; an approximate right angle indicates a low correlation. The length of a vector is an indication of how well the associated variable is approximated and how much it contributes to the analysis. For equally scaled axes, the arrows should lie approximately on a circle. The relative positions of the vectors and groups are indicative of the groups' chemical positions (Baxter and Buck, 2000; Baxter, 2004). In biplots we also can have an estimation of which is the most critical parameter in group differentiation (Moropoulou and Polikreti, 2009).

### 3.2.3 Interpretation of the data by PCA

In the interpretation of the datasets, first of all, the concentrations of major and minor elements were subjected to PCA mainly to discriminate clay-based and siliceous bodies within the bodies. To do so, SiO<sub>2</sub> was omitted from the dataset because of its diluting effect. The data was firstly standardised and PCA was then performed on the correlation matrix. The Kaiser-Meyer-Olkin measure of sampling adequacy was 0.684 which indicates that PCA was a suitable technique for this dataset. 62.63% and 14.03% of the total variance were accounted for the first and second principal components respectively. 76.67% of the total variance results for the first principal components in a good estimation of the overall composition of the samples (11.27% of total variance was also accounted for the third PC) ([Appendices 1](#)). The biplot of PCA analysis was however plotted based on the first two components presented in [Figure 3.1a](#).

First of all, according to the biplot presented in [Figure 3.1a](#), the percentages of Al<sub>2</sub>O<sub>3</sub>, K<sub>2</sub>O, and TiO<sub>2</sub> in the Āmul's sample (no. 43 in Māzandarān) should be relatively higher than the other samples, which is in concordance with the data showed in [Table 3.1](#). Furthermore, as it is demonstrated in [Figure 3.1a](#), the Āmul's sample (no. 43), as well as the Bihshahr's samples (nos. 40 to 42), does not contain considerable amount of CaO in its chemical composition which is perfectly matched with the dataset presented in [Table 3.1](#). (Note that the CaO content in the Āmul's sample is relatively higher than the Bihshahr's samples) In fact, these bodies are low-lime clay bodies. In addition, the samples of Bihshahr (nos. 40 to 42) and Āmul (no. 43) are specified with relatively high amount of iron oxide in their composition. On the other hand, the Qazvīn's samples (nos. 37 to 39) tend to be considered as calcareous bodies however the CaO content in their compositions is less than the Isfahan's samples (nos. 1 to 33) and more than the samples of the first group (Māzandarān samples, *i.e.* nos. 40 to 43). Moreover, a group of Isfahan's tiles belonged to the Masjid-i Jāme' 'i Abbāsī (nos. 28 to 33), Bethlehem church (nos. 8 and 9), and the samples of Ali-Qapu Palace (nos. 1 to 7) have formed a single cluster. Here, the separated group of Jame' Abbasi Mosque (nos.

28 to 33) might probably be considered as tiles incorporated in the original tileworks throughout successive interventions or during a restoration project. Moreover, Qazvīn's tiles (nos. 37 to 39) show more or less the same characteristics as the Isfahan's tiles.

Another point which can be deduced from [Figure 3.1a](#) is that MgO and CaO are strongly correlated to each other and the rest of the elements (except Na<sub>2</sub>O) are correlated to each other. The biplot also shows that all of the samples are not always correlated to one of the variables (the elements) and the amount of each element is equally distributed amongst the samples, except for the few abovementioned samples. One should consider that all the analysed bodies cannot be considered as siliceous paste (stonepaste bodies) which were commonly in use in the medieval Iran for making ceramics' bodies (Mason, 1996) since the silica content of these bodies is much lower than that of siliceous paste bodies which is usually above than 90 percent (Tite *et al.*, 2012) (compare with less than 70 wt% SiO<sub>2</sub> content of the bodies in [Table 3.1](#)). Except the samples of Māzandarān (Bihshahr and Āmul cities corresponded to nos. 40 to 43), which are low-lime clay-bodies, the rest of the bodies are essentially calcareous clay-based bodies. Calcareous clay-bodies have been using since the very beginning of ceramic making either on pottery-making (Yelon *et al.*, 1992) or as the bodies of first architectural polychrome glazed bricks in Iran (Caubet, 2007) until now.

Although the biplot represented in [Figure 3.1a](#) revealed very useful information about the samples, we interpreted the data obtained from the trace elements because they generally provide more realistic outlines for grouping ceramic materials in their provenance studies (Partha Sarathi *et al.*, 2008) and represent better geochemical characteristics of the clay from which the bodies are prepared. Therefore, Co, Cr, Ni, Sr, Zr, and Rb were also subjected to PCA data analysis. The standardised data showed that the Kaiser-Meyer-Olkin measure of sampling adequacy equals 0.610 and 67.14% of the total variance is accounted for the first two principal components resulting in a suitable estimation of the overall composition of the bodies ([Appendices 2](#)). The obtained biplot is shown in [Figure 3.1b](#). In contrast with [Figure 3.1a](#), in [Figure 3.1b](#) all the Isfahan's tiles (nos. 1 to 33) are very well discriminated from the rest of the samples. The tiles of Āmul (no. 43), Bihshahr (nos. 40 to 42), Qazvīn (nos. 37 to 39), and Mashhad (nos. 34 to 36) are also distinguished in different clusters. Moreover, the samples of Āmul and Bihshahr (nos. 40 to 43 in Māzandarān) are characterised by relatively high amount of Rb and, to some extent, Co in their compositions, which can be easily confirmed looking at [Table 3.2](#). Here, the sample of Muṣallā in Mashhad (n. 34) has come out of the results and shows a different behaviour in comparison with the rest of the samples. The biplot also shows that the Āmul and Bihshahr's tiles (nos. 40 to 43) are poor in Sr compared to those of Isfahan (nos. 1 to 33).

In another PCA biplot, rare earth elements (La, Nd, Y, Ce, and Sc), Vanadium (V), and Thorium (Th) were also handled by PCA in order to see their relationship with the rest of the dataset ([Figure 3.1c](#)). Again, 0.679 Kaiser-Meyer-Olkin measure of sampling adequacy and 63.13% of the total variance for the first two principal components showed a suitable estimation of the overall composition of the bodies ([Appendices 3](#)). In accordance with the other biplots, the biplot of [Figure 3.1c](#) also discriminates the samples of Āmul and Bihshahr (nos. 40 to 43) very well. However, a distinct group of Isfahan tiles can be seen in the biplot which, as discussed before, are related to the Masjid-i Jāme'-i 'Abbāsī (nos. 27 to 33) which are most probably the results of a recent intervention in the tileworks of the mosque. The biplot of [Figure 3.1c](#), in addition, shows an interesting feature of the samples. As can be seen, very highly correlated elements of Y, Th, Nd, Zr, Nd, and La are placed in the right side of the biplot (note that due to the high correlation and closeness, Th and Y are not appeared in the biplot of [Figure 3.1c](#)) and, on the

other hand, the other trace elements are gathered together on the left. It is well-known that the ratio of contents of trace elements in clays is similar to those found in parent rocks from which the clays originate (Aubert and Pinta, 1980). Due to this fact, trace elements are often used to predict the general area of ceramic bodies' production, as their presence and quantity are usually very specific for a given geological origin of the raw materials (Adriaens, 2005). For example, high concentrations of Cr, Co, Ni, and V indicate the presence of basic mineral inclusions (Aubert and Pinta, 1980; Blackman *et al.*, 1989) and rare earth elements and some elements, such as Zr and Rb, are usually associated with acidic rocks (Blackman *et al.*, 1989). Considering these remarks, the clays used to manufacture the Isfahan's tiles (nos. 1 to 33) should have originated from basic rocks due to the relatively high amount of Cr, Ni, and V in their compositions. Looking for clay deposits near Isfahan, the widespread Quaternary clay deposits can be found in the north towards south-eastern Isfahan (32° 39' N, 51° 40' E) (Bayat *et al.*, 2011). These clay deposits overlay the middle-late Eocene extrusive basic rocks, middle-late Eocene basic volcanic rocks, and Pliocene basic volcanic rocks (Zahedi *et al.*, 1978; Khodami *et al.*, 2010) (Figure 3.2a) and are still used as the main source of supplying raw material for local brick factories (Fathianpour and Tabaei,

2008). The abundance of the basic rocks near clay deposits of Isfahan could show that the bodies of Isfahan's tiles are most probably local products.

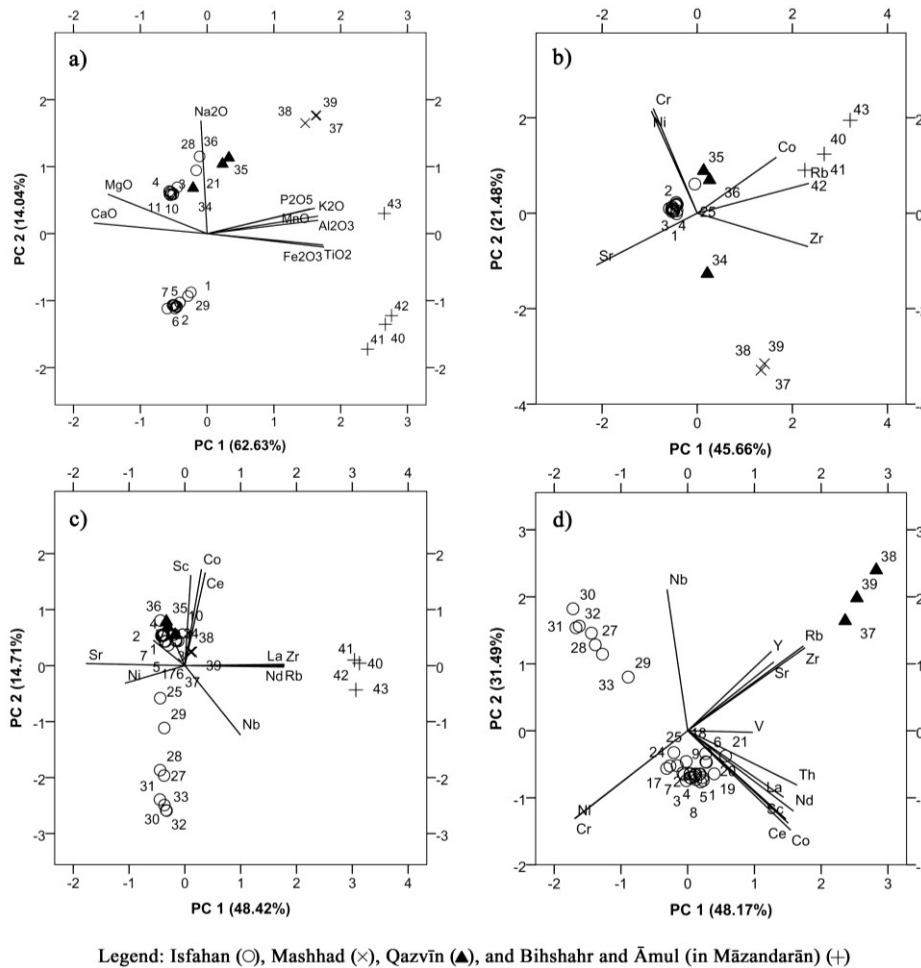


Figure 3.1 PCA biplots derived from first two principal components of a) major, minor, b) trace elements and c) rare earth and other trace elements of the samples. PCA biplot of Qazvin and Isfahan's samples are represented in the biplot d).

On the other hand, the bodies of the Mashhad's tiles show an intermediate behaviour in terms of the presence of the elements exist in basic and acidic rocks (Figure 3.1b,c). It is probable that the clays of Mashhad's tiles are supplied from the local clay sources (36° 17' N, 59° 36' E) since the northern and central clay deposits of Mashhad Basin (Yousefi *et al.*, 2007) are close to the meta-Permian ultra-basic

rocks, which change to Jurassic and early Eocene acidic rocks towards the south (Jalilian *et al.*, 1986; Alavi, 1991) (Figure 3.2b).

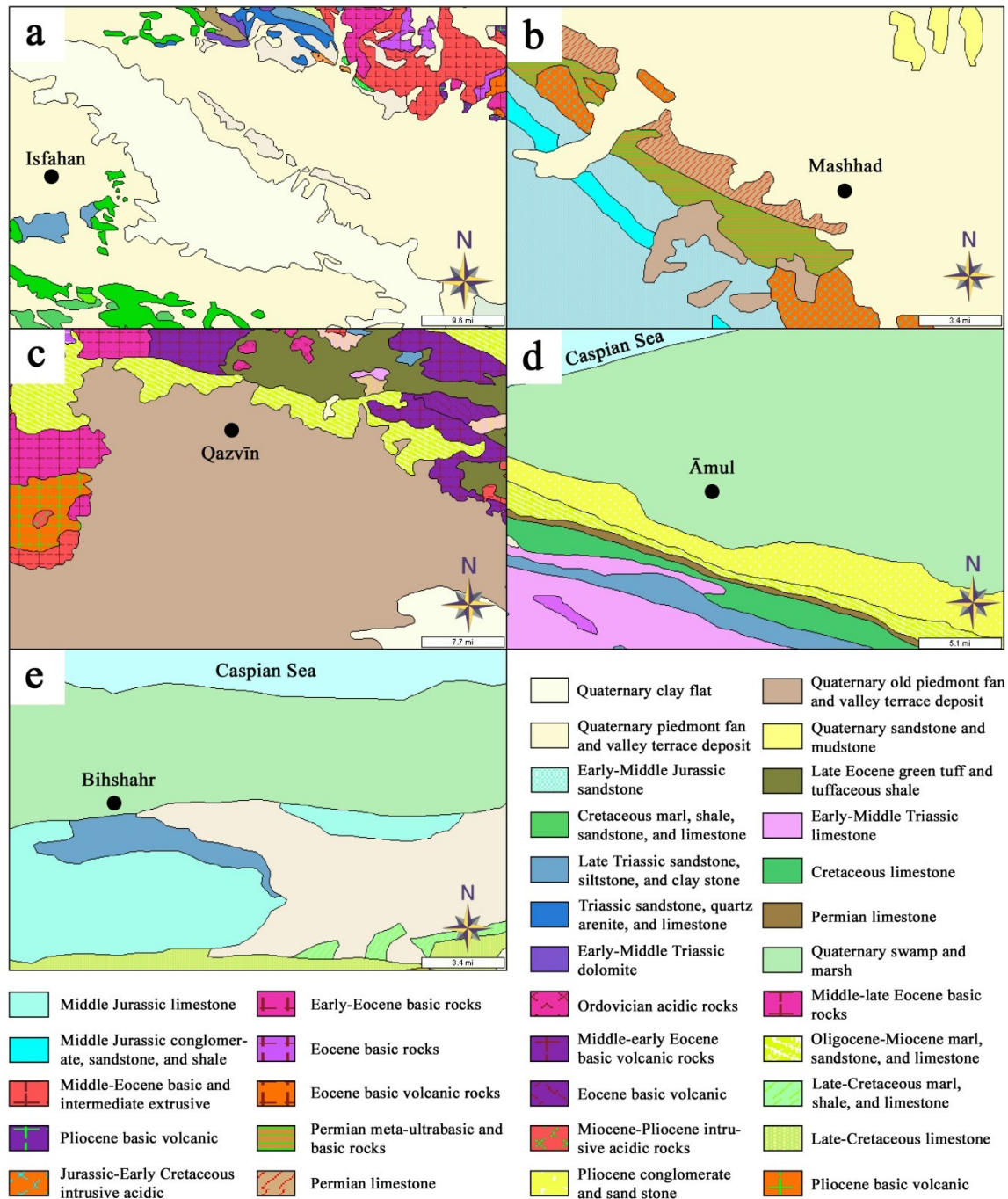


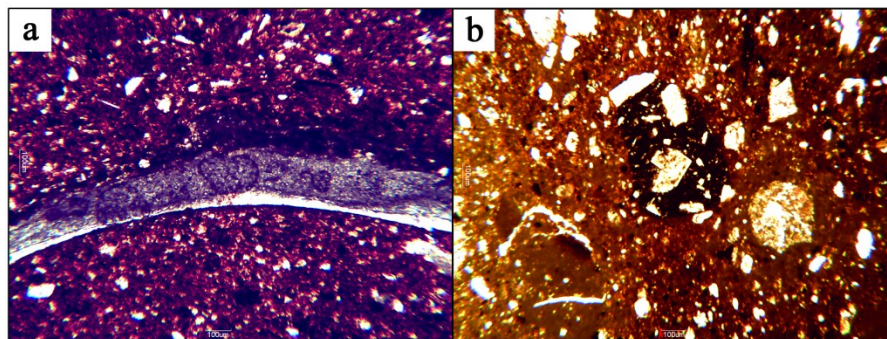
Figure 3.2 Geological context of the studied areas. (Source: National Geosciences Database of Iran)

Furthermore, the samples of Āmul and Bihshahr in Māzandarān (nos. 40 to 43) have been probably manufactured with clays deposits originating from the weathering of acidic rocks because of relatively high amount of the rare earth elements in their chemical composition (Figure 3.1b,c). The high quantity of SiO<sub>2</sub> in these samples (Table 3.1) also confirms this fact. This hypothesis is probable because, as far as

geological maps of these regions are concerned (Ghandchi *et al.*, 1991; Hossieni *et al.*, 1991), the Māzandarān province is mainly covered by Pliocene conglomerates and sandstones, Jurassic limestones, early-middle Triassic argillaceous limestones, and sparse Ordovician intrusive acidic rocks. Here, the only clay source near Bihshahr city (36° 41' N, 53° 32' E) is located on its south-eastern margins and its age is Quaternary (Figure 3.2e). However, the abundance of limestone and dolomite in this zone is in contradiction with low Ca content of the Bihshahr samples (nos. 40 to 42). It might end in the fact that the clays of the Bihshahr's tiles have not been supplied from local sources. Nevertheless, the presence of crushed shell fragments in the bodies of Bihshahr tiles (Figure 3.3a) showed that the source of the tiles' clay has been near a sea (in this case, the Caspian Sea (Figure 3.2e)).<sup>3</sup> On the other side, the clay deposits of the Āmul city (36° 28' N, 52° 21' E) derive from sediments transported by Heraz, Talar, and Tajar rivers. These deposits consist of sands, gravels, and clays of Quaternary and Late Tertiary age. The sources of these materials are in the Alborz Mountains, which comprise of volcanic rocks, limestones, and sandstones of Mesozoic and Early Tertiary age (Andriese, 1960) (Figure 3.2d). The higher Ca content of the Āmul's tile (no. 43) (Table 3.1) might derive from the limestones which cover this region.

Due to the fact that Isfahan's tiles (nos. 1 to 33) showed very close discrimination with those of Qazvīn (nos. 37 to 39) in the previous biplot (Figure 3.1c), the samples of these two cities were only subjected to PCA. The new dataset (including Isfahan and Qazvīn's samples) showed a 0.746 Kaiser-Meyer-Olkin measure of sampling adequacy and 79.56% of the total variance for the first two PCs (Figure 3.1d) (Appendices 4). Figure 3.1d discriminates very well these two groups of tiles and, moreover, separates the distinct group of the Masjid-i Jāme'-i 'Abbāsī (nos. 27 to 33) in a cluster. Figure 3.1d, in addition, shows that the tiles of Qazvīn (nos. 37 to 39) have more acidic properties compared to those of Isfahan (nos. 1 to 33) due to the higher amount of Zr, Y, and Rb in the composition of the tiles' bodies. These chemical characteristics are in accordance with the petrographical features of this region. Recent Quaternary clay deposits of Qazvīn geologic zone (36° 16' N, 50° 0' E) cover the southern margins of the homonymous city and they probably originate from the northern-middle Eocene extrusive basic rocks, middle-late Eocene basic volcanic rocks, middle-early Eocene basic rocks, middle-late Eocene acidic intrusive rocks, and Miocene-Pliocene acidic to intermediate intrusive rocks (Annells *et al.*, 1985). Qazvīn basin is also geologically well-known for its various types of volcanic tuffs that extensively cover this zone (Asiabandha *et al.*, 2009) (Figure 3.2c). The presence of these volcanic tuffs in the petrofabrics of the Qazvīn's tiles (Figure 3.3b) was another evidence for the provenance of these tiles showing a local tile-manufacturing tradition in this area.

Figure 3.3 Plane polarised light image of thin sections of a) a Bihshahr tile (no. 40) which shows a crushed shell fragment in the body's clayey matrix and b) a Qazvīn tile (no. 39) which shows a plagioclase crystal embedded in a volcanic tuff ash particle in the body's paste.



<sup>3</sup> Petrographic sections were obtained by taking a sample and then grinding one side flat. The fragments were impregnated in vacuum with a mixture from five parts of Hardrock 554 epoxy resin (lotto 090704) and one part of Hardrock 554 hardener (lotto 090927). The flat surface was then fixed to a glass slide and the rest of the sample was ground down so that a section 0.03 mm thick remained.

### 3.3 Interpretation of the dataset by bivariate plots

Bivariate plots are generally used to examine correlations between variables, identify obvious groups, detect outlier specimen (Glascock *et al.*, 2008), and evaluate validity of hypothetical groups suggested by PCA (Tite, 1999). Figure 3.4 shows some of possible bivariate plots between pairs of major, minor, and trace elements within the bodies. As it can be seen in Figure 3.4a, Bihshahr's tiles (nos. 40 to 42 demonstrated with + sign), due to a low concentration of CaO, are categorised as non-calcareous bodies, those of Isfahan (demonstrated with ○ sign) are to be considered as calcareous bodies, and those of Qazvin and Mashhad as low-calcareous bodies. The same results were previously suggested by PCA (Figure 3.1a).

In concordance with the PCA results, the Muşalla's sample (no. 34 from Mashhad) shows its different behaviour compared to the rest of the samples of Mashhad (nos. 35 and 36 demonstrated with × sign) (Figure 3.4c). This distinction is mainly derived from its lower concentration of iron, which is also the reason of its pale cream colour in body. In contrary, the samples of Bihshahr (nos. 40 to 42 demonstrated with + sign) show a higher amount of Fe<sub>2</sub>O<sub>3</sub> (Figure 3.4b,c), as PCA analyses showed before (Figure 3.1a). This can be the reason of their red colour (Figure 2.14) because when a body is formed from non-calcareous clays, iron is crystallised in the form of hematite at oxidising atmosphere and, as a result, exhibits a red colour (Maniatis, 2009). On the other hand, Figure 3.4a,b shows that the majority of the bodies are calcareous which can explain their creamy colour. The creamy colour of the bodies, in fact, is due to the dissociation of calcium carbonate into CaO and CO<sub>2</sub> and, subsequently, reacting CaO with iron oxides present in the clayey matrix. This decreases the size and amount of iron oxide particles and, consequently, bleaches the red colour to creamy or whitish (Maniatis, 2009). Molera *et al.* (1998) have provided in detail the mechanism of this transformation in colour from red to cream in clay minerals.

The bivariate plots obtained from trace elements also confirmed the validity of PCA analyses (Figure 3.4d-h). The same groups were again discriminated within the samples (Figure 3.4f). Again, the Muşalla's sample (no. 34 from Mashhad) showed its different behaviour (Figure 3.4d,h) with a high amount of Cr and a low amount of Ni giving reason for its strange behaviour. Instead, a low amount of Cr and a relatively high amount of Y, Nd, Rb, and Zr in Māzandarān's tiles suggest again that these samples are formed from acidic rocks (Figure 3.4f,g). In Figure 3.4e,h the pre-mentioned samples of the Masjid-i Jāme'-i 'Abbāsī are again discriminated, in accordance with PCA biplots illustrated in Figure 3.1c,d.

### 3.4 Concluding remarks

This paper represented the first analytical data derived from Persian *haft rang* tiles. As far as PCA interpretation of WDXRF analyses on the tiles' bodies is concerned, the 17th century Safavid *haft rang* tiles, regardless where they are found, are local products. Although it is well documented that the tiles have always been transporting from each city to another city to decorate architectural facades, this research demonstrates that the industry of tile-making in the Safavid era in Iran has been, with high probability, self-sustaining in cities where Safavid tiles are discovered. Amongst the samples collected from Isfahan, however, a group of the Masjid-i Jāme'-i 'Abbāsī was discriminated which have probably been added to the tile revetments of the mosque as a result of a latter intervention or a recent restoration plan. As a future perspective, other periods of making *haft rang* tiles should be taken into account in order to define these results in the context of Persian tile-making over the centuries of making *haft rang* tiles. In

other words, our results show only a piece of a complicated puzzle which should be gradually completed to achieve an overall knowledge of *haft rang* tile-making. Finally, WDXRF was found as an important method of quantitative elemental analysis which should be taken into consideration in the provenance studies of ceramic materials.

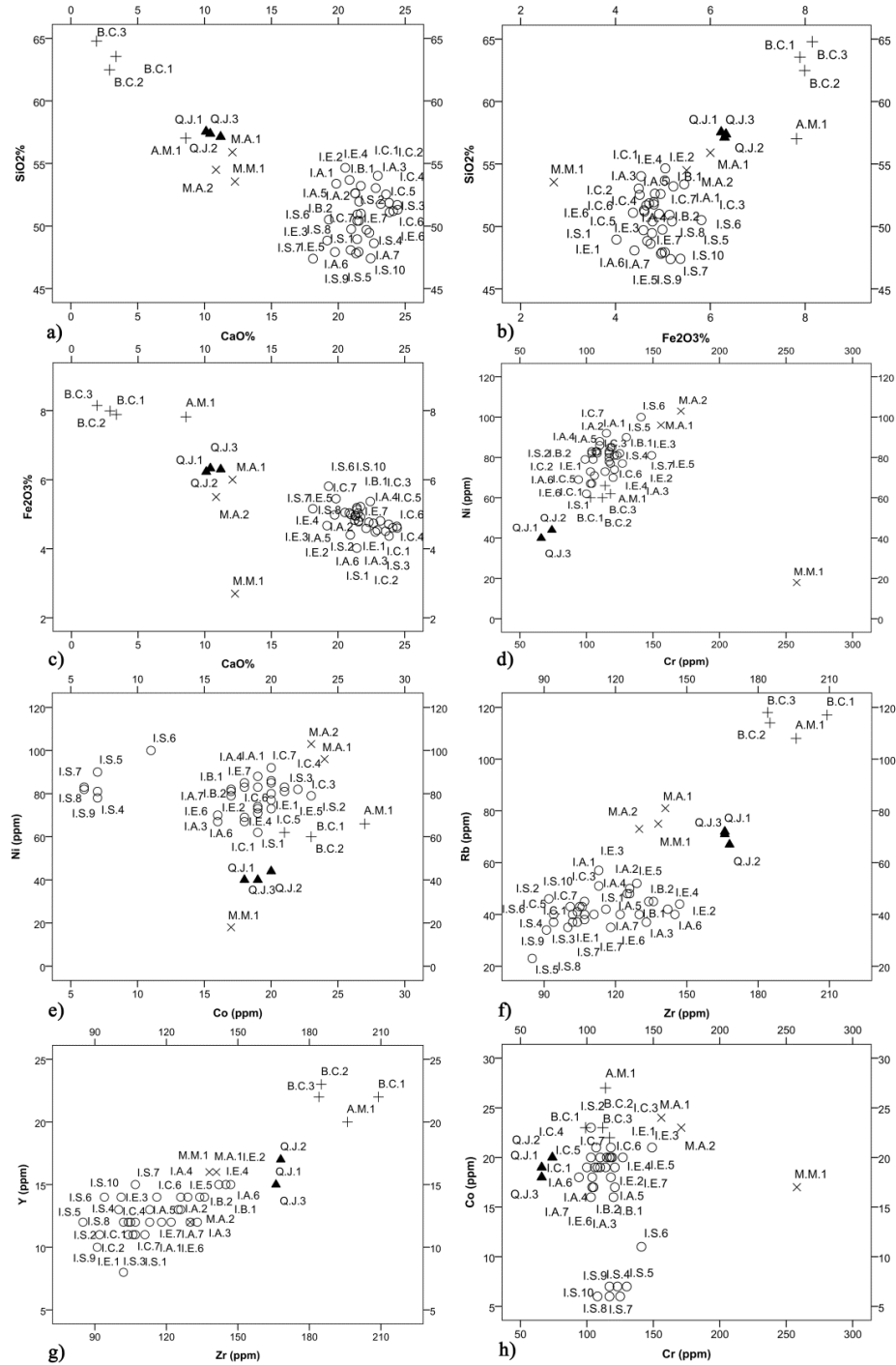


Figure 3.4 Bivariate plots of major, minor, and trace elements obtained from WDXRF data



## Chapter Four: X-ray diffraction on assessing firing temperature

### 4.1 Introduction

The study of thermal behaviour of archaeological ceramics has always been considered as one of the subjects attracted much attention in archaeological sciences because, first, it yields information about technology of making potteries and firing regimes in an ancient society (Heimann and Franklin, 1972) and, second, the estimation of firing temperature can be used in other fields of archaeological science related to ancient ceramics materials like thermoluminescence dating (Tite, 1969). Despite this fact, the study of firing temperature of the ceramic materials found in Iran, apart from few examples (Blackman, 1981; Yelon *et al.*, 1992; Shoval, 1994; Marghussian *et al.*, 2009), is rather an unexplored area. Moreover, our knowledge of firing techniques and methods from traditional and ethological documents in Iran is also limited to some medieval Persian treatises (Nayshābūrī, 1196; Tiflīsī, 12th Century; Abu'l Qasim, 1301; Ali Mohamed, 1888) and some recent observations on traditional ceramic firing (Olmer, 1908; Wulff, 1966; Bazl, 1965; Şadīq and Karīmī, 1965; Centlivres-Demont, 1971; Zamānī, 1972; Şadīq, 1976; Aḥmadīyān, 1977; Gluck, 1977; Nādirī, 1978; Kīyān-Aşl, 1993; Caiger-Smith, 2001; Floor, 2003). In the most of these treatises, the major emphasis on firing is laid on the glaze firing and less attention is paid to the biscuit firing. Some of these observations are, on the other hand, related to firing stonepaste bodies rather than clay based ones which are under question in this paper.

Studies concerning the thermal history of archaeological ceramics have always been accompanied with various methods of analysis. These methods usually track relationships between the firing temperature and changes occurred in mineralogy and microstructure of ceramics' bodies. These changes have been usually studied by the analytical methods such as FTIR (Eiland and Williams, 2000; De-Benedetto *et al.*, 2002; Shoval and Beck, 2005; Velraj *et al.*, 2009a, 2009b; Shoval *et al.*, 2011 and reference therein), thermal analysis (Cole and Crook, 1962; Roberts, 1963; Tite, 1969; Enriquez *et al.*, 1979; Mejdahl, 1980; Schomburg, 1991; Moropoulou *et al.*, 1995; Campanella *et al.*, 2003; Drebuschak *et al.*, 2005; Papadopoulou *et al.*, 2006; Drebuschak *et al.*, 2007; Ion *et al.*, 2011), Mössbauer spectroscopy (Wagner and Wagner, 2004 and references therein), or by studying of the properties associated with changes in mineralogy such as colour (Hulthén, 1976; Mirti, 1998), porosity (Cole and Crook, 1962; Morariu *et al.*, 1977; Lach, 1978; Maggetti and Schwab, 1982), hardness (Heimann and Franklin, 1972 and references therein), and magnetic properties (Velraj *et al.*, 2010; Mangureira *et al.*, 2011; Rasmussen *et al.*, 2012). Sometimes the changes associated with firing process are observed by scanning electron microscope in terms of estimation of interconnection and vitrification observed within the clay matrix of pottery (Tite and Maniatis, 1975; Maniatis and Tite, 1981; Tite, 1992). Readers may find a quite comprehensive list of methods used for assessing firing temperature of archaeological ceramics provided by Heimann and Franklin (1972).

Despite the vast application of the term ‘firing temperature,’ there are some problems associated with determining such a concept. First of all, the size of clay and non-plastic ingredients of the bodies has an important impact on ‘firing temperature’ of clay-based bodies. In other words, small size clay particles cause a decrease of the temperature at which the structure bound hydroxyl groups are usually released (Balek *et al.*, 2007). In addition, there is normally a large difference between the maximum temperatures reached in different parts of a kiln even in a single firing (Tite, 1995). Another problem is raised from soaking time of firing ceramic bodies since it drastically affect physical (Norton and Hodgdon, 1931) and micro-structural and mineralogical properties (Norton, 1931) of ceramic bodies. The problem of firing and its soaking time gets more complicated when an individual ceramic undergoes two or three firings. For instance, in our *haft rang* tiles at least two firing processes have most probably carried out on a single tile (Ali Mohamed, 1888): biscuit firing, firing a white glaze on top of the fired body (according to Ali Mohamed (1888), these two firings could have been done in one stage), and finally firing coloured glazes on top of the white glaze. This can make a complicated firing regime for glazed bodies since every firing process could have had its own maximum firing temperature (MFT) and a soaking time at the MFT. Although lower firing temperatures for the subsequent glaze firings are generally expected in *haft rang* tiles, sometimes a longer soaking time at a lower temperature can result to a same outcome with a probable shorter soaking time and higher firing temperature (Norton, 1931). Therefore, it is better to estimate an overall range of firing temperatures rather than high precision determinations of firing temperature (Tite, 1995). Thus, the term ‘equivalent firing temperature’ (EFT), as Tite (1969, 1995) suggested, is frequently used in this paper which is the temperature at which an identical mineralogy or microstructure could have been produced in one hour.

## 4.2 Materials and method

### 4.2.1 Instrumentation

X-ray diffraction (XRD) has always been one of the most important techniques for estimating firing temperature of archaeological ceramic materials. Application of XRD on ancient ceramics, which are a mixture of clay minerals, additive minerals, and their transformation products, provide useful data of the mineral composition of objects and, indirectly, contributes to achieve information about details of firing temperatures and kiln atmospheres (Cultrone *et al.*, 2001). Although it is not in general possible to use XRD to determine which clay minerals were originally present in a clay (Tite, 1999), detecting clay minerals by XRD in the clay bodies could be used as an indication of firing history of the bodies. The estimation of firing temperature by XRD is based on this fact that the mineralogical composition of clays changes during firing. These changes normally comprise of the loss of water from the clay minerals and other hydroxides, the decomposition of the carbonates with loss of CO<sub>2</sub>, and the formation of various new phases and crystalline minerals. These changes occur during heating of clay bodies may be monitored by XRD. Considering this fact, XRD, as a direct method, has always been of major interest in determining firing temperature of ancient ceramic materials (Grattan-Bellew and Litvan, 1978; Maggetti and Schwab, 1982; Shoval, 1994; Eiland and Williams, 2001; Buxeda i Garrigós *et al.*, 2002; Drebushchak *et al.*, 2005; Cultrone *et al.*, 2005b; Odriozola and Martínez-Blanes, 2007; Kristály *et al.*, 2011; Mangueira *et al.*, 2011; König and Serneels, 2013).

About 100 mg of the bodies were powdered and analysed by XRD powder method. Measurements were performed using a Philips PW 1830 generator with a PW 1820 goniometer working with Cu-K $\alpha$

radiation ( $\lambda = 1.5406 \text{ \AA}$ ), at 40 kV and 30 mA and a step size of  $1^\circ/2\theta/\text{min}$  in the  $4\text{--}73^\circ 2\theta$  range. Identification of crystalline phases by XRD was carried out using the International Centre for Diffraction Data Powder Diffraction Files (ICDD PDF). The detected phases were semi-quantitatively measured by X Powder Software Package Version 30.01.2012 (Martin, 2004).

#### 4.2.2 Statistical treatment

XRD patterns were statistically handled with PCA. In treating all the handled datasets, the datasets were firstly standardised and, then, subjected to PCA. Since the most diagnostic region of XRD patterns for ceramic materials are detectable in the  $2\theta$  range of  $8\text{--}40^\circ$  (Riccardi *et al.*, 1999; Eiland and Williams, 2001), intensity data points in this range statistically handled by PCA, where the samples (observations) in rows and their intensity data points (variables) in columns formed our dataset matrix. The distribution of the samples was observed in a score plot with the observations projected in two dimensions. In general, PCA is usually used to reduce the large number of variables to a smaller number without damaging the actual relationships between cases and variables. Despite an increasing use of PCA in handling datasets derived from chemical composition of the archaeological ceramics, the use of principal component analysis in observing XRD patterns is quite a new subject. Apart from few examples in the application PCA in investigating XRD pattern of polymorphs patterns (Barr *et al.*, 2004 and references therein; Matos *et al.*, 2007) and ceramic materials (Obeidat *et al.*, 2011), the use of PCA in observing XRD patterns of archaeological ceramics is entirely new. Other than XRD patterns, this paper also uses PCA for grouping samples in terms of other variables including quartz,  $\text{SiO}_2$ , and amorphous content of the samples. All statistical analyses of the samples and plots were developed using IBM SPSS Statistics 20 package.

#### 4.2.3 Density measurement

The bodies of the samples were cut in small bulk cubs with about 3 to 7 g and their density were calculated by dividing the mass of the samples to their volume measured by an AccuPyc 1330 pycnometer. This type of pycnometer determines volume by measuring the change of the pressure of helium in a calibrated volume. Five measurements were acquired for each sample where a small standard deviation from 0.0006 to 0.0020 showed a good precision of the measured values. One should consider that in measuring the volume of the samples, helium fills only the open pores of the porous clay bodies and the closed pores are included in the total real volume of the samples. Therefore, the measured values are lower than the real density values. This was however of interest in our studies because, as will be seen later, it could give an idea about the bubbles and ‘bloating’ of the bodies.

### 4.3 On the potential phases composing the bodies

Sometimes reactions occurred in terracotta bodies by firing in a kiln are compared with those take place in the metamorphic rocks (Riccardi *et al.*, 1999). To do so, it is usual to plot triangular phase diagrams from which the  $\text{CaO-Al}_2\text{O}_3\text{-SiO}_2$  system has been the most important for studying terracotta bodies. Although in reality the composition of ancient ceramics is always more complex than these three oxides, it is usually sufficiently accurate to have a general idea about the potential phases composed terracotta bodies (Pollard and Heron, 2008). Together with this conventional system, the relation between the chemical constituents of the bodies’ tiles the ternary plots of  $\text{SiO}_2\text{-CaO-MgO}$  is presented in Figure 4.1. First, Figure 4.1 shows that the chemical composition of the tiles’ bodies collected from each city is quite well-discriminated from

the rest of the samples, which is previously discussed with more descriptions and details in *Chapter Two*. On the other hand, plotting the bulk chemical composition of bodies' tiles on the ternary diagrams, almost all the bodies, except those of Māzandarān's samples (Āmul and Bihshahr tiles' bodies corresponded to nos. 40 to 43 in Table 4.1), would suggest wollastonite, tridymite, mullite, anorthite, and cristobalite are the probable phases formed during firing of the rest of the bodies. Here, the samples of Isfahan (illustrated with × sign in the ternary diagrams of Figure 4.1), tend to fall in anorthite and wollastonite zone; however, the samples of Qazvīn and Mashhad tend towards tridymite and cristobalite phases. Si-rich bodies of Māzandarān, nevertheless, show a tendency towards mullite and cristobalite. One should consider that although these plots allow the composition and proportion of phases present to be predicted with reasonable confidence, some circumstances, as will be seen later, can limit the usefulness of such an approach associated with equilibrium conditions (Pollard and Heron, 2008). Under these circumstances, XRD patterns could contribute better to investigate possible phases present in the bodies.

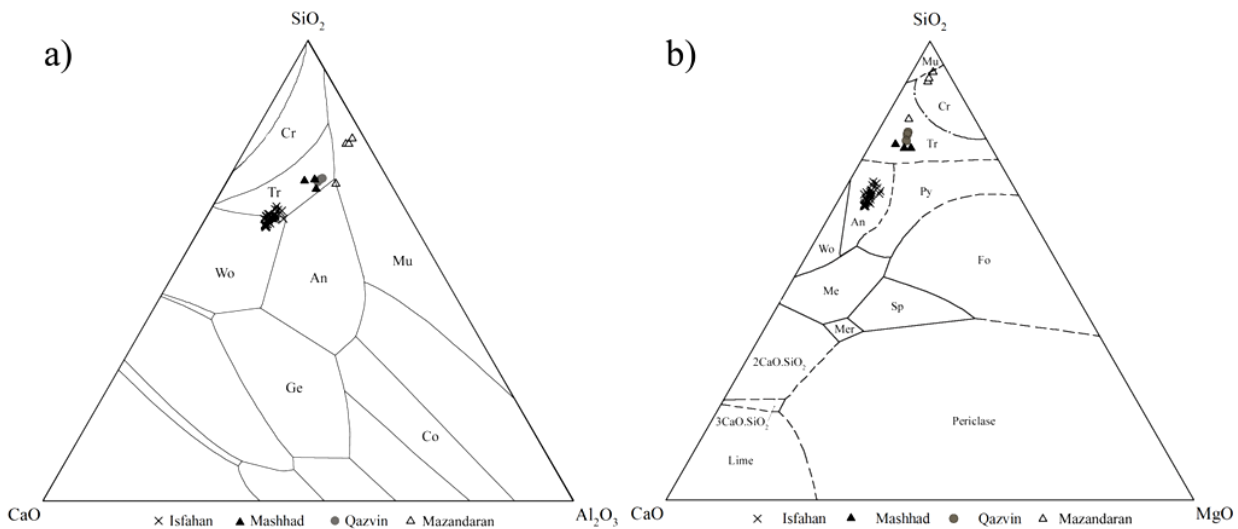
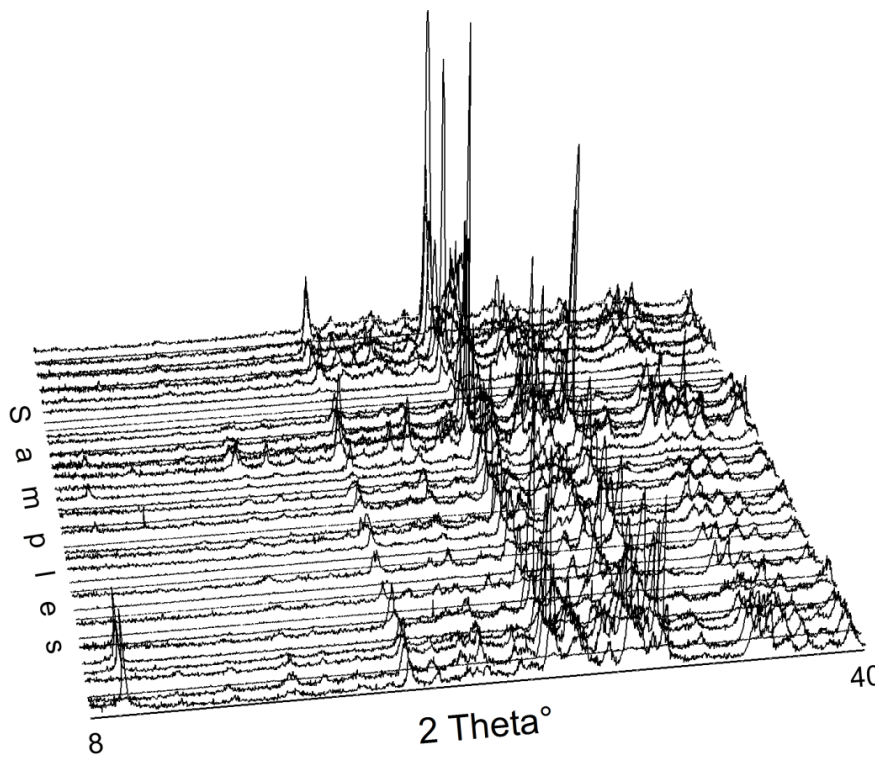


Figure 4.1 Ternary diagrams plotted for the chemical composition of the tiles' bodies. Legend: An (anorthite), Co (corundum), Cr (cristobalite), Fo (forsterite), Ge (gehlenite), Me (mellilite), Mer (merwinite), Mu (mullite), Py (pyroxene), Sp (spinel), Tr (tridymite), and Wo (wollastonite)

#### 4.4 Estimation of EFT of the bodies

Figure 4.2 shows the  $2\theta$  range of  $8\text{--}40^\circ$  region of XRD pattern of the samples, where the presence of an amorphous phase (*i.e.* vitreous phase) was evidenced by a rise of the background noise in the XRD pattern (Cultrone *et al.*, 2001) in nine XRD patterns out of forty three patterns (*i.e.*, nos. 3, 11, 12, 14, 19, 33, 34, and 42). In fact, background noise due to existence of amorphous phase in these samples does not allow us to search for any crystalline phase in the samples. The phase components of the rest of the samples were semi-quantitatively measured whose results are showed in Table 4.1. As can be seen in Table 4.1, calcite, gehlenite, muscovite (illite), feldspars (anorthite and sanidine), pyroxene (diopside), wollastonite, hematite, and variable amounts of amorphous phase are the main phases within the samples.

According to the phases detected in the bodies, four main groups were discriminated in the bodies whose thermal history has most probably been different in terms of the dominant phases present in each group. First group is highlighted with high noise background in its XRD patterns suggesting a relatively



high firing temperature at which these bodies are fired (probably higher than 1000°C) or a long soaking time. These samples are consisted of I.A.3, I.B.2, I.C.2, I.C.3, I.C.5, I.E.3, I.S.10, M.M.1, and B.C.3 corresponded respectively to the numbers 3, 9, 11, 12, 14, 19, 33, 34, and 42 in Table 4.1.

Figure 4.2 XRD patterns of the 43 samples in the range of 8–40° in  $2\theta$  scale

The second group consists of four samples of I.A.6, M.A.2, and A.M.1 tiles (respectively corresponded to nos. 6, 36, and 43). These samples contain a relatively high amount of illite (muscovite) usually abundantly found in secondary clays. The presence of illite in the tiles' bodies can be used to determine the firing temperature of these bodies. The dehydroxylation of illite is usually reported to take place between 350 and 600°C causing collapse and transformation of crystal structures and it is finally broken down up to 800°C (Maritan *et al.*, 2006), until 900°C (Bohor, 1963; Isphording, 1974; Duminuco *et al.*, 1996; Murad and Wagner, 1998; Jordán *et al.*, 1999; Riccardi *et al.*, 1999; Cultrone *et al.*, 2001; Wolf, 2002; Lumbreras *et al.*, 2003; McConville and Lee, 2005; Moroni and Conti, 2006; Trindade *et al.*, 2009; Tschegg *et al.*, 2009) or even at 1000°C (Buxeda i Garrigós *et al.*, 2002). In any case, illite structure breaks down and liquid phases begin to form. The octahedral portion of the illite structure then crystallises to form a spinel, which increases in crystal size until above 1100°C and melts by 1300°C (Cultrone *et al.*, 2001; McConville and Lee, 2005; Sedmale *et al.*, 2006). Due to the detected illite in this group's bodies, they should not therefore have been fired above 850°C.

Since illites play an important role in the formation of new firing minerals in the calcareous clay bodies, a description on its thermal behaviour needs to be provided here. Interaction of illite with calcite can be considered as an important point in diagnosing firing temperature of clay bodies. Mixtures of illitic clays containing  $\text{CaCO}_3$  form gehlenite, wollastonite, and anorthite from temperatures of 950°C onwards. However, illites which are poor in  $\text{CaCO}_3$  give a very simple mineralogical composition (quartz and hematite) after their decompositions (Jordán *et al.*, 1999). Considering these remarks, the thermal stability of calcite has also a crucial impact on the formation of new minerals and, consequently, determining EFT. At 700°C calcite begins to decompose yielding CaO (lime) with release of  $\text{CO}_2$  (Cultrone *et al.*, 2001; Buxeda i Garrigós *et al.*, 2002; Trindade *et al.*, 2009; Tschegg *et al.*, 2009). At 850-900°C calcite disappears, however, lime is present as a minor constituent (Buxeda i Garrigós *et al.*, 2002; Cultrone *et al.*,

2005a; Moroni and Conti, 2006). At this temperature calcite is completely transformed into Ca-bearing silicates due to the reaction with the phyllosilicatic paste matrix (Tschegg *et al.*, 2009; Rathossi *et al.*, 2010). Therefore, calcite is not expected in the bodies fired at temperatures above 900°C. However, this phase is sometimes detected even in the bodies fired above this temperature. This may suggest a secondary's origin calcite formed by either filtration of calcareous aqueous solutions during burial conditions, followed by the recrystallization of secondary calcite, or formed by the decomposition of gehlenite or wollastonite under post-manufacturing chemical leaching (Owen and Terence, 1998; Rathossi *et al.*, 2010) or the recarbonation of  $\text{Ca}(\text{OH})_2$  generated by the hydration of unreacted lime ( $\text{CaO}$ ) (Sánchez Ramos *et al.*, 2000; Nodari *et al.*, 2007; Rathossi *et al.*, 2010).

The third group comprises of I.B.1, I.A.7, I.C.1, I.S.4, I.E.5, I.S.1, I.S.2, I.E.4, I.E.6, I.E.7, I.A.5, I.S.3, I.S.5, I.S.6, I.S.7, I.S.8, and I.S.9 samples (corresponded to nos. 8, 7, 10, 27, 21, 24, 25, 20, 22, 23, 5, 26, 28, 29, 30, 31, and 32 respectively) which are compositionally associated with considerable content of gehlenite in the compositions. According to the ternary diagrams (Figure 4.1), gehlenite was not however expected in the XRD patterns. An explanation for this observation is that ternary diagrams are plotted based on homogeneous and ideal composition of the constituents. In the real situations where all the constituents are not homogeneously mixed this can be changed. On the other hand, during firing process, the interface between calcite and clay minerals participate in the interactions. It means that internal parts of clay minerals are remained intact and only the rims of clay crystals will be transformed. It changes stoichiometric ratio of the constituents in the reaction. Therefore, the amount of quartz participating in the reactions declines and consequently instead of high temperature minerals the chemical composition drops in the gehlenite zone in ternary diagrams.

Gehlenite, which is from melilite group, is formed from the decomposition of illite and calcite at 800–850°C (Maniatis *et al.* 1983; Sánchez Ramos *et al.*, 2000; Cultrone *et al.*, 2001; Maritan *et al.*, 2006; Trindade *et al.*, 2009). Gehlenite forms as the first phase around the calcite grains, especially if the calcite is coarse grained (Rathossi *et al.*, 2004). Gehlenite can be initially crystallised at temperatures ranging from 800 to 850°C. However, it is stable mainly at temperatures around 850–950°C. The stability field of gehlenite depends on the  $\text{SiO}_2$  saturation of the reaction; *i.e.* the higher Si-contents, the lower the equilibrium temperature at which gehlenite is stable (Cultrone *et al.*, 2001; Moroni and Conti, 2006; Tschegg *et al.*, 2009). At 950°C, Gehlenite is practically unchanged (Moroni and Conti, 2006); however, it is totally decomposed at 1050°C (Buxeda i Garrigós *et al.*, 2002; Moroni and Conti, 2006). Nonetheless, gehlenite is a metastable phase and forms wollastonite and anorthite at temperatures above 950°C (Rathossi *et al.*, 2004).

Diopside is another phase detected in this group of bodies whose thermal behaviour can contribute to estimate EFT of the bodies placed in this group. Diopside appears at 850°C and is drastically formed at 950°C (Moroni and Conti, 2006). It shows a significant increase in their main diffraction peak at higher temperatures (Cultrone *et al.*, 2001; Buxeda i Garrigós *et al.*, 2002). The presence of diopside in the tiles' bodies suggests the presence of carbonates (maybe dolomite) in the clayey material which react with quartz at high temperatures. Moreover, diopside can explain the yellowish colour of the bricks, since carbonates inhibit the growth of iron oxides favoring the development of lighter colours in ceramic bodies (Cultrone *et al.*, 2005b). Considering the thermal stability of gehlenite and diopside detected in the second group's bodies, EFT of these bodies can be roughly estimated at about 850 to 900°C (Table 4.1).

## Chapter Four: X-ray diffraction on assessing firing temperature

*Table 4.1 Semi-quantitative values of various phases detected by XRD in the bodies. Legend: Qz (quartz), An (Anorthite), Mu (muscovite), Ge (gehlenite), Ca (calcite), Di (diopside), La (laumontite), Wo (wollastonite), He (hematite), Am (amorphous phase), Sa (sanidine), Ab (abundant), EFT (equivalent firing temperature), n.m. (not measured), and n.d. (not detected)*

<i>n.</i>	<i>Samples</i>	<i>Qz</i>	<i>Ca</i>	<i>An</i>	<i>Wo</i>	<i>Ge<sup>i</sup></i>	<i>Mu</i>	<i>He</i>	<i>Di</i>	<i>Sa</i>	<i>La</i>	<i>Am</i>	<i>EFT (°C)</i>	<i>SiO<sub>2</sub><sup>ii</sup></i>	<i>Alkalis<sup>ii</sup></i>	<i>Density (g/cm<sup>3</sup>)</i>
1	I.A.1	11.4	6.5 <sup>(iii)</sup>	7.3	n.d.	8.9	n.d.	tr	10.9	n.d.	10.7 <sup>(iv)</sup>	44.7	950-1000	53.38	27.47	2.8821
2	I.A.2	17.8	n.d.	12.3	n.d.	16.7	n.d.	tr	14.4	n.d.	n.d.	38.8	950-1000	52.60	28.56	2.8807
3	I.A.3	tr	n.d.	n.d.	n.d.	n.d.	n.d.	n.d.	n.d.	n.d.	n.d.	<i>Ab</i>	>1000	53.03	30.28	n.m. <sup>(v)</sup>
4	I.A.4	17.9	n.d.	9.3	n.d.	17.2	n.d.	tr	15.2	n.d.	n.d.	39.7	950-1000	51.95	28.94	2.8502
5	I.A.5	15.2	n.d.	n.d.	n.d.	16.2	n.d.	tr	15.0	n.d.	10.5 <sup>(iv)</sup>	43.1	850-900	52.62	28.58	2.8507
6	I.A.6	15.9	15.2	n.d.	n.d.	12.1	13	n.d.	12.1	n.d.	n.d.	31.6	800-850	48.08	28.24	2.8673
7	I.A.7	22.0	n.d.	n.d.	n.d.	17.5	n.d.	n.d.	n.d.	13.7	9.5 <sup>(iv)</sup>	37.3	850-900	48.62	29.73	2.7714
8	I.B.1	21.3	n.d.	n.d.	n.d.	19.3	n.d.	n.d.	18.3	n.d.	n.d.	41.1	850-900	53.21	28.91	2.8666
9	I.B.2	n.d.	n.d.	n.d.	n.d.	n.d.	n.d.	n.d.	n.d.	n.d.	n.d.	<i>Ab</i>	>1000	50.41	28.49	n.m.
10	I.C.1	16.5	n.d.	n.d.	n.d.	18.5	n.d.	tr	23.5	n.d.	n.d.	41.5	850-900	54.02	29.98	2.8809
11	I.C.2	tr	n.d.	tr	tr	n.d.	n.d.	n.d.	n.d.	n.d.	n.d.	<i>Ab</i>	>1000	52.53	31.1	n.m.
12	I.C.3	tr	n.d.	tr	tr	n.d.	n.d.	n.d.	tr	n.d.	n.d.	<i>Ab</i>	>1000	51.76	30.91	n.m.
13	I.C.4	15.4	n.d.	8.9	n.d.	19.3	n.d.	tr	15.1	n.d.	n.d.	41.4	950-1000	51.85	31.39	2.9042
14	I.C.5	n.d.	n.d.	n.d.	n.d.	n.d.	n.d.	n.d.	n.d.	n.d.	n.d.	<i>Ab</i>	>1000	51.69	31.97	n.m.
15	I.C.6	9.1	n.d.	5.8	14.9	14.4	n.d.	tr	14.4	n.d.	n.d.	41.4	950-1000	51.19	32.12	2.9033
16	I.C.7	30.1	n.d.	8.0	n.d.	17.4	n.d.	tr	15.0	n.d.	n.d.	42.1	950-1000	50.93	28.99	n.m.
17	I.E.1	9.1	9.9 <sup>(iii)</sup>	5.8	9.7	11.1	n.d.	tr	9.4	n.d.	n.d.	45.1	950-1000	49.70	28.88	2.8320
18	I.E.2	23.9	n.d.	19.0	n.d.	19.7	n.d.	tr	n.d.	n.d.	n.d.	37.5	950-1000	54.65	27.4	2.8284
19	I.E.3	n.d.	n.d.	n.d.	n.d.	n.d.	n.d.	n.d.	n.d.	n.d.	n.d.	<i>Ab</i>	>1000	48.84	29.5	n.m.
20	I.E.4	25.1	n.d.	n.d.	n.d.	20.1	n.d.	n.d.	18.0	n.d.	n.d.	36.8	850-900	53.68	27.74	2.8041
21	I.E.5	24.5	n.d.	n.d.	n.d.	18.7	n.d.	tr	16.4	n.d.	n.d.	40.4	850-900	47.92	27.81	2.7383
22	I.E.6	22.4	n.d.	n.d.	n.d.	24.2	n.d.	tr	14.1	n.d.	n.d.	39.2	850-900	51.10	31.2	2.8272
23	I.E.7	26.8	n.d.	n.d.	n.d.	29.8	n.d.	tr	n.d.	n.d.	n.d.	43.4	850-900	50.41	28.8	2.8312
24	I.S.1	20.0	12.8	n.d.	n.d.	16.6	n.d.	n.d.	12.7	n.d.	n.d.	37.9	850-900	48.95	28.72	2.7797
25	I.S.2	22.9	13.3	n.d.	n.d.	17.3	n.d.	n.d.	12.7	n.d.	n.d.	33.8	850-900	51.00	28.78	2.8048
26	I.S.3	20.9	n.d.	n.d.	n.d.	26.8	n.d.	n.d.	15.8	n.d.	n.d.	36.4	850-900	51.30	32.05	2.8511
27	I.S.4	23.6	n.d.	n.d.	n.d.	19.8	n.d.	n.d.	17.1	n.d.	6.7 <sup>(iv)</sup>	32.9	850-900	49.46	29.5	n.m.
28	I.S.5	20.8	14.5	n.d.	n.d.	14	n.d.	n.d.	14.5	n.d.	n.d.	36.2	850-900	47.93	28.72	2.8136
29	I.S.6	17.7	14.1	n.d.	n.d.	14.4	n.d.	n.d.	12.6	n.d.	n.d.	41.2	850-900	50.51	26.56	2.8673
30	I.S.7	20.5	14.3	n.d.	n.d.	13.5	n.d.	n.d.	15.2	n.d.	n.d.	36.6	850-900	47.39	25.73	2.7572
31	I.S.8	21.4	n.d.	n.d.	n.d.	19.5	n.d.	n.d.	17.6	n.d.	n.d.	41.5	850-900	49.75	27.98	2.6824
32	I.S.9	20.8	n.d.	n.d.	n.d.	21.8	n.d.	n.d.	14.3	n.d.	n.d.	43.2	850-900	47.81	28.72	2.7519
33	I.S.10	n.d.	n.d.	n.d.	n.d.	n.d.	n.d.	n.d.	n.d.	n.d.	n.d.	<i>Ab</i>	>1000	47.41	29.49	n.m.
34	M.M.1	n.d.	n.d.	n.d.	n.d.	n.d.	n.d.	n.d.	n.d.	n.d.	n.d.	<i>Ab</i>	>1000	53.55	26.49	n.m.
35	M.A.1	31.7	n.d.	24.1	n.d.	n.d.	n.d.	n.d.	n.d.	n.d.	n.d.	44.2	950-1000	54.49	21.55	2.6921
36	M.A.2	30.4	11.4	n.d.	n.d.	11.0	7.7	n.d.	10.5	n.d.	n.d.	29.1	800-850	55.90	21.25	2.7295
37	Q.J.1	20.5	n.d.	20.3 <sup>(vi)</sup>	n.d.	n.d.	n.d.	n.d.	15.8	n.d.	n.d.	43.4	950-1000	57.55	19.08	2.7539
38	Q.J.2	18.6	n.d.	27.6 <sup>(vi)</sup>	n.d.	n.d.	n.d.	tr	16.5	n.d.	n.d.	37.2	950-1000	57.13	20.25	2.8412
39	Q.J.3	20.4	n.d.	20.2 <sup>(vi)</sup>	n.d.	n.d.	n.d.	tr	16.4	n.d.	n.d.	43.0	950-1000	57.38	19.49	2.7474
40	B.C.1	23.6	n.d.	n.d.	n.d.	n.d.	n.d.	13.6	n.d.	21.8	n.d.	41.0	950-1000	63.55	10.61	2.7062
41	B.C.2	39.3	n.d.	n.d.	n.d.	n.d.	n.d.	15.8	n.d.	14.4	n.d.	30.5	800-850	62.48	9.94	2.6756
42	B.C.3	n.d.	n.d.	n.d.	n.d.	n.d.	n.d.	n.d.	n.d.	n.d.	n.d.	<i>Ab</i>	>1000	64.78	9.37	2.7845
43	A.M.1	15.4	12.7	n.d.	n.d.	11	9.6	n.d.	n.d.	8.8	n.d.	42.5	800-850	57.02	16.4	2.8821

(i) Since any reliable discrimination between the gehlenite and äkermanite by XRD patterns is not generally easy and possible (Dondi *et al.*, 1999), we used gehlenite to cover the term äkermanite as well. (ii) SiO<sub>2</sub> content and alkali sum (MgO+CaO+Na<sub>2</sub>O+K<sub>2</sub>O) are derived from WDXRF data presented in *Chapter Three*. (iii) Due to the high amorphous and firing minerals (anorthite, wollastonite, and gehlenite) content, the calcite content has most probably a secondary origin. (iv) Laumontite (CaAl<sub>2</sub>Si<sub>4</sub>O<sub>12</sub>·4(H<sub>2</sub>O)) is most probably a secondary phase originated from either anorthite or gehlenite in post-manufacturing wet-conditions. (v) The density of samples with small size was not measured. The density of the samples with high amorphous content was considered as ‘not measured’ due to the problems associated with density measurement of highly vitreous bodies. (vi) Anorthite might be originated from the primary anorthite crystals embedded in the tuff glassy matrix found in Qazvin tiles’ bodies (see Figure 3.3)

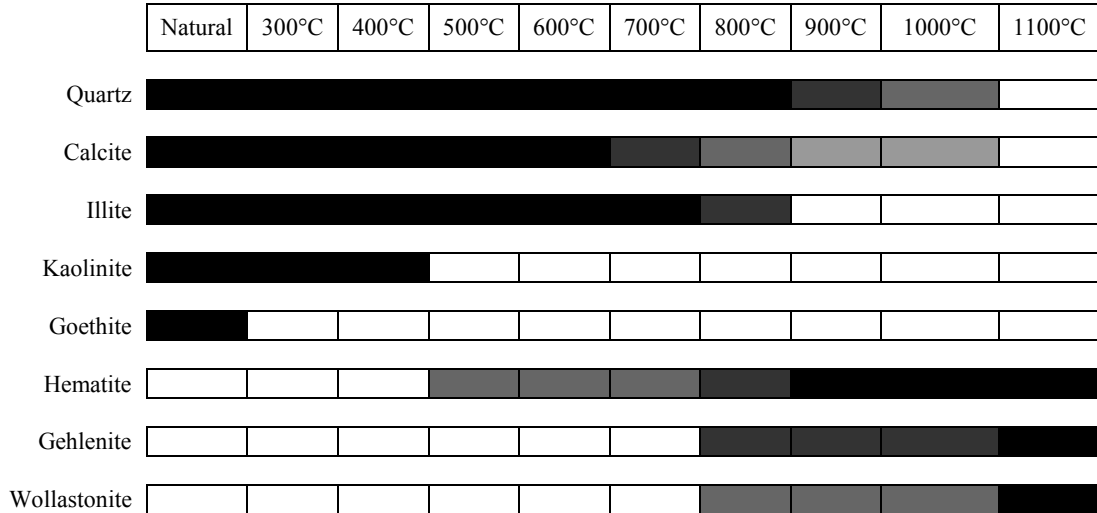
The fourth group encompasses I.A.1, I.C.4, I.C.6, I.A.2, I.A.4, I.E.2, I.C.7, I.E.1, M.A.1, Q.J.1, Q.J.2, and Q.J.3 tiles' bodies (nos. 1, 13, 15, 2, 4, 18, 16, 17, 35, 37, 38, and 39 respectively). These clay bodies are well-characterised by the presence of anorthite in their composition (Table 4.1) whose existence plays very important role in assessing EFT. Anorthite is in general crystallised in Ca-rich clays between 950°C and 1000°C (Buxeda i Garrigós *et al.*, 2002; Moroni and Conti, 2006). If sufficient amounts of calcium are available in the reaction, anorthite forms either consuming the existing gehlenite together with amorphous clay mineral breakdown products or only by reaction of decomposed clay minerals and lime (Tschegg *et al.*, 2009) in the rims of the grains (Duminuco *et al.*, 1998). The breakdown of plagioclase is occurred in the range of 900–1000°C and the progressive disappearance of potassium feldspar is slightly higher than 1100°C (Wolf, 2002). On the other hand, wollastonite is another phase which was detected two bodies of this group (nos. 15 and 17). This phase starts to form from 800-850°C (Cultrone *et al.*, 2001; Moroni and Conti, 2006; Trindade *et al.*, 2009) when unreacted CaO attacks the large quartz grains (Maniatis *et al.*, 1983). Wollastonite can also be formed as result of decomposition of gehlenite. At temperatures above 950°C and in the presence of sufficient silica, gehlenite will breakdown providing anorthite and wollastonite (Tschegg *et al.*, 2009). All the aforementioned remarks regarding anorthite and wollastonite can convey that the fourth group's bodies have most probably been fired at temperatures from 950°C until 1000°C (Table 4.1).

There are, however, some issues concerning the firing temperature of two bodies (B.C.1 and B.C.2, *i.e.* nos. 40 and 41) which did not show any firing mineral. Therefore, based on the amorphous phase and hematite contents, a rough estimation of EFT was suggested. Both of these bodies are non-calcareous bodies which contain a considerable amount of hematite in the composition. In non-calcareous clays the destruction of the original clay minerals contain iron is completed above 800 to 850°C. In these temperatures iron is released from the minerals and, if the atmosphere is oxidising, iron oxides form (Maniatis *et al.* 1983; Riccardi *et al.*, 1999). In Ca-poor systems, the total amount of hematite increases with increasing firing temperature (Mirti, 1998; Riccardi *et al.*, 1999; Buxeda i Garrigós *et al.*, 2002; Nodari *et al.*, 2007). This, first, explains the strong red hue of these bodies and, second, shows that these two bodies have at least been fired at 800°C. We, however, established a higher EFT for B.C.1 body to about 950 to 1000°C due to its higher vitreous content (41 wt%) (Table 4.1). On the other hand, the absence of mullite, a phase which according to ternary diagrams (Figure 4.1) should be expected, showed that the firing temperature of these bodies has not passed from 1050°C (Wolf, 2002). The absence of iron oxides in the rest of the bodies can be explained by the high calcium content of these bodies. Usually, maghemite, goethite, and hematite are the most familiar iron oxides which can be present in clay and ceramic minerals. Maghemite forms as an intermediate phase between 200 and 280°C and transforms to hematite at higher temperatures (Murad and Wagner, 1998). Goethite also becomes unstable at low temperatures (230–280°C) and decomposes to form hematite at 370 to 600°C (Palacios *et al.*, 2011). Ca-rich bodies, however, when fired at high temperatures under oxidising conditions, provide light creamy colour and show a significant decrease of red hue (Rathossi *et al.*, 2004; Nodari *et al.*, 2007; Rasmussen *et al.*, 2012).

Considering the abovementioned remarks, the EFT of the *haft rang* tile bodies falls between 800 to 1000°C which is entirely expected in the context of archaeological ceramic technology in the medieval Iran. Due to the coloured glazes over the *haft rang* tile bodies, the firing of *haft rang* tiles has certainly been a kiln firing, which is entirely compatible with the materials provided in the literature (Ali Mohamed, 1888). The kiln firing has always been in use in the Near East (Hansen Streily, 2000) and Iran

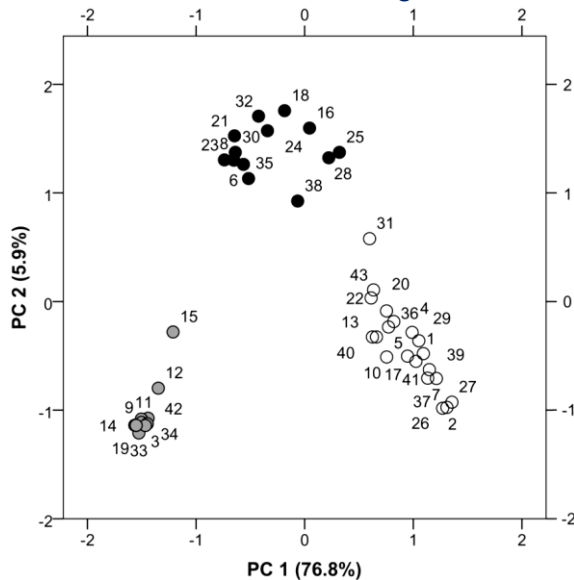
(Majidzadeh, 1975) from the antiquities. The maximum firing temperature which could have been achieved in these kilns has most probably been in the 600 to 1000°C range, where 750 to 1000°C encompasses the most achieved range. The temperatures higher 1100°C could have only been achieved by insulating kilns and using hot gases (Tite, 1995) which has most certainly been out of access in the medieval Iran. All the aforementioned remarks are represented in Table 4.2.

Table 4.2 Schematic diagram from behaviour of different phases during firing in the calcareous bodies (Trindade et al., 2009)



#### 4.5 Principal component analysis on the XRD data

Statistically handling the XRD data by PCA, 82.7% percent of total variance was accounted for the first two principal components showing a good estimation of representing data by PCA. The score plot of PCA on the XRD data is showed in Figure 4.3. The results of PCA on XRD patterns revealed very interesting



features about the samples and their phase components. As can be seen in Figure 4.3, three distinct groups are discriminated within the bodies. The first group corresponds to the bodies showed no crystalline phase in their compositions and were almost vitrified. Represented with grey circles, these samples are placed in down left of the PCA score plot of Figure 4.3.

Figure 4.3 PCA score plot on the XRD patterns in 8–40 2θ degree

The other two groups are represented with void circles on the upper part and filled circles on the down right side of the score plot. To ease our interpretations, the samples grouped on the upper part of the score plot (I.A.6, I.B.1, I.C.7, I.E.2, I.E.5, I.E.7, I.S.1, I.S.2, I.S.5, I.S.7, I.S.9, M.A.1, and Q.J.2 corresponded to

nos. 6, 8, 16, 18, 21, 23, 24, 25, 28, 30, 32, 35, and 38 respectively) are called ‘FFR’ (First Firing Regime) and those grouped on the right side of the score plot (I.A.1, I.A.2, I.A.4, I.A.5, I.A.7, I.C.1, I.C.4, I.C.6, I.E.1, I.E.4, I.E.6, I.S.3, I.S.4, I.S.6, M.A.2, Q.J.1, Q.J.3, B.C.1, B.C.2, A.M.1, and I.S.8 corresponded to 1, 2, 4, 5, 7, 10, 13, 15, 17, 20, 22, 26, 27, 29, 36, 37, 39, 40, 41, 43, and 31) are called ‘SFR’ (Second Firing Regime) by then. Due to the fact that the sample no. 15 (*i.e.* I.C.6) shows a high background noise in its XRD pattern, it is grouped with the amorphous bodies. In the further statistical treatment of the datasets, this sample is considered as a part of SFR set.

To make it clear that which factors have resulted such a discrimination, a PCA biplot was developed considering quartz, SiO<sub>2</sub>, alkali and alkali earth element sum (Na<sub>2</sub>O+K<sub>2</sub>O+CaO+MgO), and amorphous contents of these bodies as the variables. Silica (SiO<sub>2</sub>) and alkalis sum were inserted in our dataset from WDXRF quantitative analysis presented in *Chapter Three*. Here, about 84.4% of total variance was calculated for the first two PCs (Figure 4.4) (Appendices 5).

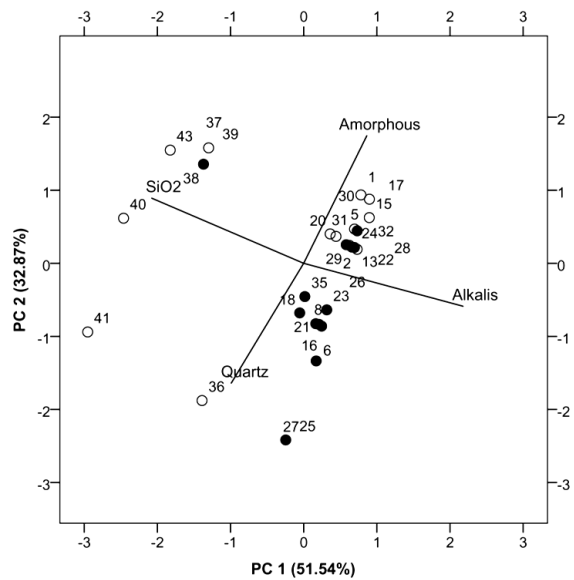


Figure 4.4 PCA biplot on quartz, SiO<sub>2</sub>, alkalis, and amorphous contents of the bodies

According to the biplot presented in Figure 4.4, the FFR samples are characterised by relatively higher quantities of quartz compared to the SFR samples. This fact is also clear in the quartz versus SiO<sub>2</sub> bivariate plot (Figure 4.5), which suggests the relatively higher quartz content of the FFR samples. On the contrary, the SFR samples show a relatively higher amorphous content in their composition suggesting a higher background noise in their XRD patterns. In addition, if we exclude few exceptions (nos. 37, 38, 39, 40, 41, and 43), both FFR and SFR samples contain relatively an equal sum of alkalis and SiO<sub>2</sub> in their chemical composition (Figure 4.4). This leads to this fact that the difference between FFR and SFR samples is essentially a difference in thermal treatments that these samples have undergone during firing.

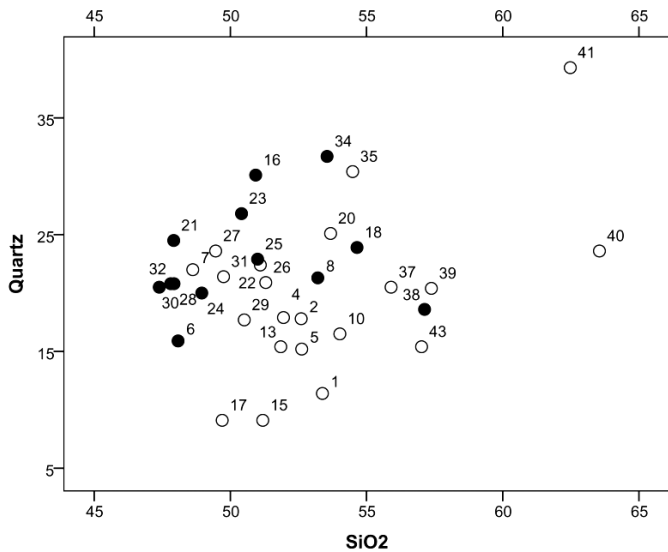


Figure 4.5 Bivariate plot of quartz versus SiO<sub>2</sub> for FFR and SFR samples

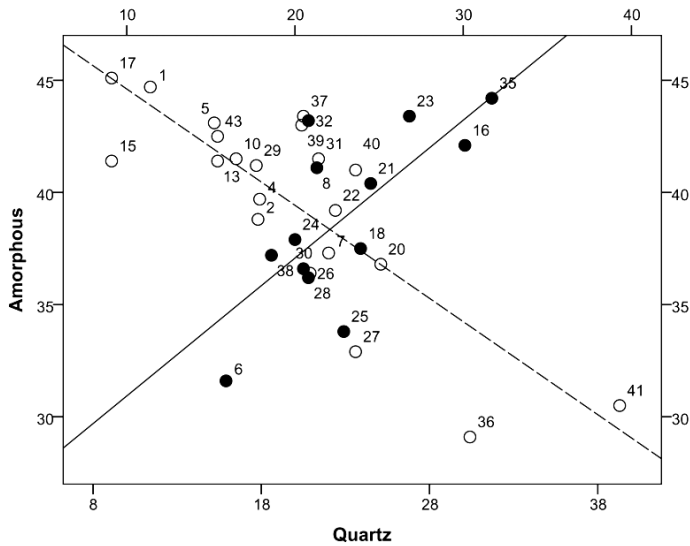


Figure 4.6 Quartz versus amorphous contents on the bivariate plot of FFR and SFR samples

Plotting amorphous and quartz contents of both of these two groups on a bivariate plot (Figure 4.6), very interesting results were observed. First, both groups of FFR and SFR samples can be fitted closely by their own regression lines which make them significantly differing. Seeking the best straight-line relationship between the two variables, the FFR samples are seen grouped together with R-squared value of 0.50 and correlation coefficient of 0.70 showing the increase in quartz content rises with increasing amorphous content. In contrast, the SFR samples are fitted with a linear regression line with R-squared value of 0.66 and a high negative correlation coefficient of -0.81 suggesting a relatively high negative correlation between quartz and amorphous contents in this group; in other words, by increasing quartz, amorphous content is drastically decreased. This could be a result of two main factors: the alkali content of the bodies and the firing process. Concerning the earlier, the ratio of SiO<sub>2</sub> to the alkali content of the bodies can be important. As can be seen in PCA score plot of Figure 4.4, a majority of the bodies has a constant quantity of alkalis in its composition. This fact is also evident in the bivariate plot showed in Figure 4.7 suggesting that, apart from few exceptions, the alkalis content in both groups of the bodies is more or less distributed equally. This shows that something other than chemical composition should have been the reason of the different trends in the two groups. This fact pushed us to delve into the second factor; *i.e.*, the firing condition.

Plotting amorphous and quartz contents of both of these two groups on a bivariate plot (Figure 4.6), very interesting results were observed. First, both groups of FFR and SFR samples can be fitted closely by their own regression lines which make them significantly differing. Seeking the best straight-line relationship between the two variables, the FFR samples are seen grouped together with R-squared value of 0.50 and correlation coefficient of 0.70 showing the increase in quartz content rises with increasing amorphous content. In contrast, the SFR samples are fitted with a linear regression line with R-squared value of 0.66 and a high negative correlation coefficient of -0.81 suggesting a relatively high negative correlation between quartz and amorphous contents in this group; in other words, by increasing quartz, amorphous content is drastically decreased. This could be a result of two main factors: the alkali content of the bodies and the firing process. Concerning the earlier, the ratio of SiO<sub>2</sub> to the alkali content of the bodies can be important. As can be seen in PCA score plot of Figure 4.4, a majority of the bodies has a constant quantity of alkalis in its composition. This fact is also evident in the bivariate plot showed in Figure 4.7 suggesting that, apart from few exceptions, the alkalis content in both groups of the bodies is more or less distributed equally. This shows that something other than chemical composition should have been the reason of the different trends in the two groups. This fact pushed us to delve into the second factor; *i.e.*, the firing condition.

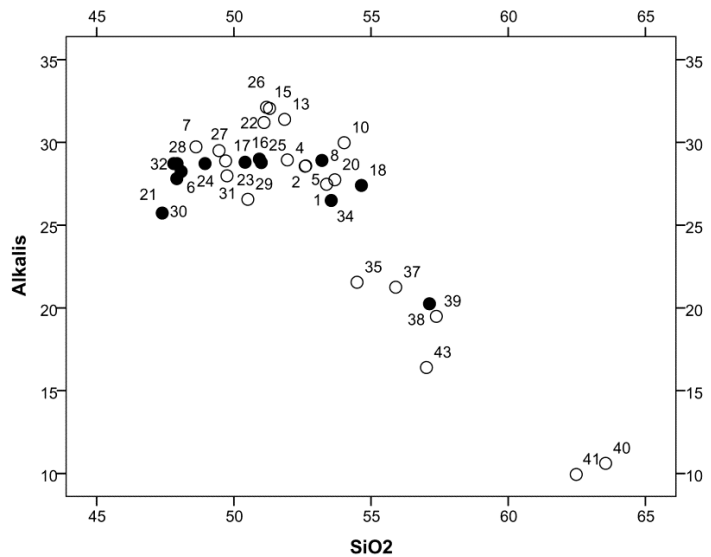


Figure 4.7 Bivariate plot of SiO<sub>2</sub> versus the alkali contents of both FFR and SFR groups

The same bivariate plot of Figure 4.6 was labelled with the estimated EFT (Table 4.1) in order to see any possible correlation between EFT and the XRD patterns of the bodies (Figure 4.8). As it is evident in Figure 4.8, the low fired bodies are located on the down side of the plot suggesting a low amorphous content can be the result of a low firing process. On the contrary, bodies with higher EFT are placed on the upper part of the bivariate plot implying a higher amorphous content can most probably be resulted from a higher firing temperature. The more interesting issue about the plot presented in Figure 4.8 is the observed trends in increasing and decreasing EFT of the bodies of both FFR and SFR groups following

their regression lines. Having a look at Figure 4.8, it can be seen that the FFR group shows a trend in increasing EFT by increasing the quartz content and, in contrast, the SFR group demonstrates a decreasing tendency in EFT with increasing quartz content. This can be a starting point for predicting EFT of unknown clay bodies with a reliable accuracy. Knowing that an unknown sample belongs to FFR or SFR and, moreover, how much amorphous phase or quartz are developed in that sample, one can roughly estimate an EFT for that body. This can be the subject of further studies in the future where different clays are fired in various temperatures with different soaking times and heating regimes in order to delve into their XRD patterns and find out the correlation between these parameters.

Another interesting point which can be inferred from Figure 4.8 is about the soaking time in the FFR and SFR groups. Since the amount of alkalis and SiO<sub>2</sub> is almost equally distributed in both groups (apart from the mentioned exceptions), the lower quartz content in SFR group in higher temperature could be the result of a longer soaking time; that is, a longer soaking time has contributed to the formation of high amorphous content and consumption of quartz in the SFR group. In contrast, the higher quartz content of high temperature FFR group members can be the result of a shorter soaking time; in other words, the soaking time has not been long enough to consume a large amount of the quartz content in FFR group.

The longer soaking time of the FFR group of tiles' bodies can be the result of one more firing process which could have been occurred in the biscuit firing; in other words, the FFR group have undergone a biscuit firing however the bodies of the SFR group have been fired with the upper white glaze in the same firing process (note that these bodies are glazed). Nevertheless, this hypothesis can be criticised because, first, it is quite unusual that two bodies of a single monument undergo two different firing regimes (for instance, M.A.1 and M.A.2 belong to two FFR and SFR groups respectively). Second, in a single firing process it is very normal to have different MFT and various parts of a traditional kiln (Tite, 1995) which can result to different firing outcomes in mineralogy and microstructure of the fired bodies.

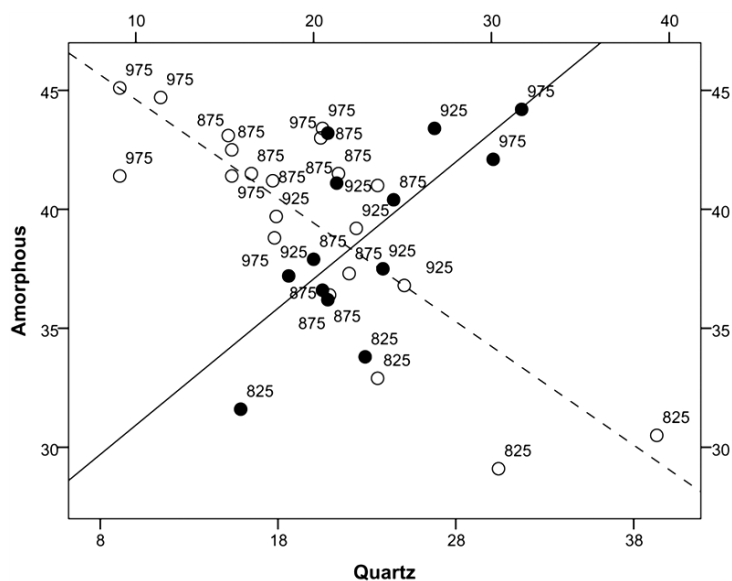


Figure 4.8 EFT of the bodies on Figure 4.6's data (note that in presenting the firing temperature the average values of the EFT are inserted)

As mentioned before, these two different trends in these two groups of bodies are mostly associated with firing temperature rather than the chemical composition. To prove this fact, the ratio of quartz to alkali and amorphous contents of the bodies could be developed in order to shed light on such a claim. The bivariate scatter plot demonstrating these variables is showed in Figure 4.9 suggesting both groups of FFR and SFR show an increasing trend of quartz/amorphous ratio by increasing quartz/alkali ratio. (Correlation coefficient and R-squared values were calculated for FFR group 0.75 and 0.55 respectively and these values for the SFR group were 0.86 and 0.73 respectively.) This can be an explanation for this

fact that the major difference between the FFR and SFR groups is laid on their firing regime rather than their chemical composition.

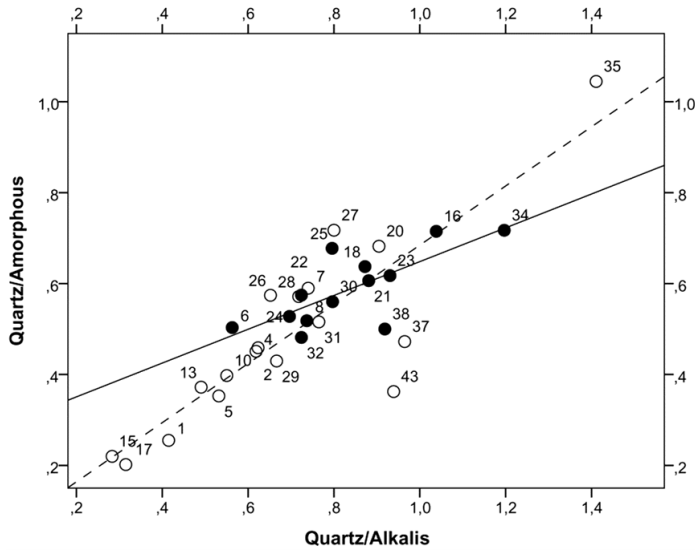


Figure 4.9 Quartz/alkali ratio versus quartz/amorphous ratio plotted for the FFR and SFR groups (note that nos. 39, 40, and 41 are removed from the SFR group to ease observing the data)

#### 4.6 Density measurement

As it is generally believed, calcite is the most important component which forms glassy phase in the clay matrix of clay bodies and changes their physical properties, especially their bulk density (Traoré *et al.*, 2007), although the presence of heavy minerals also affects the density of the clay bodies (Peacock, 1967). Density is, in fact, a physical property which can sometimes be described as a function of the volume fraction of the amorphous glassy matrix and crystalline phases in ceramics. In fact, density variation may reveal the crystallinity of ceramic bodies and the extent of the amorphous phase within them (Karamanov and Pelino, 1999). Therefore, the correlation between the amorphous glassy phase, the most frequent crystalline phases (quartz), and the density of the samples (Table 4.1) was studied in various bivariate plots. The bivariate plot of quartz versus density of both FFR and SFR groups (Figure 4.10) shows a decreasing trend of density by increasing quartz content of the bodies (correlation coefficient for FFR and SFR groups are calculated -0.58 and -0.72 and R-squared values for these groups are 0.34 and 0.52 respectively). On the other hand, amorphous content of these two groups of FFR and SFR shows a different trend against the density of the bodies; that is, by increasing the amorphous content, the density value increases in the SFR group. In contrast, within the FFR group, the density decreases when the amorphous content increases (Figure 4.11). However, one should consider that the correlation coefficient for the bivariate plot represented in Figure 4.11 for FFR and SFR groups is relatively small (-0.48 and 0.39 for FFR and SFR groups respectively) and R-squared values for these groups are also quite low (0.23 and 0.15 for FFR and SFR groups respectively). Considering these remarks, the quartz content of unknown clay bodies can be considered as a criterion for determining their bulk density; however, amorphous phase content does not seem to be a reliable parameter for establishing density of the clay bodies.

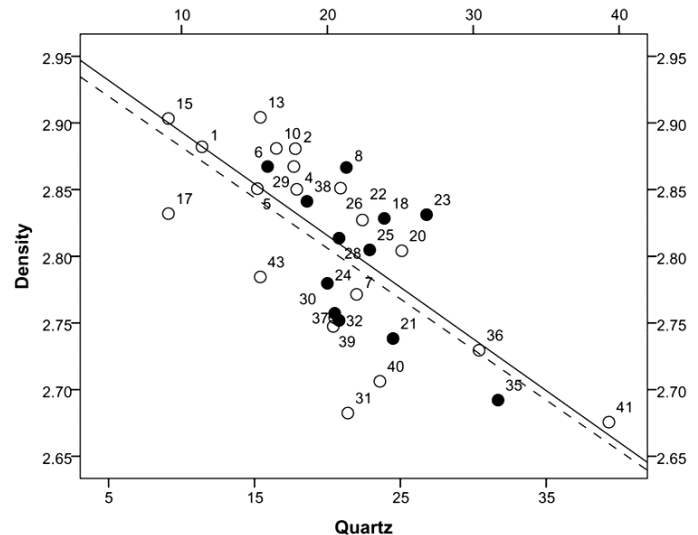
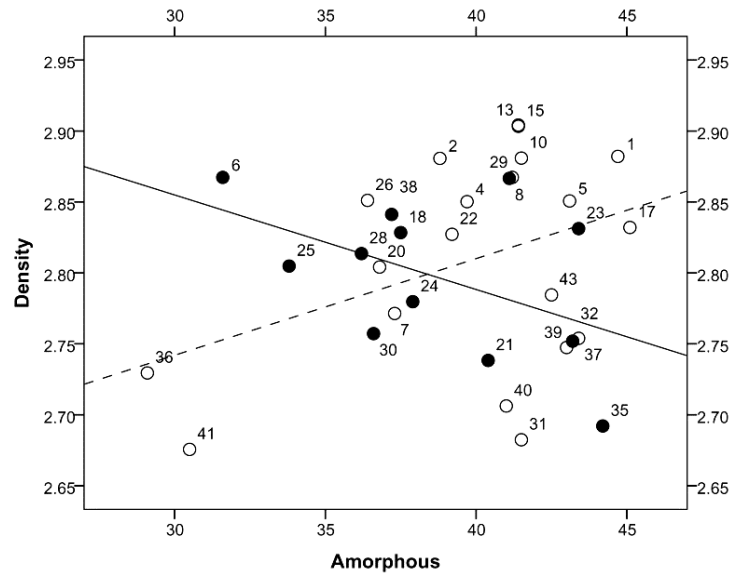


Figure 4.10 Quartz versus density contents in FFR and SFR groups

Figure 4.11 Amorphous versus density contents in FFR and SFR groups

Having in mind this fact that quartz content of the clay bodies is an important factor of density determination, looking for a firing trend within these bodies could be of interest. Figure 4.12 shows the same bivariate plot of Figure 4.10 where the average EFT of the both FFR and SFR bodies are represented instead of the samples' number. The results of this observation are quite interesting where the FFR groups shows an increasing EFT trend by increasing the quartz content and decreasing the density. In contrast, the SFR group bodies exhibit a decreasing trend in EFT by increasing quartz content and decreasing the density. It should be taken into consideration that the decreasing trend of bulk density in both groups is quite a normal trend which can be described by the specific gravity of minerals present in the bodies. Considering the lower specific gravity of quartz ( $2.6 \text{ g/cm}^3$ ), the heavier firing minerals such as gehlenite, anorthite, wollastonite, and diopside with specific gravity of about 3.0, 2.7, 2.9, and  $3.2 \text{ g/cm}^3$  respectively (Klein and Hurlbut, 1999) result a higher total bulk density in the calcareous clay bodies. This can be used as a criterion for determining EFT of the calcareous clay bodies. One should nonetheless consider the 'bloating effect' which can take place in high temperatures can affect the bulk density of the calcareous bodies. As Norris *et al.* (1979) have shown, when a ceramic body is fired, its bulk density increases and by increasing firing temperature, the bulk density continues to increase. By increasing heating, the density reaches to a maximum value and then decreases as the closed porosity increases due to the bloating effect. Considering this fact, it can be concluded that the bloating has not probably occurred in high temperature bodies of the SFR group due to their relatively high bulk density values. Even, the longer soaking time of high temperature bodies of the SFR group (look at Figure 4.8 and its



descriptions) has not ended to bloating of these bodies. As far as the high temperature bodies of FFR are concerned (for instance no. 35 corresponded to M.A.1), however, their lower density can be the result of its mineralogical composition because it is mainly formed from anorthite (Table 4.1), which has essentially a specific gravity ( $2.7 \text{ g/cm}^3$ ) close to quartz.

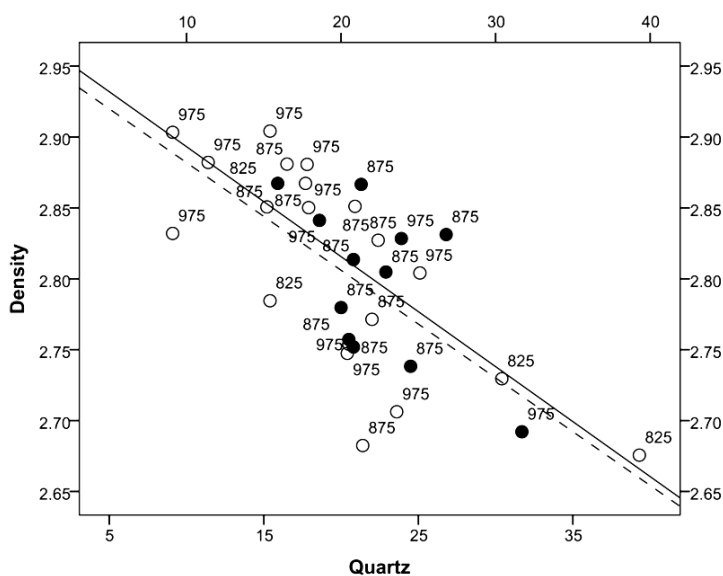


Figure 4.12 Quartz versus density contents in FFR and SFR groups representing average EFT

#### 4.7 Concluding remarks and future perspective

This chapter provides the first data concerning the thermal history of the polychrome *haft rang* tiles vastly used during the seventeenth century in Iran. This objective is achieved by interpreting XRD patterns of the samples with already well-established data provided on phase transformations in the calcareous and non-calcareous clay bodies. The results showed that the *haft rang* bodies are basically clay based and have most probably fired in the range of 800 to 1000°C. The novelty of this work is, however, the use of PCA for visualising the XRD patterns. PCA discriminated very well the bodies with high amorphous content. Moreover, particular trends were recognised in various cluster discriminated by PCA which were basically correlated to firing temperature and amorphous and quartz contents. Density of the clay bodies was also found to be considered as an important factor for clarifying the thermal history of the clay bodies. Despite these useful observations, there are many issues which deserve to be investigated more. Various clays with different chemical compositions may be fired in different temperatures with various soaking times. The quartz content and the amorphous phase of the bodies can then be monitored in order to find a reasonably predictable trend between the firing conditions and the quartz and amorphous content in the various types of clay. The density of the fired bodies, consisting both real and apparent density, should also be monitored and their correlation with soaking time and firing temperature may be studied. Although it needs a lot of efforts, samples, and time, the results can be used to have a quite realistic image of thermal history of archaeological ceramics.



# Chapter Five: Optical spectroscopy and colourimetry

## 5.1 Introduction

Over the past two decades, UV-Vis spectroscopy and colourimetry has extensively been used in the identification and survey of object of arts and historic artefacts from which artists' pigments and painting have devoted the majority of bulk research and publication (Kühn, 1968; Kühn, 1993; Mühlethaler and Thissen, 1993; Bacci, 1995; Mirti *et al.*, 1995; Bacci and Picollo, 1996; Bacci, 2000; Johnston-Feller, 2001; Pagès-Camagna and Colinart, 2003; Bacci, 2004; Bacci *et al.*, 2007a). Besides, coloured glass materials have increasingly been surveyed by UV-Vis spectroscopy either in industrial (Weyl, 1999; Bates and Douglas, 1959; Bamford, 1962; Bamford, 1977; Duran *et al.*, 1986; Eppler, 1990; Keppler, 1992; Bae and Weinberg, 1994) or in artistic and archaeological glasses (Schreurs and Brill, 1984; Sanderson and Hutchings, 1987; Brill, 1988; Mirti *et al.*, 1993a; Orlando *et al.*, 1996; Mirti *et al.*, 2000, 2002; Bianchin *et al.*, 2005; García-Heras *et al.*, 2005a; 2005b; Jackson, 2005; Bacci *et al.*, 2007b; Bingham and Jackson, 2008; Carmona *et al.*, 2008; Schibille *et al.*, 2008; Fernández, 2009; Croveri *et al.*, 2010; Meulebroeck *et al.*, 2011; Ceglia *et al.*, 2012). On the other hand, archaeological glazes, as glassy materials, have also received an increasing attention in being investigated by UV-Vis spectroscopy (Molera *et al.*, 1997; Mirti, 1998; Vendrell *et al.*, 2000; Borgia *et al.*, 2002; Padeletti *et al.*, 2004; Roqué *et al.*, 2006; Reiche *et al.*, 2009). The application of this method comes from the fact that transition metals in glassy matrixes yield different colours in various atmospheres of firing imposed to glazed or glass objects. UV-Vis spectroscopy can be used to identify the transition metal ions present in glass and their oxidation states. It is often performed in conjunction with elemental analysis techniques to determine the glass colourant in addition to its oxidation state (Mass, 1999). Sometimes, in fact, a simple reflectance spectrum in the visible region suffices for the identification of an unknown material (Bacci, 2000).

Optical spectroscopy works based on the transitions of electrons between the outer energy levels of the atoms, whose energies are in the range from near infrared, through visible, to ultraviolet (Artioli, 2010). In other words, the energy ranges spanned by ultraviolet and visible radiation encompass the energies required to promote electrons from their ground states in the outer shells (*d* shells) of transition metal ions (such as  $\text{Co}^{2+}$ ,  $\text{Cu}^{2+}$ , and  $\text{Fe}^{3+}$ ) into excited states. To do so, a transition metal absorbs light at the wavelength that matches the difference in energy between its ground and excited electronic states. The particular wavelength of maximum absorbance for a transition metal ion is characteristic of a particular metal and also its oxidation state (Mass, 1999; Pollard *et al.*, 2007; Stuart, 2007). The mechanism of the absorption is generally defined by the ligand field theory in which a metal ion is surrounded by ligand ions (or atoms, or molecules) that produce a field acting upon the central ion orbitals, so as to resolve the degeneracy of the five *d* orbitals of the transition-metal ion, where, the energy of the different *d* orbitals is a function of the ligand type, number, and geometrical arrangement (Bacci, 2000). We do not go further into the theoretical aspects of the ligand field theory in glassy matrixes. Readers may find the relevant materials in Bates (1961), Bamford (1962), Wong and Angell (1991), and Guloyan (2007).

## 5.2 Instrumentation and the optical dataset

In general, two types of optical spectrum analysers are currently available: high-end and portable spectrometers. High-end spectrometers are characterised by their high spectral resolution. They can measure the intensity as a function of the wavelength with high resolution. The measurement procedure corresponds to an automatic scanning of the spectrum where the measurement of a single spectrum takes a few minutes. These instruments are relatively large and can only be used in laboratory conditions. Portable spectrometers, on the other hand, measure the spectrum in real-time. The signal is diffracted into the separate wavelength components and focused on a detector array inside the apparatus. This configuration results a smaller spectral resolution compared to the high-end equipment (Johnston-Feller, 2001; Meulebroeck *et al.*, 2011). This technique is fast, non-destructive, and low-cost compared with the expensive equipment for standard chemical analysis. These features make optical spectroscopy appropriate for a first-line analysis of coloured materials especially glazes and glasses. Moreover, this technique is non-destructive as it requires only a limited cleaning of glass and glaze. Another strong point is the availability on the market of portable spectrum analysers, which would allow in situ measurements (Ceglia *et al.*, 2012).

Due to the frequent need in cultural heritage to measure the absorption spectra in situ, for example ancient glazes, the transmission measurements are obviously impossible and, therefore, techniques based on surface reflectance have been developed (Artioli, 2010). Reflectance is described in two terms: *diffuse*, meaning ‘specular component excluded (SCE)’ or *total*, meaning ‘specular component included (SCI)’ (Johnston-Feller, 2001). Reflectance spectroscopy measures the spectral composition of the radiation specularly or diffusely reflected by the object surface, to which radiation emerging from the inside of the object is added. The balance between specular and diffuse reflection depends on how smooth or matte the surface is (Bacci, 2000). On highly polished or very glossy materials, the surface reflection is mirror like, that is, light will be reflected at an angle equal and opposite to the incident angle. This type of mirror reflection is called specular or Fresnel reflection. When surfaces are matte (non-glossy), all of the surface reflection is diffuse; that is, the light is scattered in all directions (Johnston-Feller, 2001). In dielectric materials (non-metals like glazes), the surface reflection is simply the character of the illuminant. Colour is produced from the internal absorption and scattering of the incident light inside the material. Therefore, to describe the colour as observed, it is desirable to exclude the specular reflection on glossy samples. This is what human observers do; they ignore very bright brightness. For collecting reflected light, three basic types of optical design are used in spectrophotometers from which integrating sphere geometry with either 0° illumination and diffuse viewing (0°/d) or near-normal incidence, such as 8°, and diffuse viewing (8°/d) is popularly used. In most commonly used type of integrating sphere geometry the angle of illumination is about 8° so that light reflected specularly at -8° strikes the integrating sphere wall and is included in the measurement. They are generally equipped to exclude the specular reflection, if desired (Johnston-Feller, 2001).

The colour of an object can be expressed by the values of three coordinates which may be directly or indirectly related to tint, lightness, and saturation. Commercial instruments for colour measurement perform calculations of colour coordinates according to a few conventional systems. The oldest and yet widely used way of expressing colour coordinates is the Munsell system, which uses the variables H (hue, *i.e.* tint), C (chroma, *i.e.* saturation), and V (value, *i.e.* lightness). More recent is the CIEL\*a\*b\* system, proposed in 1976 by *the Commission Internationale de l’Eclairage*. In this system, the coordinate  $L^*$  is

directly related to the lightness of the colour, while  $a^*$  and  $b^*$  depend on both tint and saturation. In more detail, the CIEL $^*a^*b^*$  space is defined in such a way that red and green colours are characterised by values of  $b^*$  close to 0, and  $a^*>0$  and  $a^*<0$ , respectively, while yellow and blue are characterised by values of  $a^*$  close to 0, and  $b^*>0$  and  $b^*<0$ , respectively (Mirti *et al.*, 1993b; Bacci, 2004). To describe a colour in CIEL $^*a^*b^*$  terms, diffuse reflectance must be used. To analyse the intensity of the light beam, the total reflectance has to be considered (Johnston-Feller, 2001). The calculations and mathematics behind CIEL $^*a^*b^*$  can be found elsewhere (Bacci, 2004; Johnston-Feller, 2001).

In our studies, both *diffuse* and *total* reflectances (SCE and SCI respectively) of a clean surface of the coloured glazes were acquired simultaneously in the range of 360–740 nm with 10 nm interval using a Konica Minolta spectrophotometer CM-2600D quipped with a barium sulfate integrating sphere with d/8° configuration to collect reflected light. Colour coordinates were expressed in the CIEL $^*a^*b^*$  colour system, with reference to the illuminant D65 (average solar light) and the 10° viewing angle and spectroscopic data were processed by the SpectraMagicNX software. Over 460 measurements were acquired from the coloured glazes of *haft rang* tiles.

### 5.3 Interpretation of the dataset

Figure 5.1 shows the points representing colours of the glazes projected on  $a^*$  and  $b^*$  coordinate system of the CIEL $^*a^*b^*$  colour space. As can be seen in Figure 5.1, all the blue glazes are placed in the right down quadrant of the plot, which can roughly be correspond to deep blue hues. However, some samples (I.E.6, B.C.1, B.C.3, I.E.1, and M.A.1) demonstrate lighter hues towards the white direction. Having a look at these samples with naked eyes (see Figure 2.10 and Figure 2.14), it can be apparently seen that these samples have been corroded and, consequently, seem whitish. Amongst the blue glazes there are also three samples which show a tendency towards the yellow colours. These samples (I.C.1, I.C.3, and I.C.4), however, seem to be quite transparent and thin enough to allow the incident light to reach to the white glaze underneath. In Figure 5.1, moreover, all the white and dark violet glazes are displayed close to the illuminant source nonetheless with completely different degree of  $L^*$  (look at Figure 5.2) so that the violets are almost appear black and the whites exhibit very pale yellow hue. Within the dark violet glazes, however, I.A.3 exhibits a lighter hue towards the red hues which is visually confirmed by looking at the sample with naked eyes.

The yellow glazes are discriminated on top of the diagram (Figure 5.1) with four exceptions (I.S.9, B.C.1, M.A.1, and M.A.2) which show a hue near the green colours. In contrary, the green glazes are situated in the up left quadrant of the plot with ten exceptions (I.A.7, I.B.1, I.E.2, I.E.4, I.E.6, M.M.1, Q.J.3, I.C.4, I.C.7, and I.E.1) towards the yellow hues. The turquoise glazes, on the other hand, demonstrate negative values of  $a^*$  and  $b^*$  in the left down quadrant of Figure 5.1 except two samples (I.E.6 and Q.J.2) which show a tendency to the white hues due to their deteriorated matte surfaces. In addition, another group amongst the turquoise glazes (I.A.7, I.B.2, I.E.1, I.E.2, I.E.4, I.E.6, M.M.1, and Q.J.2) exhibits a greenish hue. Finally, the brown glazes are located nearby the yellow glazes in the upright quadrant of Figure 5.1 so that it seems that they are placed in the corpus of the yellow glazes' group. As a general result, it can also be inferred from Figure 5.1 that green, yellow, white, and brown glazes are placed in the upper part of the  $a^*$  vs.  $b^*$  diagram and, on the other hand, blue, turquoise, and violet glazes in the bottom.

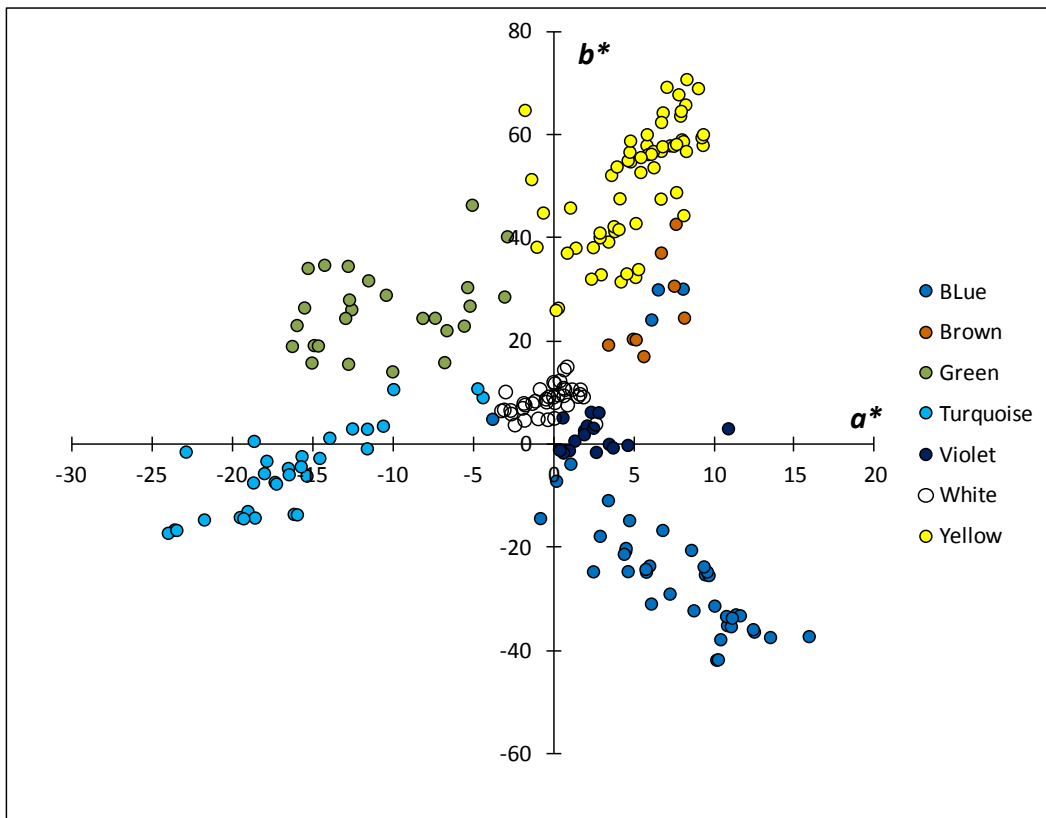


Figure 5.1 Projection of  $a^*$  and  $b^*$  SCE values of the coloured glazes on the CIEL\*a\*b\* colour plane

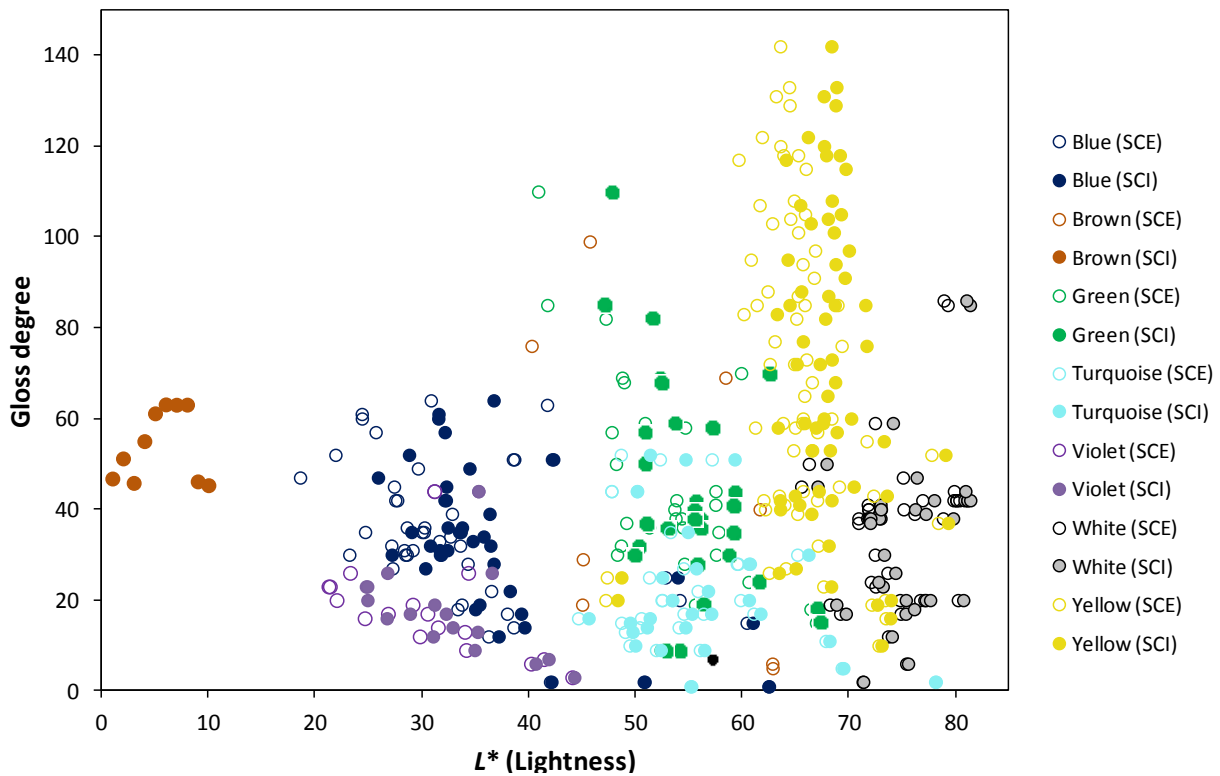


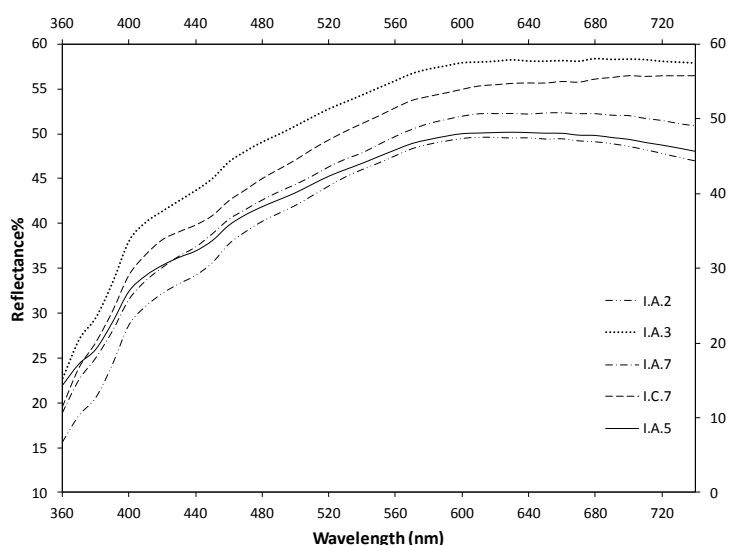
Figure 5.2 Lightness versus gloss degree for both SCE and SCI values of the various coloured glazes

Due to the fact that diagrams like that of Figure 5.1 do not exhibit  $L^*$  value of the samples and, furthermore, the degree of glossiness (gloss), as an important factor for glassy surfaces of glazes, is not considered in the colour interpretation, these two parameters are plotted in one individual diagram to observe how lightness is changed with gloss within the coloured glazes (Figure 5.2). The first issue which is clearly seen in Figure 5.2 is that all the glazes demonstrate the same value for gloss degree in both SCE and SCI modes except the brown glazes. Moreover,  $L^*$  value in the SCE mode is naturally less than that of SCI mode. In addition,  $L^*$  value is gradually decreased from white > yellow > turquoise > green > blue > violet > brown. Moreover, yellow, white, brown (just in SCI mode) and green glazes show a relatively higher degree of glossiness rather than blue, violet and turquoise glazes. The optical measurements were not limited, however, to this level and our studies were extended to study the visible spectra of each group of the coloured glazes as follows.

### 5.3.1 Whites

A white glaze is actually transparent glazes in which something causes scattering of the light and, consequently, opacifying the transparent glaze. In general, a glaze is opacified due to separation of crystalline phases during cooling, creation of gas bubbles within the glaze, or addition of insoluble crystals such as quartz, calcite, or tin oxide (Schabbach *et al.*, 2008; Croveri *et al.*, 2010). One of the most famous methods in opacifying glazes is the distribution of small particles of tin oxide within a colourless glaze, resulting in the reflection and the scattering of the light. The opacification achieved is changed by various parameters such as the number of particles (which has the effect of increasing the path length for the light), the size of the particles, the presence of clean faces to the crystalline particles, and the difference of refractive index between crystals and glass matrix (Vendrell *et al.*, 2000) so that the larger the difference between these refraction indexes, the larger the opacification will be (Schabbach *et al.*, 2008).

If no compositional data for a glaze is available, then the total reflectance spectra, obtained non-destructively with a portable spectrophotometer, can be used to provide an indication of the tin oxide and lead oxide contents of the glaze. However, the total reflectance also depends on the glaze thickness, the tin



oxide particle size, the presence of other crystalline phases in the glaze and the body colour (Vendrell *et al.*, 2000). Almost all the white substrate glazes of *haft rang* tiles demonstrated identical spectral curves like those plotted in Figure 5.3. These curves are also identical with those of Islamic lead-tin Islamic glazes obtained by Vendrell *et al.* (2000).

Figure 5.3 Optical spectra of total reflectance (SCI mode) for five white glazes of *haft rang* tiles

It should be indicated that the spectral curves of the white glazes obtained from diffuse reflectance light also exhibited the same behaviour as those of total reflectance. Generally, the light reaching the interface between white glazes and body paste is reflected at the surface of the paste and then travels back

again through the thickness of the glaze to the outer surface. As the paste is normally a fired clay containing several percent of iron oxide, the colour of this diffuse reflection is reddish or creamy rather than colourless; that is, the reflected intensity is higher for the red than for the blue or the green parts of the visible spectrum (Vendrell *et al.*, 2000). However, as mentioned before, the curves of white glazes acquired from diffuse and total reflectance were the same. It is most probably because of the fact that the white glazes have been opacified enough to cover the creamy (and in some occasions red) colour of the bodies.

Another issue which can be perceived from Figure 5.3 is that the white colours are lead-based glaze because in lead-rich glasses there is an important absorption in the near ultraviolet which can be detected in the blue end of the visible spectrum. This absorption is the reason for tin-opacified lead glazes appearing white, even when the crystal size of the tin oxide is small enough to produce scattering with a higher intensity in the blue (Vendrell *et al.*, 2000). In fact, the absorption of glazes in the blue and near UV region of the spectrum increases scattering in the blue region enhances the whiteness of the glaze (Vendrell *et al.*, 2000).

### 5.3.2 Yellows

We obtained a typical curve for the majority of the yellow glazes like that of showed in Figure 5.4a with high absorbance in the wavelengths lower than about 450 nm. This spectrum is similar with those of lead-tin yellow type II ( $\text{PbSn}_2\text{SiO}_7$ ) suggested by Kühn (1993, 1968). The high absorbance occurred in wavelengths lower than 450 nm is probably due to the high lead content of the glaze (Padeletti *et al.*, 2004), as mentioned also for that of the white glazes. Moreover, according to Kühn (1993), the yellow glaze should have been fired at temperature above  $650^\circ\text{C}$  (probably around  $750^\circ\text{C}$ ) to yield such a spectrum. Four yellow glazes (I.C.7, I.E.1, I.E.7, and Q.J.2), however, showed a slightly different spectra (Figure 5.4b). This might be from the fact that these glazes were severely altered on the surface (look at Figure 2.10 and Figure 2.11 in *Chapter Two*). Moreover, one should take into account that the yellows are from opacified yellow glazes and do not have anything in common with those of iron(III) yellow glazes described later on.

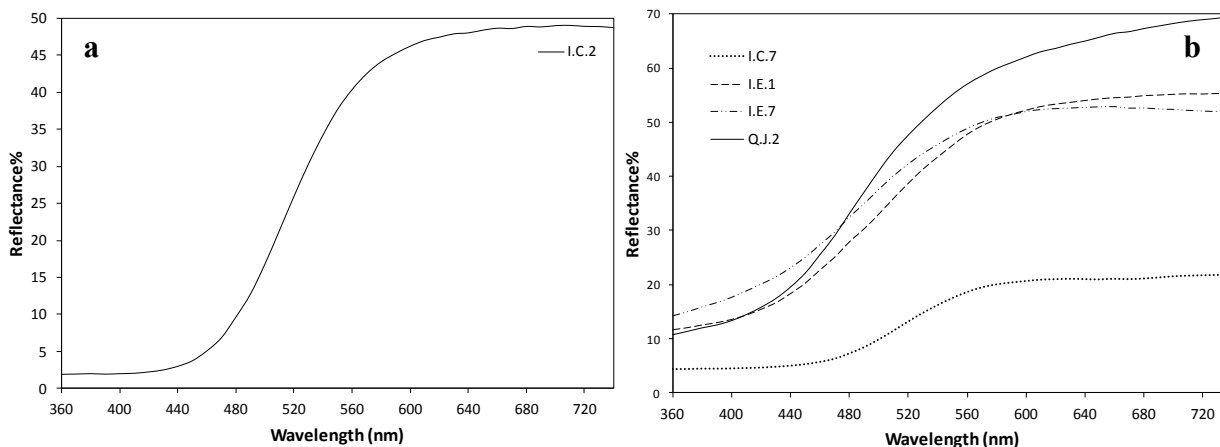
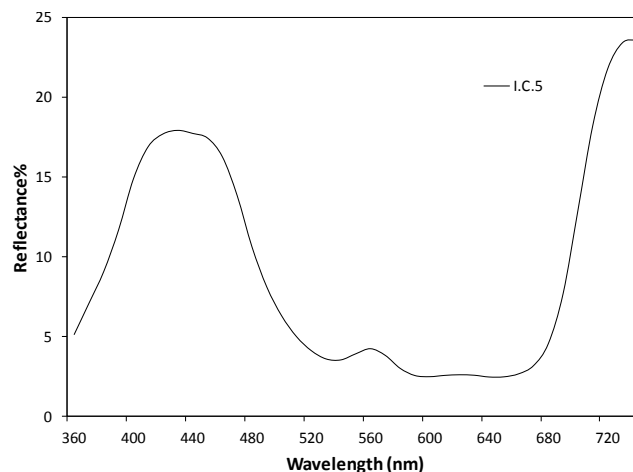


Figure 5.4 a) Optical spectral curve of I.C.2 yellow glaze b) and four deteriorated yellow glazes of I.C.7, I.E.1, I.E.7, and Q.J.2

## 5.3.3 Blues

The blue glazes showed the absorbance bands at 540, 590, and 650 nm as illustrated in Figure 5.5. These bands have been frequently attributed to a glassy matrix in which cobalt(II), in a tetrahedral symmetry ( $3d^7$  electronic configuration), have yielded a deep blue hue (Bamford, 1977; Staniforth, 1985; Duran *et al.*, 1986; Nelson and White, 1986; Mühlethaler and Thissen, 1993; Bacci and Picollo, 1996; Mirti *et al.*, 2000; Llusar *et al.*, 2001; Bacci, 2004; Padeletti *et al.*, 2004; Bianchin *et al.*, 2005; García-Heras *et al.*, 2005; Bacci *et al.*, 2007b; Fernández, 2009; Reiche *et al.*, 2009; Croveri *et al.*, 2010; Ceglia *et al.*, 2012). The cobalt(II) electronic spectra depend on the spin state (doublet or quartet) of the metal ion in the ground state and on its stereochemistry, that is, the spatial arrangement of the ligands around it. The most common arrangements in pigments are four-coordination (tetrahedral symmetry), six-coordination (octahedral symmetry), and eight-coordination (cubic symmetry). This last, although found with certainty in only a few synthetic compounds, cannot be ruled out in glass (Bacci and Picollo, 1996). The blue colour is developed when cobalt is tetrahedral coordinated by four oxygen ions. For this configuration, three transitions are allowed, but only two are detectable with normal spectrophotometers. These come from electronic  $d-d$  transitions from the  $^4A_2$  ground state to  $^4T_1(P)$  and  $^4T_1(F)$  states (Duran *et al.*, 1986; Keppler, 1992; Bacci and Picollo, 1996; Borgia *et al.*, 2002; Reiche *et al.*, 2009; Croveri *et al.*, 2010; Ceglia *et al.*, 2012). Both bands are characterised by three sub-peaks located around 530, 590, and 650 nm in the visible region (Llusar *et al.*, 2001; Ceglia *et al.*, 2012).

Figure 5.5 Optical curve of I.C.5 blue glaze in diffuse reflectance mode



The position of the first absorption band at around 540 nm may provide further information on the composition of glaze. In general, potash and soda glassy matrixes (where K and Na are used in flux agent) push this band towards higher wavelengths (Bacci and Picollo, 1996; Bacci, 2000; Bacci *et al.*, 2007b) in contrast with that of Ca-bearing glaze whose first band tends to lower wavelengths about 520 nm (Ceglia *et al.*, 2012). It may convey that our blue glazes are mainly obtained from cobalt ions in alkaline potash and soda glazes rather than calcium based glazes. Another issue which confirms this hypothesis is a weak shoulder at about 450 nm (Figure 5.5) reported by Bacci and Picollo (1996) as a shoulder in potash glasses. This shoulder has also been attributed to iron(III) ions which usually occurred in ancient glazes as a contamination (Ceglia *et al.*, 2012).

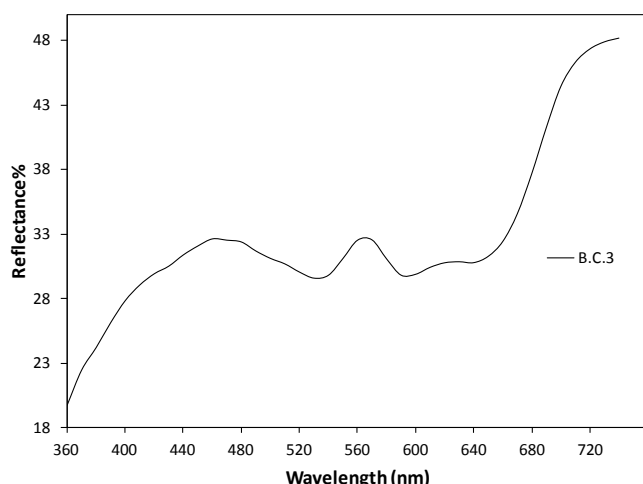
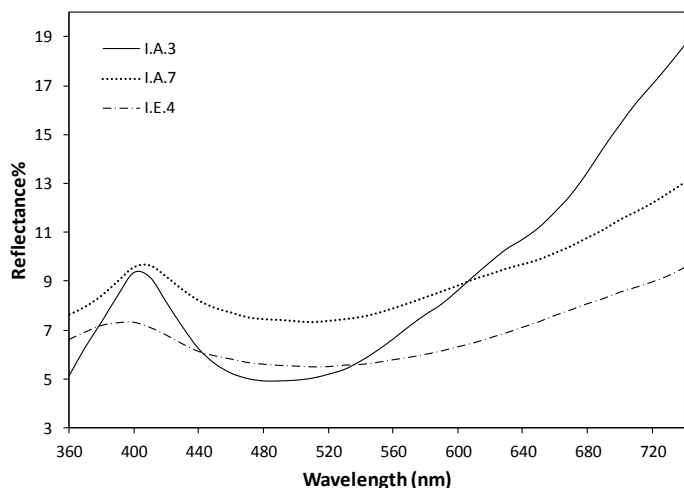


Figure 5.6 Reflectance spectra of the altered blue glaze of B.C.3

Other than the abovementioned optical spectrum, there are some blue glazes (*i.e.*, B.C. serie) which show the identical bands as those demonstrated in Figure 5.6. Having a look at these glazes, it can be seen that they are highly corroded and to a high extent are deteriorated (Figure 2.14). It is in accordance with the optical spectrum suggested by Mühlethaler and Thissen (1993) for degraded smalt blue. Figure 5.6 suggests an increased contribution of octahedral coordination of cobalt(II) in the degraded blue glaze to the tetrahedral coordinated cobalt(II) (Mühlethaler and Thissen, 1993) with electronic transitions from  $^4T_1$  to  $^4T_1$  and  $^4A_2$  (P) (Duran *et al.*, 1986).

### 5.3.4 Violets

A broad absorption band at around 490 nm and a weak shoulder at around 680 nm are characteristics absorption bands for the dark violet (almost black appearance) (Figure 5.7) attributed of manganese(III) ion in glass (Bamford, 1977; Brill, 1988; Mirti *et al.*, 1993b; Orlando *et al.*, 1996; Bacci *et al.*, 2007b; Bingham and Jackson, 2008; Carmona *et al.*, 2008; Fernández, 2009). This band can be assigned to the  $^5E_g$  to  $^5T_{2g}$  transition of octahedral coordinated manganese(III) (Keppler, 1992; Bingham and Jackson, 2008; Reiche *et al.*, 2009) which yields a purple and violet colour to the glazes. Moreover, due to the intensified violet colour of the glazes, manganese(III) ions have yielded such a hue in a high alkaline content glaze rather than a lead-based one (Carmona *et al.*, 2008).



Moreover, absence of chromium(III) absorption bands in an octahedral coordination at around 400 and 600 nm (Keppler, 1992; Jagannadha Reddy and Frost, 2005) rejects any possibility of the use of chromite ( $FeO.Cr_2O_3$ ) for obtaining the violet and black colours as it is reported to be a black colourant in ancient Persian glaze-making (see *Chapter Eight*, p. 98).

Figure 5.7 Typical reflectance spectra of the violet glazes

On the other hand, two violet glaze (I.E.3 and I.E.5) exhibited absorption bands of cobalt(II) other than those of manganese(III) (Figure 5.8). It shows that Co-bearing substance, as those for the blue glazes, have been probably added to manganese compounds to obtain a darker hue.

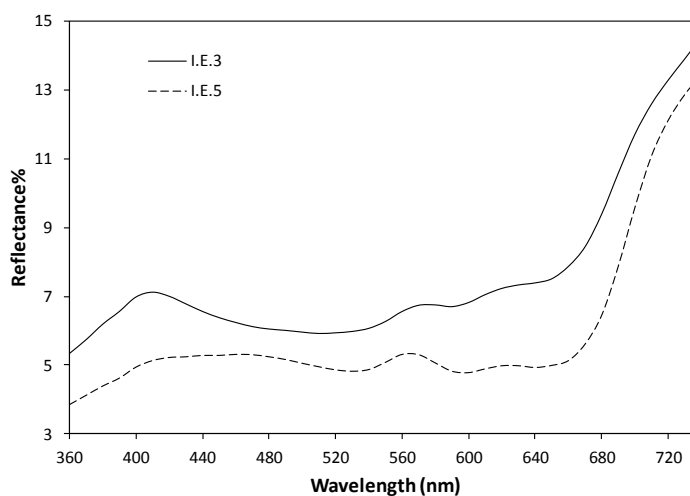


Figure 5.8 Absorption bands of the dark blue glazes of I.E.3 and I.E.5

## 5.3.5 Browns

Apart from few exceptions, all the brown glazes showed the absorption bands as those plotted in Figure 5.9. According to what stated about yellow glazes, the strong and broad absorption at wavelengths lower than 480 nm are associated to high quantity of lead content in the glazes. It seems that the brown glazes are chemically similar to the yellow glazes in which iron(III), with an absorption band at 580 nm in lead glazes (Stroud, 1971; Molera *et al.*, 1997), and manganese(III) with a weak shoulder at around 660 nm, have yielded a brown hue. This situation is more evident for the brown glaze of M.A.2 where two absorbance bands at about 490 and 650 nm are identical to those of manganese(III) in glaze matrix (Figure 5.10). The attribution of 580 nm band to iron(III) is, however, challengeable. Generally accepting, the bands at 380, 415, and 445 nm are attributed to iron(III) (Mirti *et al.*, 2000; Garcia-Heras *et al.*, 2005; Bacci *et al.*, 2007b; Bingham and Jackson, 2008; Schibille *et al.*, 2008; Reiche *et al.*, 2009; Ceglia *et al.*, 2012) giving a yellow hue to the glaze. The absence of these bands in the brown glazes may be justified by high lead content of the glazes which covers strongly the wavelengths lower than 480 nm and creates a lenser hue of brown glaze (Hampton, 1946). Meulebroeck *et al.* (2011), however, have attributed the absorbance peak at around 580 nm to ferri-sulfide ( $\text{Fe}^{3+}-\text{S}^{2+}$ ) bond formed under reducing atmosphere. Nonetheless, this attribution to the band at 580 nm to ferri-sulfide may not be valid in this case since the atmosphere of firing glazes has undoubtedly been oxidising (Wakamatsu *et al.*, 1987) (see Chapter Eight, p. 101).

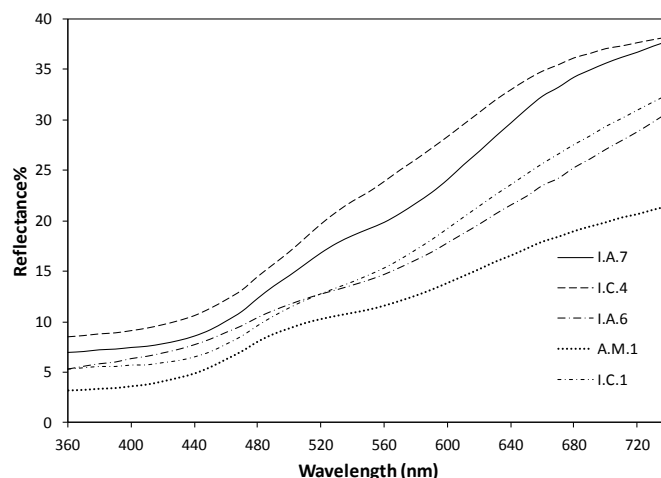
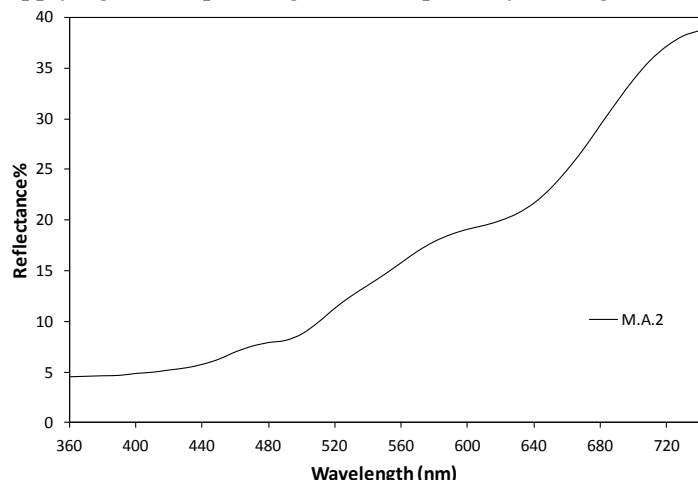


Figure 5.9 Optical reflectance spectra of some brown glazes

There are, at the same, two brown glazes (I.E.2 and I.E.4) which show an interesting feature. As their spectra show (Figure 5.11), they exhibit the same optical behaviour as the yellow glazes. Visual appearance of these samples (see Chapter Two, p. 21) suggests that these colours have been obtained by applying a transparent glaze on top of a yellow glaze to yield a brown hue. It simply suggests that the



optical spectra of the substrate yellow glazes have been recorded by spectrometer. Nonetheless, it should be noted that the absorbance bands of the upper transparent brownish glaze could not be most likely detected by the instrument because of low concentration of the colourant agent.

Figure 5.10 Optical reflectance spectra of M.A.2 brown glaze with two absorbance at 490 and 650 nm attributable to manganese(III)

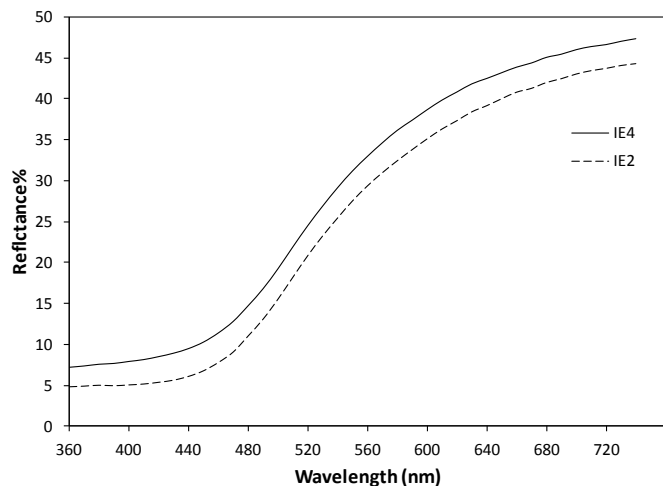


Figure 5.11 Optical reflectance spectra of the brown glazes of I.E.4 and I.E.2 demonstrate the identical lead-tin yellow type II spectra

### 5.3.6 Greens

All the green glazes show a broad absorption band after 720 nm. Moreover, there can be seen a high absorbance band at the wavelengths lower than 440 nm attributed to lead content of the glazes (Figure 5.12a-c). The green colour within the glazes has been most probably

obtained by copper(II) ions which show a high and broad absorption band at the 700-900 nm (Bamford, 1977; Mirti *et al.*, 1993b, 2000; Padeletti *et al.*, 2004; Bacci *et al.*, 2007b; Carmona *et al.*, 2008; Croveri *et al.*, 2010) (Unfortunately, because of the low band range detection of the spectrophotometer, the tail of the band can only be observed in Figure 5.12).

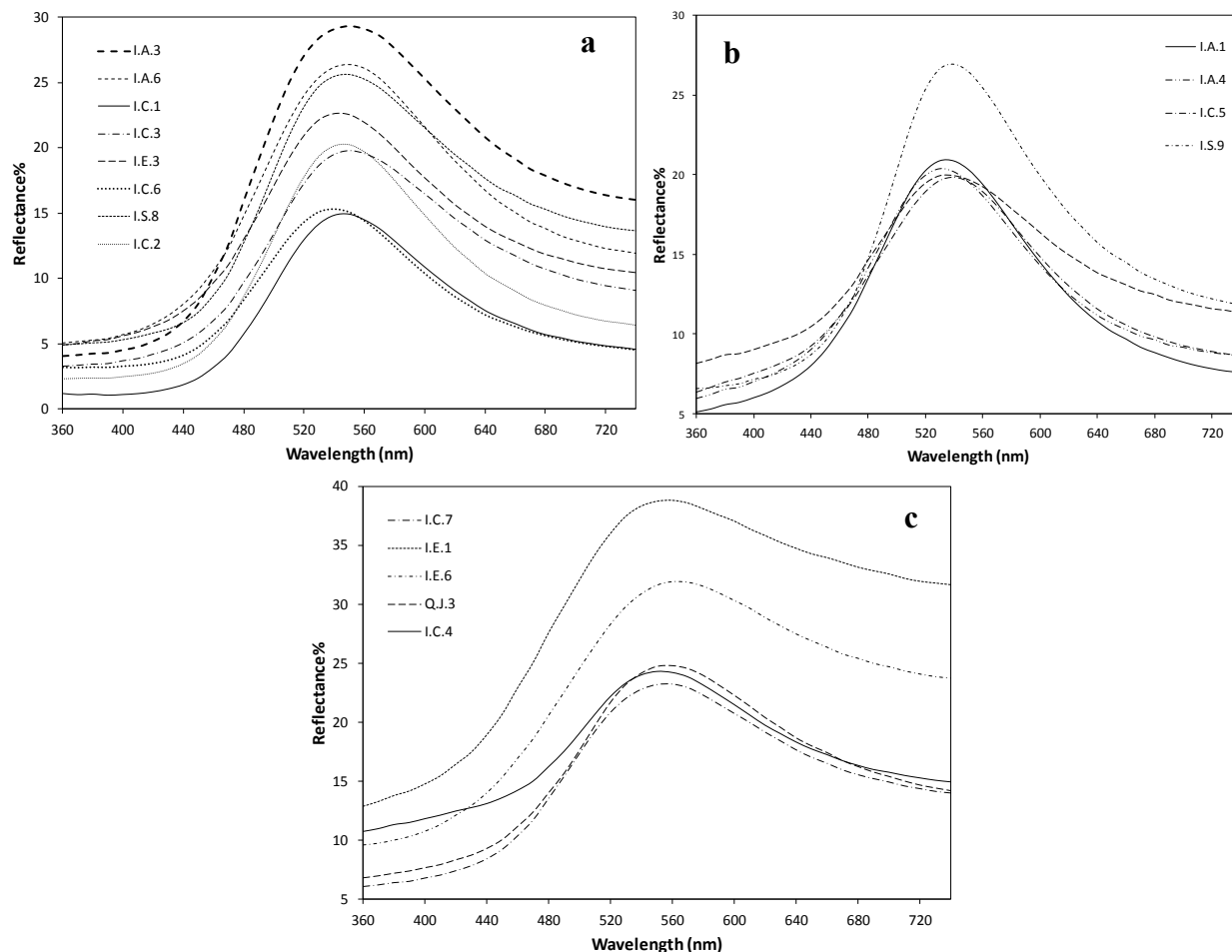


Figure 5.12 Different optical spectra of the green glazes: a) emerald green hue with the minimum absorbance at around 550 nm; b) dark green hue with the minimum absorbance at around 530 nm; c) light green hue with the minimum absorbance at around 570 nm

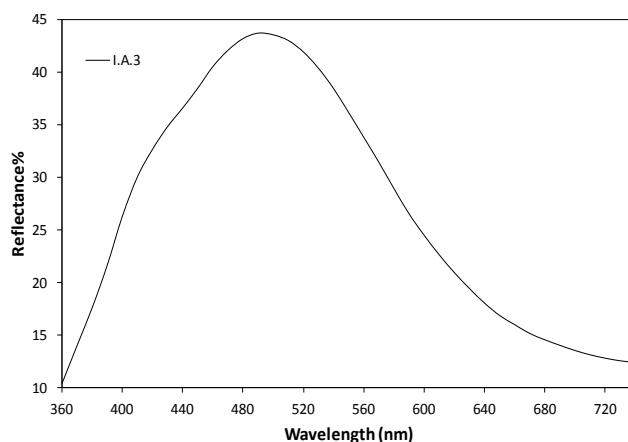
The copper(II) ion partially fill  $d$  orbitals creating colour centres in glass via an absorption band in the visible spectrum. In fact, the octahedral coordination of copper(II) in glass produces a ligand field splitting of the free ion energy level (Bae and Weinberg, 1994). The absorption bands are commonly assigned to the transition  ${}^2E_g(D)$  to  ${}^2T_{2g}(D)$  associated with the presence of copper(II) ions in an octahedral coordinaton (Keppler, 1992; Mirti *et al.*, 1995). Another issue concerning the green colour of the glaze is that this has nothing in common with the green colours obtained from chromium(III) in glaze with absorption bands at 630, 650, and 675 nm (Bamford, 1977; Carmona *et al.*, 2008; Reiche *et al.*, 2009).

Generally, by increasing the lead content of the glaze, maximum absorbance shifts towards lower wavelength and the glaze's colour tends to be more greenish (Carmona *et al.*, 2008), as for our green glazes. Both the facts (high absorption at lower 480 nm and higher 720 nm) show that the green glazes are to be classified as high-lead glazes. The minimum absorbance of copper(II)-bearing green glazes, on the other hand, is usually placed at around 530 nm (Padeletti *et al.*, 2004). As can be seen in Figure 5.12a-c, this minimum has been shifted in green glazes with various glazes and, therefore, different hues are appeared within the green glazes. It is probably due to different amounts of lead in the various types of the green glazes (see *Chapter Eight*, p. 100). Another issue which can be inferred from UV-Vis spectrum of the green glazes is that the atmosphere of firing was most certainly oxidising (Wakamatsu *et al.*, 1986).

### 5.3.7 Turquoises

Figure 5.13 shows the optical spectrum of I.A.3's turquoise glaze, which is similar with that of other turquoise glazes. The spectrum is characteristic of copper(II) in an octahedral symmetry in the soda glaze matrix fired in an oxidising atmosphere (Wakamatsu *et al.*, 1986). In fact, characteristic bands of copper(II) in a sodium silicate glass at 450 nm (shoulder) and 780 nm (Bamford, 1977; Carmona *et al.*, 2008; Reiche *et al.*, 2009) are clearly seen in Figure 5.14a. The minimum absorption for turquoise glazes, in contrary with the green glazes, is shifted to 480 nm due to the sodium content of the glazes (Padeletti *et al.*, 2004). Moreover, low absorbance in the wavelengths lower than 400 nm shows that the lead content of the glazes is not high. However, as for the green glazes, although the maximum absorbance band of copper(II) cannot be seen in Figure 5.13, due to low wavelength range of the spectrum, the maximum absorption has been probably shifted to the wavelengths longer than 780 nm. It shows that the turquoise glaze contain some amounts of lead oxide on their composition. Moreover, having a look at Figure 5.1, the hue and colour coordinates of the turquoise glazes is very similar to those suggested by Pagès-Camagna and Colinart (2003) for Egyptian blue pigment quenched rapidly.

Figure 5.13 Typical optical spectrum of the turquoise glazes with diffuse reflectance light



Due to the tendency of sodium silicate glazes to deterioration through the time, some turquoise glazes exhibited different optical spectral curves like those showed in Figure 5.14. The minimum absorption in these turquoise glazes has been shifted to higher wavelengths and they almost reflect the wavelengths higher than 520 nm and, thus, they look like a matte surface with a weak hue of turquoise colour.

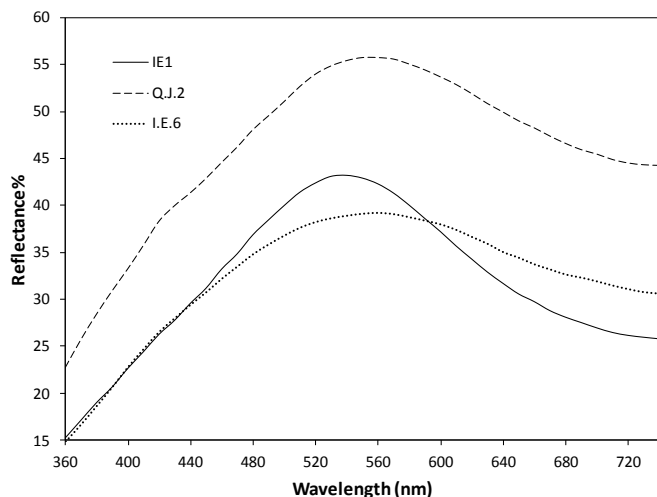


Figure 5.14 Optical spectra of deteriorated turquoise glazes

### 5.3.8 Final discussion

Sometimes it is not so simple to attribute a given spectrum to an identical compound and, hence, correlation analysis is often necessary. Derivative spectroscopy can be useful in this regard to discriminate different colours easier (Bacci, 1995; Bacci *et al.*, 2007a). Figure 5.15 demonstrates the first derivative extraction of the various coloured glazes differentiating very well the glazes and their maximum and minimum absorption bands. The derivative values of each glaze were obtained from their representative showed in the previous optical spectra. In Figure 5.15, maxima and minimum absorbance of the various coloured glazes can also be seen well-demonstrated.

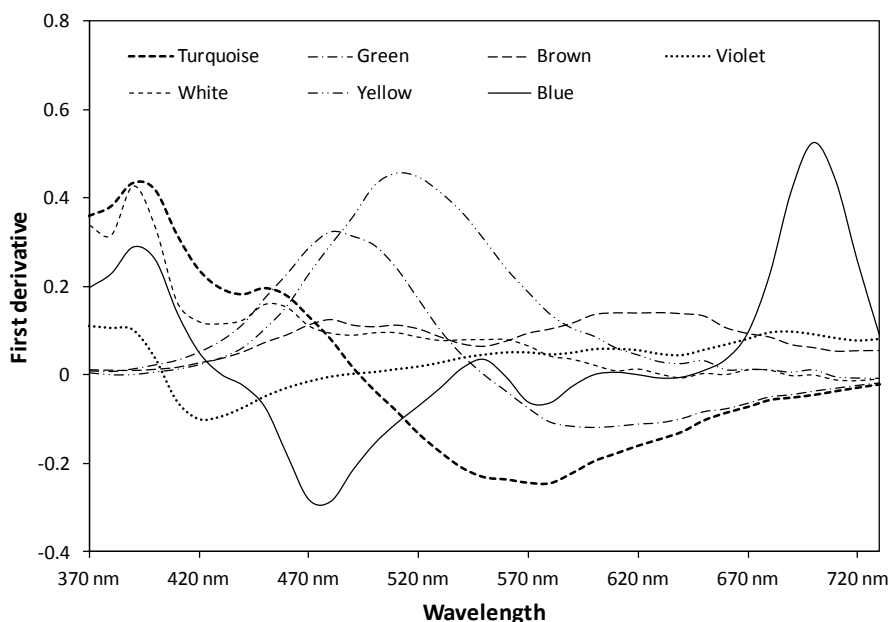


Figure 5.15 First derivatives of visible spectra of the coloured glazes

## Chapter Six: Micro-Raman spectroscopy on glaze characterisation

### 6.1 Introduction

Since 1928, when Raman scattering was discovered by Sir Chandrasekhra Venkata Raman, Raman spectroscopy has been widely used in different scientific fields, including art conservation and archaeological sciences (Cariati and Bruni, 2000; Vandenberghe, 2004; Baraldi and Tinti, 2008). Various types of archaeological materials such as pigments, dyes, textiles, corrosion products of metallic objects, *etc.* have been increasingly investigated so far by Raman spectroscopy (Cariati and Bruni, 2000; Smith and Clark, 2004; Madariaga, 2010). Raman spectroscopy, however, in archaeological ceramics and glassy materials has not been extensively considered as a primary analytical alternative. Usually, due to the weak Raman scattering of vitreous silica (Smith and Clark, 2004) and the strong fluorescence as a result of burial environments or artifact handling, no useful Raman spectra could be usually obtained for pottery or faience fragments (Clark and Gibbs, 1997b; Cariati and Bruni, 2000; Smith and Clark, 2004). Moreover, the problem of defocusing of the laser excitation upon passing through the glassy material, which itself can act as a lens (Smith and Clark, 2004), is another challenge of using Raman spectroscopy for investigating glass and glazed materials. Nonetheless, despite these problems, Raman spectroscopy has recently found its appropriate position in surveying these sorts of samples either in industrial applications (Brawer and White, 1975, 1977; Worrell and Henshall, 1978; Furukawa *et al.*, 1981; McMillan, 1984; Ho *et al.*, 1995; Robinet *et al.*, 2008) or archaeological uses (Bertoluzza *et al.*, 1995; Clark *et al.*, 1997a; 1997b; Clark and Gibbs, 1997b; Clark and Curri, 1998; Edwards and Tait, 1998; Brooke *et al.*, 1999; Zuo *et al.*, 1999; Colomban and Treppoz, 2001; Colomban *et al.*, 2001, 2003; Liem *et al.*, 2002; Sakellariou *et al.*, 2004; Colomban, 2003, 2005; Barilaro *et al.*, 2005; Colomban and Paulsen, 2005; Colomban *et al.*, 2004; 2005; Colomban and Milande, 2006; Robinet *et al.*, 2006; Sandalinas *et al.*, 2006; Catalano *et al.*, 2007; Kock and De Waal, 2007; Ricci *et al.*, 2007; Prinsloo and Colomban, 2008; Ricciardi *et al.*, 2009; Rosi *et al.*, 2009; Kirmızı *et al.*, 2010; Miao *et al.*, 2010; Sendova *et al.*, 2010; Tournié *et al.*, 2010; Rosi *et al.*, 2011).

Raman spectroscopy yields information about molecular and crystal lattice vibrations and, therefore, is sensitive to the composition, bonding, chemical environment, phase, and crystalline structure of materials. These characteristics make it an exceptional method for identifying materials in any physical form (Smith and Clark, 2004). Raman scattering is, in fact, derived from inelastic collisions of the electromagnetic radiation with a substance. When the electromagnetic radiation collides a molecule, as a matter of fact, it can be transmitted, absorbed or scattered. When the incident and the scattered radiations have the same frequency (elastic collision) the effect of Rayleigh scattering is occurred. On the contrary, in the Raman scattering, produced by an inelastic collision, the differences in energy between the incident and the scattered photons are quantised which corresponds with the vibrational or the rotational levels of the molecule (Cariati and Bruni, 2000; Smith and Clark, 2004). We do not go further in the details of the

phenomenon since more details about Raman effects and its basics can be referred to the previously published literature (Long, 2002; Ferraro *et al.*, 2003; Long, 2005).

## 6.2 Sample preparation and the instrumentation

Samples subjected to micro-Raman spectroscopy were the same as those whose optical properties were measured by UV-Vis spectroscopy. More than 300 Raman spectra were obtained from various coloured glazes. Nonetheless, sampling for Raman investigations demanded a slight difference with that of UV-Vis spectroscopy. As far as the literature regarding Raman spectroscopy on glazed objects is concerned, the major application of Raman spectroscopy has been focused on focusing the laser on the pigment grains suspended in the glazes by exposing them. Hence, cross sections of glazed samples, where the pigment can be exposed at the edges of the cracked fragments, are generally suggested to be investigated by Raman spectroscopy (Clark *et al.*, 1997a; Clark and Gibbs, 1997b; Clark and Curri, 1998; Cariati and Bruni, 2000; Barilaro *et al.*, 2005). Apart from the suspended pigment in glaze matrixes, structural vibrations of the glaze matrixes were also investigated by Raman spectroscopy in our studies.

To reduce the problem of fluorescence associated with glazed objects, one can use longer wavelengths of exciting laser. In other words, the longer wavelength of laser radiation used as an excitation source, the lower intensity of fluorescence could be (Smith and Clark, 2004). The use of lasers with lower wavelength, like red light laser, is preferred to analyse specifically the low wavenumbers below  $200\text{ cm}^{-1}$ . However, it should be considered that Raman scattering with low wavelength lasers is rather weak. One can also overcome the problem of fluorescence using ‘bleaching’ laser radiation prior to the final measurements which allows better recording of the Raman spectrum (Colomban, 2005). On the other hand, the use of a confocal system in micro-Raman spectroscopy also can enhance the spatial resolution of Raman spectra. It, in fact, allows us to focus on an appropriate grain or pigment suspended in a glaze and to eliminate Raman signals originating from above and below this position (Colomban, 2005). The exciting line power used is also an important issue in the Raman spectroscopy. Typically, the power of illumination is kept low to reduce local heating which can modify the material nature by oxidation (Castro *et al.*, 2005; Colomban, 2005).

Considering abovementioned remarks, Raman spectra of the samples were obtained from cross sections of the samples using an Olympus BXFM microscope coupled to a LabRam HR800 spectrometer (Horiba Jobin Yvon, France) fitted with an air-cooled CCD detector ( $1024 \times 256$  pixels) at  $-70^\circ\text{C}$ . The spectrometer had a focal length of 80 mm and was equipped with two 600 and 1800 groove/mm gratings. Raman spectra were recorded using a He-Ne laser as excitation source with wavelength of 632.81 nm. The laser power was always kept between 0.2 and 4 mW and the exposure time varied between 5 and 10 seconds with 10 accumulations. Spectra were recorded by placing the samples on the X-Y motorised stage and observing them with 50x and 100x objectives. The spectrometer was calibrated and checked with silicon at  $520\text{ cm}^{-1}$ . The removal of spikes of cosmic rays was performed by LabSpec 5 software.

## 6.3 Interpretation of the Raman spectra of various coloured glazes

Prior to get into the interpretation of Raman spectra of the different coloured glazes, it is necessary to be indicated that transition metal ions ( $\text{Cu}^{2+}$ ,  $\text{Co}^{2+}$ ,  $\text{Mn}^{3+}$ , *etc.*) usually become part of the glassy lattice in the process of making colour in glazes. Here, the Raman scattering will not be very sensitive and only the glassy matrix fingerprint will appear (Colomban, 2005; Colomban *et al.*, 2001). However, it is worth to

observe precisely this glassy fingerprint since it suggests solid facts about the nature of a glaze: alkalinity or being Pb or Ca-bearing. Nonetheless, Raman spectra of amorphous phases are sometimes difficult to interpret because of the low content of spectral features (Sendova *et al.*, 2010). On the other hand, apart from dissolution of the transitional metal ions, a colour can arise from precipitation of a new phase in the glass matrix or dispersion of a phase which has been formed before incorporation into the glaze (Colomban *et al.*, 2001). Therefore, besides the investigations carried out on the structure of the glazes, another essential part of this chapter is to focus on the newly formed particles and primary crystals in the glazes.

### 6.3.1 General facts about Raman spectra of amorphous glazes

Before to start explaining how the interpretation Raman spectra of glassy lattices works, it should be noted that ancient and historic glazes have complex compositions with many different cations present at varied concentrations, each cation having an effect on the silicate structure and consequently on the Raman spectrum. All these effects will be superimposed in the Raman spectra, making the interpretation more difficult (Robinet *et al.*, 2006). The literature presented here is just obtained from pure and previously known materials and may not be valid for the interpretation of ancient technology. However, they may also push us towards a more realistic image of the materials under question.

In silicate glazes, the backbone structure is composed of silicate tetrahedra,  $\text{SiO}_4$ , joined by bridging oxygens. Network modifiers are normally added to modify the properties of the glazes. For instance, alkali ions lessen the melting point while alkaline-earth and aluminum ions stabilise the glaze towards alteration. Lead can be present either as a network modifier or a network former. Incorporating the modifier cations into the structure breaks the Si–O connectivity by replacing Si cations, leading to the creation of ‘non-bridging oxygens’ (NBOs) within the silicate structure (Brawer and White, 1975). The presence of NBOs in the structure enhances the susceptibility of silicate glasses to alteration, primarily as a result of the depolymerisation of the silicate network. The notation  $Q^n$ , where  $n$  is the number of bridging oxygens, is used to distinguish between the different tetrahedral species in the network; that is,  $Q^3$  corresponds to silicate species with one NBO ( $\text{Si}_2\text{O}_5$ ),  $Q^2$  to silicate species with two NBOs ( $\text{SiO}_3$ ) and  $Q^4$  to silicate species with no NBO ( $\text{SiO}_2$ ) (Brawer and White, 1977; Ho, 1995; Robinet *et al.*, 2008). The cation type and concentration, thus, influence the Q distribution through the conservation of the charge balance and stoichiometry in the glass structure (Robinet *et al.*, 2006). The more electronegative the metal cation, the stronger is its tendency to form bonds with NBO in the least polymerised  $Q^n$  species. Thus, alkali cations are preferentially bonded to NBO from  $Q^3$  units, while alkaline earth or polyvalent cations are preferentially bonded to NBO from  $Q^2$  units (Brawer and White, 1977; Ho, 1995; Robinet *et al.*, 2008).

The Raman spectra of amorphous glazes are usually composed of two broad bands. The first one is located at about  $500\text{ cm}^{-1}$  related to the bending mode (McMillan, 1984; Ho, 1995; Liem *et al.*, 2002; Colomban *et al.*, 2003; Robinet *et al.*, 2006, 2008; Prinsloo and Colomban, 2008; Rosi *et al.*, 2011) and to be associated with  $\alpha$ -quartz line at  $464\text{ cm}^{-1}$ . As the silica content of the glass is reduced, the band moves to a higher wavenumber (Ho, 1995). This Raman line corresponds to a displacement of the bridging oxygen along a line bisecting the Si–O–Si angle and is the strongest mode for structures composed of connected  $\text{SiO}_4$  tetrahedral units. Thus, this mode is very sensitive to the modification of the tetrahedral network imposed by the vicinity of alkali or alkali earth cations. Consequently, it can be used as a probe for detecting a given aluminosilicate network, either amorphous or crystalline (Colomban *et al.*, 2003).

The other main band in glazes spectra is located at around  $1000\text{ cm}^{-1}$  and originates from Si–O stretching mode (Ho, 1995; Liem *et al.*, 2002; Colomban *et al.*, 2003; Robinet *et al.*, 2006; 2008; Rosi *et al.*, 2011). The centre of gravity of the two bands is very different depending on the nature of glazes (Colomban *et al.*, 2003). Raman bands at  $550$  to  $600\text{ cm}^{-1}$  is a blending of several modes. The  $\text{Si}_2\text{O}_5$  unit has several strong modes near these frequencies (Brawer and White, 1975, 1977). The band near  $550\text{ cm}^{-1}$  in the spectra of soda silicate glazes is probably caused by the Si–O–Si bending vibration of the linkage associated with the  $\text{Q}^3$  species, while the component near  $600\text{ cm}^{-1}$  is often assigned to Si–O–Si bending vibrations in depolymerised species such as  $\text{Q}^2$  (Robinet *et al.*, 2006). In fact, the locations of the Raman bands in the  $400$ – $700\text{ cm}^{-1}$  region are associated with the degree of polymerization involving Si–O–Si linkages between the silicate tetrahedral. The wavenumber changes accompanying glass compositional changes could be attributed to differences in the nature of the silicate clustering.

Vitreous glazes usually show an asymmetric band near  $800\text{ cm}^{-1}$ , with probable components at  $790$  and  $830\text{ cm}^{-1}$ . In alkali silicate glass systems, this band broadens and shifts to slightly lower frequency with decreasing silica content, to around  $750\text{ cm}^{-1}$  (McMillan, 1984). This band is linked to the motion of Si against its tetrahedral cage (Robinet *et al.*, 2006, 2008) and, for lead glazes, it is often not clear. It could be indicative of a stronger interaction between the lead and the oxygen atoms bonded to the silicon, resulting in a decrease in the silicon-oxygen bond strengths, thus displacing this bond-stretching mode to a lower frequency (Worrell and Henshall, 1978).

The region  $900$ – $1000\text{ cm}^{-1}$  is associated with the Si–O stretching vibration of  $\text{Q}^2$  species (Furukawa *et al.*, 1981; Robinet *et al.*, 2006). An enhancement of this region is observed with the increase in calcium content (Robinet *et al.*, 2006). However, it can be said that the replacement of soda by lime has a relatively small effect on the Si–O network. It increases the amount of disorder, probably in the form of bond length and angle fluctuations, but the glass network is qualitatively unaltered (Brawer and White, 1977). At the same time, Robinet *et al.* (2008) believe that the peak at  $950\text{ cm}^{-1}$ , which is likely associated with the presence of alkaline-earth cations in the glass, often disappeared in the decomposition when no or very little alkaline-earth cations were present.

The peak around  $1100\text{ cm}^{-1}$ , particularly intense in alkali silicate glass spectra, is associated with the symmetric Si–O stretching vibration of the major  $\text{Q}^3$  species (Robinet *et al.*, 2006). The width of the  $1100\text{ cm}^{-1}$  peak varies systematically as a function of composition and the type of modifier. The order of the Si–O network decreased with increasing field strength of the modifier (Brawer and White, 1977). In lead glazes, the high electronegativity of the lead cation induces a weakening of the Si–O bonds causes the intense peak at around  $1070\text{ cm}^{-1}$  shift (Robinet *et al.*, 2008). The peak at  $1035\text{ cm}^{-1}$  in lead glazes is probably equivalent to the  $1040\text{ cm}^{-1}$  component in the alkali silicate glass spectra model, and therefore is likely associated with the vibration of bridging Si–O bonds in silicate species that are not fully polymerised (Robinet *et al.*, 2008). Moreover, the component at  $1150\text{ cm}^{-1}$  results from the superimposition of the Si–O stretching vibration of  $\text{Q}^4$  and a different type of  $\text{Q}^3$  species (Robinet *et al.*, 2008). Fully polymerised silicates  $\text{Q}^4$ , corresponding to vitreous silica regions, display a weak Si–O stretching vibration around  $1150\text{ cm}^{-1}$  (Robinet *et al.*, 2006).

Raman spectra of the lead alkali silicate glasses and the high lead silicate glazes display different profiles. The main distinction between these two types of glazes is the presence of an intense peak around  $1070\text{ cm}^{-1}$  in the spectra of lead alkali silicate glazes, which corresponds to the vibration of  $\text{Q}^3$  species. In general, the lead content increase induces a shift of the stretching region towards lower wavenumbers, the

band being centered around  $1050\text{ cm}^{-1}$  in lead alkali silicate and  $950\text{ cm}^{-1}$  in the high lead silicate glazes (Robinet *et al.*, 2008) due to the large atomic mass of the lead atom (Worrell and Henshall, 1978). An explanation of this band is that introduction of  $\text{Pb}^{2+}$  ions into the silica network breaks some of the silicon-oxygen bonds, with the production of groups of the type  $\equiv\text{Si}-\text{O}^0$  or  $\equiv\text{Si}-\text{O}^- \dots \text{Pb}^{2+}$ . Thus, the presence of the lead atoms weakens the Si-O bond, and displaces this type of silicon-oxygen bond-stretching mode to lower frequencies (Worrell and Henshall, 1978). In lead glazes, moreover, the intensity of the  $300\text{-}600\text{ cm}^{-1}$  region is decreased and the weak band around  $800\text{ cm}^{-1}$  is disappeared. All changes are directly associated with the decrease of the silica content and the depolymerisation of the network (Robinet *et al.*, 2008).

## 6.4 Coloured glazes and micro-Raman spectroscopy

### 6.4.1 Turquoise glazes

Almost all the Raman spectra of the turquoise glazes showed an identical spectrum demonstrated in Figure 6.1. According to the aforementioned literature, this spectrum is representative of an alkaline lattice. Two bands at ca.  $470$  and  $550\text{ cm}^{-1}$  show an alkaline lattice for the turquoise glazes. Moreover, the clear evidence of alkaline structure of the glazes is the band centered at  $1090\text{ cm}^{-1}$ . The band at  $470\text{ cm}^{-1}$  can also show a less amorphous lattice since this feature is related to  $\alpha$ -quartz and not shifted to higher wavenumbers as a result of network modifiers. Moreover, another feature which shows alkaline nature of the turquoise glaze is the broad band at about  $800\text{ cm}^{-1}$  which generally is not appeared in lead based glazes. The tendency of this band towards higher wavenumbers (around  $800\text{ cm}^{-1}$ ) also shows the high content of crystalline silica in its composition. An evidence of high silica content of the turquoise glazes was the abundant unsolved quartz particles inside the glazes with the Raman bands at  $201$ ,  $262$ ,  $359$ ,  $400$ , and  $463\text{ cm}^{-1}$  (Figure 6.2) (Brooke *et al.*, 1999; Barilaro *et al.*, 2005).

Figure 6.1 Raman spectra of the turquoise glaze of I.A.2

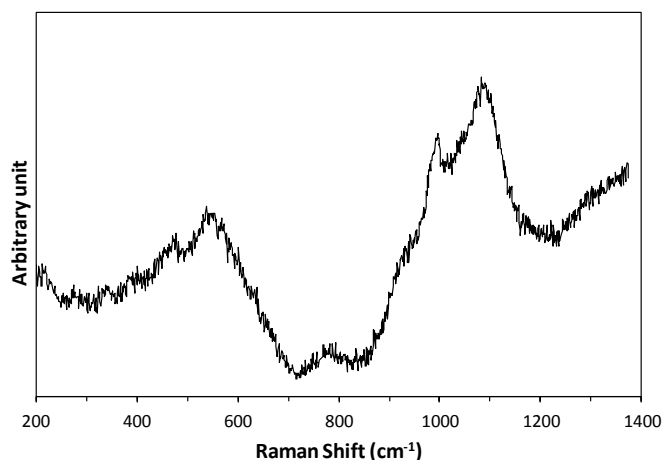
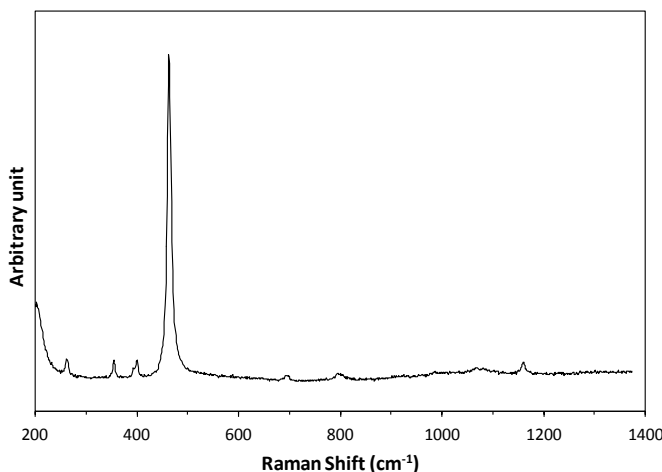


Figure 6.2 Quartz in the turquoise glaze of I.B.1

Another technological aspect, which was revealed by Raman spectroscopy survey through the turquoise glazes, was the identification of the black particles in the glassy matrix (Figure 6.3a). Raman spectra of this particle showed bands at  $285$ ,  $332$ , and  $619\text{ cm}^{-1}$ , corresponding to the  $A_g$ ,  $B_{1g}$  and  $B_{2g}$  symmetries respectively,



which are characteristic of the black copper oxide (tenorite) (Guha *et al.*, 1991; Chou *et al.*, 2008; Mattei *et al.*, 2008) (Figure 6.3b). Copper oxide was commonly used in the form of flakes in the composition of alkaline glazes to yield a turquoise hue (see *Chapter Eight*, p. 99).

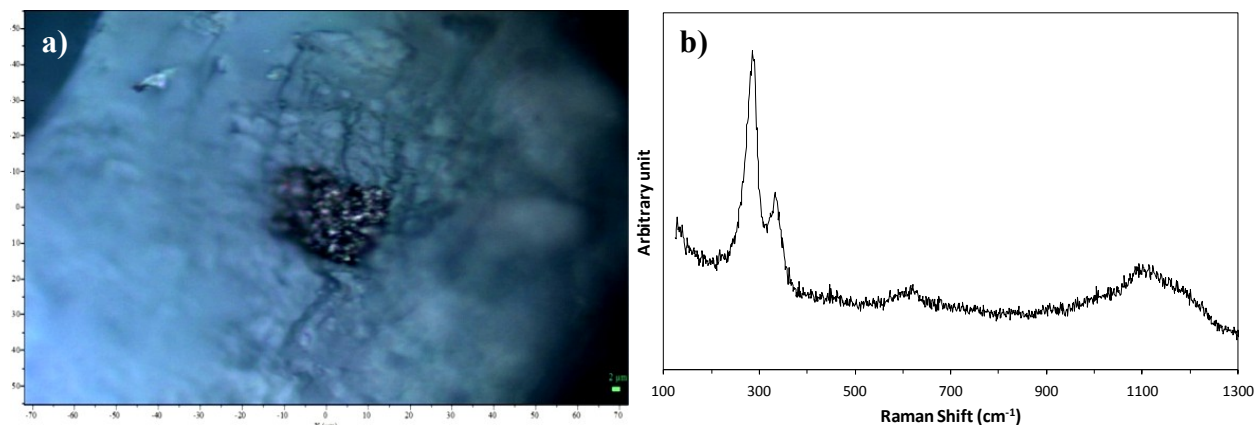
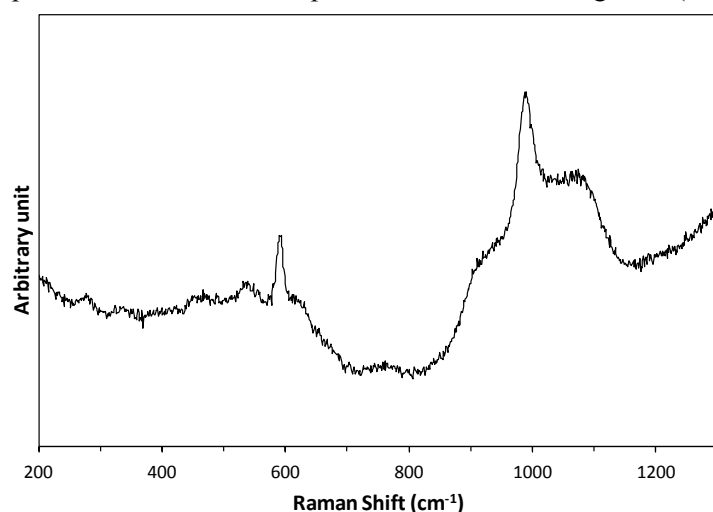


Figure 6.3 a) Copper oxide in the turquoise glaze of I.E.3 b) and its Raman spectrum

A distinct group of the turquoise glazes comprising of I.E.3, I.A.7, I.B.1, I.B.2, I.C.3, I.E.1, Q.J.1, I.S.9, I.E.6, I.E.2, and I.A.3 demonstrate two sharp peaks at about 590 and 990  $\text{cm}^{-1}$ . The typical spectrum of this group is showed in Figure 6.4. These two bands might most likely be associated to calcium (or the other alkaline-earth element, magnesium) content of the glazes. Another probable hypothesis for the sharp band at 990  $\text{cm}^{-1}$  is the presence of copper cations in the glazes since the cations generally induce a sharp peak at 990  $\text{cm}^{-1}$  in the spectra of alkali silicate glazes (Robinet *et al.*, 2008). The sharpness of the band



may indicate that copper ions are within a more organised structure (Robinet *et al.*, 2006). It seems, however, that the second hypothesis for the turquoise glazes is more valid since the usual way of making turquoise hues in the alkaline glaze has been the use of copper ions inside the glaze's lattice.

Figure 6.4 Sharp bands at 590 and 990  $\text{cm}^{-1}$  in the turquoise glaze of I.A.7

#### 6.4.2 Blue glazes

First of all, it should be noted that all the blue glazes, apart from some exceptions, were entirely transparent and their Raman spectra almost did not show any special band concerning to a particular blue colourant. Previously detected in archaeological ceramics, neither azurite (Brooke *et al.*, 1999), nor lapis lazuli (Clark *et al.*, 1997b; Colombari, 2003; Catalano *et al.*, 2007; Sendova *et al.*, 2010; Tournié *et al.*, 2010), nor the cobalt blue ( $\text{CoAl}_2\text{O}_4$ ) (Kock and De Waal, 2007) were detected in the Raman spectra of

the blue glazes. The typical blue spectrum of the blue glazes is showed in Figure 6.5. The fact is that the blue hue is most probably derived from cobalt ions since no specific Raman band is expected hen from a dissolved cobalt(II) in glaze lattice (Colomban *et al.*, 2004; Barilaro *et al.*, 2005). In addition, the glazes were not saturated enough by cobalt ions to see a spinel or olivine types in the composition of the glaze (Colomban *et al.*, 2001, 2004).

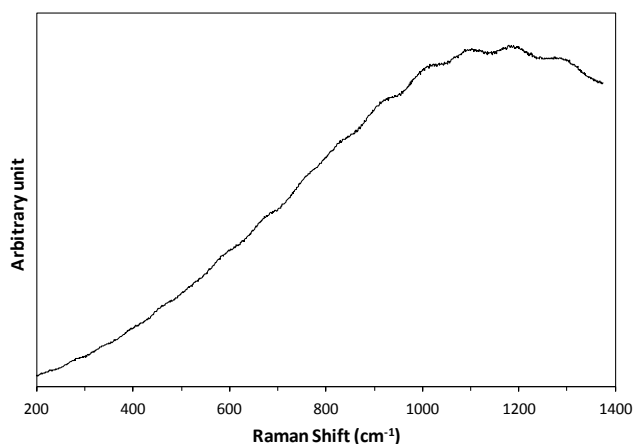


Figure 6.5 Raman spectrum of the I.E.5 blue glaze

Among the blue glazes, some exceptions showed undissolved particles which could act as opacifiers in their compositions. For instance, I.A.5, I.E.6, and B.C.2 blue glazes showed tin oxide (cassiterite) opacifier with Raman bands at 472, 633, and 775  $\text{cm}^{-1}$  (Barilaro *et al.*, 2005; Kock and De Waal, 2008; Ricciardi *et al.*, 2009; Kırmızı *et al.*, 2010; Rosi *et al.*, 2011) corresponded to  $E_g$ ,  $A_{1g}$ , and  $B_{2g}$  respectively (Diéguez *et al.*, 2001) (Figure 6.6a) and, furthermore, I.A.1 and I.B.1 demonstrated quartz with the previously mentioned Raman bands in their composition (Figure 6.6b).

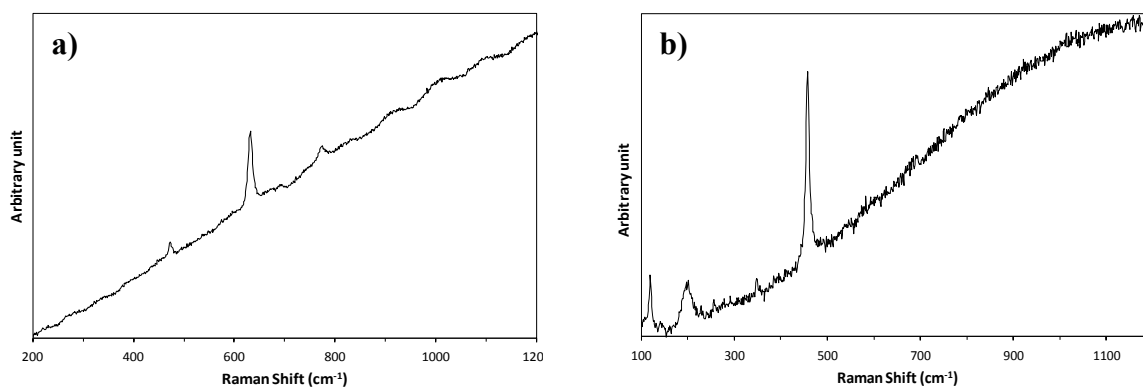
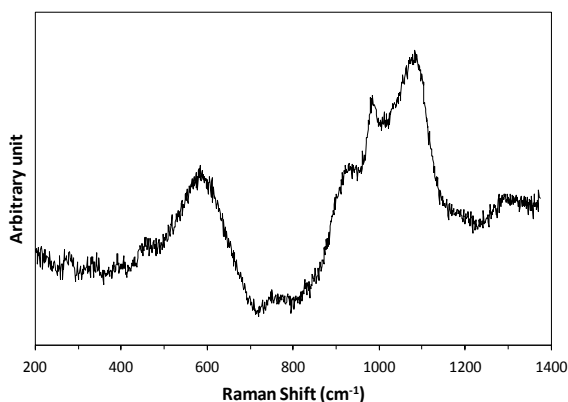


Figure 6.6 a) Raman spectrum of cassiterite in I.A.5 and b) quartz in I.A.1 blue glazes

#### 6.4.3 Violet glazes



The violet glazes, apart from some exceptions, showed the same Raman spectra as those of the turquoise glazes from which the Raman spectrum of I.C.2 is showed in Figure 6.7. As suggested for the turquoise glazes, the alkaline lattice of the glazes is clearly seen in Figure 6.7 due to two bands at about 470 and 590  $\text{cm}^{-1}$ , a broad band at around 800  $\text{cm}^{-1}$  and the peaks at 930, 980, and 1080  $\text{cm}^{-1}$  which are characteristic of alkaline glassy matrixes.

Figure 6.7 Raman spectrum of the violet glaze of I.C.2

#### 6.4.4 White glazes

As mentioned in the previous chapter, the main cause of a white colour in glazes is the scattering of the incident light by dispersed particles in a given glazes lattice. In accordance with the previous results, the unique particle used as opacifier in the white glazes of the *haft rang* tiles was identified as tin oxide (cassiterite). The bands at 474, 633, and 775  $\text{cm}^{-1}$  were frequently seen in the white glazes proved the presence of  $\text{SnO}_2$  as the opacifier of the glazes. The absence of the Raman bands of calcium antimonate (Ricciardi *et al.*, 2009; Tournié *et al.*, 2010), zircon (Colomban *et al.*, 2004), and titanium oxide (Zuo *et al.*, 1999), as usual opacifiers of glazes, gave more validity to tin oxide as the main opacifier of the glazes.

#### 6.4.5 Yellow glazes

All the yellow glazes are opacified with an opacifier exhibited a Raman spectrum like that showed in Figure 6.8. Two narrow bands at 68 and 80  $\text{cm}^{-1}$  together with, the strongest one at around 133  $\text{cm}^{-1}$ , a small shoulder at 253  $\text{cm}^{-1}$ , a broad band at 322  $\text{cm}^{-1}$ , another weak peak at about 450  $\text{cm}^{-1}$ , and a broad band centered at about 950  $\text{cm}^{-1}$  were the characteristic Raman bands of the yellow pigment suspended in glassy lattice of the yellow glazes. The aforementioned Raman bands are very close to those of lead tin yellow type II ( $\text{PbSn}_{1-x}\text{Si}_x\text{O}_3$ ) presented in the literature (Clark *et al.*, 1995; Bell *et al.*, 1997; Prinsloo and Welter *et al.*, 2007; Colomban, 2008; Miao *et al.*, 2010). The Raman bands at approximately 100  $\text{cm}^{-1}$  occur due to the presence of  $\text{Pb}^{2+}$  ions in the glaze lattice. This band might originate from a perturbation of a lattice mode of silicon due to the presence of  $\text{Pb}^{2+}$  ions (Worrell and Henshall, 1978). Moreover, the strong band at 133  $\text{cm}^{-1}$  is characteristic of lead silicate glazes witnessing Pb–O stretching mode (Worrell and Henshall, 1978; Sakellariou *et al.*, 2004). By increasing the lead content, the intensity of this band is accordingly increased (Furukawa *et al.*, 1978). In addition, the shoulder at the region of 450  $\text{cm}^{-1}$  is associated with the Raman active OSiO angular bending mode of vibration (Worrell and Henshall, 1978). Ultimately, the broad band around 800–1200  $\text{cm}^{-1}$  confirms that the lead glassy phase is formed above 600°C (Ricci *et al.*, 2007).

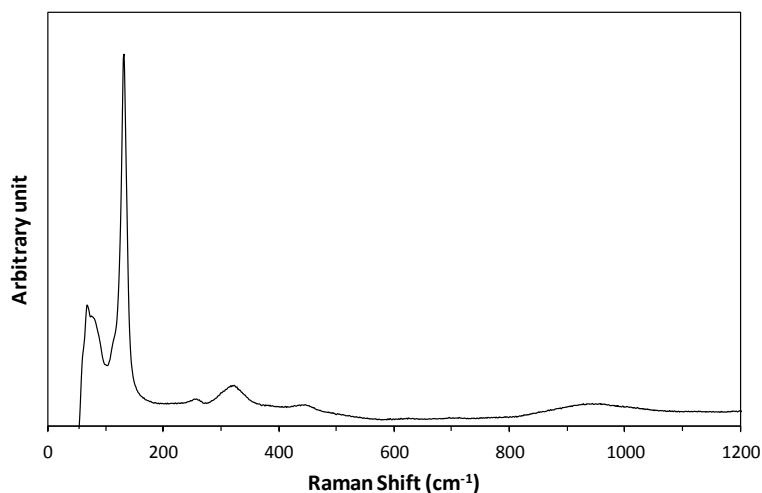


Figure 6.8 Raman spectrum of I.C.7 yellow glaze

One should consider that there is always a challenge in discriminating lead tin yellow type II against the lead antimonate yellow (Naples yellow) since they show almost an identical Raman spectrum which makes it difficult to distinguish them by Raman spectroscopy (Clark *et al.*, 1995; Ruiz-Moreno *et al.*, 2003; Sakellariou *et al.*, 2004; Tournié *et al.*, 2010). Nonetheless, a small difference in slight shift of the strongest stretching Raman band at 133  $\text{cm}^{-1}$  in lead tin bearing glazing towards higher wavenumbers (about 145  $\text{cm}^{-1}$ ) for lead antimonate yellow (Ruiz-Moreno *et al.*, 2003; Barilaro *et al.*, 2005; Miao *et al.*, 2010; Rosi *et al.*, 2011) and, furthermore, the presence of another band at about 510  $\text{cm}^{-1}$  for lead antimonate yellow (Sandalinas *et al.*, 2006; Rosi *et al.*, 2009; Miao *et al.*, 2010; Rosi *et al.*, 2011) made us

able to identify that all the yellow glazes are achieved by lead tin yellow type II. This peak at about 510  $\text{cm}^{-1}$  can be ascribed to the  $A_{1g}$  mode and corresponds to the totally symmetric elongation of the  $\text{SbO}_6$  octahedra (Rosi *et al.*, 2009) which is not entirely observed in our yellow glazes.

#### 6.4.6 Green glazes

The typical Raman bands, as those of the yellow glazes, were observed for the green glazes; *i.e.*, 63, 83, 132, 260 (a shoulder), 325, 450, and a broad band from 850 to 1100  $\text{cm}^{-1}$  (Figure 6.9). The only difference between the green and the yellow glazes' Raman spectra was the bands at about 65  $\text{cm}^{-1}$  which in the green glazes represented a higher intensity. It seems that the green hue is obtained by adding a colouring agent in the matrix of the yellow glazes. Since no significant Raman band was observed which can be assigned to another substance other than the lead-tin yellow type II, it can be concluded that the colouring agent is most probably dissolved in the glazes' lattices.

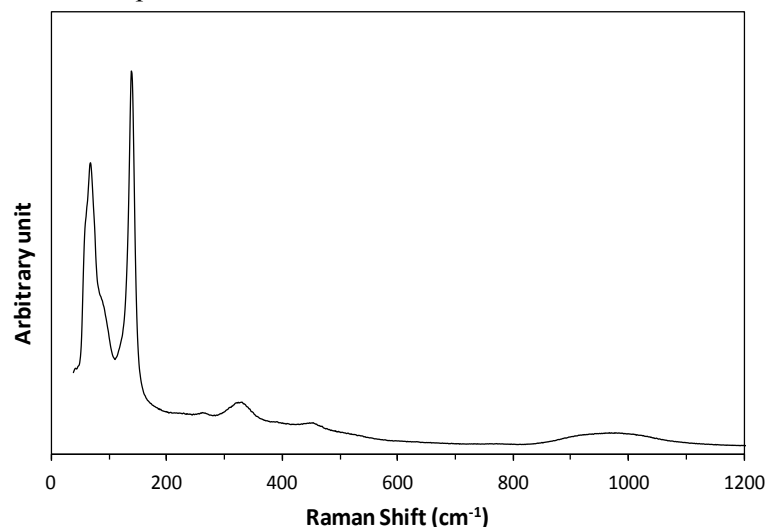
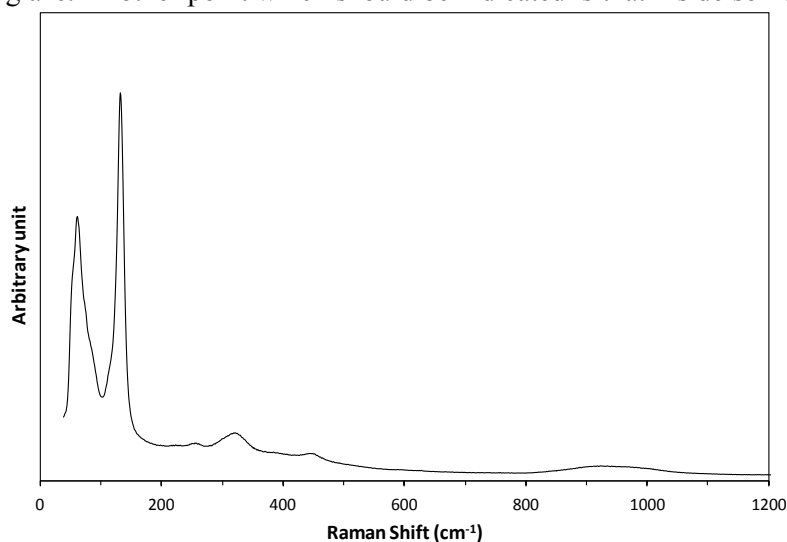


Figure 6.9 Raman spectrum of the I.A.4's green glaze

#### 6.4.7 Brown glazes

As for the green glazes, the brown glazes showed the same Raman bands as the yellow glazes at 59, 79, 255, 320, 449  $\text{cm}^{-1}$  along with a broad band from 850 to 1050  $\text{cm}^{-1}$  (Figure 6.10). Evidently, the brown hue also has been achieved by dissolving a colouring agent inside a yellow opacified glaze, as the green glaze.



Another point which should be indicated is that inside some brown glazes, several dark spots could be visually observed (Figure 6.11a) whose Raman spectrum is represented in Figure 6.11b. The peaks at 218, 281, 335 (shoulder), 396, 592, and 1295  $\text{cm}^{-1}$  shows that the black spots comprise of hematite (red iron oxide) (Brooke *et al.*, 1999; Zuo *et al.*, 1999; Colomban *et al.*, 2001, 2004; Barilaro *et al.*, 2005; Kock and De Waal, 2007; Clark and Curri, 1998).

Figure 6.10 Raman spectrum of I.C.1 brown glaze

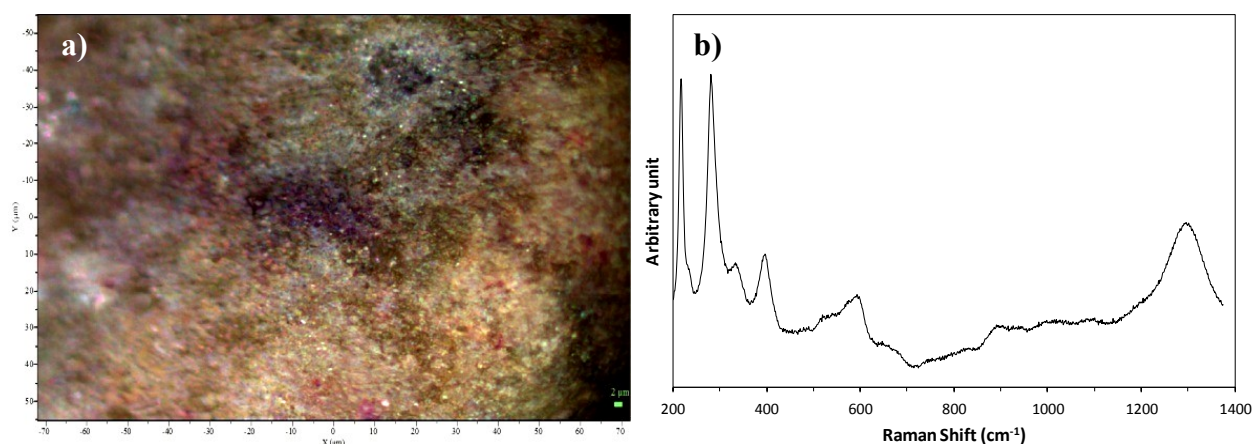


Figure 6.11 a) Red spots in the brown glaze of M.A.2 and b) its Raman spectrum

#### 6.4.8 Black lines

The majority of black lines showed a strong Raman band at  $653\text{ cm}^{-1}$ , along with two small bands at  $314$  and  $365\text{ cm}^{-1}$  (Figure 6.12a), which is attributed to manganese oxide ( $\text{Mn}_3\text{O}_4$ , hausmannite) (Strohmeier and Hercules, 1984; Brooke *et al.*, 1999; Buciuman *et al.*, 1999; Julien *et al.*, 2002; Mironova-Ulmane *et al.*, 2009). One should, however, consider that the band at  $653\text{ cm}^{-1}$  can be resulted from local laser heating (Buciuman *et al.*, 1999); in other words, the original composition prior to the analysis has probably been changed to another form of manganese oxide. Another group of the black lines (I.A.4, I.C.1, I.C.2, I.C.3, I.C.5, I.E.1, I.E.4, I.E.5, I.S.9, I.S.8, B.C.1, and B.C.3) showed a broad and strong Raman band at about  $630\text{ cm}^{-1}$  (Figure 6.12b) which can be attributed again to  $\text{Mn}_3\text{O}_4$  with a crystal size of about  $30\text{ nm}$ . The difference between these two types of  $\text{Mn}_3\text{O}_4$  detected by Raman spectroscopy is basically their crystal size where a lower crystal size of  $\text{Mn}_3\text{O}_4$  ( $30\text{ nm}$ ) has resulted the strongest band to be centred at  $630\text{ cm}^{-1}$  however the higher crystal size of  $\text{Mn}_3\text{O}_4$  ( $>100\text{ nm}$ ) caused broadening and a shift of this band to higher wavenumbers centred at  $653\text{ cm}^{-1}$  (Zuo *et al.*, 1998).

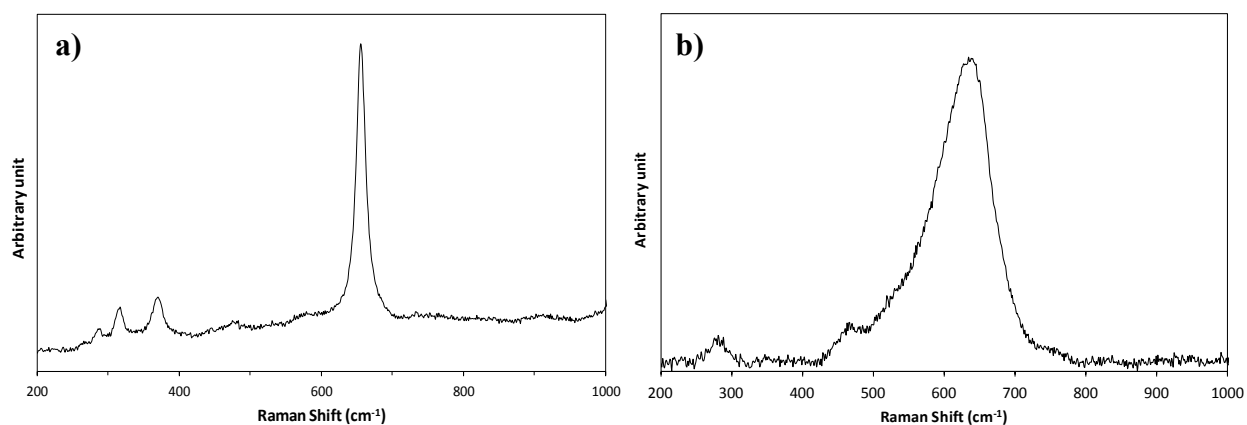


Figure 6.12 a) Raman profile of  $\text{Mn}_3\text{O}_4$  in the black line of I.C.4 and b) Raman profile of  $\text{Mn}_3\text{O}_4$  in the black line of I.E.5

## Chapter Seven: SEM observations and EDS microanalyses

### 7.1 Introduction

It may not be needed to justify the use of scanning electron microscope (SEM) and its adjacent method of microanalysis, energy dispersive X-ray spectroscopy (EDS), for the investigations presented in this chapter since they have been extensively used in investigating various types of materials including archaeological ceramics. The literature of using SEM and EDS is extremely well-developed that it needs a particular volume to be discussed. Here, only to give a general idea, it is briefly mentioned that SEM micrographs have principally used to examine firing temperature and structure of potteries (Maniatis and Tite, 1981; Freestone and Middleton, 1987; Tite, 1992), to survey the distribution of elements incorporated in both glazes and bodies and to observe their microstructure (Tite, 1992; Guilherme *et al.*, 2009) and to provide information on raw materials and production methods (Tite, 1992). EDS microanalysis has also been widely applied in identifying ancient bodies and glazes' constituents and determining their chemical compositions qualitatively and quantitatively (Freestone, 1991; Pérez-Arantegui *et al.*, 1999; Sánchez Ramos *et al.*, 2002; Alaimo *et al.*, 2004; Chapoulie *et al.*, 2005; Moroni and Conti, 2006; Tite, 2009). The introduction of SEM and EDS to the examination of ancient ceramics during the 1970s provided a powerful technique for the investigation of these surface treatments (Tite, 2008).

When the surface of a sample is scanned with a beam of electrons back-scattered electrons, secondary electrons, Auger electrons, and X-ray fluorescence can occur. When the electron beam strikes a sample, some electrons are elastically scattered by the sample atoms without a significant loss of energy. These electrons preserve somewhat less energy than the beam and are known as back-scattered electrons. Other electrons produce an inelastic collision and may cause the sample atom to ionise. These electrons lose more energy and are known as secondary electrons (Stuart, 2007; Artioli, 2010). If a nonconductive sample is examined, secondary electrons leaving the sample generate an excess of positive charge of the surface. This will deflect electrons travelling to the detector and result in a blurred image. Thus, samples are usually coated with a conductive film (Stuart, 2007). To achieve this, a 1–10 nm thick conducting film is usually deposited onto the sample. The most commonly used method is sputtering with gold or carbon (Froh, 2004).

Secondary electrons are widely used for obtaining image in scanning electron microscopy. In fact, because of their low energy, low energy electrons emerge from a very thin surface layer of the specimen of about 10 nm thickness or even less (Froh, 2004). Secondary electron emission has a high depth of field and forms the principal SEM imaging tool through topographic contrast (Adriaens and Dowsett, 2005). Using electrons with wavelengths of 0.123–0.012 nm, magnifications over 100,000 times, compared to the

low magnifications of about 1000 offered by optical microscopes, can be achieved by SEM (Artioli, 2010).

By backscattered electrons, however, image formation about a comparatively thick layer of around a micrometer can be achieved. Backscattered electron images, moreover, contain information on the element composition in addition to information on the topography of the specimen (Froh, 2004). The detection of the higher energy backscattered electrons, in fact, gives rise to a number of sources of contrast including topographic contrast, atomic number contrast, *etc.* Atomic number contrast arises because the backscattering coefficient rises monotonically with atomic number of the scattering atoms. The effect is sufficiently large to discriminate between adjacent elements in the periodic table and high- and low-density phases in a ceramic body may easily be distinguished (Adriaens and Dowsett, 2005).

Concerning EDS microanalyses, it can be mentioned that before the backscattered electrons leave the sample they may result in inelastic collisions and generate secondary electrons. Electrons from outer energy atomic shells fill the holes produced by the emission of secondary electrons from the inner energy shells. During this process, energy is released in the form of a characteristic x-ray. EDS analysis involves the analysis of the X-rays and allows elements to be identified (Stuart, 2007). Energy dispersive EDS spectrometres simultaneously measure the whole X-ray spectrum and hence provide a quick determination of the element composition of the sample (Froh, 2004).

## 7.2 Samples and experimental

More than 250 coloured glazes pushed us to select a representative sample from each type of coloured glazes previously determined by UV-Vis and Raman spectroscopy because it was not practically feasible to analyse more than three points from each sample. To do so, twenty eight samples were selected and three spots in each sample were semi-quantitatively analysed by EDS. SEM-EDS analyses were performed with a Zeiss EVO 40 scanning electron microscope equipped with an INCA Energy 300 Oxford EDS microanalysis system using 18 kV, 0.12 nA, 100 s counting time and 8.5 mm working distance. Elemental data were prepared using the INCA Energy 300 software, the calibration was carried out by cobalt, and the obtained data were normalised to 100%. Samples were coated with carbon and the analyses were carried out by scanning a large area of the glaze. The relative errors were 6 to 10 % for the majority of the elements and the detection limits were about 0.1 wt% for most of the elements however for manganese and lead was about 0.3 wt%. The samples and the results of EDS microanalyses can be found in Table 7.1.

## 7.3 Results

To have an overall idea about the analysed glazes, a PCA biplot of the samples for Na<sub>2</sub>O, MgO, Al<sub>2</sub>O<sub>3</sub>, SiO<sub>2</sub>, K<sub>2</sub>O, CaO, and PbO were plotted (Figure 7.1). A 0.668 Kaiser-Meyer-Olkin measure of sampling adequacy and 90.78% of the total variance for the first two principal components (69.81% for PC1 and 20.97% for PC2) showed that PCA is a suitable statistical approach for interpreting the dataset (the calculations behind this biplot can be found in [Appendices 6](#)). Figure 7.1 clearly shows that blue, turquoise, violet, and white glazes (nos. 1 to 12) are apparently alkaline glazes due to the relatively high alkali content (K<sub>2</sub>O and Na<sub>2</sub>O). On the contrary, brown, yellow, and green glazes (nos. 13 to 23) are lead based glazes due to the high content of lead in their glassy matrix. On the other hand, the black lines do not show a behaviour by which a glassy matrix can be perceived. In other words, the chemical

composition of the black lines is not laid within the glassy matrixes due to the relatively high amount of alumina and the low silica and alkali contents.

Table 7.1 The semi-quantitative results of EDS microanalyses on the coloured glazes (normalised to 100%)

n.	Glaze	Label	Na <sub>2</sub> O	MgO	Al <sub>2</sub> O <sub>3</sub>	SiO <sub>2</sub>	K <sub>2</sub> O	CaO	Fe <sub>2</sub> O <sub>3</sub>	MnO	CoO	PbO	CuO	SnO <sub>2</sub>	ZnO	PbO/ SnO <sub>2</sub>	SiO <sub>2</sub> / Na <sub>2</sub> O+K <sub>2</sub> O	Na <sub>2</sub> O/ K <sub>2</sub> O
1	Blue	I.C.5	18.6	1.9	1.7	65.9	4.7	4.2	2.1	n.d.*	0.2	0.7	n.d.	n.d.	n.d.	n.c.**	8.2	4.0
2	Blue	I.E.5	6.1	1.4	3.6	66.6	4.7	5.0	4.2	n.d.	0.8	6.3	1.4	n.d.	n.d.	n.c.	15.6	1.3
3	Blue	I.S.8	12.6	1.2	4.2	58.8	12.0	3.6	3.9	n.d.	0.4	3.4	n.d.	n.d.	n.d.	n.c.	16.7	1.0
4	Turquoise	I.A.2	15.0	2.1	7.2	54.4	4.1	6.5	2.4	n.d.	n.d.	5.4	3.0	n.d.	n.d.	n.c.	7.7	3.7
5	Turquoise	I.A.3	17.7	1.5	4.8	47.3	5.1	4.5	2.3	n.d.	n.d.	8.6	2.7	5.6	n.d.	1.5	7.8	3.4
6	Turquoise	I.A.7	20.9	3.5	4.2	52.3	3.2	3.5	n.d.	n.d.	n.d.	11.5	0.8	n.d.	n.d.	n.c.	5.7	6.5
7	Violet	I.A.3	15.1	1.4	3.9	46.1	5.4	4.9	1.6	2.2	n.d.	19.2	n.d.	n.d.	n.d.	n.c.	8.5	2.8
8	Violet	I.C.3	8.5	2.3	2.8	63.1	6.6	6.4	1.7	3.9	n.d.	4.6	n.d.	n.d.	n.d.	n.c.	14.0	1.3
9	Violet	I.E.5	15.4	1.6	5.9	44.0	4.9	5.2	1.3	2.2	n.d.	19.4	n.d.	n.d.	n.d.	n.c.	7.7	3.2
10	White	A.M.1	16.8	2.3	4.9	53.6	4.6	5.3	n.d.	n.d.	n.d.	9.7	n.d.	2.8	n.d.	3.5	7.8	3.6
11	White	I.C.2	11.7	2.1	2.8	57.4	6.1	6.0	2.1	n.d.	n.d.	7.9	n.d.	3.9	n.d.	2.0	11.0	1.9
12	White	I.C.7	11.9	1.9	3.6	51.4	8.2	4.9	0.8	n.d.	n.d.	9.3	n.d.	7.9	n.d.	1.2	12.5	1.5
13	Brown	I.A.7	4.8	1.0	3.0	28.6	2.1	1.9	1.2	0.4	n.d.	46.5	n.d.	10.4	n.d.	4.4	8.1	2.3
14	Brown	I.C.1	5.3	0.7	2.2	34.4	1.1	0.9	1.2	0.7	n.d.	44.4	n.d.	9.1	n.d.	4.9	7.6	4.9
15	Brown	I.E.2	6.2	0.4	2.1	33.4	2.0	1.8	1.0	n.d.	n.d.	46.3	n.d.	6.9	n.d.	6.7	7.4	3.0
16	Brown	I.E.4	2.9	0.7	3.6	35.2	3.5	2.0	1.5	0.2	n.d.	41.4	n.d.	7.3	1.7	5.7	15.6	0.8
17	Brown	M.A.2	7.8	1.6	6.7	34.3	3.4	2.5	5.3	n.d.	n.d.	38.5	n.d.	n.d.	n.d.	n.c.	7.8	2.3
18	Green	I.A.4	2.4	0.5	2.0	30.4	0.3	1.4	1.6	n.d.	n.d.	44.6	1.0	15.0	0.7	3.0	13.1	7.2
19	Green	I.A.7	3.8	0.4	2.4	29.0	1.5	2.2	2.7	n.d.	n.d.	49.5	0.5	7.4	0.6	6.7	9.1	2.5
20	Green	I.C.2	3.7	0.5	2.2	25.8	0.3	2.5	1.4	n.d.	n.d.	54.2	1.5	6.8	1.2	7.9	7.3	12.0
21	Yellow	I.C.6	3.8	0.5	3.8	29.8	1.3	1.1	n.d.	n.d.	n.d.	50.8	n.d.	9.0	n.d.	5.6	9.0	3.1
22	Yellow	I.C.7	2.2	0.8	3.1	40.9	2.1	1.9	1.8	n.d.	n.d.	37.0	n.d.	10.1	n.d.	3.7	20.4	1.1
23	Yellow	I.S.9	8.4	0.6	2.8	35.4	1.9	3.0	n.d.	n.d.	n.d.	40.1	n.d.	7.7	n.d.	5.2	6.1	4.5
24	Black line	I.A.4	1.4	1.8	7.7	33.3	2.5	7.4	9.9	1.8	n.d.	33.2	1.0	n.d.	n.d.	n.c.	26.0	0.6
25	Black line	I.C.4	3.6	3.1	16.8	35.6	4.0	11.7	6.8	11.5	n.d.	7.1	n.d.	n.d.	n.d.	n.c.	13.9	0.9
26	Black line	I.E.7	4.5	2.3	12.7	38.9	4.1	4.3	8.8	19.7	n.d.	4.7	n.d.	n.d.	n.d.	n.c.	12.7	1.1
27	Dark spot	I.E.2	2.3	2.6	17.0	31.0	0.4	33.3	9.7	n.d.	n.d.	3.6	n.d.	n.d.	n.d.	n.c.	14.0	5.5
28	Dark spot	I.E.4	5.5	4.1	19.8	38.0	9.7	5.7	6.5	0.4	n.d.	10.4	n.d.	n.d.	n.d.	n.c.	16.6	0.6

\*not detected; \*\*not calculable

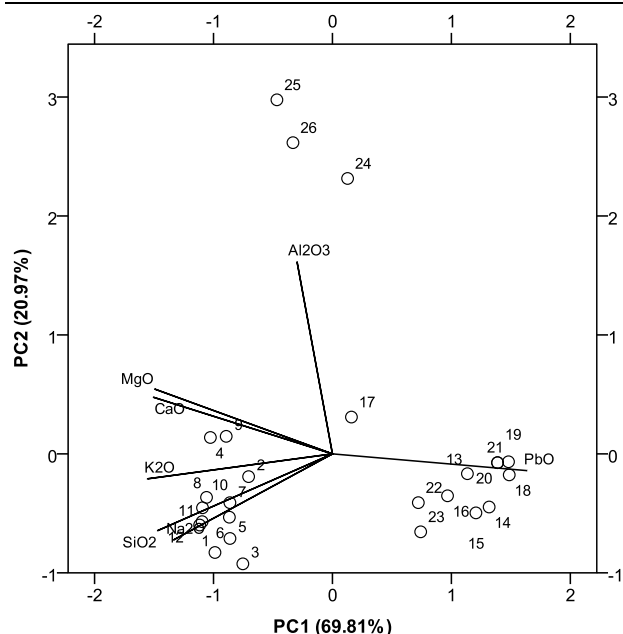


Figure 7.1 PCA biplot of the first two principal components resulted from the EDS data on the coloured glazes

Another issue which can be inferred from the biplot and Table 7.1 is that plant ash has most probably been the main resource for supplying flux content of the glazes because, as it is generally well-known, the plant ash alkali content is usually associated with magnesia and potash (Henderson, 1985; Brill, 1992; Freestone, 2006; Tite *et al.*, 2006; Rehren, 2008). The Na<sub>2</sub>O:K<sub>2</sub>O ratio of the glazes varies from 1 to 12, which is in accordance with the analytical results of the plant ashes discovered in Iran (Brill, 1999; Tite *et al.*, 2006).

On the other hand, wood ash has not been used as flux since it contains low soda and high potash contents (Stern and Gerber, 2004). Generally known, plant ash is rich in lime and magnesia. However, Turner (1956) suggests that the ash from any particular plant has different composition according to the locality where it is grown. That is, the plants which were grown near the sea or on salt desert land were associated with a relatively high soda content whilst those inland regions were relatively rich in potash. Nonetheless, these hypotheses about the plant ash source of the alkali contents of the glazes can be challenged since any purification as those suggested in old treatises (Rāzī, 9-10th century AD; Ali Mohamed, 1888) resulting alkali contains much less lime, magnesia, alumina, and other less soluble components of the ash. Moreover, one should consider other sources of supplying alkali contents in the ancient ceramic technology. For instance, in the case of saltpeter and niter, the former of which was definitely used in Chinese glassmaking, and the latter of which was used in Europe for a wide variety of purposes in the centuries (Brill, 1992).

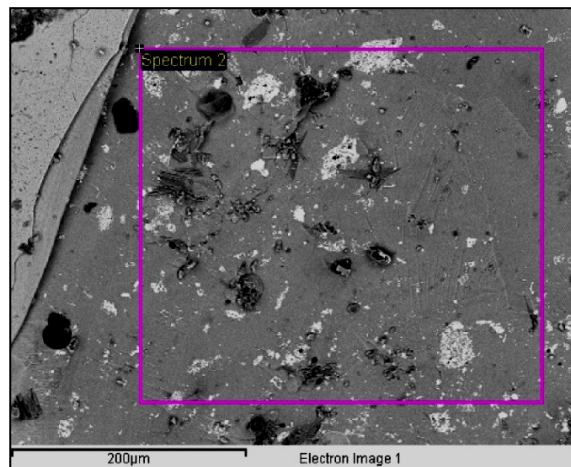
On the other hand, significant amounts of alumina and lime in the glazes' composition can be associated with both the silica source and the glazes' bodies. Nevertheless, since coloured glazes are applied on a white low alumina content glaze, it seems that the alumina and lime contents are associated with the silica source which is most probably sand or quartz pebbles (Turner, 1956). As generally known, from two sources of sand and quartz pebbles, quartz pebbles have a low alumina and lime contents (Tite and Shortland, 2003). This pushed us to attribute the silica source to sand. However, one should bear in mind that the lime contents could have been originated both quartz sand and plant ash (Tite and Shortland, 2003) or may be incorporated deliberately as a separate component, either lime or limestone (Shortland and Eremin, 2006).

### 7.3.1 Whites

According to the EDS results (Table 7.1), SnO<sub>2</sub> (cassiterite) can be considered as the opacifier used to opacify the white glazes. The EDS results, moreover, show that the PbO:SnO<sub>2</sub> ratio is 1.2:1, 2:1, and 3.5:1 for the white glazes of I.C.7, I.C.2, and A.M.1 respectively which is entirely compatible with the relative PbO:SnO<sub>2</sub> ratio suggested in Abu'l Qasim (1301) and Ali Mohamed (1888) treaties. This fact,

furthermore, implies that all the lead content of the glazes has been stoichiometrically satisfied by the tin content in order to opacify the glazes. In other words, the white glazes are basically alkali-based and the lead content has only participated in the opacification of the glazes. The presence of cassiterite as the opacifier and the nature of the glassy matrix of the glazes have been previously positively detected by UV-Vis spectroscopy and micro-Raman spectroscopy (see *Chapter Five*, p. 61 and *Chapter Six*, p.76). It should be noted that the semi-translucent appearance of A.M.1 white glaze can be a result of lower tin content of this glaze. Backscattered image of the white glazes also showed that the size of tin oxide dispersed in the alkaline glazes is varying between 0.5 to 35  $\mu\text{m}$  resulting in the reflection and scattering of light and, consequently, opacifying the glazes (Figure 7.2).

Figure 7.2 Backscattered image of the white glaze of I.C.7 sample



### 7.3.2 Yellows

According to the dataset presented in Table 7.1, yellow glazes are apparently high lead glazes with more than 35 wt% PbO. The EDS results, moreover, show about 6.3:1, 4.3:1, and 6.2:1 for the Pb:Sn weight ratio in I.C.6, I.C.7, and I.S.9 yellow glazes respectively suggesting lead-tin yellow as the yellow opacifier. Tite *et al.* (2008), on the other hand, have gathered together all ancient recipes of making lead-tin yellow opacified glazes suggesting that the ratio obtained in our studies is close to that of Islamic yellow glazes and has less in common with the European lead-tin yellow glazes spanning from the Roman periods until the eighteenth century. Moreover, it is showed that the lead stannate responsible for the opaque yellow of the glasses is the cubic form ( $\text{PbSnO}_3$ ) and not the orthorhombic form ( $\text{Pb}_2\text{SnO}_4$ ). It is shown that, when mixtures of lead oxide and tin oxide are heated to temperatures in the range 700–900°C, it is the orthorhombic  $\text{Pb}_2\text{SnO}_4$  that is formed. However, if silica is added to the  $\text{Pb}_2\text{SnO}_4$  and the resulting mixture is heated to 850°C, the  $\text{Pb}_2\text{SnO}_4$  is converted to the cubic  $\text{PbSnO}_3$  (Rooksby, 1964; Tite *et al.*, 2008),

### 7.3.3 Green glazes

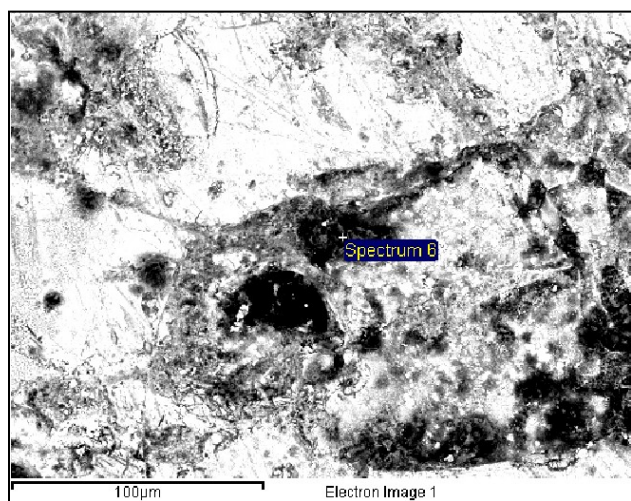
With 1, 0.5, and 1.5 wt% copper oxide in the composition of the I.A.4, I.A.7, and I.C.2 green glazes respectively, the green colour is apparently caused by copper ions in the glazes' matrixes (Table 7.1). This fact was previously showed by micro-Raman and optical spectroscopy (see *Chapter Five*, p. 66 and *Chapter Six*, p. 77). EDS microanalyses, in addition, showed that the chemical composition of the green glazes is entirely comparable with the yellow glazes (Table 7.1). Comparing the PbO:SnO<sub>2</sub> ratio within the green and yellow glazes (Table 7.1) (5.9:1 on average for the green and 4.8:1 on average for the yellow glazes), it can be hypothesised that the green glazes are in fact the same yellow glazes in which copper ions have yielded a greenish colour. The only difference between the green and the yellow glazes, however, is laid on the presence of zinc in the composition of the green glazes. The relatively high amount of zinc oxide (0.7, 0.6, and 1.2 for I.A.4, I.A.7, and I.C.2 respectively) cannot be attributed to the traces of zinc which are usually associated with copper ores. Two hypotheses, however, can be suggested in this

regard: first, it can be assumed that zinc oxide is deliberately added to the green glazes' batch and, the second: a brass based alloy has been principally the source of supplying copper content of the glazes. As far as the first hypothesis is concerned, although Abu'l Qasim (1301) has mentioned the use of a zinc compound (*tūtīyā*) for making glazes, he does not indicate where and how it is used in glaze-making. The second hypothesis is more probable since any copper-bearing material, including metallic copper, bronze, and brass, could have been roasted and used in the glaze in order to make a green hue.

#### 7.3.4 Brown glazes

As the green glazes, the brown glazes are high lead content glazes in which iron and, in the case of I.A.7 and I.C.1 samples, manganese have created a brown hue. The PbO:SnO<sub>2</sub> ratio of 4.4:1, 4.9:1, 6.7:1, and 5.7:1 for I.A.7, I.C.1, I.E.2, and I.E.4 respectively is totally comparable with that of the yellow glazes (Table 7.1). The only samples which shows different behaviour is M.A.2 brown sample which is a tin-free opacified brown glaze. The visual appearance of this sample is entirely different from the others, which was previously showed with the optical spectrum of this glaze (see *Chapter Five*, p. 65). This could be related to the relatively high iron content (5.3 wt%) of this glaze and the absence of manganese, by which it is opacified.

The I.E.2 and I.E.4 brown glazes, as seen in the previous chapters, are brown glazes in which undissolved dark spots were dispersed. EDS microanalysis of these spots shows an iron rich substances which is fairly affected by the lead based glaze surrounded them (Table 7.1). Raman spectra of these spot



had previously showed the presence of hematite (iron oxide) in the composition of these spots which is totally consistent with EDS results. Figure 7.3 shows a backscattered SEM image of one of these dark spots embedded in the lead rich glaze matrix of I.E.2. It seems that the iron oxides particles, which were supposed to be dissolved in the glaze's matrix, are remained intact in the glazes.

Figure 7.3 Dark iron rich spots in the brown glaze of I.E.2

#### 7.3.4 Turquoise glazes

These glazes are apparently low lead-alkali glazes with less than 10 wt% PbO in which about 3 wt% copper oxide is responsible of the turquoise colour (the lower copper oxide content (0.8 wt%) of the I.A.7 turquoise glaze can be the result of the deteriorated surface of the glaze). As it is showed, the black particles of tenorite (CuO) were previously detected in Raman spectra of these glazes (see *Chapter Six*, p. 73) which confirms this fact. On the other hand, tin oxide has been responsible of the opacity of two out of the three glazes (I.A.7 and I.A.3). Figure 7.4 demonstrates the distribution of tin oxide particles in the backscattered SEM image with small white particles (with a 5 μm diameter on average) within the low lead-alkali glaze of I.A.3. However, the transparent appearance of the I.A.2 turquoise glaze is the result of

the absence of tin oxide in the glaze matrix (Table 7.1). Moreover, the turquoise glazes did not show any trace of zinc in their chemical compositions. This can convey that the sources for supplying copper for the green and turquoise glazes are probably different.

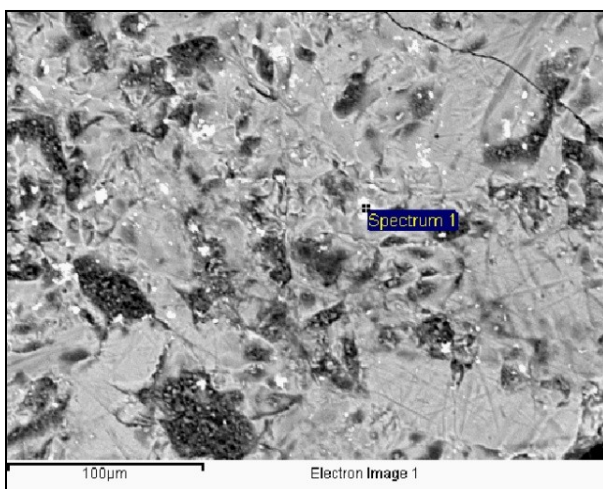


Figure 7.4 Small tin oxide particles in the turquoise glaze of I.A.3

### 7.3.5 Blue glazes

The EDS results showed that blue glazes were low lead-alkaline glazes which are not opacified with tin oxide (Table 7.1). The  $\text{Na}_2\text{O}:\text{K}_2\text{O}$  ratio in the blue glazes for I.C.6, I.E.5, and I.S.8 was 4:1, 1.3:1, and 1:1 respectively showing that a soda rich plant is used as flux. The low  $\text{Na}_2\text{O}:\text{MgO}$  ratio also confirmed this hypothesis since, as it is previously mentioned, the plant ash soda is Iran has always been associated with magnesia. What is evident is that the use of natron source as flux can be most likely excluded. The colouring agent, on the other hand, was diagnosed cobalt for the blue glazes nevertheless I.E.5 blue glaze showed copper oxide as well as another colourant (Table 7.1). Concerning the presence of copper in the blue glaze, copper might have been added to the blue glaze batch in order to create a particular hue of blue colour.

### 7.3.6 Violet glazes

Except I.C.3 violet glaze, the two violet glazes not only show high alkali content (more than 15 wt%) but also show a relatively high amount of PbO in their compositions (more than 19 wt%) suggesting lead-alkali character of the glazes. The I.C.3 violet glaze can also be considered as lead-alkali glaze but with higher silica content. The low  $\text{Na}_2\text{O}:\text{K}_2\text{O}$  ratio and the magnesia content of the violet glazes suggest that plant ash has been used as flux rather than natron. On the other hand, manganese ions are the principal colourants of these glazes as the EDS results suggest (Table 7.1). It should be noted that the relatively high amount of manganese indicate that the manganese content cannot have an external source as it is suggested that sometimes manganese can be introduced from external sources and blacken potash glassy matrixes (Watkinson *et al.*, 2005). Iron content of the glazes do not seem to have any role in colouring the glazes and it can be interpreted as inclusion since iron is usually associated with the raw materials used to produce ancient glazes.

### 7.3.7 Black lines

Black lines are not apparently real glazes since the high amount of  $\text{Al}_2\text{O}_3$  and low  $\text{SiO}_2$  and alkali oxide ( $\text{Na}_2\text{O}$  and  $\text{K}_2\text{O}$ ) contents cannot molten to be used as a glaze in the conventional temperature achieved in old kilns. The relative high amount of manganese oxide in the composition of the black lines (more than 10 wt%) justifies the black colour of the lines which was previously identified as  $\text{Mn}_3\text{O}_4$  with different crystal size by micro-Raman spectroscopy. The refractory behaviour of these lines with high alumina content has most probably kept the lines to be molten during their firing process. This feature has certainly been in favor in the firing process; that is, the higher softening point temperature of these black lines has not allowed the runny coloured glazes to run together during the firing. In other words, this black line has kept the different coloured glazes separated during firing. Furthermore, the iron content of these black lines is relatively high which aid the black manganese oxides to be intensified in colour.

### 7.4 Estimation of maturing temperature of the glazes

Since the maturing temperature of the glazes has a substantial impact on the formation of the glazes, the model suggested by Fluegel (2006, 2007) and Lakatos *et al.* (1972) was selected to estimate different temperature at which the glazes show different behaviours. These approaches, despite their limitations in ancient glaze technologies<sup>1</sup>, give a reasonable indication for the range of firing temperatures probably used in the manufacture of these glazes and have been previously used to characterise the thermal behaviour of the archaeological glazes (Tite *et al.*, 1998; Gill and Rehren, 2011; O’Kane, 2011).

In our calculations, the Fluegel (2006)<sup>2</sup> model was selected to estimate the temperature at which a viscosity of  $10^4$  poise of the different glazes could have been achieved since this viscosity is assumed to be appropriate for melting the glazes. In the case of the lead glazes (yellow, brown, and green glazes) the quantity of  $\text{SnO}_2$  was subtracted from that of  $\text{PbO}$ , because it is assumed that since the  $\text{SnO}_2$ : $\text{PbO}$  ratio for a yellow glazes is 1:1 in the yellow opacifier of  $\text{PbSnO}_3$  (Tite *et al.*, 2008b), the same amount of  $\text{SnO}_2$  is stoichiometrically consumed by  $\text{PbO}$  and the rest of  $\text{PbO}$  participates as a flux in the glazes. Since the green and brown glazes were initially supposed basically as yellow-colourant-modified glazes, the same approach was selected for these glazes as well. The results of these calculations are shown in Table 7.2.

According to data presented in Table 7.2, the maturing temperature for the alkali glazes (blue, violet, and turquoise) is on average about  $700^\circ\text{C}$  (if we exclude two outliers of as results of alkali leaching and glazes deterioration), for the white glazes is about  $860^\circ\text{C}$ , for the high lead glazes (yellow, green, and brown) is around  $615^\circ\text{C}$ , and this temperature for the black lines is above  $1150^\circ\text{C}$ . The first point, which can be perceived from these results, is that the black lines have been resistant enough in the low maturing temperature of the other glazes not to be molten during firing. This could keep separated the molten glazes and avoid running the glazes together during firing. The manganese content seems only to have the role not more than of a colouring agent to keep visually the glazes separated not practically during firing. On the other hand, the maturing temperature of the white glazes is about  $150^\circ\text{C}$  and  $240^\circ\text{C}$  higher than the alkali and the high lead glazes respectively giving it this possibility to act as a substrate for the coloured glazes and lessening the chances of the other glazes running or of re-melting with the substrate glaze. The

<sup>1</sup> For instance, Lakatos *et al.* (1972) considers only the six most common glass oxides but does not include any of the colourants or lead oxide and, further, the Fluegel’s approach (Lakatos *et al.*, 1972) is determined for lead oxide concentrations in a specific range.

<sup>2</sup> This was achieved by a Microsoft Excel spreadsheet available at: <http://glassproperties.com/viscosity/>

coloured glazes have a relatively low maturing temperature suitable for a low firing temperature process. However, since this temperature for the alkali glazes is about 100°C higher than that of high lead glazes, it can be said that for an intermediate firing temperature, the alkali glazes do not receive sufficient heat and, on the contrary, the high lead glazes are over-fired. This can be the main reason for accelerating the deterioration process of the polychrome *haft rang* colours.

Table 7.2 Calculated maturing temperature of the coloured glazes

Coloured glaze	Samples	T (°C) at which 10 <sup>4</sup> poise is achieved (Fluegel, 2006)
Blue	I.C.5	770
Blue	I.E.5	942
Blue	I.S.8	787
Turquoise	I.A.2	819
Turquoise	I.A.3	708
Turquoise	I.A.7	637
Violet	I.A.3	613
Violet	I.C.3	888
Violet	I.E.5	615
White	A.M.1	843
White	I.C.2	902
White	I.C.7	844
Brown	I.A.7	616
Brown	I.C.1	627
Brown	I.E.2	545
Brown	I.E.4	664
Brown	M.A.2	547
Green	I.A.4	755
Green	I.A.7	551
Green	I.C.2	497
Yellow	I.C.6	585
Yellow	I.C.7	783
Yellow	I.S.9	596
Black line	I.A.4	1168
Black line	I.C.4	1176
Black line	I.E.7	1159



## Chapter Eight: Discussion

Here, in this chapter, the results of the analytical studies of WDXRF, XRD, UV-Vis spectroscopy, micro-Raman spectroscopy, SEM, and EDS microanalyses on the bodies and glaze layers of the seventeenth century Safavid *haft rang* tiles are discussed.

### 8.1 Bodies

According to the WDXRF and XRD results, the bodies of the studies *haft rang* tile are entirely clay based. These bodies, as their name conveys, have been made of clay. As it is generally well-known, clays are divided into two groups of primary and secondary. Sources of the primary clays in Iran are rare; however, some of ceramic-manufacturing centres in Iran, such as Shahriḡā and Zunūz, are still using primary clays in making ceramic bodies (Şadīq, 1976; Jināb, 1997). Nonetheless, no account either in ancient Iranian ceramics or in analytical data showing the application of this type of clay as the main ingredient of bodies. Secondary clays, however, may contain various constituents such as quartz, organic matters, and iron minerals, which are not basically clay minerals. Moreover, some materials that were sometimes added to clay to enhance workability of the clay may change its chemical composition. For instance, salt (Aḡmadīyān, 1977), bentonite (Nādirī, 1978), sand, plant ash (Ali Mohamed, 1888), ground bricks, crushed potteries, organic materials, and crushed shell (Holakooei *et al.*, 2013), have been using in Iran to improve the consistency of the body and control drying and firing shrinkage of the bodies. This is an important issue in the provenance studies of the ceramics since these additives can drastically change the chemical composition of the bodies and introduce new elements and, consequently, mislead the interpretation of analytical results. Although some efforts have been made to eliminate the effect of such additives in the provenance studies of clay bodies (Cogswell *et al.*, 1998), it is still a controversial issue since the variety of materials used as temper is quite vast and unpredictable.

As far as the analytical studies on ceramics materials found in Iran are concerned, the majority of these bodies have a high calcium content with colour variety of cream to buff (Kamilli and Lamberg-Karlovsky, 1979; Yelon *et al.*, 1992; Holakooei, 2013; Holakooei *et al.*, 2013). Sometimes, low calcium content clay bodies have been reported in the literature where iron oxide has yielded an orange to red colour (Kamilli and Lamberg-Karlovsky, 1979; Holakooei *et al.*, 2013). It can be explained by the fact that when a non-calcareous clay is fired, iron is crystallised in the form of hematite and, consequently, become red in colour. On the other hand, when clays containing calcite are fired, calcium carbonate is dissociated to CaO and CO<sub>2</sub>. The freed CaO reacts then with iron oxides which decreases the size iron oxide particles and, as a result, bleaches the red colour to cream and buff (Maniatis, 2009). Readers may find the mechanism of this transformation in Molera *et al.* (1998). The buff colour of the calcareous bodies can be more easily concealed by an opacified glaze than in the case of red body with low calcium content. Moreover, due to a

higher thermal expansion coefficient of calcareous clay bodies, which is close to those of lead-alkali glazes, the risk of glaze crazing during the cooling following a second firing is lessened (Tite *et al.*, 1998).

Clay bodies are used in Iran from the beginning of pottery making (Yelon *et al.*, 1992) and making glazed objects spanning from historic times (Holakooei, 2013) through the medieval Iran (Holakooei *et al.*, 2013). In fact, the first applications of clay bodies covered by a vitreous layer are found the architectural glazed bricks at Chughā Zānbīl (Dur Untash) dated back to the middle Elamite period (13th century BC). These bricks are most probably the first experiences of the application of polychrome glazes on the clay body in the Near East (Moorey, 1994).

Our studies showed also that the bodies are biscuit fired prior to apply the white glaze substrate on. Biscuit firing has some advantages which have provoked glaze-makers to do it in the production of glazed products. Tite *et al.* (1998) suggest that a successful application of a glaze suspension to a biscuit-fired body is more readily achieved since the structure of such a body is undisturbed by the displacement of air and no expansion occurs as a result of water transfer from the suspension, nor contraction during the subsequent drying. In addition, because biscuit-fired bodies tend to have higher open porosity than unfired bodies and because the pores do not already contain water, biscuit-fired bodies absorb water from the glaze suspension more easily and more predictably. Therefore, the glaze dries more rapidly and its thickness is more readily controlled. Other advantages of prior biscuit firings are that they facilitate the complete oxidation of the body, thereby avoiding darker areas of unoxidised body beneath the glaze, and that there is less reaction between body and glaze which allows better transparency and control of glaze colour. However, the addition of clay, gum or starch to the suspension is still advisable in order to ensure good adhesion between the glaze powder after drying and the body. On the debit side, since the use of a biscuit fired body involves a double firing, are the increased costs in terms of fuel and time (Tite *et al.*, 1998).

Another type of the body which was usually used in the seventeenth century Safavid ceramics is the ‘processed body’ (Agosti and Schweiser, 2002; Tite *et al.*, 2011). The term ‘processed body’ is selected to refer the bodies whose main component is quartz to which other ingredients are added for certain purposes. This term roughly covers the terms such as stonepaste, frit, quartz-frit, faïence, artificial paste, *kāshī* (Mason, 1996), silicate pottery, composite material (Keblow-Brensted, 2003), and *jismī* (Nādirī, 1978; Zumarshīdī, 2006) which have been frequently used to describe quartz-based bodies. Based on the Abu’l Qasim’s treatise, it is suggested that the ratios of the principal ingredients of stonepaste bodies are 80 wt% quartz, 10 wt% white clay, and 10 wt% glass powder (Mason, 1996). However, as it will be showed, there is variety of body, based on geographical and chronological variations (Tite *et al.*, 2011), which cannot be technologically matched with this description. Here, therefore, the expression ‘processed body’ is used to cover the other terms since ingredients of the bodies are usually selected and processed prior to firing.

The first use of processed bodies has been reported in Iran from the Elamite period at Haft Tepe (Negahban, 1991). In the Middle Elamite period (1550-1100 BC), this new technology was widely used to make glaze bricks at Susa, which was then inherited by the Achaemenids to decorate the friezes of the Apadana palaces at Susa and Persepolis (Heim, 1992; Caubet and Kaczmarczyk, 1998; Tite *et al.*, 2008a; Holakooei, 2013). It is reported that the main components of the Achaemenid glazed bricks are sand and lime (Caubet, 1992). Processed bodies were also extensively used in the Islamic lands including Iran. In the Abū Dulaf’s treatise (950 AD) there are some hints about making the technology of processed bodies.

As far as the treatise is concerned, quartz, glass powder, and tin oxide are the main components of a processed body. These components were knocked, ground and, sifted and, thereafter, mixed with water until the proper paste become ready to work with (Morgan, 1994). Contemporary Persian processed bodies, however, have other ingredients; for instance, in Naṭanz, the combination of kaolin and flint powder (Wulff, 1966) and in Maybud combination of 75 wt% silica, 12.5 wt% a white clay, and 12.5 wt% glass powder (Centlivres-Demont, 1971). According to Abu'l Qasim (1301), in *'Arā'yis al-Javāhir va Nafā'yis al-Aṭā'tib*, quartz is the main component of these bodies, along with a white, sticky, strong clay called *lūrī*. Ali Mohamed (1888) has also mentioned quartz (flint stone) and a white colour clay called *gil-i būta*<sup>1</sup> as the main components of a processed body. Moreover, Chardin (1811) in his observations of the potters of Isfahan briefly mentions that the fine powder of river pebbles, mixed with some mould<sup>2</sup>, was used to compose the bodies. Referring to the potters of Isfahan, Qum, Naṭanz and Kāshān, Wulff (1966) also notes that the dry river bed flint stone found near Naṭanz are gathered, crushed, ground, and then seventy to eighty percent of the powdered flint stone is mixed with ten to twenty percent of fine clay and ten percent of glass powder to make a body paste.

Abu'l Qasim (1301) describes how to take ten parts crushed quartz and mix it with one part ground glass frit and one part white *lūrī* clay dissolved in water. This mixture should be kneaded well like dough and left to be matured for one night, Abu'l Qasim (1301) mentions. Rochechouart (1867) and Ali Mohamed (1888) also describe a method which is more or less similar to that Abu'l Qasim's way of making the processed body. As it can be seen, other than quartz and the white clay, glass frit is another component. (The way of preparation of glass frit will be discussed in the upcoming parts.) Nowadays, glass powder is also used to make the processed bodies (Bier *et al.*, 1993; Caiger-Smith, 2001).<sup>3</sup> The role of the powdered glass was to be molten at high temperature and bind the quartz and clay particles together after cooling (Mason, 1995). In other words, during firing and sintering process, the powdered glass is molten and, due to its surface tension and capillary action, is penetrated between clay and quartz particles. Accordingly, alkaline elements in the glass frit react with the quartz grains and clay minerals and modify physical properties of the body (Tite and Mason, 2011).

Processed bodies have a high amount of silicon and, in contrary, calcium and iron contents are less than the clay bodies if we exclude those Achaemenid glazed bricks in which a relatively high amount of calcium is very usual (Caubet and Kaczmarczyk, 1998; Tite *et al.*, 2008a). As a general fact, it can be said

<sup>1</sup> Regardless of what *lūrī* may be, it could be said that it is the same as that of Ali Mohamed's *gil-i būta*. *Gil-i būta*, in fact, is a white clay which still being used to enhance physical properties of the bodies in Iran. According to Abū al-Qāsim's description, *lūrī* clay should be a special type of slimy clay with good plasticity. This white clay has been interpreted as bentonite (Caiger-Smith, 2001; Wulff, 1977). The use of bentonite, as well as quartz, in processed bodies has also been noted in some contemporary sources (Māhir al-Naqsh, 2002; Zumarshīdī, 2006). Moreover, *lūrī* clay can be also interpreted as kaolin (Keblow-Brensted, 2003). The use of kaolin in the composition of ceramic bodies was common in Nā'īn since recent times (Olmer, 1908), which is expectable due to the kaolin mines around found nearby Nā'īn (Olmer, 1908; Fūmanī and Bīrīnjīyān, 2005). Zamānī (1972) has also indicated a clay so-called *khāk-i būta*, which is a kind of kaolin used as a substitute for quartz in ceramic-making in Mind, Gunābād. According to Zamānī (1972), *khāk-i būta* is mixed with bentonite to produce a substrate of under-glaze decorations. Apparently, in this case *khāk-i būta* cannot be bentonite. Bahrāmī (1944) attributes *lūrī* clay to chalk, which is most certainly inappropriate.

<sup>2</sup> Ibn Battuta mentions a process by which Chinese potters leave the clay and let bacteria grow inside the clay. The fermentation occurred ends up to higher degree of plasticity of the clay (Ruggles, 2011). Nayshābūrī (1195) also indicates that a same procedure was common in Iran during the eleventh century. He states that potters inherit the clay of potteries from their fathers and call it 'paternal clay.' Nonetheless, Rochechouart (1867) records that Iranian, unlike Chinese, do not ferment the clay of pottery-making. On the other hand, al-Bīrūnī (c.1050) states Chinese potters mix white tin oxide with fermented clay and make cups with.

<sup>3</sup> Caustic soda and borax have also been reported to be used in the composition of the processed bodies (Rochechouart, 1867) to aid the formation of a glassy phase in the bodies.

that, due to the small amount of colouring agents like iron oxides, in the composition of the processed bodies, they are usually light in colour (white to pale pink). Moreover, processed bodies emit less volatile gases during firing process because the amount of decomposable and combustible materials is much low. (We exclude the Ca-bearing processed bodies.) Hence, the processed body could have been baked together with upper glazes in one individual firing process (Caiger-Smith, 1973) and, thus, one firing process (biscuit firing) was eliminated. It is necessary to explain that, the heating regime in the kiln for firing and cooling processed bodies is quite different from that of the clay bodies. Basically, the binder agent between the particles of the processed body is molten glass. Therefore, it can be said that before melting frit glass, the processed body is very susceptible to collapse because of thermal fluctuations in the kiln. Furthermore, during the cooling stage, due to relatively high amount of glassy phase, processed bodies should be cooled very slowly to reduce the risk of fracture and cracking. Hence, the processed bodies are fired and cooled slower than the clay bodies. Although the firing temperature of the processed bodies is not specified yet, it can be said the temperature has not gone further 1200°C (Tite and Mason, 2011). An advantage of using the processed bodies is their low volumetric and linear shrinkage due to lack of decomposable and volatile materials. Furthermore, due to the almost same coefficient of expansion with alkaline glazes layers, these glazes are not subjected to high tension and, therefore, the risk of crazing and crackling was drastically lessened (Caiger-Smith, 1973; Tite *et al.*, 2008a). Another advantage of the processed body is that, in the case of chipping the upper white glaze, the body is not in high contrast with the white glaze (Caiger-Smith, 1973). Also, the white upper glaze does not need high percentage of tin oxide to be opacified since the body is already white. Therefore, the tin oxide was economised in the glazes (Tite *et al.* 1998). Generally, in Iran, underglaze decorations, lustre, *lājvardīna*, and *mīnā`ī* ware were executed on the processed bodies although there are some reports of the use of the processed bodies in mosaic (Nādirī, 1978; Zumarshīdī, 2006), and monochrome tiles.

Regarding the bodies used to be produced in the same time in the adjacent cultures of the Safavid dynasty one can mention Iznik underglaze decorations which are executed on processed bodies (Henderson, 2004). Iznik ware bodies are of the quartz-frit type consisting of quartz particles bonded together by interstitial glass. These bodies are then normally coated with a quartz-frit slip made from finer quartz particles (Tite, 1989). Moreover, lead and tin-rich inclusions detected in the body of Iznik tiles (Henderson and Raby, 1989). Tiles' bodies in India, in the first half of the seventeenth century, essentially comprise angular quartz grains of different sizes and minor amounts of other minerals with varying, but generally limited, development of a phase of interstitial glass binding them together, corresponding to the stonepaste (Gill and Rehren, 2011).

## 8.2 Glazes

### 8.2.1 Network formers

A network former is an element which comprises of the main composition of a glaze and it can be said that the glaze would not be formed without (Hamer and Hamer, 2004). Chemically, silicon, germanium, phosphorus, and boron are able to have this characteristic (Eppler and Eppler, 2000). Undoubtedly, silicon has been using from antiquity as the main ingredient and network former of glazes. Silicon, in the form of quartz and other silicates, has been very cheap to be supplied and it has been quite easy to have access to. Besides, according to old Persian texts, boron has been an important network former in the composition of glazes. Ali Mohamed (1888) speaks about borax in the composition of red and blue glazes. Unfortunately,

except few examples (Tite, 1989), this element is neglected in the scientific literature published on ancient glazes. Regarding the ancient knowledge of borax, the use of this substance in the composition of the glazes seems probable since Jābir ibn Ḥayyān (al-Hassan, 2009), al- Bīrūnī (ca.1050), Nayshābūrī (1195), and Ali Mohamed (1888) have pointed out the application of borax in the glazes and glasses. Few recent observations also confirm the use of borax in the composition of Iranian contemporary glazes and glasses (Wulff, 1966; Floor, 2003). Another network former usually detected in the literature is phosphorus, whose presence in the archaeological glazes can be associated to plant ash (Rye, 1976) (see 8.2.2 *Fluxes*).

Another material, which should have a network former in its composition, is *qamṣarī* stone, according to Abu'l Qasim (1301). He states that *qamṣarī* stone is fired and molten with plant ash to create a frit. Therefore, in the composition of this stone one network former element should have been existed. Wulff (1966) believes that this stone probably is boro-calcite, but Keblow-Bernsted (2003) interprets this stone as dolomite, which does not seem to be interpreted appropriately. However, according to Allan (1973), *qamṣarī* should be magnesium silicate. Nevertheless, as far as the analytical approaches of Islamic glazes are concerned, the quantity of magnesium reported in the Islamic glazes could have been originated from plant ashes usually used in the composition of the glazes since they usually contain a considerable amount of magnesium (Tite *et al.*, 2006). Anyhow, the nature of *qamṣarī* stone is not well-defined yet and it merits to be subjected to more research.

### 8.2.2 *Fluxes*

The EDS microanalyses confirmed the use of plant ash in the composition of the coloured glazes. Old evidences of the use of plant ash in the ancient Near East (Gadd and Thompson, 1936; Henderson, 1985; Freestone, 1991) and old Persian glasses (Brill, 1992) also support the use of plant ash as the main alkali supplier as a long tradition in Iran and the Near East. Another source of supplying the alkali content of Islamic glaze has been natron which, according to our observations, can be ruled out of in the case of the *haft rang* glazes. In medieval Persian manuscripts, there are some terms used to explain such a material, such as *shakhār*, *qalīyā*, *kalīyāb*, *qalīyāb*, *qalī*, *kilā*, and *kālī* (Nayshābūrī, 1195; Abu'l Qasim, 1301; Majmū'at al-Ṣanāya', 1582<sup>4</sup>; Ali Mohamed, 1888; Wulff, 1966) from which *shakhār* has been used more. Abu'l Qasim calls *shakhār* as a unifier which unifies all glaze ingredients (Ritter *et al.*, 1935). He describes this substance is made by burning pure, fully-grown *ushnān* plant which has a red-coloured centre when broken, with a strong smell.

The factors that determine the compositions of plant ash include the plant species; the stage in the growing season and the component of the plants (woody part or leaves); the composition of the soil and ground water in which the plants are growing; and the way in which the plants are ashed (Tite *et al.*, 2006). Practically, the alkalis (sodium and potassium) should be predominantly in the form of carbonates, bicarbonates, sulphites, sulphides and hydroxides rather than either chlorides or sulphates. Here, the alkali chlorides are practically non-reactive, melting and volatilising without decomposition. Similarly, the alkali sulphates react only slowly prior to decomposition (occurring at about 1200°C for sodium sulphate) unless

<sup>4</sup> There are six manuscripts kept in the Library of Islamic Parliament of Iran which contain more or less the same content. The oldest one's name is *Majmū'at al-Ṣanāya'* (Registration No. 15617) written in 1582 by an unknown author. Other copies whose names are *Chihil Bāb dar Kīmīyā* (Registration No. 15672), *Majmū' al-Ṣanāya'* (Registration No. 315), *Majmū' al-Ṣanāya'* (Registration No. 12586), *Majma' al-Ṣanāya'* (Registration No. 14284), and *Javāhir al-Ṣanāya'* (Registration No. 2849) are more recent and date back respectively to 1707, 1820, 1845 and the last two with unknown date. Here, in this text, we use the oldest one as the main reference and cite it as (*Majmū'at al-Ṣanāya'*, 1582).

reduced to sulphites or sulphides as a result of the presence of carbonaceous matter. Therefore, unlike the carbonates which dissociate to form oxides and are then readily incorporated into the glaze, only small amounts of chlorides or sulphates can be incorporated into a glass with the remainder forming an immiscible melt that remains separate from the glass (Tite *et al.*, 2006).

To produce *shakhār*, Wulff (1966) explains that the plant *ushnān*, which is a variety of *Salsola*, *Kali Solsola*, *Soda*, *Seiditziarosmarinus*, is slowly fired without long flame in a shallow well with two meters in depth. Then, the obtained ash is fired again in a particular furnace to calcine it. They load the furnace with five to seven kilograms of this ash from which five kilograms *shakhār* would be collected after the calcination.<sup>5</sup> Ali Mohamed (1888) describes *shakhār* is obtained from burning glasswort (*shūra*) and to purify it one can dissolve it in water in a kettle and place it on fire and boil it. Crystallised form of *shakhār* will be gathered after boiling and pouring it into an earthen bowl and leaving it all night.<sup>6</sup> There is, however, a puzzling description in the Abu'l Qasim's treatise. He states that *shakhār* should not be mixed with *shūra* because it destroys the glaze. Allan (1973) attributes *shūra* to *Salsola Tragus*. He also mentions that this plant, due to small amount of alkaline content, destroys the glazes. However, it should be taken into consideration that in old Persian manuscripts *shūra* has been also used to describe potassium nitrate (saltpeter) (Zāvush, 1996) and, therefore, the interpretation of Allan about *shūra* might be revised.

### 8.2.3 Intermediates

An intermediate acts sometimes as a network former and occasionally plays flux's role in the glaze. In historical glazes, as today, aluminum has always been the main intermediate element. Although aluminum cannot be a glass former, it could help network formers to make glassy matrix. More aluminum content in the glaze, more viscose glaze will be. A high viscosity glaze works for vertically placed objects inside the kiln to avoid glaze running. Other than aluminum, lead and zinc have also the same characteristic to act as aluminum in the matrix of glazes (Eppler and Eppler, 2000). Abū al-Qāsim (1301) has written about *tūfiyā* (zinc oxide (Zāvush, 1996) or zinc sulphide (Allan, 1973)) used in the glazes. However, zinc, except for a sample, was not observed in our studies on the *haft rang* glazes. Moreover, calcium and magnesium are two alkaline earth elements which act as intermediate in the glaze matrix. These elements, together with aluminum, stabilise the glazes' structure and enhance their resistance against weathering usually caused by moisture. These elements could have been introduced in the archaeological glazes as a plant ash's minor constituent (Tite *et al.*, 2006). Sometimes, calcium could be added to the glaze's batch deliberately as calcium carbonate (Shortland and Eremin, 2006).

The most important intermediate element in the *haft rang* tile which its presence in the glazes was proved by different analytical methods was lead. Perhaps lead, after silicon, is the most important element used in archaeological and modern glazes. Pb-bearing compounds, as fluxes, have been widely used in the ancient Persian glazes after the Achaemenids period until the recent times although the application of lead in making lead antimonate yellow glazes had been started much earlier from the middle Elamite period

<sup>5</sup> According to old treatises of glaze-making, the plant ash has most probably been the only source of supplying alkali content of Iranian glazes. The significant quantity of potassium and magnesium content detected in the ancient Iranian glazes can be originated from the plant ash used as flux (Freestone, 2008).

<sup>6</sup> Rāzī (9-10th century AD), in *Kitāb al-Asrār*, also mentions almost the same procedure for purifying the plant ash. He states that to make a purified *qalī*, one should grind and dissolve it in water and leave it for a weak. Then, it should be boiled until the quantity of the water is halved. Afterwards, it should be filtered ten times and poured in a thin permeable pot. The pot should be hung over a vase to gather the dropped alkali solution inside, which can be used as the purified *qalī*. One can also gather the efflorescenced *qalī* on the surface of the pot for two or three times, powder it and use it as a purified *qalī*.

(Caubet, 2007; Holakooei, 2013). Lead compounds have been applied in historical glazes with a reciprocal function; that is, they act as flux and intermediate in the same time. Although lead is not network former, high amounts of lead in the glazes does not end to the devitrification phenomenon and the glaze with sixty five percent of lead can even be easily formed with good properties (Eppler and Eppler, 2000). The earliest evidences of the use of lead-based glazes date back to the first century BC in Anatolia (Walton and Tite, 2010); however, it seems that the oldest evidences of using lead-based glazes in Iran date to the Parthian period (Hill *et al.*, 2004). In contrast with alkaline glazes, lead-based glazes have always had some advantages which provoked ancient glaze-makers to use it. Lead glazes can be easily used without any need to be fritted. Hence, time and fuel could have been economised. In addition, lead glazes have more wetting effect than alkaline glazes and, therefore, crawling occurs less in the lead glazes. Another advantage of lead glazes their low thermal expansion coefficient in comparison to that of alkaline glazes which permits glaze-makers to apply it easier on the clay bodies. Furthermore, lead glazes look very shiny and glossy due to their high refractive index (Tite *et al.*, 1998).

#### 8.2.4 The transparent frit

A transparent frit has necessarily been an essential part of the *haft rang* tiles. According to our studies, it has been prepared by quartz and plant ash even in the high lead glazes of yellow, green, and brown glazes. Al-Bīrūnī (ca.1050) mentions a kind of transparent enamel obtained from powdered flint stone and red lead ( $Pb_3O_4$ ). Moreover, Nayshābūrī (1196) describes how to make the transparent frit by grinding, washing, and drying quartz and, then, mixing and firing it with the plant ash. Abu'l Qasim (1301), however, describes this frit is prepared by melting 105 parts quartz and 100 parts plant ash in a kiln for a day and suddenly cooling the molten material in the water. The cooled glass is then ground, sifted and used as the transparent frit. Ali Mohamed (1888) suggests equal amounts of quartz and the plant ash should be molten and, like Abu'l Qasim, describes how to stir the molten glass. Ḥusaynī (19th Century), however, in *Kashf al-Ṣanāya*<sup>5</sup>, provides a description about making a lead-based frit by mixing sixteen parts red lead, four parts powdered flint, three parts powdered glass, and twelve parts quartz and, then, heating them for twenty four hours on a pungent fire. He also adds the molten materials should be suddenly cooled in water and, thereafter, dried, pounded, ground, and used as a transparent frit. In Maybud and Naṭanz, a similar method is still used to create transparent frits (Centlivres-Demont, 1971; Kīyān-Aṣl, 1994).

#### 8.2.5 The opaque frit (white glaze)

Any material which is not dissolved in the glassy matrix of the transparent frit produces an opaque frit. As a definition, undissolved materials scatter light beam and, as a consequence, the glaze appears opaque. Higher refractive index of the dispersed particles, the more opaque glaze will be. Moreover, particle size and shape, together with the degree of dissolution of the particles, are the other important factors in opacifying glazes (Mason and Tite, 1997). During the Middle Elamite period, lime and air bubbles, along with calcium antimonate, have been the main causes of opacifying alkaline glazes (Caubet, 2007; Holakooei, 2013); however, in the Achaemenid era calcium antimonate and tin oxide have been basically used as opacifiers (Caubet and Kaczmarczyk, 1998; Caubet, 2007). Opacified glazes are also achieved by adding quartz, wollastonite, diopside, air bubbles (Mason and Tite, 1997), feldspar together with air bubbles (Mason and Keall, 1991) and undissolved silicates (Pace *et al.*, 2008). Although tin oxide has

been used as an opacifying agent in pre-Islamic glazes (Caubet, 1992), it was largely used in Islamic World from the ninth century onwards (Mason and Tite, 1997).

In spite of the extensive use of tin oxide in the Iranian glaze industry, tin mines have brought up controversial issues. According to old quotes, tin was apparently an imported merchandise (Tūsī, 1255; Manşūr, 1454–1478). However, Mustufī (1339) notes that tin mines are found in Luristān. In fact, the presence of tin ore in Luristān is probable because of many bronze objects excavated by archaeological expeditions in this region (Muscarella, 1988). Moreover, based on various old texts, Zāvush (1996) suggests seven zones in Iran as probable resource of tin even though there is no recent research confirming these old quotes.

Al-Bīrūnī (ca.1050) indicates some hints about tin opacified glazes which are perhaps the oldest quotes in this regard. He writes about a white enamel which is obtained from one part flint-stone powder, equal amount glass powder, one-fourth part natural sodium carbonate (natron), and two-thirds part tin oxide powder. He also mentions that borax could also be added to the mixture to lower the melting temperature. Nonetheless, what Abu'l Qasim (1301) states about opaque frit are different. The opaque frit of Abu'l Qasim demands two steps to be developed. In the first step, lead and tin are molten together to produce lead and tin oxides and in the second phase the mixture of *qamşarī* stone and the plant ash is fired with the product of the first step. To produce lead-tin oxides, three parts white lead and a third part tin should be fired together. However, Ali Mohamed (1888) suggests four parts lead and one part tin to achieve the first mixture. To make such a mixture from tin and lead, Abu'l Qasim (1301) says that lead should be molten in the kiln for a while, and tin is then added on top of it. When this mixture brings up an earthy substance on its surface, it is completely ready. Ali Mohamed (1888) also describes more or less the same procedure with more details. Nowadays, the lead and tin oxide mixture is still being manufactured in the traditional Persian workshops with the same procedure (Şadıq and Karīmī, 1965; Wulff, 1966; Holakooei *et al.*, 2012). The reason of oxidising lead and tin together may be laid on the fact that tin oxide is more easily produced from heating tin and lead metals together rather than by heating tin by itself (Paynter *et al.*, 2004). Ḥusaynī (1669), in *Tuḥfa-ye Ḥakīm-i Mu'min*, also describes a similar procedure with little difference. He suggests adding some sulfur to the mixture of lead and tin. All the mentioned treatises suggest that the mixture should be stirred by an iron ladle to reach good results. Tin, in fact, was always oxidised with lead because it is very difficult to be oxidised in the pure state (Mason and Tite, 1997). To make the opaque glaze, one part *qamşarī* stone and one part plant ash are then roasted together and after cooling, three parts of this frit are added to one part of the lead-tin oxide. This mixture is molten and cooled in water and, then, ground to be used (Abu'l Qasim, 1301). However, Ali Mohamed (1888) briefly suggests mixing one part of the tin-lead oxides with three parts of the transparent frit to make a white glaze. Ḥusaynī (19th Century), nevertheless, describes an almost different procedure about the white frit. According to his treatise, the glaze-maker should put both lead and tin into a furnace and brew the mixture to make froth on the top of the melted material like a cream. Then, he removes it with a spoon, grinds and puts it in a large pot of water. When it is precipitated in the water, he should pour the water out of the pot and dry the washed material inside the pot in the sunlight. Then, he should take the dried material and add the same amount of sand and one fourth part table salt to it. The glaze-maker must fuse this mixture in a kiln to prepare the white glaze, according to Ḥusaynī (19th Century).

The development of Islamic tin-opacified glazes has traditionally been attributed to the need to copy imports of Chinese whitewares into the Islamic world. The fact that the early Islamic opaque-glazed wares

were overwhelmingly used as backgrounds for overglaze decoration in blue, green and metallic lustre paints would also argue that the impetus was the local demand, not foreign influence (Mason and Tite, 1997). To produce the white colour, the tin oxide must exist as small particles (crystals), the size of which should be of the same order of magnitude as the visible wavelength of white light. However, as scattering follows the Rayleigh formula, where the scattered intensity is proportional to the fourth power of the wavelength, the scattered light should be bluish. This does not occur because the lead glazes absorb light in the blue region, compensating for this effect (Vendrell-Saz *et al.*, 2006). Molera *et al.* (1999) have shown that, during the production of tin-opacified lead glazes, the lead oxide reacts with the tin oxide to produce lead stannate, which then goes into solution as the glaze itself forms. Normally, the tin oxide would subsequently recrystallise out from the glaze. Since lead glazes absorb in the blue region, tin-opacified lead-alkali glazes appear whiter than would the corresponding tin-opacified alkali glazes (Tite *et al.*, 1998).

### 8.2.6 Blue glazes

According to UV-Vis spectroscopy and EDS microanalyses, cobalt is the colourant of the blue glazes of the *haft rang* tiles. Dark blue hues have been traditionally achieved by adding a Co-bearing material into a glaze. However, the first clues about blue hues in glazes are derived from the use of copper and iron compounds in an alkaline glaze as those of Middle-Elamite blues used in decorating glazes bricks of Susa and Chughā Zānbīl (Caubet, 2007). The traces of using cobalt together with copper in yielding dark blue colours date back to the relief glazed bricks of the Achaemenid period (Caubet and Kaczmarczyk, 1998). The use of blue cobalt, nonetheless, was flourished in the Islamic periods. The quotes of Nayshābūrī (1196) might be the oldest indications about making dark blue hues from cobalt-bearing materials when he states it is provided by taking 100 parts quartz, five parts *lājvard* rock [a cobalt compound], and borax of natron. Abu'l Qasim (1301), however, describes this colour is achieved by adding *sulaymānī lājvard*<sup>7</sup> to the transparent frit and, for a greyer hue, less *lājvard* and a small amount of red lead should be added. Unknown author of *Majmū'at al-Ṣanāya* (1582) also speaks clearly about using *sulaymānī* stone in making blue colours in glazes. Ali Mohamed (1888) also describes cobalt ores in environs of Kāshān which look like blossoms. Jahāngīr Pādīshāh (1627) in *Mirāt al-Javāhir* has mentioned three different types of *sulaymānī* stone, but there is no indication about their use. However, the author of Burhān-i qāṭa' has described *sulaymānī* stone as manganese oxide which is a black mud supplied from the mountains of Kāshān (Khalaf Tabrīzī, 1652). (Certainly, manganese oxide does not yield blue colour in the glaze, and the Khalaf Tabrīzī' state is probably inappropriate.) Allan (1973) suggests that *sulaymānī* stone is sulpharsenide of cobalt, cobaltite (CoAsS), which at high temperatures is transformed to cobalt oxide, zaffer in Arabic (Keblow-Bernsted, 2003).

<sup>7</sup> There is a controversial discussion about the word *lājvard*, a component responsible for azure colour in the glaze. *Lājvard* in Persian means lapis lazuli. According to Abu'l Qasim (1301), it yields blue or sapphire colour in the transparent frit. But, lapis lazuli is a chain silicate which sulfur in its crystalline lattice causes the blue colour (Plesters, 1966). Evidently, at high temperatures, sulfur is given off the crystalline lattice, as sulfur trioxide and dioxide, and subsequently, it becomes colourless. Hence, most of researchers do not attribute Abu'l Qasim's *lājvard* to lapis lazuli, and have interpreted it as a cobalt ore (Allan, 1973; Keblow-Bernsted, 2003; Bier, 1993). Nevertheless, having an interpretation of the Raman spectrum of a Safāvid blue glaze, Colombari (2003) believes that the Abu'l Qasim's *lājvard* is, in fact, natural ultramarine which reflects blue colour from the interface of glaze and body. He suggests that lapis lazuli causes the blue colour in the glaze at the temperatures below its decomposition temperature. Accordingly, Gueit *et al.* (2010) has reported the application of natural lapis lazuli in *mīnā'ī* decorations. Also, Catalano *et al.* (2007) have published a paper in which lapis lazuli has been introduced as a colouring agent of Italian blue glazes. In the contrast, a recent Raman study has declined this hypothesis and gives another interpretation of the band by which the previous studies have concluded to the use of lapis lazuli in the glazes (Sendova *et al.*, 2010). It should be noted that Abū al-Qāsim (1301) himself clearly describes the appearance of *lājvard* which has nothing in common with natural lapis lazuli.

Abu'l Qasim (1301) describes that sources of this stone are in Qamṣar and it is like white silver shining in a sheath of hard black stone. The cobalt ores near Kāshān and Qamṣar have been frequently cited in old and contemporary recipes of glaze-making (Dānishpazhūh, 1447; Polak, 1865; Rochechouart, 1867; Olmer, 1908; Allan, 1973; Wulff, 1966; Mudarrisī Ṭabāṭabā'ī, 1985; Kalāntar Ḍarrābī, 1999; Floor, 2003; Keblow-Bernsted, 2003; Harātī, 2004). Moreover, cobalt mines near the mountain of Quhrūd (Wulff, 1966), Tehran, Anārak, Balūchistān (Keblow-Bernsted, 2003), and Nā'in (Gluck, 1977) are also mentioned. It is suggested that the cobalt mines of Kāshān are now either exhausted (Nīyāzmand, 1964; Gluck, 1977) or out of access because of the constructions on top of the mines (Harātī, 2004). However, what appears in the reports of Schindler (Floor, 2003) and Olmer (1908) demonstrates that there have been cobalt ores in a large amount around Qamṣar. Unknown author of *Javāhir-nāma* notes that the ores were exported to Saudi Arabia and Iraq (Dānishpazhūh, 1447). However, Polak (1865) mentions that these ores were exported to Russia. Moreover, the cobalt ores were apparently exported to China, where it was called 'su ma li qing' which means Mohammedan blue (Feng and BaoRu, 2008). In China, *sulaymānī* stone has been as precious as gold during Ming dynasty (Gluck, 1977), however, it was differently purified and processed in China (Wen and Pollard, 2009). Nevertheless, it should be noted that studies performed on the trace elements of blue glazes produced in Iraq and China shows that their cobalt ores were not only mined in Kāshān. That is, cobalt was possibly provided from Saudi Arabia or Yemen (Wood *et al.*, 2007).

Ali Mohamed (1888), Olmer (1908), Wulff (1966), Mudarrisī Ṭabāṭabā'ī (1985), Kalāntar Ḍarrābī (1999), and Schindler (Floor, 2003) have fairly similar descriptions about the preparation of a key component of a blue glaze. Usually, in the process of purifying cobalt ore, earthy cobalt was washed with water, and then fired with potash and borax to obtain a concentrated colourant for blue. Ali Mohamed (1888) explains that, to make a blue colour from the colourant, one should take one part of the earthy cobalt, three parts of the powdered glass, four parts of the transparent frit, sixty five grams of the purified colourant, and half a kilogram the plant ash and, then, bray the whole and finally use it in the mixture with the Arabic gum. Rochechouart (1867) describes another way of making blue glaze. He writes that tile-makers take one part cobalt oxide, one part borax, and one-fourth part grape juice, mix well, and then, melt in a pot in the kiln. Then, they break the pot and take out the contents and powder it. Five grams of this powder is mixed with the following mixture: 100 grams powdered glass, fifty grams saltpeter, fifty grams borax, and fifty grams caustic soda. They melt the mixture, and after cooling the mixture, they powder it and mix with Tragacanth gum and use as a blue glaze.

### 8.2.7 Violet glazes and black lines

Basically, manganese oxide had been responsible for black to violet tints in both lead and alkaline glazes. This was again positively proved in all black and violet glazes of *haft rang* tiles by micro-Raman spectroscopy, UV-Vis spectroscopy, and EDS microanalyses. Abu'l Qasim (1301) describes if one adds one part *maghnīsīyā* to ten parts of the transparent frit, it outs of kiln black. According to Abu'l Qasim, lesser amount of *maghnīsīyā*, however, yields a violet hue. *Maghnīsīyā* is, in fact, manganese oxide (pyrolusite) known also as *gil-i maghnī*, *maghn*, and *gil-i kāsaḡarān* (Maṣṣur, 1454–1478; Zāvush, 1996). Abu'l Qasim (1301), moreover, mentions two types of *maghnīsīyā*: male and female which based on the hardness of different manganese ores, Zāvush (1996) believes that the male one is pyrolusite (with higher value of hardness) and female one is rhodochrosite [manganese carbonate] (with lower hardness). *Maghnīsīyā* was also known as 'black of glassmakers' because it was used in the glass industry (Khalaf

Tabrīzī, 1652).<sup>8</sup> Ali Mohamed (1888) notes that the black colour can be obtained by mixing and braying together powdered glass, the transparent frit, and maghn stone, as well as liquid Arabic gum. Another way to produce black and violet glazes was to mix red and azure glazes together (Ali Mohamed, 1888). A mixture of five parts dark blue glaze and one part red glaze is the composition of violet glaze, Rochechouart (1867) records. According to Rochechouart, manganese violet does not have the same quality as the former violet glaze.

Concerning the black lines of *haft rang* tiles, the colouring agent was also identified definitely manganese oxide black in contrast with the black lines of the seventeenth century Safavid underglaze decorations where chromite has been used for making a separating black line of the blue and white wares (Agosti and Schweiser, 2002). It should be noted that chromite in the Safavid underglazes acts as a separating line due to its refractory behaviour. In the *haft rang* tiles, however, the main reason, which does not allow the coloured glazes run together, is the high alumina content whilst manganese oxide is solely responsible for the black hue.

### 8.2.8 Turquoise glazes

Basically, turquoise hues have been achieved by bivalent copper ions dissolved in alkaline glazes and opaque turquoise colours have been attained by white tin-opacified glaze and copper oxide, as the analytical studies pursued in this thesis proved this fact. Copper oxide has been always known the most important colouring agent in pre-Islamic and Islamic Iranian glazes. The application of copper in the alkaline glazes from the Elamite (Caubet and Pierrat-Bonnefois, 2005; Caubet, 2007) and Achaemenid glazed bricks (Caubet and Kaczmarczyk, 1998) towards Parthian and Sassanian periods in pre-Islamic Iran (Hill *et al.*, 2004) is reported. Almost in all old Persian manuscripts copper compounds are suggested as the main colourant of turquoise glazes. Unknown author of *Majmū'at al-Şanāya'* (1582) suggests mixing and fritting ten parts transparent frit, one part burnt copper, one part tin oxide, and half a part cobalt ore to achieve a turquoise glaze. Ali Mohamed (1888), however, notes a turquoise colour is achieved by adding one sixteenth part copper dross (the pieces which chip off when copper is hammered) to one part of the white glaze and heating in the kiln. Rochechouart (1867) mentions how glaze-makers mix 400 grams lead and tin oxides, 660 grams glass powder, eighty grams copper oxide, eighty grams powdered flint stone, and 240 grams caustic soda, and afterwards, frit them together to obtain a turquoise glaze. Furthermore, Olmer (1908) describes the ingredients used in Nā'in to make a turquoise glaze: two parts lead oxide, two parts tin oxide, one part copper oxide (burnt copper), one part sand, and six parts glass powder. The presence of undissolved particles of burnt copper in the composition of the turquoise glazes previously proved by micro-Raman spectroscopy confirms the quotes of the old recipes.

### 8.2.9 Yellow glazes

The *haft rang* yellow glazes were definitely diagnosed lead-tin yellow type. However, the oldest evidences of using yellow glazes in Iran date back to the Middle Elamite dynasty when lead antimonate was being used as a yellow opacifier (Caubet, 2007). This tradition was on use until the decline of the Achaemenid period when yellow glazes were disappeared and experienced a long period of absence (Caubet, 1992; Caubet and Kaczmarczyk, 1998). Although Nayshābūrī (1196) and Abu'l Qasim (1301)

---

<sup>8</sup> Very low amounts of this substance were also used to discolour greenish hues obtained by iron content in glassware (Rāzī, 9-10th Century; Tūsī, 1255; Khalaf Tabrīzī, 1652).

have mentioned a substance so-called *atmad* (antimony sulfide or stibnite) which could have been used in glazes in order to produce yellow glaze, there is no analytical data supporting the application of antimony in making Iranian yellow glazes in Islamic Persia. However, Tite's (personal communication) studies shows that lead antimonate yellow had been using from the eighth century in Egypt and Syria.

On the other hand, another type of yellow glaze is lead-tin yellow used as a common yellow glaze in Islamic era of Iran. Ali Mohamed (1888) notes that it is yielded by melting sixteen parts lead and one part tin, taking the froth and heating it again in order to change all to froth. The yellow glaze is then obtained by mixing and heating this mixture with a quarter of its quantity of flint stone. By heating and being molten this mixture, a glaze-maker should take out that yellow colour with an iron ladle, bray it, mix it with a solution of Tragacanth gum and apply it on bricks or vases. Nowadays, this method is used for making yellow in Lalajīn near Hamadān (Ṣadīq and Karīmī, 1965). Rochechouart (1867), also, notes that how glaze-makers obtain a yellow hue from three kilograms lead, 320 grams tin and 640 grams powdered flint stone. It should be emphasised that the lead stannate responsible for the opaque yellow of the glasses is the cubic form ( $\text{PbSnO}_3$ ) and not the orthorhombic form ( $\text{Pb}_2\text{SnO}_4$ ). It is shown that, when mixtures of lead oxide and tin oxide are heated to temperatures in the range 700–900°C, it is the orthorhombic  $\text{Pb}_2\text{SnO}_4$  that is formed. However, if silica is added to the  $\text{Pb}_2\text{SnO}_4$  and the resulting mixture is heated to 850°C, the  $\text{Pb}_2\text{SnO}_4$  is converted to the cubic  $\text{PbSnO}_3$ , complete conversion occurring for a  $\text{Pb}_2\text{SnO}_4$  to  $\text{SiO}_2$  molar ratio of 3 to 2 (*i.e.*, equivalent to 69.9 wt% PbO, 23.8 wt% SnO<sub>2</sub> and 6.3 wt% SiO<sub>2</sub>) (Tite *et al.*, 2008b).

One type of yellow glaze is also described by Tiflīsī (12th Century) and the unknown author of *Majmū'at al-Ṣanāya'* (1582) which contains neither tin nor antimony in its composition. They just simply suggest mixing and fritting lead white, plant ash and quartz to obtain a yellow hue in a vitreous matter. They would have probably mentioned a pale and transparent glaze which might be obtained from iron content of the body introduced in the bulk of the glaze. The examples of such a yellow glaze can be found in Darb-i Imam in Isfahan and many other tenth century AD monuments in Iran.

#### 8.2.10 Green glazes

According to micro-Raman and EDS microanalyses, green glazes were a green tinted yellow glazes achieved by copper ions. According to Nayshābūrī (1196), mixing and heating one part flint stone, two parts lead oxide, two parts plant ash and ten parts burnt copper can lead to a green hue in the glaze. He also records another kind of green glaze obtained from silica powder, powdered red lead, copper oxide, verdigris and borax of natron. Unknown author of *Majmū'at al-Ṣanāya'* (1582), moreover, suggests fritting two parts quartz, one part plant ash and one part tin oxide and copper oxide together and using it as the green opaque glaze. Interesting point in his descriptions is the use of two crucibles one top of another. He explains that the upper crucible should have a hole beneath in order to pass the molten materials to the downer one during heating. He clearly speaks about fritting and not simply mixing the ingredients to make a green glaze. Ali Mohamed (1888), however, describes a green glaze comes out of the kiln when one part copper dross, three parts lead oxide, six parts glass, six parts flint stone, and six parts alkaline transparent frit are mixed and heated in the kiln. Rochechouart (1867) also describes four different types of green glaze prevailed in the nineteenth century in Maybud, central Iran. At the same time, in Nā'īn, however, green glazes were obtained by mixing and firing three parts lead oxide, two parts copper oxide, two parts sand and three parts glass powder (Olmer, 1908). Since antiquity, to make opaque green glazes either

copper-bearing materials were added to tin or antimony opacified glazes or tin or antimony compounds were added to a green frit (Nayshābūrī, 1196; Rochechouart, 1867; Ṣadīq and Karīmī, 1965). Sometimes, a tiny amount of cobalt compounds was also added to achieve other tonalities of green glazes (Nayshābūrī, 1196; Ṣadīq and Karīmī, 1965).

#### 8.2.11 Brown glazes

Brown glazes are rarely used in *haft rang* tiles. However, three brown glazes analysed in our studies showed iron oxides has yielded a brown hue the lead-tin yellow glazes. This fact can also be tracked in old manuscripts of glaze-making. Ali Mohamed (1888) describes iron filings should be dissolved in aqua regia firstly in order to make the iron saffron (burnt-green vitriol). This can yield an orange or jujube colour to the glaze. Rochechouart (1967), also, explains two brown glazes which had been using over the nineteenth century in Iran. The first one, which is tobacco-like in colour, is achieved by mixing yellow and black glazes equally. For the second one, however, glaze-makers mix, at first, five parts iron filings and two parts sal ammoniac together. Then, they take two parts of this mixture and mix with five parts flint stone and two parts saltpeter. By heating this mixture, a brown glaze comes out of the kiln.



## Final Remarks and Conclusions

This thesis represented the first analytical data derived from Persian *haft rang* tiles and was focused on the technological study of the tiles during the seventeenth, when all of crafts seem to have undergone a dramatic change as a result of a global market flourished in the Safavid Persia. The most important centres of using polychrome *haft rang* tiles in the Safavid period, including Mashhad, Isfahan, Māzandarān (Āmul and Sārī), and Qazvīn, were selected as the area of sampling. Forty three samples were analysed by WDXRF, XRD, micro-Raman spectroscopy, UV-Vis spectroscopy, SEM, and EDS microanalyses whose results were presented in various chapters. An individual chapter was devoted to discuss these results in the context of Persian ceramic industry spanning the first millennium BC through the recent times. The aim of the current chapter is, however, to illustrate an overall view on the *haft rang* tiles and to compare technologically this style of tile-making with Spanish *cuerva seca* tiles as the Persian technique is frequently referred to the Spanish one.

As far as PCA interpretation of WDXRF results on the tiles' bodies is concerned, the tile fragments are totally calcareous clay-based and each centre of Safavid tilework have its identical chemical composition, which distinguishes it from the others. Amongst the samples obtained from Isfahan, however, a group was discriminated, which has probably been added to tile revetments of the mosque due to a latter intervention or a recent restoration plan. On the other hand, statistically handling the values of trace elements and considering geological specifications of the zones from where samples were obtained, it can be suggested that *haft rang* tiles' bodies have probably been manufactured from the local clays resources. In other words, the bodies of the tiles could be local products and, therefore, not imported from other regions. Moreover, XRD analyses established the firing temperature of the samples at about 850-1000°C, which is entirely expected from the traditional and old kilns of ceramic kilns in Iran. On the other side, although it is well-documented that the tiles have always been transporting from each city to another city to decorate architectural facades, this research demonstrates that the industry of tile-making in the Safavid era in Iran has been, with high probability, self-sustaining in cities where Safavid tiles are discovered. As a future perspective, other periods of making *haft rang* tiles should be taken into account in order to define the obtained results in the context of Persian tile-making over the past centuries. In other words, our results show only a piece of a complicated puzzle, which should be gradually completed to achieve an overall knowledge of *haft rang* tile-making.

Having a comparative view, the bodies of the Ottoman Iznik tiles and Indian mosaic tiles, which were in use during the seventeenth century with a more or less a same time of period with the studied *haft rang* tiles, it should be said that the bodies of *haft rang* technique is totally different from their contemporary Indian and Ottoman techniques. Quartz based bodies of Iznik underglaze (Paynter *et al.*, 2004) and Indian mosaic tiles (Gill and Rehren, 2011; Gulzar, *et al.*, 2012) seem to be adjusted for the two techniques of

underglaze and mosaic. Therefore, it has been a great evolution for ceramic technology in the seventeenth century to use clay bodies for making polychrome tiles when in the same period of time, quartz based bodies were in use for making underglaze blue and white wares (Agosti and Schweiser, 2004). This could suggest a fast production with more diversity in colour which was in privilege during the rapid evolution of the Safavid Empire during the seventeenth century.

On the other hand, there is Spanish *cuerva seca* technique, which uses clay body as a substrate for the subsequent glazes. Although the Persian and Spanish techniques both are created on clay bodies, there is a slight difference in firing the biscuit. According to our studies, a biscuit firing has most probably been done for a group of *haft rang* tiles (see *Chapter Four*, p. 52) prior to the use of coloured glazes. However Pérez-Arantegui *et al.* (1999) suggest that Spanish *cuerva seca* glaze decorations are painted on a raw body before firing and the coloured glazes are fired in the same firing with the body. Thus, it seems that the bodies of *haft rang* tiles have pursued a same tradition of the fifteenth century Timurid polychrome tiles rather than an external Spanish evolution since the composition and the technology of *haft rang* tiles is quite similar to their Timurid antecedents (O’Kane, 2011).

Concerning the white substrate glaze of *haft rang* tiles, it should be noted that it is practically an alkali glaze in which tin oxide particles have been incorporated. The lead content of the white glaze can however be attributed to the pigment obtained from oxidising lead and tin together which is frequently mentioned in old and recent manuscripts as the main constituent of the opacification in archaeological glazes (see *Chapter Eight*, p. 95). According to the calculations carried out on the semi-quantitative EDS results, the maturing temperature at which the white substrate glaze has a viscosity of  $10^4$  poise is about 900°C. This temperature is quite comparable with the temperature calculated for the antecedents Timurid *haft rang* tiles (O’Kane, 2011). Considering the maturing temperature of the upper coloured glazes, which according to our calculations was on average about 700°C (see *Chapter Seven*, p. 86), it could be hypothesised that when the upper glazes are runny enough to wet the surface of the white glaze, the white substrate glaze does not change its behaviour under the lower maturing temperature of the coloured glazes. This lessens the chance of re-melting and unifying the white glazes with the upper coloured glazes.

Having a comparison the substrate of coloured glazes in *haft rang* with *cuerva seca*, a significant difference is raised; that is, total absence of a white substrate glaze for coloured glazes in *cuerva seca* technique. Technological studies on Spanish *cuerva seca* ware have showed that the coloured glazes are directly applied on a clay-based body and any white glaze or slip is entirely absent in this kind of glazed decorations (Pérez-Arantegui *et al.*, 1999; Chapoulie *et al.* 2005). On the other hand, there are Iznik tiles in which different coloured pigments are applied on a white slip and a transparent glaze has covered both the white slip and the pigments. The Iznik tiles, however, are apparently underglaze decorations and technically different from those of *haft rang*. It seems that *haft rang* technique is a unique technique which uses a white glaze as substrate to apply other glazes on. *Haft rang* technique is nonetheless similar with Persian *mīnā’ī* and *lājvardīna* techniques in which a substrate glaze (white and dark blue for *mīnā’ī* and *lājvardīna* respectively) is used for subsequent overglaze decoration.

Another point which makes unique *haft rang* tiles is its coloured glazes, which are used on the white substrate. The first issue is the variety of colour used in *haft rang* tiles, which comprises of white, turquoise, blue, violet, yellow, black, green, and brown (and in more recent instances from 18th century onwards, pink glaze). This variety is less achieved in Spanish *cuerva seca* tiles, where yellow, green, turquoise, white, and black glazes are all variety of colours executed ever on Spanish *cuerva seca*

ceramics. This dissimilarity between these two types of polychrome glazed ceramics is more evident in the chemical composition of the coloured glazes. According to the results obtained in this thesis, turquoise, white, blue, and violet glazes of *haft rang* technique are apparently alkali glazes with probably plant ash origin of flux and brown, yellow, and green glazes are high lead glazes (see *Chapter Seven*). Analytical approaches on the  *cuerda seca*  glazes, however, have showed that the glazes are high lead glazes with low alkali content (Pérez-Arantegui *et al.*, 1999; Chapoulie *et al.* 2005). It seems that the source of flux agent is entirely different in these two styles of making polychrome tiles, i.e. *haft rang* and  *cuerda seca* . Another difference in the glaze composition of *haft rang* and  *cuerda seca*  is related to the opacifiers used in the bulk glazes. Based on the results of micro-Raman spectroscopy and EDS microanalyses, the opacifier of the white glazes in *haft rang* style is tin oxide prepared by roasting tin and lead together, as it has been a routine practice in Iran from the very beginning of the use of tin oxide as opacifier (see *Chapter Eight*, p. 95). However, there are some examples of  *cuerda seca*  specimens which are not opacified by tin oxide or a quantity of tin oxide is very low respect to the Persian technique of *haft rang*. Another opacifier used in *haft rang* technique is lead stannate yellow which seems to be totally absent in  *cuerda seca*  technique. In the Islamic Persia, lead stannate has always been used as the yellow opacifier in yellow, green, and brown glazes, as was proved in our studies on *haft rang* tiles (see *Chapter Six*, p. 76). It seems, nevertheless, that lead stannate has never been used in  *cuerda seca*  technique. As far as the yellow glazes of  *cuerda seca*  technique are concerned, they are transparent high lead glazes in which iron oxide had yielded a yellowish hue. Only common point between  *cuerda seca*  and *haft rang* technique in the coloured glazes is the colourants of green and black glazes which are copper and manganese oxides respectively. This similarity, however, cannot make these techniques close together as the usual ways of obtaining such colours have always been using copper and manganese in antiquity.

The main reason by which *haft rang* technique is called ‘ *cuerda seca* ’ is the use of a black line for delineating designs and separating different coloured glazes. The term  *cuerda seca*  is usually translated in the scholarly literature as ‘dry cord,’ but this can be misleading. The term itself was not used in Spain before the early sixteenth century, much after the technique was first used on pottery, in the eleventh century (O’Kane, 2011). According to the published analytical data, the colouring agent of black lines in both *haft rang* and  *cuerda seca*  styles is manganese oxide. In the Persian technique of *haft rang*, nonetheless, high alumina content has dramatically increased the maturing temperature of this glaze up to about 1150°C (see p. 86), which is desirable for keeping separated the melted coloured glazes in lower temperature in order to avoid mixing and running together. However, in the case of  *cuerda seca*  technique except few samples, the alumina content of the black lines is relatively lower than that of Persian technique. On the other hand, it is claimed that in the Spanish technique a fatty substance was mixed with manganese oxide, which could keep the watery suspensions of the coloured glazes on the body prior to firing. To the best of our knowledge, the use of a fatty substance in *haft rang* tiles has not been reported yet. The use of a black line for separating coloured glazes, on the other hand, cannot be a concrete reason by which we can technologically attribute *haft rang* to the Spanish technique of  *cuerda seca*  since prototypes of using a dark line for separating coloured glazes are dated back to much earlier times in Iran. The Elamite polychrome glazed bricks at Chughā Zānbīl and Susa, and the Achaemenid polychrome glazed bricks at Persepolis and Susa are only pre-Islamic examples of the use of a black line to delineate designs and patterns in Iran. If we come through the Islamic Persia, abundant examples of using a black line in the underglaze decorations and overglaze *mīnā ī* ware show a rich and long tradition of using a dark separating colour between different colours. However, the most similar technique, which uses the same functionality of the black line with the more or less a similar chemical composition, is that of the

fifteenth century Timurid polychrome *haft rang* technique. Apparently, the similarity in materials and technique between Timurid and Safavid overglaze polychrome tiles suggest that we should look for the origins of *haft rang* in Iran. In fact, considering the technological differences between *haft rang* and *cuerda seca*, it could be probably appropriate to consider the Persian technique as an independent development rather than an external influence. Unconnected with earlier Spanish examples, *haft rang* technique can be considered as a development from previous overglaze-painted techniques of *mīnā`ī* ware (O’Kane, 2011). Therefore, it would be appropriate to have a look at Islamic overglazes of *mīnā`ī* in the following paragraphs.

Jābir ibn Ḥayyān, in *al-Durra al-Maknūna*, is the first person who describes how to make *mīnā`ī* decorations on glassware (al-Hassan, 2009). The Tiflīsī’s treatise can also be considered as an important resource of materials and techniques of *mīnā`ī* decorations (Tiflīsī, 12th Century). Moreover, Abu’l Qasim (1301) gives details for achieving white, red, black, and yellow colours on glazes. A more recent treatise is written in the sixteenth century which clearly describes different techniques for obtaining various colours on a glassy surface (Majmū‘at al-Ṣanāya‘, 1582). Concerning the colourants used in *mīnā`ī* decorations, Tiflīsī (12th Century) discusses that a red overglaze hue is to be achieved by copper compounds (black copper oxide, orpiment, and verdigris) and reducing agents (marcasite and vinegar). Since this composition is suitable for making lustre overglazes, the red hue can be attributed to the shiny metallic red layers usually seen in lustreware. Unlike the Tiflīsī’s recipe, the analytical approach on *mīnā`ī* overglazes show that red colour is obtained from hematite (Mason *et al.*, 2001; Smith, 2001; Koss *et al.*, 2009; Gueit *et al.*, 2010). Chemical analyses of *mīnā`ī* red overglazes show that the amount of fluxes in this colour is low, and accordingly quartz content is high. Therefore, iron oxide is not dissolved in the glassy matrix and, hence, the red colour is not usually bright enough in *mīnā`ī* overglazes. Traditional glaze-makers, by experience, have not used high amount of flux in the composition of the red overglazes, because dissolved iron oxide in the glassy layer could produce a brownish colour to the layer (Smith, 2001). Another red hue, as that of ruby, is suggested by unknown author of *Majmū‘at al-Ṣanāya‘* (1582) in which two parts of red orpiment, three parts of sulfur, and one part of Yemeni vitriol are mixed and ground with vinegar and, then painted on a glassy surface. Like the Tiflīsī’s recipe, the ingredients suggested by *Majmū‘at al-Ṣanāya‘* are close to those of lustre pigment.

Concerning green and white colours, Tiflīsī (12th Century) explains that they are yielded from copper compounds and tin oxides respectively. The results of analytical studies also confirm that green and white overglazes have always been achieved by these constituents (Mason *et al.*, 2001; Smith, 2001; Koss *et al.*, 2009; Gueit *et al.*, 2010).<sup>1</sup> Turquoise hues have usually been created as inglaze colours (Mason *et al.*, 2001; Smith, 2001; Koss *et al.*, 2009) despite the Tiflīsī’s description which refers to an overglaze hue (Tiflīsī, 12th Century). Dark blues have always been associated with cobalt compounds and are usually achieved as inglaze decorations (Mason *et al.*, 2001; Smith, 2001; Koss *et al.*, 2009). However, unknown author of *Majmū‘at al-Ṣanāya‘* (1582) describes that it is achieved as an overglaze decoration by mixing, grinding, and painting twelve parts iron oxide, twelve parts burnt silver, four parts cobalt ore and vinegar on a glassy surface. Tiflīsī (12th Century) also describes that a dark purple hue is attained by manganese oxide, which is in accordance with scientific analyses carried out on overglaze purple glazes (Mason *et al.*, 2001; Smith, 2001; Koss *et al.*, 2009). Black colour is usually used to lineate designs and is achieved by

<sup>1</sup> Gueit *et al.* (2010) report a white overglaze on glassware contained significant amount of calcium.

chromite (Smith, 2001), as Abu'l Qasim's (1301) has also mentioned. This black colour is usually used as inglaze underdrawings (in *mīnā'ī* ware) or overglaze decorations (in *lājvardīna* ware) (Koss *et al.*, 2009).

Based on Abu'l Qasim's treatise and experimental observations, Mason *et al.* (2001) suggest that the pigments of *mīnā'ī* overglazes are simply obtained by mixing metallic oxides and the powdered frit of the substrate glaze. On the other hand, some believe that a colouring agent is fritted together with other ingredients in order to obtain its correspondent overglaze pigment (Hobson, 1965; Wulff, 1966; Smith, 2001). Another alternative suggests the application of colouring agents directly applied on the substrate glaze, being neither fritted nor mixed with other compounds (Freestone, 2002; Koss *et al.*, 2009), which is in accordance with the Tiflīsī's treatise. Concerning the firing process of *mīnā'ī* ware, it is generally believed that these decorations are created at low temperatures with long time firing (Smith, 2001; Koss *et al.*, 2009). Moreover, Henderson and Allan (1990) have suggested that the firing temperature of the overglaze decorations had been about 650 to 750°C, while that of the substrate glassware had been around 850°C. However, Mason *et al.* (2001) and Freestone (2002) have suggested that the firing temperature of the overglaze decorations and the substrate glaze had been about 890 to 920°C, but in a short time. This opinion is in contrast with the descriptions of *Majmū'at al-Šanāya* (1582) which specify that the firing temperature of *mīnā'ī* overglazes should be the half of that of glassy substrate.

As far as *lājvardīna* overglazes are concerned, Abu'l Qasim (1301) describes different types of colourant including tin oxide, red hematite, chromite, and dissolved iron mixed with a transparent frit and fired on a pre-fired glaze in order to create white, red, black, and yellow respectively. Frequently, gold leaf is also used as an overglaze to decorate *lājvardīna* ware which is in accordance with Abu'l Qasim treatise. A recent study on *lājvardīna* ware has showed that the turquoise glaze is achieved by copper with tin oxide as the opacifier, the opaque white by tin oxide, the transparent yellow by iron oxide, and the opaque yellow by lead stannate. The black line applied to one of the bodies is again coloured by manganese oxide (O'Kane, 2011). These colourants, as well as gold leaf, are the same colours used in the fifteenth century Timurid polychrome glazes which are then inherited by the Safavids in producing *haft rang* tiles. The same tradition was afterward acquired by the Qajars in the nineteenth century for making polychrome glazes when this technique was called *haft rangī*, *kār-rū-rang*, or *khishī*. Ali Mohamed describes with detail how to produce a single *haft rang* tile (see *Chapter One*, p. 5), which is entirely comparable with the results obtained in this thesis.

To sum up, it can be concluded that *mīnā'ī* decorations are to be considered as the precedents of *haft rang* technique since technique and materials used in these two styles are quite similar. Another similarity between these two styles of polychrome-making is related to the term *haft rang*, which was previously used by Abu'l Qasim to describe the decorations we know today as *mīnā'ī*. This term, centuries later, was still used by Ali Mohamed (1888) for describing polychrome overglaze decorations which today are known as *cuerva seca*. Therefore, it would be more appropriate to reconsider the use of the term '*cuerva seca*' for the seventeenth Safavid polychrome glazes. We suggest the term '*haft rang*' for the seventeenth Safavid polychrome glazed tiles and their Timurid antecedents since they originally used to be called '*haft rang*.' This nomination still in use in today's Iran for describing this type of polychrome glazed ceramics and merits to be used in scholarly literature as well.



## References

- Abu'l Qasim, A.K., 1301, *'Arā'yis al-Javāhir va Nafā'yis al-Aṭā'yib*, ed. Afshār, Ī., 1966, Anjuman-i Āṭār-i Millī-i Īrān Press, Tehran. [in Persian]
- Adriaens, A., 2005, Non-destructive analysis and testing of museum objects: an overview of five years of research, *Spectrochimica Acta Part B*, 60, 1503-1516.
- Agosti, M.D. and Schweiser, F., 2002, Technical analyses, in *Persia and China: Safavid blue and white ceramics in the Victoria and Albert Museum*, ed. Crowe, Y., Thames and Hudson, London, pp. 293-304.
- Ahmadi, M., 2010, *Technical Studies and Conservation of Glazed Bricks of Tepe Rabat Sardasht*, M.A. Thesis, Art University of Isfahan, Dept. of Conservation and Restoration of Cultural Heritage. [in Persian]
- Aḥmadīyān, M.A., 1977, Pottery-making in Sāva, *Hunar va Mardum Magazine*, 177-178, 55-62. [in Persian]
- Aitchison, J., 1994, Principles of compositional data analysis, *Multivariate Analysis and Its Applications*, 24, 73-81.
- Alaimo, R., Bultrini, G., Fragalà, I., Giarrusso, R. and Montana, G., 2004, Microchemical and microstructural characterisation of medieval and post-medieval ceramic glaze coatings, *Applied Physics A*, 79, 263-272.
- Alavi, M., 1991, Sedimentary and structural characteristics of the Paleotethys remnants in northeastern Iran, *Geological Society of America Bulletin*, 103, 983-992.
- al-Bīrūnī, c. 1050, *Al-Jamāhir fī Ma'rifat al-Javāhir*, trans. Said, H.M., 1891, Pakistan Hijra Council, Islamabad.
- Alemi, M., 1996, Documents: the Safavid royal gardens in Sari, environmental design, *Journal of the Islamic Environmental Design Research Centre*, 1, 98-103.
- al-Hassan, A.Y., 2009, An eighth century Arabic treatise on the colouring of glass: Kitāb al-Durra al-Maknūna (the Book of the Hidden Pearl) of Jābir ibn Ḥayyān (c. 721- c. 815 AD), *Arabic Sciences and Philosophy*, 19, 1, 121-156.
- Ali Mohamed, U., 1888, On the manufacture of modern kashi earthenware tiles and vases in imitation of the ancient, in *Leadless Decorative Tiles, Faience, and Mosaic. History, Materials, Manufacture and Use of Ornamental Flooring Tiles, Ceramic Mosaic, and Decorative Tiles and Faience. Recipes for Tile-bodies, and for Leadless Glaze and Art-tile Enamels*, ed. Furnival, W.J. 1904, Stone, Staffordshire, Furnival, W.J., pp. 215-223.
- Allan, J.W., 1973, Abu'l Qasim's treatise on ceramics, *Iran*, 11, 111-120.

## References

---

- Anderson, G.D. and Rosser-Owen, M., 2007, *Revisiting Al-Andalus: Perspectives on the Material Culture of Islamic Spain and Beyond*, Brill, Leiden.
- Andriessse, J.P., 1960, The soils of Mazandaran in northern Iran and their suitability for paddy-rice irrigation, *Journal of Soil Science*, 11, 2, 227-245.
- Annells, R.N., Arthurton, R.S., Bazley, R.A.B., Davies, R.G., Hamed, M.A.R. and Rahimzadeh, F., 1985, *Geological quadrangle maps of Iran nos. E3 and E4: Qazvin and Rasht '1:250000'*, Ministry of Mines and Metals, Tehran Naqshah Office Press, Tehran.
- Añón, J.M.C., 2009-2010, Vestigios olvidados de nuestra ciudad cilniana, *Revista de la Asociación Cilniana para la Defensa y Difusión del Patrimonio Cultural*, 22-23, 73-84.
- Arakeliyan, H., 2001, *Bethlehem Church of New Julfa in Isfahan*, Nāīrī, Isfahan. [in Persian]
- Ardalan, N., 1974, Colour in Safavid architecture: the poetic diffusion of light, *Iranian Studies*, 71-2, 164-178.
- Arnold, D.E., Neff, H. and Bishop, R.L., 1991, Reviewed compositional analysis and 'sources' of pottery: an ethnoarchaeological approach, *American Anthropologist*, 93, 1, 70-90.
- Arnold, D.E., Neff, H. and Glascock, M.D., 2000, Testing assumptions of neutron activation analysis: communities, workshops, and paste preparation in Yucatan, Mexico, *Archaeometry*, 42, 2, 301-216.
- Artioli, G., 2010, *Scientific Methods and Cultural Heritage: an Introduction to the Application of Materials Science to Archaeometry and Conservation Science*, Oxford University Press, Oxford.
- Asiabanha, A., Ghasemi, H. and Meshkin, M., 2009, Paleogene continental-arc type volcanism in North Qazvin, North Iran: facies analysis and geochemistry, *Neues Jahrbuch für Mineralogie-Abhandlungen*, 186, 2, 201-214.
- Aubert, H. and Pinta, M., 1980, *Trace Elements in Soils*, Elsevier, Burlington.
- Babaie, S. and Haug, R., 2007, Isfahan x. Monuments, *Encyclopædia Iranica*, available at: <http://www.iranicaonline.org/articles/isfahan-x-monuments>
- Bacci, M. and Picollo, M., 1996, Non-destructive spectroscopic detection of cobalt(II) in paintings and glass, *Studies in Conservation*, 41, 3, 136-144.
- Bacci, M., 1995, Fibre optics applications to works of art, *Sensors and Actuators B: Chemical*, 29, 190-196.
- Bacci, M., 2000, UV-VIS-NIR, FT-IR, and FORS spectroscopies, in *Modern Analytical Methods in Art and Archaeology*, eds. Ciliberto, E. and Spoto, G., John Wiley & Sons, New York, pp. 321-362.
- Bacci, M., 2004, Optical spectroscopy and colourimetry, in *Proceedings of the International School of Physics 'Enrico Fermi'*, eds. Martini, M., Milazzo, M. and Piacentini, M., IOS Press, Amsterdam, pp. 1-15.
- Bacci, M., Picollo, M., Trumpy, G., Tsukada, M., and Kunzelman, D., 2007a, Non-invasive identification of white pigments on 20th-century oil paintings by using fiber optic reflectance spectroscopy, *Journal of the American Institute for Conservation*, 46, 1, 27-37.

- Bacci, M., Corallini, A., Orlando, A., Picollo, M. and Radicati, B., 2007b, The ancient stained windows by Nicolò di Pietro Gerini in Florence. A novel diagnostic tool for non-invasive in situ diagnosis, *Journal of Cultural Heritage*, 8, 235-241.
- Bae, B.-S. and Weinberg, M.C., 1994, Optical absorption of copper phosphate glasses in the visible spectrum, *Journal of Non-Crystalline Solids*, 168, 223-231.
- Bahrāmī, M., 1944, a Lustre Pitch, *Yādigār Magazine*, 6, 72-77. [in Persian]
- Balek, V., Pérez-Maqueda, L.A., Poyato, J., Černý, Z., Ramírez-Valle, V., Buntseva, I.M. and Pérez-Rodríguez, J.L., 2007, Effect of grinding on thermal reactivity of ceramic clay minerals, *Journal of Thermal Analysis and Calorimetry*, 88, 1, 87-91.
- Bamford, C.R., 1977, *Colour Generation and Control in Glass*, Elsevier, Amsterdam.
- Baraldi, P. and Tinti, A., 2008, Raman spectroscopy in art and archaeology, *Journal of Raman Spectroscopy*, 39, 963-965.
- Barilaro, D., Barone, G., Crupi, V., Donato, M.G., Majolino, D., Messina, G. and Ponterio, R., 2005, Spectroscopic techniques applied to the characterization of decorated potteries from Caltagirone (Sicily, Italy), *Journal of Molecular Structure*, 744-747, 827-831.
- Barr, G., Dong, W. and Gilmore, Ch.J., 2004, High-throughput powder diffraction. II. Applications of clustering methods and multivariate data analysis, *Journal of Applied Crystallography*, 37, 243-252.
- Bastani Parizi, M.E., 2000, Ganj-‘Alī Khan, *Encyclopædia Iranica*, available at: <http://www.iranicaonline.org/articles/ganj-ali-khan>
- Baxer, M.J. and Buck, C.E., 2000, Data handling and statistical analysis, in *Modern Analytical Methods in Art and Archaeology*, eds. Ciliberto, E. and Spoto, G., John Wiley & Sons, New York, pp. 681-746.
- Baxter, M.J., 1994, *Exploratory Multivariate Analysis in Archaeology*, Edinburgh University Press, Edinburgh.
- Baxter, M.J., 1995, Standardization and transformation in principal component analysis, with applications to archaeometry, *Journal of the Royal Statistical Society*, 44, 4, 513-527.
- Baxter, M.J., 2004, Distance and transformation in the multivariate analysis of archaeometric data, in *Proceedings of the International School of Physics ‘Enrico Fermi’*, eds. Martini, M., Milazzo, M. and Piacentini, M., IOS Press, Amsterdam, pp. 17-36.
- Baxter, M.J., Beardah, C.C., Cool, H.E.M. and Jackson, C.M., 2005, Compositional data analysis of some alkaline glasses, *Mathematical Geology*, 37, 2, 183-196.
- Baxter, M.J., Cool, H.E.M. and Jackson, C.M., 2005, Further studies in the compositional variability of colourless Romano-British glass, *Archaeometry*, 47, 1, 47-68.
- Bayat, O., Karimzadeh, H.R. and Khademi, H., 2011, Clay minerals in two paleosols on geomorphic surfaces in eastern Isfahan, *Iranian Journal of Crystallography and Mineralogy*, 19, 1, 45-58. [in Persian]

## References

---

- Bazl, F., 1965, The ceramic arts, D: contemporary techniques, in *A Survey of Persian Art: from Prehistoric Times to the Present*, Vol IV, eds. Pope, A.U. and Ackerman, Ph., Oxford University Press, London; New York, pp. 1703-1706.
- Bell, I.M., Clark, R.J.H. and Gibbs, P.J., 1997, Raman spectroscopic library of natural and synthetic pigments (Pre 1850 AD), *Spectrochimica Acta Part A*, 53, 2, 159-2179.
- Ben-Shlomo, D., Maeir, A.M. and Mommsen, H., 2008, Neutron activation and petrographic analysis of selected late Bronze and Iron Age pottery from Tell es-Safi/Gath, Israel, *Journal of Archaeological Science*, 35, 956-964.
- Berti, G., 1997, Pisa: ceramiche e commerci 2° metà X - 1° metà XIV sec, in *I Congresso Nazionale di Archeologia Medievale*, ed. Gelichi, S., Firenze, pp. 346-351.
- Bianchin, S., Brianese, N., Casellato, U., Fenzi, F., Guerriero, P., Vigato, P.A., Battagliarin, M., Nodari, L., Russo, U., Galgani, M. and Mendera, M., 2005, Medieval and renaissance glass technology in Valdelsa (Florence). Part 3: vitreous finds and crucibles, *Journal of Cultural Heritage*, 6, 165-182.
- Bieber, A.M., Brooks, D.W., Harbottle, G. and Sayre, E.V., 1976, Application of multivariate techniques to analytical data on Aegean ceramics, *Archaeometry*, 18, 1, 59-74.
- Bier, C., Ebrahimian, M., Ala-Firouz, I. and Gluck, J., 1993, Crafts, *Encyclopædia Iranica*, available at: <http://www.iranica.com/articles/crafts->, Date of Access 07.07.2011.
- Bingham, P.A. and Jackson, C.M., 2008, Roman blue-green bottle glass: chemical-optical analysis and high temperature viscosity modeling, *Journal of Archaeological Science*, 35, 302-309.
- Blackman, M.J., 1981, The mineralogical and chemical analysis of Banesh period ceramics from Tal-e Malyan, Iran, in *Scientific Studies in Ancient Ceramics*, Hughes, M.J. ed., British Museum Occasional Studies, 19, pp. 7-20.
- Blackman, M.J., Mery, S. and Wright, R.P., 1989, Production and exchange of ceramics on the Oman peninsula from the perspective of Hili, *Journal of Field Archaeology*, 16, 1, 61-77.
- Blair, S. and Bloom, J., 1994, *The Art and Architecture of Islam, 1250-1800*, Yale University Press, New Haven.
- Blair, S., 1989, Āmol: Islamic monuments, *Encyclopædia Iranica*, Vol. I, 980-982.
- Blunt, W., 1966, *Isfahan, Pearl of Persia*, Stein and Day, New York.
- Bohor, F., 1963, High-temperature phase development in illitic clays, *Clays and Clay Minerals*, 12, 1, 233-246.
- Borgia, I., Brunetti, B., Mariani, I., Sgamellotti, A., Cariati, F., Fermo, P., Mellini, M., Viti, C. and Padeletti, G., 2002, Heterogeneous distribution of metal nanocrystals in glazes of historical pottery, *Applied Surface Science*, 185, 206-216.
- Borjian, H., 2007, Isfahan xiii. Crafts, *Encyclopædia Iranica*, available at: <http://www.iranicaonline.org/articles/isfahan-xiii-crafts>

## References

---

- Bouchard, M. and Gambardella, A., 2010, Raman microscopy study of synthetic cobalt blue spinels used in the field of art, *Journal of Raman Spectroscopy*, 41, 1477-1485.
- Brawer, S.A. and White, W.B., 1975, Raman spectroscopic investigation of the structure of silicate glasses. I. The binary alkali silicates, *Journal of Chemical Physics*, 63, 2421-2432.
- Brawer, S.A. and White, W.B., 1977, Raman spectroscopic investigation of the structure of silicate glasses (II). Soda-alkaline earth-alumina ternary and quaternary glasses, *Journal of Non-Crystalline Solids*, 23, 2, 261-278.
- Brill, R.H., 1988, Scientific investigations of the Jalame glass and related finds, in *Excavations at Jalame: site of a glass factory in late Roman Palestine*, ed. Weinberg G.D., Columbia, University of Missouri Press, pp. 257-294.
- Brill, R.H., 1992, Chemical analyses of some glasses from Frattesina, *The Journal of Glass Studies*, 34, 11-22.
- Brill, R.H., 1999, *Chemical Analyses of Early Glasses, Vols 1 and 2*, The Corning Museum of Glass Corning, New York.
- Brill, R.H., 2005, Chemical analysis of some Sassanian glasses from Iraq, in *Sasanian and Post-Sasanian Glass in the Corning Museum of Glass*, eds. Whitehouse, D. and Brill R.H., Corning Museum of Glass, New York, pp. 65-88.
- Brooke, C.J., Edwards, H.G.M. and Tait, J.K.F., 1999, The Bottesford blue mystery: a Raman spectroscopic study of post-mediaeval glazed tiles, *Journal of Raman Spectroscopy*, 30, 429-434.
- Buciuman, F., Patcas, F., Craciun, R. and Zahn, D.R.T., 1999, Vibrational spectroscopy of bulk and supported manganese oxides, *Physical Chemistry Chemical Physics*, 1, 185-190.
- Buko, A., 1984, Problems and research prospects in the determination of the provenance of pottery, *World Archaeology*, 15, 3, 348-365.
- Buscaglia, G., 1992, Criterios de identificación de los azulejos sevillanos y ligures y una producción inédita savonense del siglo XVI, laboratorio de arte, *Revista del Departamento de Historia del Arte*, 52, 325-339.
- Buxeda i Garrigós, J., Mommsen, H. and Tzolakidou, A., 2002, Alterations of Na, K and Rb concentrations in Mycenaean pottery and a proposed explanation using X-ray diffraction, *Archaeometry*, 44, 2, 187-198.
- Caiger-Smith, A., 1973, *Tin-Glaze Pottery in Europe and the Islamic World*, Faber and Faber Limited, London.
- Caiger-Smith, A., 2001, Esfahan: an Unexpected Pottery Workshop, Unpublished Article. URL: <http://islamicceramics.ashmolean.org/Glossary/isfahan.htm>
- Campanella, L., Favero, G., Flamini, P. and Tomassetti, M., 2003, Prehistoric terracottas from the Libyan Tadrart Acacus: thermoanalytical study and characterization, *Journal of Thermal Analysis and Calorimetry*, 73, 127-142.

## References

---

- Canby, S.R., 2002, Pounces for textiles or pounces for pictures? in *Safavid Art and Architecture*, ed. Canby, S.R., British Museum Publications, London, pp. 67-71.
- Cariati, F. and Bruni, S., 2000, Raman Spectroscopy, in *Modern Analytical Methods in Art and Archaeology*, eds. Ciliberto, E. and Spoto, G., John Wiley & Sons, New York, pp. 255-278.
- Carmona, N., García-Heras, M., Villegas M. A., Jiménez, P. and Navarro, J., 2008, Study of chromophores of Islamic glasses from Al-Andalus (Murcia, Spain), in *Lasers in the Conservation of Artworks*, eds. Castillejo *et al.*, Taylor & Francis, London, pp. 73-78.
- Carswell, J., 1968, *New Julfa: the Armenian Churches and Other Buildings*, Clarendon Press, Oxford.
- Castro, K., Pérez-Alonso, M., Rodríguez-Laso, M.D., Fernández, L.A. and Madariaga, J.M., 2005, On-line FT-Raman and dispersive Raman spectra database of artists' materials (e-VISART database), *Analytical and Bioanalytical Chemistry*, 382, 248-258.
- Catalano, I.M., Genga, A., Laganara, C., Laviano R., Mangone, A., Marano, D. and Traini, A., 2007, Lapis lazuli usage for blue decoration of polychrome painted glazed pottery: a recurrent technology during the middle ages in Apulia (southern Italy), *Journal of Archaeological Science*, 34, 503-511.
- Caubet, A., 1992, Achaemenid brick decoration, in *The Royal City of Susa: Ancient Near Eastern Treasures in the Louvre*, Metropolitan Museum of Art, New York, pp. 223-226.
- Caubet, A. and Kaczmarczyk, A., 1998, Les briques glaçurées du palais de Darius, *Techne*, 23-26.
- Caubet, A. and Pierrat-Bonnefois, G., 2005, *Faïences de l'Antiquité de l'Égypte à l'Iran*, Musée du Louvre, Paris.
- Caubet, A., 2007, *Faïences et Matières Vitreuses de l'Orient Ancient*, Musée du Louvre, Paris.
- Ceglia, A., Meulebroeck, W., Baert, K., Wouters, H., Nys, K., Thienpont, H. and Terryn, H., 2012, Cobalt absorption bands for the differentiation of historical Na and Ca/K rich glass, *Surface and Interface Analysis*, 44, 219-226.
- Centlivres-Demont, M., 1971, *Une Communauté de Potiers en Iran: Le Centre de Meybod (Yazd)*, Présentée à la Faculté des Lettres de l'Université de Neuchâtel pour Obtenir le Grade de Docteur es Lettres.
- Chapoulie, R., Déléry, C., Daniel, F. and Vendrell-Saz, M., 2005, *Cuerda seca* ceramics from al-Andalus, Islamic Spain and Portugal (10th–12th centuries AD): investigation with SEM-EDX and cathodoluminescence, *Archaeometry*, 47, 3, 519-534.
- Chardin, J., 1811, *Voyages du Chevalier Chardin en Perse et autres Lieux de l'Orient*, Tome 8, le Normant, Imprimeur-Libraire, Paris.
- Chou, M.H., Liu, S.B., Huang, C.Y., Wu, S.Y. and Cheng, C.-L., 2008, Confocal Raman spectroscopic mapping studies on a single CuO nanowire, *Applied Surface Science*, 254, 7539-7543.
- Clark, R.J.H., Cridland, L., Kariuki, B.M., Harris, K.D.M. and Withnall, R., 1995, Synthesis, structural characterisation and Raman spectroscopy of the inorganic pigments lead tin yellow types I and II and lead

- antimonate yellow: their identification on medieval paintings and manuscripts, *Journal of the Chemical Society, Dalton Transactions*, 16, 2577-2582.
- Clark, R.J.H. and Gibbs, P.J., 1997a, Identification of lead(ii) sulfide and pararealgar on a 13th century manuscript by Raman microscopy, *Chemical Communications*, 1003-1004.
- Clark, R.J.H. and Gibbs, P.J., 1997b, Non-Destructive in situ study of ancient Egyptian faience by Raman microscopy, *Journal of Raman Spectroscopy*, 28, 99-103.
- Clark, R.J.H., Curri, L., Henshaw, G.S. and Laganara, C., 1997a, Characterization of brown-black and blue pigments in glazed pottery fragments from Castel Fiorentino (Foggia, Italy) by Raman microscopy, x-ray powder diffractometry and x-ray photoelectron spectroscopy, *Journal of Raman Spectroscopy*, 28, 105-109.
- Clark, R.J.H., Curri, M.L. and Laganara, C., 1997b, Raman microscopy: the identification of lapis lazuli on medieval pottery fragments from the south of Italy, *Spectrochimica Acta Part A*, 53, 597-603.
- Clark, R.J.H. and Curri, L.M., 1998, The identification by Raman microscopy and x-ray diffraction of iron-oxide pigments and of the red pigments found on Italian pottery fragments, *Journal of Molecular Structure*, 440, 105-111.
- Cogswell, J.W., Neff, H. and Glascock, M.D., 1996, The effect of firing temperature on the elemental characterization of pottery, *Journal of Archaeological Science*, 23, 283-287.
- Cogswell, J.W., Neff, H. and Glascock, M.D., 1998, Analysis of shell-tempered pottery replicates: implications for provenance studies, *American Antiquity*, 63, 1, 63-72.
- Cole, W.F. and Crook, D.N., 1962, A Study of Fired-Clay Bodies from Roman Times, *Transactions of the British Ceramic Society*, 61, 299-315.
- Colomban, Ph. and Treppoz, F., 2001, Identification and differentiation of ancient and modern European porcelains by Raman macro and micro-spectroscopy, *Journal of Raman Spectroscopy*, 32, 93-102.
- Colomban, Ph., Sagon, G. and Faurel, X., 2001, Differentiation of antique ceramics from the Raman spectra of their coloured glazes and paintings, *Journal of Raman Spectroscopy*, 32, 351-360.
- Colomban, Ph., 2003, Lapis lazuli as unexpected blue pigment in Iranian lâjvardina ceramics, *Journal of Raman Spectroscopy*, 34, 420-423.
- Colomban, Ph., Liem, N.Q., Sagon, G., Tinh, H. X. and Ba Hoành, T., 2003, Microstructure, composition and processing of 15th century Vietnamese porcelains and celadons, *Journal of Cultural Heritage*, 4, 187-197.
- Colomban, Ph., Milande, V. and Le Bihan, L., 2004, On-site Raman analysis of Iznik pottery glazes and pigments, *Journal of Raman Spectroscopy*, 35, 527-535.
- Colomban, Ph., 2005, Chapter 13: Case study: glasses, glazes and ceramics - recognition of ancient technology from the Raman spectra, in *Raman Spectroscopy in Archaeology and Art History*, eds. Edwards, H.G.M. and Chalmers, J.M., Royal Society of Chemistry, Cambridge, pp. 192-206.

## References

---

- Colomban, Ph. and Paulsen, O., 2005, Non-destructive determination of the structure and composition of glazes by Raman spectroscopy, *Journal of the American Ceramic Society*, 88, 2, 390-395.
- Colomban, Ph., de Laveaucoupet, R. and Milande, V., 2005, On-site Raman spectroscopic analysis of Kütahya fritwares, *Journal of Raman Spectroscopy*, 36, 857-863.
- Colomban, Ph. and Milande, V., 2006, On-site Raman analysis of the earliest known Meissen porcelain and stoneware, *Journal of Raman Spectroscopy*, 37, 606-613.
- Conesa, J.C., 2008, La loza decorada en España, *Ars longa, Cuadernos de Arte*, 17, 151-168.
- Croveri, P., Fragalà, I. and Ciliberto, E., 2010, Analysis of glass tesserae from the mosaics of the 'Villa del Casale' near Piazza Armerina (Enna, Italy). Chemical composition, state of preservation and production technology, *Applied Physics A*, 100, 927-935.
- Crowe, Y., 1991, Ceramics xv. The Islamic Period, 16th-19th Centuries, *Encyclopædia Iranica*, Vol. V, 327-331.
- Crowe, Y., 2004, A late Safavid dish: a cluster of exotic trees and foliage, *Muqarnas: An Annual on the Visual Culture of the Islamic World*, 21, 121-128.
- Cultrone, G., Rodriguez-Navarro, C., Sebastian, E., Cazalla, O. and De La Torre, M.J., 2001, Carbonate and silicate phase reactions during ceramic firing, *European Journal of Mineralogy*, 13, 3, 621-634.
- Cultrone, G., Sebastian, E. and de la Torre M.J., 2005a, Mineralogical and physical behaviour of solid bricks with additives, *Construction and Building Materials*, 19, 39-48.
- Cultrone, G., Sidraba, I. and Sebastian, E., 2005b, Mineralogical and physical characterization of the bricks used in the construction of the Triangul Bastion, Riga (Latvia), *Applied Clay Science*, 28, 297- 308.
- Dānīshpazhūh, M.T. ed., ca. 1447, Javāhir-nāma (Unknown Author), in *Farhang-i Īrānzamīn*, 1965, Vol. XII, Tehran, pp. 266-273. [in Persian]
- Davis, J.C., 2002, *Statistics and Data Analysis in Geology*, John Wiley & Sons, New York.
- De Vleeschouwer, F., Renson, V., Claeys, Ph., Nys, K. and Bindler, R., 2011, Quantitative WDXRF calibration for small ceramic samples and their source material, *Geoarchaeology*, 26, 3, 440-450.
- De-Benedetto, G.E., Laviano, R., Sabbatini, L., Zambonin, P.G., 2002, Infrared spectroscopy in the mineralogical characterization of ancient pottery, *Journal of Cultural Heritage*, 3, 177-186.
- Degeorge, G. and Porter, Y., 2002, *The Art of the Islamic tile*, Flammarion, Paris.
- Déléry, C., 2004, un reflejo de la lorca islámica a través del estudio de la cerámica de cuerda seca encontrada en su entorno, Alberca, *Revista de la Asociación de Amigos del Museo Arqueológico de Lorca*, 2, 167-176.
- Déléry, C., 2009, Using *cuerda seca* ceramics as a historical source to evaluate trade and cultural relations between Christian ruled lands and Al-Andalus, from the tenth to thirteenth centuries, *Al-Masaq: Islam and the Medieval Mediterranean*, 21, 1, 31-58.
- Der Hovhanean, H., 2000, *History of New Julfa*, Zinda Rūd and Naqsh-i Khurshīd, Isfahan. [in Persian]

- Descantes, C., Speakman, R.J. and Glascock, M.D., 2008, Compositional studies of Caribbean ceramics: an introduction to instrumental neutron activation analysis, *Journal of Caribbean Archaeology*, 2, 1-14.
- Diéguez, A., Romano-Rodríguez, A., Vilà, A. and Morante, J.R., 2001, The complete Raman spectrum of nanometric SnO<sub>2</sub> particles, *Journal of Applied Physics*, 90, 1550-1557.
- Doménech-Carbó, A. and Doménech-Carbó, M.T., 2005, Electrochemical characterization of archaeological tin-opacified lead-alkali glazes and their corrosion processes, *Electroanalysis*, 17, 21, 1959-1969.
- Drebushchak, V.A., Mylnikova, L.N. and Molodin, V.I., 2007, Thermogravimetric investigation of ancient ceramics metrological analysis of sampling, *Journal of Thermal Analysis and Calorimetry*, 90, 1, 73-79.
- Drebushchak, V.A., Mylnikova, L.N., Drebushchak, T.N. and Boldyrev, V.V., 2005, The investigation of ancient pottery, application of thermal analysis, *Journal of Thermal Analysis and Calorimetry*, 82, 3, 617-626.
- Drennan, R.D., 2009, *Statistics for Archaeologists: a Commonsense Approach*, Springer, Boston.
- Duminuco, P., Messiga, B. and Riccardi, M.P., 1998, Firing process of natural clays: some microtextures and related phase compositions, *Thermochimica Acta*, 321, 185-190.
- Duran, A., Fernandez Navarro, J.M., Casariego, P. Joglar, A., 1986, Optical properties of glass coatings containing Fe and Co, *Journal of Non-Crystalline Solids*, 82, 1, 391-399.
- Edwards, H.G.M. and Tait, J.K.F., 1998, FT-Raman spectroscopic study of decorated stained glass, *Applied Spectroscopy*, 52, 5, 679-682.
- Ehlers, E., 1989, Behšahr, older Ašraf, *Encyclopædia Iranica*, Vol. IV, 113.
- Eiland, M.L. and Williams, Q., 2000, Infra-red Spectroscopy of Ceramics from Tell Brak, Syria, *Journal of Archaeological Science*, 27, 993-1006.
- Eiland, M.L. and Williams, Q., 2001, Investigation of Islamic ceramics from Tell Tuneinir using X-Ray diffraction, *Geoarchaeology: An International Journal*, 16, 8, 875-903.
- Encyclopædia Iranica*, available at: <http://www.iranicaonline.org/pages/guidelines>
- Enriquez, C.R., Danon, J. and Beltrão, M. Da C.M.C., 1979, Differential thermal analysis of some Amazonian archaeological pottery, *Archaeometry*, 21, 2, 183-186.
- Eppler, R.A. and Eppler, D.R., 2000, *Glazes and Glass Coating*, American Ceramic Society, Westerville.
- Falcone, R., Renier, A. and Verità, M., 2002, Wavelength-dispersive X-ray fluorescence analysis of ancient glasses, *Archaeometry*, 44, 4, 531-542.
- Fathianpour, N. and Tabaei, M., 2008, Classification of alluvium deposits in north northeast Isfahan in order to supply raw material for brick production, *Proceedings of the First Brick and Clay Blocks Symposium*, Isfahan University of Technology, Isfahan, Iran, pp. 3-15. [in Persian]

## References

---

- Fehérvári, G., 1973, *Islamic Pottery: A Comprehensive Study based on the Barlow Collection*, Faber and Faber Limited, London.
- Fehérvári, G., 2000, *Ceramics of the Islamic World in the Tareq Rajab Museum*, I. B. Tauris Publishers, London and New York.
- Feng, D. and BaoRu, S., 2008, Further study of sources of the imported cobalt-blue pigment used on Jingdezhen, *Science in China Series E: Technological Sciences*, 51, 3, 249-259.
- Fernández, F.V., 1988, Cerámica de cuerda seca en un documento de la geniza de El Cairo, *Cuadernos de Prehistoria y Arqueología*, 15, 379-384.
- Fernández, J.G., 2009, *Optical Characterization and Analysis of Archaeological Glass Artefacts*, Master Thesis, Universitat Politècnica de Catalunya, Departament d'Òptica i Optometria.
- Ferraro, J.R., Nakamoto K. and Brown, Ch.W., 2003, *Introductory Raman Spectroscopy*, Elsevier, Amsterdam.
- Floor, W., 2003, *Traditional Crafts in Qajar Iran (1800-1925)*, Mazda Publishers, California.
- Fluegel, A., Varshneya, A.K., Earl, D.A., Seward, T.P. and Oksoy, D., 2006, Improved composition-property relations in silicate glasses, Part I: Viscosity, in *Melt Chemistry, Relaxation, and Solidification Kinetics of Glasses*, eds. Li, H., Ray, C.S., Strachan, D.M., Weber, R. and Yue, Y., John Wiley & Sons, Hoboken, pp. 129-143.
- Fluegel, A., 2007, Glass viscosity calculation based on a global statistical modeling approach, *Glass Technology*, 48, 1, 13-30.
- Fortnum, C.D.E., 1873, *A Descriptive Datalogue of the Maiolica, Hispano-Moresco, Persian, Damascus, and Rhodian wares in the South Kensington Museum: with Historical Notes, Marks and Monograms*, Chapman & Hall, London.
- Freestone, I.C. and Middleton, A.P., 1987, Mineralogical applications of the analytical SEM in archaeology, *Mineralogical Magazine*, 51, 21-31.
- Freestone, I.C., 1991, Technical examination of neo-Assyrian glazed wall plaques, *Iraq*, 53, 55-58.
- Freestone, I.C., 2002, The relationship between enameling on ceramics and on glass in the Islamic World, *Archaeometry*, 44, 2, 251-5.
- Freestone, I.C., 2006, Glass production in late antiquity and the early Islamic period: a geochemical perspective. In: *Geomaterials in Cultural Heritage*, eds. Maggetti, M. and Messiga, B., The Geological Society, London, pp. 201-216.
- Froh, J., 2004, Archaeological ceramics studied by scanning electron microscopy, *Hyperfine Interactions*, 154, 159-176.
- Fūmanī, M.R. and Bīrīnjīyān, Sh., 2005, *Mines of Iran: Active and Non-active*, Regional Library of Science and Technology, Tehran. [in Persian]

- Furukawa, T., Brawer, S.A. and White, W.B., 1978, The structure of lead silicate glasses determined by vibrational spectroscopy, *Journal of Materials Science*, 13, 2, 268-282.
- Furukawa, T., Fox, K.E. and White, W.B., 1981, Raman spectroscopic investigation of the structure of silicate glasses. III. Raman intensities and structural units in sodium silicate glasses, *Journal of Chemical Physics*, 75, 3226-3237.
- Gadd, C.J. and Thompson, R.C., 1936, A middle-Babylonian chemical text, *Iraq*, 3, 1, 87-96.
- Galdieri, E., 1974, Les palais d'Isfahan, *Iranian Studies*, 73-4, 380-405.
- Galdieri, E., 1979, *Esfahan, Ali Qapu: An architectural Survey*, IsMEO, Rome.
- García-Heras, M., Blackman, M.J., Fernández-Ruiz, R., and Bishop, R.L., 2001, Assessing ceramic compositional data: a comparison of total reflection X-ray fluorescence and instrumental neutron activation analysis on late iron age Spanish Celtiberian ceramics, *Archaeometry*, 43, 3, 325-347.
- García-Heras, M., Carmona, N., Gil, C. and Villegas, M.A., 2005a, Neorenaissance/Neobaroque stained glass windows from Madrid: a characterisation study on some panels signed by the Maumejean Frères company, *Journal of Cultural Heritage*, 6, 91-98.
- García-Heras, M., Rincón, J.Ma., Jimeno, A. and Villegas, M.A., 2005b, Pre-Roman coloured glass beads from the Iberian Peninsula: a chemico-physical characterisation study, *Journal of Archaeological Science*, 32, 727-738.
- Gardner, H. and Kleiner, F.S., 2010, *Gardner's Art through the Ages: The Western Perspective*, Wadsworth; Cengage, Boston.
- Ghandchi, M. and Afsharianzadeh, A., 1991, *Geological quadrangle maps of Iran no. G4: Sārī '1:250,000'*, Ministry of mines and metals, Tehran Naqshah Office Press, Tehran.
- Gignoux, Ph. and Bates, M., 2011, Dirham, *Encyclopædia Iranica*, available at: <http://www.iranicaonline.org/articles/dirham#pt2>
- Gill, M.S. and Rehren, Th., 2011, Material characterization of ceramic tile mosaic from two 17th-century Islamic monuments in northern India, *Archaeometry*, 53, 1, 22-36.
- Glascock, M.D., Neff, H. and Vaughn, K.J., 2004, Instrumental neutron activation analysis and multivariate statistics for pottery provenance, *Hyperfine Interactions*, 154, 95-105.
- Gluck, J., 1977, Pottery, in *A Survey of Persian Handicraft*, ed. Gluck, G. and Gluck, S.H., Bank Melli Iran, Tehran, pp. 41-96.
- Godard, A., 1965, *The Art of Iran*, Praeger, New York.
- Golombek, L., 2003, The Safavid ceramic industry at Kirman, *Iran*, 41, 253-270.
- Golombek, L., Mason, R.B. and Proctor, P., 2001, Safavid potters' marks and the question of provenance, *Iran*, 39, 207-236.
- Grattan-Bellew, P.E. and Litvan, G.G., 1978, *X-ray diffraction method for determining the firing temperature of clay brick*, American Ceramic Society Bulletin, 57, 5, 493-495.

## References

---

- Grube, E.J., 1965, The art of Islamic pottery, *The Metropolitan Museum of Art Bulletin*, 236, 209-228.
- Gueit, E., Darque-Ceretti, E. and Aucouturier, M., 2010, Glass gilding process in medieval Syria and Egypt (13th-14th Century), *Journal of Archaeological Science*, 37, 1742-1752.
- Guha, S., Peebles, D. and Wieting, J.T., 1991, Raman and infrared studies of cupric oxide, *Bulletin of Materials Science*, 14, 3, 539-543.
- Guilherme, A., Coroado, J. and Carvalho, M.L., 2009, Chemical and mineralogical characterization on glazes of ceramics from Coimbra Portugal from the sixteenth to nineteenth centuries, *Analytical and Bioanalytical Chemistry*, 395, 2051-2059.
- Guloyan, Y.A., 2007, Complete analysis of ionic staining of glasses by transition-metal compounds, *Glass and Ceramics*, 64, 5-6, 153-158.
- Gulzar, S., Wörle, M., Burg, J.-P., Chaudhry, M.N., Joseph, E. and Reusser, E., 2012, Characterization of 17th Century Mughal tile glazes from Shahdara Complex, Lahore-Pakistan, *Journal of Cultural Heritage*, doi:10.1016/j.culher.2012.03.007
- Haghnazarian, A., 2006, *Armenian Churches in New Djulfa*, Farhangistān-i Hunar, Tehran. [in Persian]
- Hājī-qāsimī, K., 2000, Madrasa of 'Abbās-qulī, in *Ganj-nama V*, Shahid-Beheshti University and Iranian Cultural Heritage Press, Tehran. [in Persian]
- Hall, E.T., 1970, Analytical techniques used in archaeometry, *Philosophical Transactions of the Royal Society of London. Series A, Mathematical and Physical Sciences*, 269, 135-141.
- Hall, M., Amraatuvshin, Ch. and Erdenbat, E., 1999, X-ray fluorescence analysis of pottery from northern Mongolia, *Journal of Radioanalytical and Nuclear Chemistry*, 240, 3, 763-773.
- Hamer, F. and Hamer, J., 2004, *the Potter's Dictionary of Materials and Techniques*, University of Pennsylvania Press, London.
- Hampton, W.M., 1946, Colour of heavy lead silicate glass, *Nature*, 158, 582-582.
- Haneda, M. and Matthee, R., 2006, Isfahan vii, Safavid Period, *Encyclopædia Iranica*, available at: <http://www.iranicaonline.org/articles/isfahan-vii-safavid-period>
- Hansen Streily, A., 2000, Early pottery kilns in the Middle East, *Paléorient*, 26, 2, 69-81.
- Harāfī, M.M., 2004, Heritage of forgotten arts, *Kayhān-i Farhangī Magazine*, 216, 5-23. [in Persian]
- Harvard Reference or Citation Generator*, [On-line] Available at: <http://www.dairyscience.info/harvard/referencegen.php>.
- Hattstein M. and Delius, P., 2001, *Islam, Art and Architecture*, Konemann.
- Heck, M., Rehren, T. and Hoffmann, P., 2003, The production of lead-tin yellow at Merovingian Schleithem (Switzerland), *Archaeometry*, 45, 1, 33-44.
- Heim, S., 1992, Glazed objects and Elamite glaze industry, in *The Royal City of Susa: Ancient Near Eastern Treasures in the Louvre*, Metropolitan Museum of Art, New York, pp. 202-210.

## References

---

- Heimann, R. and Franklin, U.M., 1972, Archaeo-thermometry: the assessment of firing temperatures of ancient ceramics, *Journal of the International Institute of Conservation-Canadian Group*, 4, 2, 23-45.
- Henderson, J., 1985, The raw materials of early glass production, *Oxford Journal of Archaeology*, 4, 3, 267-91.
- Henderson, J. and Raby, J., 1989, The technology of fifteenth century Turkish tiles: an interim statement on the origins of the Iznik industry, *World Archaeology*, 21, 1, 115-132.
- Henderson, J. and Allan, J.W., 1990, Enamels on Ayyubid and Mamluk glass fragments, *Archaeomaterials*, 4, 167-183.
- Henderson, J., 2002, Tradition and experiment in first millennium A.D. glass productions the emergence of early Islamic glass technology in late antiquity, *Accounts of Chemical Research*, 35, 594-602
- Henderson, J., 2004, The archaeologist as a detective: scientific techniques and the investigation of past societies, in *Forensic Geoscience: Principles, Techniques and Applications*, eds. Pye, K. and Croft, D.J., The Geological Society, London, pp. 147-158.
- Hernández, A.P., 1992, Sevilla y la técnica de la cuerda seca: vajilla y azulejos ss. XV-XVI, Atrio, *Revista de Historia del Arte*, 4, 17-30.
- Hill, D.V., Speakman, R.J. and Glascock, M.D., 2004, Chemical and mineralogical characterization of Sasanian and early Islamic glazed ceramics from the Deh Luran Plain, Southwestern Iran, *Archaeometry*, 46, 4, 585-605.
- Hillenbrand, R., 1986, Architecture vi. Safavid to Qajar periods, *Encyclopædia Iranica*, Vol. II, 345-349.
- Ho, C.T., LaCourse, W.C., Condrate Sr., R.A. and Jillavenkatesa, A., 1995, A Raman spectral investigation of structural variations in thin silicate glass fibers, *Materials Letters*, 23, 237-240.
- Hobson, R.L., 1965, The ceramic arts. (D): Techniques, in *A Survey of Persian Art: from Prehistorical Times to the Present*, eds. Pope, A.U. and Ackerman, Ph., Oxford University Press, London; New York, Vol. IV, pp. 1697-1702.
- Holakooei, P., Mishmastnehi, M., Petrucci, F.C. and Vaccaro, C., 2012, Contemporary Persian *haft rangi* tiles from technical point of view, *Proceedings of the AIAr Meeting Science for Contemporary Art*, ed. Petrucci, F.C., Pàtron Editore, Bologna, pp. 203-209.
- Holakooei, P., 2013, A technological study of the Elamite polychrome glazed bricks at Susa, southwestern Iran, *Archaeometry*, in press.
- Holakooei, P., Petrucci, F.C., Tassinari, R. and Vaccaro, C., 2013, Application of WDXRF in the provenance studies of Persian *haft rang* tiles: a statistical approach, *X-ray Spectrometry*, 42, 2, 105-115.
- Hunarfar, L., 1956, *Ganjīna-i Ātār-i Tārīkhī-i Isfahān*, Taqafī Library, Isfahan.
- Hossieni, Z., Afsharzadeh, A. and Chaichi, Z., 1991, *Geological quadrangle maps of Iran no. F4: Āmul '1:250,000'*, Ministry of mines and metals, Tehran Naqsheh Office Press, Tehran.
- Hulthén, B., 1976, On thermal colour test, *Norwegian Archaeological Review*, 9, 1, 1-6.

## References

---

- Husaynī, 'A., 19th Century, *Kashf al-Ṣanāya*, Manuscript kept in the Central Library of Tehran University, Registration No. M2261. [in Persian]
- Husaynī, M.M., 1669, *Tuḥfa-ye Ḥakīm-i Mu'min*, ed. 1997, Publications of Maḥmūdī Bookstore, Tehran. [in Persian]
- IJMES Transliteration System for Arabic, Persian and Turkish*, available at: [web.gc.cuny.edu/ijmes/docs/TransChart.pdf](http://web.gc.cuny.edu/ijmes/docs/TransChart.pdf)
- Iñañez, J., G., Speakman, R.J., Garrigós, J.B. and Glascock, M.D., 2008, Chemical characterization of majolica from 14th to 18th century production centers on the Iberian Peninsula: a preliminary neutron activation study, *Journal of Archaeological Science*, 35, 425-440.
- Ion, R.M., Dumitriu, I., Fierascu, R.C., Ion, M.L., Pop, S.F., Radovici, C., Bunghez, R.I. and Niculescu, V.I.R., 2011, Thermal and mineralogical investigations of historical ceramic, *Journal of Thermal Analysis and Calorimetry*, 104, 487-493.
- Isphording, W.C., 1974, Combined thermal and x-ray diffraction technique for identification of ceramicware temper and paste minerals reviewed, *American Antiquity*, 39, 3, 477-483.
- Jackson, C.M., Smedley, J.W. and Booth, C.M., 2005, Glass by design? Raw materials, recipes and compositional data, *Archaeometry*, 47, 781-795.
- Jackson, C.M., 2005, Making colourless glass in the Roman period, *Archaeometry*, 47, 4, 763-780.
- Jagannadha Reddy, B. and Frost, R.L., 2005, Spectroscopic characterization of chromite from the Moa-Baracoa Ophiolitic Massif, Cuba, *Spectrochimica Acta A*, 61, 8, 1721-1728.
- Jahāngīr Pādīshāh, 1627, *Mirāt al-Javāhir*, Manuscript kept in the National Library of Iran, Registration No. 14889-5. [in Persian]
- Jalilian, M., Jamshidi, Kh., Hosseini, Z., Kamali, Ch. and Moghimi, J., 1986, *Geological quadrangle maps of Iran no. K4: Mashhad '1:250,000'*, Ministry of mines and metals, Tehran Naqshah Office Press, Tehran.
- Janssens, K., 2005, X-ray based methods of analysis, in *Non-destructive Micro Analysis of Cultural Heritage Materials*, eds. Janssens, K. and Van Grieken, R., Elsevier, Amsterdam; London.
- Javādī, Sh., 2008, The study and analysis of architectural decorations in the Gnajali Khan complex, a masterpiece of art from the Safavian period in Kerman, *Bāgh-i Naẓar*, 59, 35-50. [in Persian]
- Jawhari, T., Roid, A. and Casado, J., 1995, Raman spectroscopic characterization of some commercially available carbon black materials, *Carbon*, 33, 11, 1561-1565.
- Jināb, M.A., 1977, *al-Eṣfahān*, ed. M.R. Rīyāzī, Mīrāth Farhangī Kishvar Press, Tehran. [in Persian]
- Johnston-Feller, R., 2001, *Colour science in the examination of museum objects: nondestructive procedures tools for conservation*, Getty Publications, Los Angeles.
- Jordán, M.M., Boix, A., Sanfeliu, T. and de la Fuente C., 1999, Firing transformations of cretaceous clays used in the manufacturing of ceramic tiles, *Applied Clay Science*, 14, 225-234.

- Jordán, M.M., Sanfeliu, T. and de la Fuente C., 2001, Firing transformations of tertiary clays used in the manufacturing of ceramic tile bodies, *Applied Clay Science*, 20, 87-95.
- Julien, C., Massot, M., Rangan, S., Lemal, M. and Guyomard, D., 2002, Study of structural defects in  $\gamma$ -MnO<sub>2</sub> by Raman spectroscopy, *Journal of Raman Spectroscopy*, 33, 223-228.
- Kalāntar Žarrābī, A.R., 1999, *History of Kāshān*, ed. Afshār, Ī., Amir Kabir Press, Tehran. [in Persian]
- Kāmbakhsh-fard, S.A., 1967, The Pottery-making of Nayshābūr in the Seljuk Period, *Historical Surveys*, 9-10, 349-360.
- Kamilli, D.C. and Lamberg-Karlovsky, C.C., 1979, Petrographic and electron microprobe analysis of ceramics from Tepe Yahya, Iran, *Archaeometry*, 21, 1, 47-59.
- Karamanov, A. and Pelino, M., 1999, Evaluation of the degree of crystallisation in glass-ceramics by density measurements, *Journal of the European Ceramic Society*, 19, 649-654.
- Karimy, A.H. and Holakoei, P., 2009, *Technological Study of the Architectural Decorations of Bethlehem Church*, Isfahan's Cultural Heritage, Handicrafts and Tourism Organization, unpublished research. [in Persian]
- Keblow-Bernsted, A.M., 2003, *Early Islamic Pottery: Materials and Techniques*, Archetype, London.
- Kennett, D.J., Sakai, S., Neff, H., Gossett, R. and Larson, D.O., 2002, Compositional characterization of prehistoric ceramics: a new approach, *Journal of Archaeological Science*, 29, 443-455.
- Keppler, H., 1992, Crystal field spectra and geochemistry of transition metal ions in silicate melts and glasses, *American Mineralogist*, 77, 62-75.
- Khalaf Tabrīzī, M.H., 1652, *Burhān-i Qāte'*, ed. Mu'īn, M., 1983, Amir Kabir Press, Tehran. [in Persian]
- Khodami, M., Noghreyan, M. and Davoudian, A.R., 2010, Geochemical constraints on the genesis of the volcanic rocks in the southeast of Isfahan area, Iran, *Arabian Journal of Geosciences*, 3, 257-266.
- Kibaroglu, M., Satir, M. and Kastl, G., 2009, Petrographic and geochemical analysis on the provenance of the Middle Bronze and Late Bronze/Early Iron Age ceramics from Didi Gora and Udabno I, Eastern Georgia, *Journal of Archaeological Science*, 36, 10, 2463-2474.
- Kırmızı, B., Colomban, Ph. and Blanc, M., 2010, On-site analysis of Limoges enamels from sixteenth to nineteenth centuries: an attempt to differentiate between genuine artefacts and copies, *Journal of Raman Spectroscopy*, 41, 1240-1247.
- Kīyān-Aşl, M., 1993, *Problems Associated with the Glaze and Body in the Iranian Traditional Ceramics (Naţanz and Shahriżā)*, B.A. Thesis, Art University of Isfahan, Dept. of Fine Arts, Isfahan. [in Persian]
- Kīyānī, M.Y., Karīmī, F. and Qūchānī, 'A., 1983, *Introduction to Art of Tilework in Iran*, Rizā 'Abbāsī Museum, Tehran. [in Persian]
- Klein, C. and Hurlbut, C.S., 1999, *Manual of Mineralogy*, John Wiley & Sons, New York.

## References

---

- Klein, M., Jesse, F., Kasper, H.U. and Golden, A., 2004, Chemical characterization of ancient pottery from Sudan by X-ray fluorescence spectrometry XRF, electron microprobe analysis EMPA and inductively coupled plasma mass spectrometry ICP-MS, *Archaeometry*, 46, 339-356.
- Kleiss, W., 1990, Čehel Sotun, Qazvīn, *Encyclopædia Iranica*, Vol. V, 116-117
- Kleiss, W., 1993, Safavid palaces, *Ars Orientalis*, 23, 269-280.
- Kliess, W., 1999, Farahābād, *Encyclopædia Iranica*, available at:  
<http://www.iranicaonline.org/articles/farahabad>
- Kock, L.D. and De Waal, D., 2007, Raman studies of the underglaze blue pigment on ceramic artefacts of the Ming dynasty and of unknown origins, *Journal of Raman Spectroscopy*, 38, 1480-1487.
- Kock, L.D. and De Waal, D., 2008, Raman analysis of ancient pigments on a tile from the Citadel of Algiers, *Spectrochimica Acta Part A*, 71, 1348-1354.
- König, D. and Serneels, V., 2013, Roman double-layered crucibles from Autun/France: a petrological and geochemical approach, *Journal of Archaeological Science*, 40, 156-165.
- Koss, K., McCarthy, B., Chase, E.S. and Smith, D., 2009, Analysis of Persian painted minai ware, in *Scientific Research on Historical Asian Ceramics*, Archetype, London, pp. 33-50.
- Kristály, F., Kelemen, É., Rozsa, P., Nyilas, I. and Papp, I., 2012, Mineralogical investigations of medieval brick samples from Békés County (SE Hungary), *Archaeometry*, 54, 2, 250-266.
- Kühn, H., 1968, Lead-tin yellow, *Studies in Conservation*, 13, 1, 7-33.
- Kühn, H., 1993, Lead-tin yellow, in *Artists' Pigments: A Handbook of Their History and Characteristics*, vol 2, ed. Roy, A., Oxford University Press, New York, pp. 131-158.
- LaBrecque, J.J., Vaz, J.E. and Cruxent, J.M., 2003, Further investigation of majolica ceramics assigned to the Puebla Mexico provenance by radioisotope induced X-ray fluorescence, *X-Ray Spectrometry*, 32, 25-28.
- LaBrecque, J.J., Vaz, J.E., Cruxent, J.M. and Rosales, P.A., 1998, A simple radioisotope x-ray fluorescence method for provenance studies of archaeological ceramics employing principal component analysis, *Spectrochimica Acta Part B*, 53, 95-100.
- Lach, V., 1978, Microstructural changes during the firing of wall tile and sanitaryware, *Ceramurgia International*, 4, 1, 28-37.
- Lachance, G.R., and Traill, R.J., 1966, A practical solution to the matrix problem in x-ray analysis, *Canadian Journal of Spectroscopy*, 11, 43-48.
- Lakatos, T., Johansson, L.G. and Simmingsköld, B., 1972, Viscosity temperature relations in the glass system SiO<sub>2</sub>-Al<sub>2</sub>O<sub>3</sub>-Na<sub>2</sub>O-K<sub>2</sub>O-CaO-MgO in the composition range of technical glasses, *Glass Technology*, 13, 88-95.
- Lane, A., 1971, *Later Islamic Pottery: Persia, Syria, Egypt, Turkey*, Faber and Faber, London.

- Leung, P.L. and Luo, H., 2000, A study of provenance and dating of ancient Chinese porcelain by x-ray fluorescence spectrometry, *X-Ray Spectrometry*, 29, 1, 34-38,
- Li, B.-P., Greig, A., Zhao, J.-X., Collerson, K. D., Quan, K.-S., Meng, Y.-H. and Ma, Zh.-L., 2005, ICP-MS trace element analysis of Song dynasty porcelains from Ding, Jiexiu and Guantai kilns, north China, *Journal of Archaeological Science*, 32, 2, 251-259.
- Liem, N.Q., Thanh, N.T. and Colomban, Ph., 2002, Reliability of Raman micro-spectroscopy in analysing ancient ceramics: the case of ancient Vietnamese porcelain and celadon glazes, *Journal of Raman Spectroscopy*, 33, 287-294.
- Llugar, M., Forés, A., Badenes, J.A., Calbo, J., Tena, M.A. and Monrós, G., 2001, Colour analysis of some cobalt-based blue pigments, *Journal of the European Ceramic Society*, 21, 8, 1121-1130.
- Long, D.A., 2002, *The Raman Effect*, Wiley & Sons, Chichester.
- Long, D.A., 2005, Introduction to Raman spectroscopy, in *Raman Spectroscopy in Archaeology and Art History*, eds. Edwards, H.G.M. and Chalmers, J.M., Royal Society of Chemistry, Cambridge, pp. 17-40.
- Lumbreras, L.G., Gebhard, R., Häusler, W., Kauffmann-Doig, F., Riederer, J., Sieben, G. and Wagner, U., 2003, Mössbauer study of ceramic finds from the Galería de las Ofrendas, Chavín de Huántar, *Hyperfine Interactions*, 150, 51-72.
- Madariaga, J.M., 2010, Raman spectroscopy in art and archaeology, *Journal of Raman Spectroscopy*, 41, 1389-1393.
- Maggetti, M. and Schwab, H., 1982, Iron Age fine pottery from Châtillon-s-Glâne and the Heuneburg, *Archaeometry*, 24, 21-36.
- Māhir al-Naqsh, M., 2002, *Tile and its Application*, Samt Publications, Tehran. [in Persian]
- Mainfort, R.C., Cogswell, J.W. O'Brien, M.J., Neff, H. and Glascock, M.D., 1997, Neutron-activation analysis of pottery from Pinson mounds and nearby sites in western Tennessee: local production vs. long-distance importation, *Midcontinental Journal of Archaeology*, 22, 43-68.
- Majidzadeh, Y., 1975, The development of the pottery kiln in Iran from prehistoric to historical periods, *Paléorient*, 3, 207-221.
- Majmū'at al-Šanāya', 1582, *Majmū'at al-Šanāya'*, manuscript kept in the Library of Islamic Parliament of Iran, Registration No. 15617. [in Persian]
- Mallory-Greenough, L.M., Greenough, J.D. and Owen, J.V., 1998, New data for old pots: trace element characterisation of ancient Egyptian pottery using ICP-MS, *Journal of Archaeological Science*, 25, 85-97.
- Mangueira, G.M., Toledo, R., Teixeira, S. and Franco R.W.A., 2011, A study of the firing temperature of archaeological pottery by x-ray diffraction and electron paramagnetic resonance, *Journal of Physics and Chemistry of Solids*, 72, 90-96.
- Maniatis, Y. and Tite, M.S., 1981, Technological examination of Neolithic - Bronze Age pottery from central and southeast Europe and from the Near East, *Journal of Archaeological Science*, 8, 59-76.

## References

---

- Maniatis, Y., 2009, The emergence of ceramic technology and its evolution as revealed with the use of scientific techniques, in *From Mine to Microscope: Advances in the Study of Ancient Technology*, eds. Shortland, A., Freestone, I.C. and Rehren, Th., Oxbow, Oxford, pp. 11-26.
- Maniatis, Y., Simopoulos, A., Kostikas, A., and Perdikatsis, V., 1983, Effect of reducing atmosphere on minerals and iron oxides developed in fired clays: the role of Ca, *Journal of the American Ceramic Society*, 66, 11, 773-781.
- Manşūr, M., 1454-1478, *Gawhar-nāma*, ed. Sutūda, M., 1956, Farhang-i Īrānzamīn, Vol. IV, Tehran, pp. 185-287. [in Persian]
- Marghussian, A.K., Fazeli, H. and Sarpoolaki, H., 2009, Chemical-mineralogical analyses and microstructural studies of prehistoric pottery from Rahmatabad, south-west Iran, *Archaeometry*, 51, 733-747.
- Maritan, L., Nodari, L., Mazzoli, C., Milano, A. and Russo, U., 2006, Influence of firing conditions on ceramic products: experimental study on clay rich in organic matter, *Applied Clay Science*, 31, 1-15.
- Martí, M.G., 1954, *Cerámica del Levante Español, Siglos Medievales*, Labor, Barcelona.
- Martin, J.D., 2004, *XPowder, a Software Package for Power X-ray Diffraction Analysis*, ISBN: 84-609-1497-6.
- Martín, M.M.M., Escobosa, I.F. and Delgado, J.L., 1999, Las producciones de un alfar islámico en Almería, *Arqueología y Territorio Medieval*, 6, 207-240.
- Mason, R.B. and Keall, E.J., 1991, The Abbasid glazed wares of Siraf and the Basra connection: petrographic analysis, *Iran*, 29, 51-66.
- Mason, R.B., 1995, New looks at old pots: results of recent multidisciplinary studies of glazed ceramics from the Islamic World, *Muqarnas*, 12, 1-10.
- Mason, R.B., 1996, Petrography and provenance of Timurid ceramics, in *Tamerlane's Tableware: a New Approach to the Chinoiserie Ceramics of Fifteenth and Sixteenth Century Iran*, eds. Golombek, L., Mason, R.B. and Bailey, G., Royal Ontario Museum and Mazda Press, Costa Mesa, pp.16-56.
- Mason, R.B. and Tite, M.S., 1997, The beginning of tin-opacifications of pottery glazes, *Archaeometry*, 39, 41-58.
- Mason, R.B., Tite, M.S., Paynter, S. and Salter, C., 2001, Advances in polychrome ceramics in the Islamic world of the 12th century AD, *Archaeometry*, 43, 2, 191-209.
- Mason, R., 2003, Petrography of pottery from Kirman, *Iran*, 41, 271-278.
- Mass, J.L., 1999, Instrumental methods of analysis applied to the conservation of ancient glasses, in *Conservation of Glass and Ceramics: Research, Practice, and Training*, ed. Tennent, N., James & James, London, pp. 15-41.

- Matos, Ch.R.S., Xavier, M.J., Barreto, L.S., Costa, N.B. and Gimenez, I.F., 2007, Principal component analysis of x-ray diffraction patterns to yield morphological classification of brucite particles, *Analytical Chemistry*, 79, 2091-2095
- Mattei, E., de Vivo, G., De Santis, A., Gaetani, C., Pelosi, C. and Santamaria, U., 2008, Raman spectroscopic analysis of azurite blackening, *Journal of Raman Spectroscopy*, 39, 302-306.
- Mathee, R., 2008, Safavid dynasty, *Encyclopædia Iranica*, available at: <http://www.iranicaonline.org/articles/safavids>
- McConville, C.J. and Lee, W.E., 2005, Microstructural development on firing illite and smectite clays compared with that in kaolinite, *Journal of American Ceramic Society*, 88, 8, 2267-2276.
- McGovern, P.E., 1989, Ancient ceramic technology and stylistic change: contrasting studies from southwest and southeast Asia, in *Scientific Analysis in Archaeology and its Interpretation*, ed. Henderson, J., University of California, Los Angeles, pp. 63-81
- McMillan, P., 1984, A Raman spectroscopic study of glasses in the system CaO-MgO-SiO<sub>2</sub>, *American Mineralogist*, 69, 645-459.
- McQuade, M.C., 1999, Las cerámicas españolas de la Hispanic society of America Archer Milton Huntington y su museo, *Cerámica y Vidrio*, 384, 353-358.
- Mejdahl, V., 1980, Further work on ceramic objects from Glozel, *Archaeometry*, 22, 2, 197-203.
- Meulebroeck, W., Cosyns, P., Baert, K., Wouters, H., Cagno, S., Janssens, K., Terryn, H., Nys, K. and Thienpont, H., 2011, Optical spectroscopy as a rapid and low-cost tool for the first-line analysis of glass artefacts: a step-by-step plan for Roman green glass, *Journal of Archaeological Science*, 38, 2387-2398.
- Miao, J., Yang, B. and Mu, D., 2010, Identification and differentiation of opaque Chinese overglaze yellow enamels by Raman spectroscopy and supporting techniques, *Archaeometry*, 52, 1, 146-155.
- Mironova-Ulmane, N., Kuzmin, A. and Grube, M., 2009, Raman and infrared spectromicroscopy of manganese oxides, *Journal of Alloys and Compounds*, 480, 97-99.
- Mirti, P., Casoli, A. and Appolonia, L., 1993a, Scientific analysis of Roman glass from Augusta Praetoria, *Archaeometry*, 35, 2, 225-240.
- Mirti, P., Ferrari, R. P., Lauranti, E. and Casoli, A., 1993b, A study of Roman glass by reflectance and electron paramagnetic resonance spectroscopies, *Spectrochimica Acta A*, 49, 9, 1361-1371.
- Mirti, P., Appolonia, L., Casoli, A., Ferrari, R., Laurenti, E., Amisano Canesi, A. and Chiari, G., 1995, Spectrochemical and structural studies on a Roman sample of Egyptian blue, *Spectrochimica Acta A*, 51, 437-446.
- Mirti, P., 1998, On the use of colour coordinates to evaluate firing temperatures of ancient pottery, *Archaeometry*, 40, 1, 45-57.
- Mirti, P., Lepora, A. and Sagui, A., 2000, Scientific analysis of seventh-century glass fragments from the Crypta Balbi in Rome, *Archaeometry*, 42, 2, 359-374.

## References

---

- Mirti, P., Davit, P. and Gulmini, M., 2002, Colourants and opacifiers in seventh and eighth century glass investigated by spectroscopic techniques, *Analytical and Bioanalytical Chemistry*, 372, 221-229.
- Moens, L., von Bohlen, A. and Vandenaabeele, P., 2000, X-ray fluorescence, in *Modern Analytical Methods in Art and Archaeology*, eds. Ciliberto, E. and Spoto, G., John Wiley & Sons, New York, pp. 55-79.
- Molera, J., Garcia-Vallés M., Pradell, T. and Vendrell-Saz, M., 1996, Hispano-Moresque pottery production of the 38 fourteenth-century workshop of Testar del Moli Paterna, Spain, *Archaeometry*, 38, 1, 67-80.
- Molera, J., Vendrell-Saz, M., Garcia-Vallés M. and Pradell, T., 1997, Technology and colour development of Hispano-Moresque lead glazed pottery, *Archaeometry*, 39, 23-39.
- Molera, J., Pradell, T. and Vendrell-Saz, M., 1998, The colours of ca-rich ceramic pastes: origin and characterization, *Applied Clay Science*, 13, 187-202.
- Molera, J., Pradell, T., Salvadó, N. and Vendrell-Saz, M., 1999, Evidence of tin oxide recrystallization in opacified lead glazes, *Journal of American Ceramic Society*, 82, 2871-2875.
- Moorey, R.S.P., 1994, *Ancient Mesopotamian Materials and Industries: the Archaeological Evidence*, Clarendon Press, Oxford; New York.
- Morariu, V.V., Bogdan, M. and Ardelean, I., 1977, Ancient pottery: its pore structure, *Archaeometry*, 19, 2, 187-221.
- Morgan, P. and Leatherby, J., 1987, Excavated ceramics from Sirjan, in *Syria and Iran, Three Studies in Medieval Ceramics*, eds. Allan, J. and Roberts, C., Oxford University Press, Oxford; New York, pp. 23-175.
- Morgan, P., 1994, Iranian stone-paste pottery of the Saljuq period: types and techniques, in *Cobalt and Lustre*, ed. Grube, E.J., The Nour Foundation, New York, pp. 155-248.
- Moroni, B. and Conti, C., 2006, Technological features of renaissance pottery from Deruta Umbria, Italy: an experimental study, *Applied Clay Science*, 33, 230-246.
- Moropoulou, A., Bakolas, A., Bisbikou, K., 1995, Thermal analysis as a method of characterizing ancient ceramic technologies, *Thermochimica Acta*, 2570, 743-753.
- Moropoulou, A. and Polikreti, K., 2009, Principal component analysis in monument conservation: three application examples, *Journal of Cultural Heritage*, 10, 73-81.
- Motos Guirao, E., 1994, Cerámica hispano-musulmana de cuerda seca de la fortaleza de balis al-Ahmar cerro del castellón. vélez rubio, Almería, colección Miguel Guirao, in *Arqueología, Comarca de los Vélez*, Instituto de Estudios Almerienses, Almería, pp. 169-178.
- Mudarrisī Ṭabāṭabā'ī, Ḥ., 1985, *Qum-nāma, Articles and Texts about Qum*, Qum. [in Persian]
- Mueller, J.W., 1974, The use of sampling in archaeological survey, *Memoirs of the Society for American Archaeology*, 28, i-xi, 1-91.

## References

---

- Mühlethaler, B. and Thissen, J., 1993, Smalt, in *Artists' Pigments. A Handbook of Their History and Characteristics*, vol. 2, ed. Roy, A., National Gallery of Art and Oxford University Press, New York; Washington; Oxford, pp. 113-130.
- Murad, E. and Wagner, U., 1998, Clays and clay minerals: the firing process, *Hyperfine Interactions*, 117, 337-356.
- Muscarella, O.W., 1988, *Bronze and Iron, Ancient Near Eastern Artifacts in the Metropolitan Museum of Art*, Yale University Press, New York.
- Mustufi, H., 1339, *Nuzhat al-Qulūb*, ed. le Strange, G., 1963, Tehran. [in Persian]
- Nādirī, B., 1978, A brief about tile-making in Mashhad, *Hunar va Mardum Magazine*, 188, 58-65. [in Persian]
- Narāqī, H., 1969, *Historical Monuments of Kāshān and Naṭanz*, Anjuman-i Āthār-i Millī-i Īrān Press, Tehran. [in Persian]
- Nasr, H., 1974, Religion in Safavid Persia, *Iranian Studies*, 71-2, 271-286.
- Naumann, R., 1971, Brennöfen für Glasurkeramik, *Istanbuler Mitteilungen*, 21, 173-190.
- Navā'ī, A.H. and Malik-zāda, E., 2005, 'Abbās-Qulī madrasa and fight among its inheritors and trustees, *Mīrās-i Jāvīdān*, 50, 34-42.
- Nayshābūrī, M.A.J., 1196, *Javāhir-nāma Niṣāmī*, eds. Afshār, Ī. and Daryāgasht, M.R., 2004, Mīrāt-i Maktūb Press, Tehran. [in Persian]
- Necipoglu, G., 1990, From international Timurid to Ottoman: a change of taste in sixteenth-century ceramic tiles, *Muqarnas*, 7, 136-170.
- Neff, H., 2002, Quantitative techniques for analysing ceramic compositional data, in *Ceramic Production and Circulation in Greater Southwest: Source Determination by INAA and Complementary Mineralogical Investigations*, eds. Glowacki, D.M. and Neff, H., Costen Institute of Archaeology, UCLA, pp. 15-36.
- Neff, H., 2003, Analysis of Mesoamerican plumbate pottery surfaces by laser ablation inductively coupled plasma mass spectrometry LA-ICP-MS, *Journal of Archaeological Science*, 30, 21-35.
- Neff, H., Bishop, R.L. and Sayre, E.V., 1988, A simulation approach to the problem of tempering in compositional studies of archaeological ceramics, *Journal of Archaeological Sciences*, 15, 159-172.
- Negahban, E.O., 1991, *Excavations at Haft Tepe, Iran*, Vol. 70 of Museum monographs, Museum of Archaeology, University of Pennsylvania, Philadelphia.
- Nelson, C. and White, W.B., 1986, Transition metal ions in silicate melts. IV. Cobalt in sodium silicate and related glasses, *Journal of Materials Research*, 1, 1, 130-138.
- Newman, A.J., 2006, *Safavid Iran: Rebirth of a Persian Empire*, Tauris, London.
- Nīyāzmand, R., 1964, Professions: pottery industry, in *Īrānshahr, Vol. II*, ed. Hikmat, A., UNESCO office in Tehran, pp. 1815-1833. [in Persian]

## References

---

- Nodari, L., Marcuz, E., Maritan, L., Mazzoli, C. and Russo, U., 2007, Hematite nucleation and growth in the firing of carbonate-rich clay for pottery production, *Journal of the European Ceramic Society*, 27, 4665-4673.
- Norris, A.W., Taylor, D. and Thorpe, I., 1979, Range curves: an experimental method for the study of vitreous pottery bodies, *Transactions of the British Ceramic Society*, 78, 102-108.
- Norrman, M., Stahl, K., Schluckebier, G. and Al-Karadaghi, S., 2006, Characterization of insulin microcrystals using powder diffraction and multivariate data analysis, *Journal of Applied Crystallography*, 39, 3, 391-400.
- Norton, F.H. and Hodgdon, F.B., 1931, The influence of time on the maturing temperature of whiteware bodies. I., *Journal of the American Ceramic Society*, 14, 3, 177-191.
- Norton, F.H., 1931, The influence of time on the maturing temperature of whiteware bodies. II, *Journal of the American Ceramic Society*, 14, 3, 192-206.
- Nuṣratī, M., 2001, Masjed-e Jāme‘ of Qazvīn, *Gulistān-i Qurān*, 99, 21-22.
- O’Kane, B., 1987, *Timurid Architecture in Khurasan*, Mazdā Publishers and Undena Publications, Costa Mesa.
- O’Kane, B., 2011, Tiles of many hues: the development of Iranian cuerda seca tiles and the transfer of tilework technology, in *And Diverse Are Their Hues: Colour in Islamic Art and Culture*, eds. Bloom, J.M. and Blair, S.S., Yale University Press, New Haven; London, pp. 177-203.
- Obeidat, S.M., Al-Momani, I., Haddad, A. and Bani Yasein, M., 2011, Combination of ICP-OES, XRF and XRD techniques for analysis of several dental ceramics and their identification using chemometrics, *Spectroscopy*, 26, 2, 141-149.
- Odriozola, C. and Martínez-Blanes, J.M., 2007, Estimate of firing temperatures through bone-based chalcolithic decorated pottery, *Journal of Thermal Analysis and Calorimetry*, 87, 1, 135-141.
- Olmer, M.L.-J., 1908, *Rapport sur une Mission Scientifique en Perse*, Vol XVI, Imprimerie Nationale, Paris.
- Orlando, A., Olmi, F., Vaggelli, G. and Bacci M., 1996, Mediaeval stained glasses of Pisa cathedral (Italy): their composition and alteration products, *Analyst*, 121, 553-558.
- ‘Oṭāridī, A.A., 2002, *Culture of Khurāsān, Ṭūs*, ‘Oṭārid, Tehran. [in Persian]
- Owen, J.V. and Terence, E., 1998, Day assessing and correcting the effects of the chemical weathering of potsherds: a case study using soft-paste porcelain wasters from the Longton Hall (Staffordshire) factory site, *Geoarchaeology: An International Journal*, 13, 3, 265-286.
- Pace, M., Bianco Prevot, A. and Mirti, P., 2008, The technology of production of Sassanian glazed pottery from Veh-Ardashir (Central Iraq), *Archaeometry*, 50, 4, 591-605.
- Padeletti, G., Fermo, P., Gilardoni, S. and Galli, A., 2004, Technological study of ancient ceramics produced in Casteldurante (central Italy) during the Renaissance, *Applied Physics A*, 79, 2, 335-339.

## References

---

- Pagès-Camagna, S., Colinart, S., 2003, The Egyptian green pigment: its manufacturing process and links to Egyptian blue, *Archaeometry*, 45, 4, 637-658.
- Palacios, P.R., Bustamante, A., Romero-Gómez, P. and González, J.C., 2011, Kinetic study of the thermal transformation of limonite to hematite by x-ray diffraction,  $\mu$ -Raman and Mössbauer spectroscopy, *Hyperfine Interact*, 203, 113-118.
- Palazón, N., 1990, *Los Materiales Islámicos del Alfar Antiguo de San Nicolás de Murcia. Fours de Potiers et 'Testares' Médiévaux en Méditerranée Occidentale*, Madrid Publicaciones de la Casa de Velázquez, Série Archéologique XII.
- Papadopoulou, D., Lalia-Kantouri, M., Kantiranis, N. and Stratis, J., 2006, Thermal and mineralogical contribution to the ancient ceramics and natural clays characterization, *Journal of Thermal Analysis and Calorimetry*, 84, 1, 39-45.
- Partha Sarathi, D., Acharya, R., Nair, A.G.C., Lakshminarayana, S., Lakshmana Das, N. and Reddy, A.V.R., 2008, Application of instrumental neutron activation analysis for chemical composition analysis of ancient potteries from Buddhist sites of Andhra Pradesh: Part I, *Journal of Nuclear and Radiochemical Sciences*, 9, 1, 7-12.
- Paynter, S., Okyar, F., Wolf, S. and Tite, M.S., 2004, The production technology of Iznik pottery- a reassessment, *Archaeometry* 46, 3, 421-437.
- Peacock, D.P.S., 1967, The heavy mineral analysis of pottery: a preliminary report, *Archaeometry*, 10, 1, 97-100.
- Pérez-Arantegui, J., Soto, M. and Castillo, J.R., 1999, Examination of the 'cuerda seca' decoration technique on Islamic ceramics from al-Andalus Spain, *Journal of Archaeological Science*, 26, 935-941.
- Persian Farsi*, available at: [transliteration.eki.ee/pdf/Persian.pdf](http://transliteration.eki.ee/pdf/Persian.pdf)
- Persian Romanization Table*, available at: [www.loc.gov/catdir/cpsd/romanization/persian.pdf](http://www.loc.gov/catdir/cpsd/romanization/persian.pdf)
- Persian*, Reports on the Current Status of United Nations Romanization Systems for Geographical Names, UNGEGN Working Group on Romanization System, Version 2.2, 2003, available at: <http://www.eki.ee/wgrs/>
- Petersen, A., 1996, *Dictionary of Islamic Architecture*, Routledge, London.
- Pickett, D., 1997, *Early Persian Tilework: the Medieval Flowering of Kāshī*, Associated University Presses, London.
- Polak, J.E., 1865, *Persien: Das Land und Seine Bewohner*, Hildesheim, New York.
- Pollard, A.M. and Heron, C., 2008, *Archaeological Chemistry*, Royal Society of Chemistry, Cambridge.
- Pollard, A.M., Batt, C.M., Stern, B. and Young, S.M.M., 2007, *Analytical Chemistry in Archaeology*, Cambridge University Press, Leiden.
- Pope, A.U., 1965, *Persian Architecture: the Triumph of Form and Color*, G. Braziller, New York.

## References

---

- Porter, V., 1995, *Islamic Tiles*, Interlink Books, New York.
- Porter, Y., 2011, *Le Prince, l'Artiste et l'Alchimiste: la Céramique dans le Monde Iranien Xe-Xviie Siècles*, Hermann Éditeurs, Paris.
- Prinsep, J., 1840, Useful Tables, *Forming an Appendix to the Journal of the Asiatic Society: Part I, Coins, Weights, and Measures of British India*, Bishop's College Press, Calcutta.
- Prinsloo, L.C. and Colomban, Ph., 2008, A Raman spectroscopic study of the Mapungubwe oblates: glass trade beads excavated at an Iron Age archaeological site in South Africa, *Journal of Raman Spectroscopy*, 39, 79-90.
- Purnaderi, H., 2010, The transformation and development of Ali-Qapu, the court house Dulat-Khana of Naqsh-e-Jahan square, a review of the IsMEO studies on the chronological development of Ali Qapu, *Şuffa*, 20, 51, 23-30. [in Persian]
- Rasmussen, K.L., De La Fuente, G.A., Bond, A.D. Mathiesen, K.K. and Vera, S.D., 2012, Pottery firing temperatures: a new method for determining the firing temperature of ceramics and burnt clay, *Journal of Archaeological Science*, 39, 6, 1705-1716.
- Rathossi, C. and Pontikes Y., 2010, Effect of firing temperature and atmosphere on ceramics made of NW Peloponnese clay sediments. Part I: reaction paths, crystalline phases, microstructure and colour, *Journal of the European Ceramic Society*, 30, 1841-1851.
- Rathossi, Ch., Tsolis-Katagas, P. and Katagas, Ch., 2004, Technology and composition of Roman pottery in northwestern Peloponnese, Greece, *Applied Clay Science*, 24, 313-326.
- Rāzī, M.Z., 9-10th century AD, *Kitāb al-Asrār*, trans. Shaybānī, Ḥ. 'A., 1992, Tehran University Press, Tehran. [in Persian]
- Reedy, T.J. and Reedy, C.L., 1988, *Statistical Analysis in Art Conservation Research*, Getty Conservation Institute, Marina del Rey.
- Rehren, Th., 2008, A review of factors affecting the composition of early Egyptian glasses and faience: alkali and alkali earth oxides, *Journal of Archaeological Science*, 35, 1345-1354.
- Reiche, I., Röhrs, S., Salomon, J., Kanngießer, B., Höhn, Y., Malzer, W. and Voigt, F., 2009, Development of a nondestructive method for underglaze painted tiles- demonstrated by the analysis of Persian objects from the nineteenth century, *Analytical and Bioanalytical Chemistry*, 393, 1025-1041.
- Riccardi, M.P., Messiga, B. and Duminuco, P., 1999, An approach to the dynamics of clay firing, *Applied Clay Science*, 15, 393-409.
- Ricci, C., Miliani, C., Rosi, F., Brunetti, B.G. and Sgamellotti, A., 2007, Structural characterization of the glassy phase in majolica glazes by Raman spectroscopy: a comparison between Renaissance samples and replica processed at different temperatures, *Journal of Non-Crystalline Solids*, 353, 1054-1059.
- Ricciardi, P., Colomban, Ph., Tournié, A., Macchiarola, M. and Ayed, N., 2009, A non-invasive study of Roman Age mosaic glass tesserae by means of Raman spectroscopy, *Journal of Archaeological Science*, 36, 2551-2559.

- Ritter, H., Ruska, J. and Winderlich, R., 1935, Orientalische steinbücher und persische fayencetechnik, *Abteilung Istanbul des Archäologischen Institutes des Deutschen Reiches*, 3, 16-56.
- Roberts, J.P., 1963, Determination of the firing temperature of ancient ceramics by measurement of thermal expansion, *Archaeometry*, 6, 21-25.
- Robertson, J.D., Neff, H. and Higgins, B., 2002, Microanalysis of ceramics with PIXE and LA-ICP-MS, *Nuclear Instruments and Methods in Physics Research B*, 189, 378-381.
- Robinet, L., Coupry, C., Eremin, K. and Hall, Ch., 2006, The use of Raman spectrometry to predict the stability of historic glasses, *Journal Raman Spectroscopy*, 37, 789-797.
- Robinet, L., Bouquillon, A. and Hartwig, J., 2008, Correlations between Raman parameters and elemental composition in lead and lead alkali silicate glasses, *Journal of Raman Spectroscopy*, 39, 618-626.
- Rochechouart, J., 1867, *Souvenirs d'un voyage en Perse*, Challamel Ainé, Paris.
- Rodríguez, J.A.E., 2006, *Antigüedades Medievales*, Real Academia de la Historia, Madrid.
- Rooksby, H.P., 1964, A yellow cubic lead tin oxide opacifier in ancient glasses, *Physics and Chemistry of Glasses*, 5, 1, 20-25.
- Roqué, J., Molera, J., Sciau, P., Pantos, E., Vendrell-Saz, M., 2006, Copper and silver nanocrystals in lustre lead glazes: development and optical properties, *Journal of the European Ceramic Society*, 26, 16, 3813-3824.
- Rosi, F., Manuali, V., Miliani, C., Brunetti, B.G., Sgamellotti, A., Grygar, T. and Hradil, D., 2009, Raman scattering features of lead pyroantimonate compounds. Part I: XRD and Raman characterization of  $Pb_2Sb_2O_7$  doped with tin and zinc, *Journal of Raman Spectroscopy*, 40, 107-111.
- Rosi, F., Manuali, V., Grygar, T., Bezdzicka P., Brunetti, B.G., Sgamellotti, A., Burgio, L., Seccaroni, C. and Miliani, C., 2011, Raman scattering features of lead pyroantimonate compounds: implication for the non-invasive identification of yellow pigments on ancient ceramics. Part II. In situ characterisation of Renaissance plates by portable micro-Raman and XRF studies, *Journal of Raman Spectroscopy*, 42, 407-414.
- Ruggles, D.F., 2011, *Islamic Art and Visual Culture: an Anthology of Sources*, Wiley-Blackwell, West-Sussex.
- Ruiz-Moreno, S., Pérez-Pueyo, R., Gabaldón, A., Soneira, M.-J. and Sandalinas, C., 2003, Raman laser fibre optic strategy for non-destructive pigment analysis. Identification of a new yellow pigment (Pb, Sn, Sb) from the Italian XVII century painting, *Journal of Cultural Heritage*, 4, 309s-313s.
- Ruvalcaba-Sil, J.L., Ontalba Salamanca, M.A., Manzanilla, L., Miranda, J., Cañetas Ortega, J. and López, C., 1999, Characterisation of pre-Hispanic pottery from Teotihuacan, Mexico, by a combined PIXE-RBS and XRD analysis, *Nuclear Instruments and Methods in Physics Research B*, 150, 591-596.
- Rye, O.S., 1976, Khār: sintered plant ash in Pakistan. Appendix 3, in *Traditional Pottery Techniques of Pakistan*, Smithsonian contributions to Anthropology, 21, Eds. O.S. Rye and C. Evans, Smithsonian Institution Press, pp. 180-185.

## References

---

- Şadīq, M. and Karīmī, A., 1965, Pottery-making in Lālaĵīn, *Hunar va Mardum Magazine*, 30, 10-16. [in Persian]
- Şadīq, M., 1976, Pottery-making in Zunūz, *Hunar va Mardum Magazine*, 174, 40-45. [in Persian]
- Sajo Bohus, L., Mackowiak de Antczak, M., Greaves, E.D., Antczak, A., Bermudez, J., Kasztovszky, Zs., Poirier, T. and Simonits, A., 2005, Incipient archaeometry in Venezuela: provenance study of Pre-Hispanic pottery figurines, *Journal of Radioanalytical and Nuclear Chemistry*, 265, 2, 247-256.
- Sakellariou, K., Miliani, C., Morresi, A. and Ombelli, M., 2004, Spectroscopic investigation of yellow majolica glazes, *Journal of Raman Spectroscopy*, 35, 61-67.
- Sánchez Ramos, S., Bosch Reig, F., Gimeno Adelantado, J.V., Yusá Marco, D.J. and Doménech Carbó, A., 2002, Study and dating of medieval ceramic tiles by analysis of enamels with atomic absorption spectroscopy, x-ray fluorescence and electron probe microanalysis, *Spectrochimica Acta Part B*, 57, 689-700.
- Sandalinas, C., Ruiz-Moreno, S., López-Gil A., and Miralles, J., 2006, Experimental confirmation by Raman spectroscopy of a Pb-Sn-Sb triple oxide yellow pigment in sixteenth-century Italian pottery, *Journal of Raman Spectroscopy*, 37, 1146-1153.
- Sanderson, D.C.W. and Hutchings, J.B., 1987, The origins and measurement of colour in archaeological glasses, *Glass Technology*, 28, 99-105.
- Sarre, F., 1924, *Ardabil: Grabmoschee des Schech Safi*, trans. Mūsavī, Ş.Kh., 2006, Farhangistān-i Hunar, Tehran. [in Persian]
- Savory, R., 1980, *Iran under the Safavids*, Cambridge University Press, Cambridge; New York.
- Sayre, E.V., Smith, R.W., 1974, Analytical studies of ancient Egyptian glass, in *Recent Advances in the Science and Technology of Materials*, Vol. 3, ed. Bishay, A., Plenum Press, New York, pp. 47-70.
- Schabbach, L.M., Bondioli, F., Ferrari, A. M., Manfredini, T., Petter, C.O. and Fredel, M.C., 2008, Colour in ceramic glazes: Analysis of pigment and opacifier grain size distribution effect by spectrophotometer, *Journal of the European Ceramic Society*, 28, 1777-1781.
- Schibille, N., Marii, F., and Rehren, T., 2008, Characterization and provenance of late antique window glass from the Petra church in Jordan, *Archaeometry*, 50, 4, 627-642.
- Schomburg, J., 1991, Thermal reactions of clay minerals: their significance as 'archaeological thermometers' in ancient potteries, *Applied Clay Science*, 6, 275-220.
- Schreurs, J.W.H. and Brill, R.H., 1984, Iron and sulfur related colors in ancient glasses, *Archaeometry*, 26, 2, 199-209.
- Sedmale, G., Sperberga, I., Sedmalis, U. and Valancius, Z., 2006, Formation of high-temperature crystalline phases in ceramic from illite clay and dolomite, *Journal of the European Ceramic Society*, 26, 3351-3355.

## References

---

- Sendova, M., Kaiser, B., Scalera, M. and Zhelyaskov, V., 2010, Della Robbia blue glaze: micro-Raman temperature study and x-ray fluorescence spectroscopy characterization, *Journal of Raman Spectroscopy*, 41, 4, 469-72.
- Shaikh, H., 1909, *Persian Self-taught in Roman Characters with English Phonetic Pronunciation*, E. Marlborough & Co., London.
- Shapur Shahbazi, A. and Bosworth, E.C., 1990, Capital Cities, *Encyclopædia Iranica*, Vol. IV: 768-774.
- Shennan, S., 1997, *Quantifying Archaeology*, Edinburgh University Press, Edinburgh.
- Shortland, A. J. and Eremin, K., 2006, The analysis of second millennium glass from Egypt and Mesopotamia, Part 1: new WDS analyses, *Archaeometry*, 48, 4, 581-603.
- Shoval, S. and Beck, P., 2005, Thermo-FTIR spectroscopy analysis as a method of characterizing ancient ceramic technology, *Journal of Thermal Analysis and Calorimetry*, 82, 3, 609-619.
- Shoval, S., 1994, The firing temperature of a Persian-period pottery kiln at tell, Michal, Israel estimated from the composition of its pottery, *Journal of Thermal Analysis*, 42, 175-185.
- Shoval, Sh., Yadin, E. and Panczer, G., 2011, Analysis of thermal phases in calcareous Iron Age pottery using FT-IR and Raman spectroscopy, *Journal of Thermal Analysis and Calorimetry*, 104, 515-525.
- Smith, D., 2001, Considering the colors of minai ware, in *MET objectives*, The Metropolitan Museum, pp. 9-11.
- Smith, G.D. and Clark, R.J.H., 2004, Raman microscopy in archaeological science, *Journal of Archaeological Science*, 31, 1137-1160.
- Soucek, P.P., 1985, 'Āli-Qapu, *Encyclopædia Iranica*, Vol. I, 871-872.
- Soucek, P.P., 1994, Decoration, *Encyclopædia Iranica*, Vol. VII, 159-197.
- Staniforth, S., 1985, Retouching and colour matching: the restorer and metamerism, *Studies in Conservation*, 30, 3, 101-111.
- Stern, W.B. and Gerber, Y., 2004, Potassium-calcium glass: new data and experiments, *Archaeometry*, 46, 1, 137-156.
- Stevens, R., 1974, European visitors to the Safavid court, *Iranian Studies*, 73-4, 421-457.
- Stievano, L., Bertelle, M., Calogero, S. and Wagner, F.E., 2004, The application of  $^{119}\text{Sn}$  mössbauer spectroscopy to the investigation of glass coatings: evolution of the tin species in lead-rich white glazes, *Hyperfine Interactions*, 154, 1, 83-94.
- Strohmeier, B.R. and Hercules, D.M., 1984, Surface spectroscopic characterization of Mn/Al<sub>2</sub>O<sub>3</sub> catalysts, *The Journal of Physical Chemistry*, 88, 4922-4929.
- Stroud, J.S., 1971, Optical absorption and color caused by selected cations in high-density lead silicate glass, *Journal of American Ceramic Society*, 54, 8, 401-406.
- Stuart, B.H., 2007, *Analytical Techniques in Materials Conservation*, John Wiley & Sons, Chichester.

## References

---

- Suárez, E.S., 2007, La cerámica de ‘*cuerda seca*’ del antiguo Convento de San Francisco de Asís de las Palmas de Gran Canaria, *Cuadernos de Prehistoria y Arqueología*, 33, 155-174.
- Tangri, D. and Wright, R.V.S., 1993, Multivariate analysis of compositional data: applied comparisons favour standard principal components analysis over Aitchison’s loglinear contrast method, *Archaeometry*, 35, 1, 103-112.
- Tiequan, Zh., Changsui, W., Hongmin, W. and Zhenwei, M., 2010, The preliminary study on kiln identification of Chinese ancient Qingbai wares by ICP-AES, *Journal of Cultural Heritage*, 11, 4, 482-486.
- Tiflīsī, Ḥ., 12th Century, *Bayān al-Ṣanā‘āt*, ed. Afshār, Ī., 1956, Vol V, Farhang-i Īrānzamīn, Tehran, pp. 298-457. [in Persian]
- Tite, M.S., 1969, Determination of the firing temperature of ancient ceramics by measurement of thermal expansion: a reassessment, *Archaeometry*, 11, 1, 131-143.
- Tite, M.S. and Maniatis, Y., 1975, Examination of ancient pottery using the scanning electron microscope, *Nature*, 257, 122-123.
- Tite, M.S., 1989, Iznik pottery: an investigation of the methods of production, *Archaeometry*, 31, 2, 115-132.
- Tite, M.S., 1992, The impact of electron microscopy on ceramic studies, *Proceedings of the British Academy*, 77, 111-131.
- Tite, M.S., 1995, Firing temperatures determination: how and why? in *The Aim of Laboratory Analyses of Ceramics in Archaeology*, eds. Lindahl, A. and Stilborg, O., Konfrenser, Stockholm, 34, pp. 37-42.
- Tite, M.S., Freestone, I., Mason, R., Molera, J., Vendrell-Saz, M. and Wood, N., 1998, Lead glazes in antiquity: methods of production and reasons for use, *Archaeometry*, 40, 2, 241-260.
- Tite, M.S., 1999, Pottery production, distribution, and consumption- the contribution of the physical sciences, *Journal of Archaeological Method and Theory*, 6, 3, 181-233.
- Tite, M.S. and Shortland, A.J., 2003, Production technology for copper- and cobalt-blue vitreous materials from the New Kingdom site of Amarna- a reappraisal, *Archaeometry*, 45, 2, 285-312.
- Tite, M.S., Shortland, A., Maniatis, Y., Kavoussanaki, D. and Harris, S.A., 2006, The composition of the soda-rich and mixed alkali plant ashes used in the production of glass, *Journal of Archaeological Science*, 33, 1284-1292.
- Tite, M.S., 2008, Ceramic production, provenance and use- a review, *Archaeometry*, 50, 2, 216-231.
- Tite, M.S., Shortland, A.J., McCarthy, B. and Paynter, S., 2008a, Production of glazed pottery and brickwork in the Near East, in *Production Technology of Faience and Related Early Vitreous Materials*, eds. Tite, M.S. and Shortland, A.J., Oxford University School of Archaeology Monograph 72, Oxford, pp. 187-198.

- Tite, M.S., Pradell, T. and Shortland, A.J., 2008b, Discovery, production and use of tin-based opacifiers in glasses, enamels and glazes from the Late Iron Age onwards: a reassessment, *Archaeometry*, 50, 67-84.
- Tite, M.S., 2009, The production technology of Italian maiolica: a reassessment, *Journal of Archaeological Science*, 36, 2065-2080
- Tite, M.S., Wolf, S. and Mason, R.B., 2011, The technological development of stonepaste ceramics from the Islamic Middle East, *Journal of Archaeological Science*, 38, 570-580.
- Tite, M.S., Personal communication via email in 12th February 2013.
- Tournié, A., Prinsloo, L.C. and Colomban, Ph., 2010, *Raman spectra database of the glass beads excavated on Mapungubwe hill and k2, two archaeological sites in South Africa*, Materials Science, Cornell University Library.
- Traoré, K., Ouedraogo, G.V., Blanchart, P., Jernot, J.-P. and Gomina, M., 2007, Influence of calcite on the microstructure and mechanical properties of pottery ceramics obtained from a kaolinite-rich clay from Burkina Faso, *Journal of the European Ceramic Society*, 27, 1677-1681.
- Trindade, M.J., Dias, M.I., Coroado, J. and Rocha, F., 2009, Mineralogical transformations of calcareous rich clays with firing: a comparative study between calcite and dolomite rich clays from Algarve, Portugal, *Applied Clay Science*, 42, 345-355.
- Tschegg, C., Ntaflos, Th. and Hein, I., 2009, Thermally triggered two-stage reaction of carbonates and clay during ceramic firing- a case study on Bronze Age Cypriot ceramics, *Applied Clay Science*, 43, 69-78.
- Turner, J., 1996, *The Dictionary of Art*, Vol. 30, Grove, New York.
- Turner, W., 1956, Studies in ancient glasses and glassmaking processes. Part V. Raw materials and melting processes, *Journal of the Society of Glass Technology*, 40, 277-300.
- Ṭūsī, M.Ḥ., 1255, *Tansūq-nāma-i Īlkhānī*, ed. Ražavī, M.T.M., 1969, *Bunyād-i Farhang-i Īrānzamīn*, Tehran. [in Persian]
- Tzelalian, A., 2006, Tra chiese e moschee: nuova giulfa, modello di simbiosi di religioni e culture, *Annali di Ca' Foscari: Rivista della Facoltà di Lingue e letterature straniere dell'Università Ca' Foscari di Venezia*, 453, 93-112.
- Valdés Fernández, F., 1995, Datos sobre el comercio peninsular durante las primeras Taifas: el reino de Badajoz, *V Semana de Estudios Medievales: Nájera*, 5, 167-174.
- Van der Weerd, J., Smith, G.D., Firth, S. and Clark R.J.H., 2004, Identification of black pigments on prehistoric Southwest American potsherds by infrared and Raman microscopy, *Journal of Archaeological Science*, 31, 1429-1437.
- Vandenabeele, P., 2004, Raman spectroscopy in art and archaeology, *Journal of Raman Spectroscopy*, 35, 607-609.

## References

---

- Velraj, G., Janaki, K., Mohamed Musthafa, A. and Palanivel, R., 2009a, Estimation of firing temperature of some archaeological pottery shreds excavated recently in Tamilnadu, India, *Spectrochimica Acta Part A*, 72, 730-733.
- Velraj, G., Janaki, K., Mohamed Musthafa, A. and Palanivel, R., 2009b, Spectroscopic and porosimetry studies to estimate the firing temperature of some archaeological pottery shreds from India, *Applied Clay Science*, 43, 303-307.
- Velraj, G., Mohamed Musthafa, A., Janaki, K., Deenadayalan, K. and Basavaiah, N., 2010, Estimation of firing temperature and ancient geomagnetic field intensity of archaeological potteries recently excavated from Tamilnadu, India, *Applied Clay Science*, 50, 148-153
- Vendrell, M., Molera, J. and Tite, M., 2000, Optical properties of tin opacified glazes, *Archaeometry*, 42, 2, 325-340.
- Vendrell-Saz, M., Molera, J., Roqué, J. and Pérez-Arantegui, J., 2006, Islamic and Hispano-Moresque (mudejar) lead glazes in Spain: a technical approach, in *Geomaterials in Cultural Heritage*, eds. Maggetti, M. and Messiga, B., The Geological Society, London, pp. 163-174.
- Wagner, F.E. and Wagner, U., 2004, Mössbauer spectra of clays and ceramics, *Hyperfine Interactions*, 154, 35-82.
- Wakamatsu, M., Takeuchi, N., Nagai, H., Ono, Y. and Ishida, Sh., 1986, Effect of furnace atmosphere on color of copper glaze, *Journal of the Ceramic Association*, 94, 1088, 387-392.
- Wakamatsu, M., Takeuchi, N. and Ishida, Sh., 1987, Effect of furnace atmosphere on color of iron glaze, *Journal of Non-Crystalline Solids*, 95-96, 2, 733-740.
- Walton, M.S. and Tite, M.S., 2010, Production technology of roman lead-glazed pottery and its continuance into late antiquity, *Archaeometry*, 52, 5, 733-759.
- Watkinson, D., Weber, L. and Antheuser, K., 2005, Staining of archaeological glass from manganese-rich environments, *Archaeometry*, 47, 1, 69-82.
- Weaver, M.E., 1986, Mouvments of Ardabīl, *Encyclopædia Iranica*, Vol. II, 357-365.
- Welch, A., 1974, Painting and patronage under Shah Abbas I, *Iranian Studies*, 73-4, 458-507.
- Welter, N., Schüssler, U. and Kiefer, W., 2007, Characterisation of inorganic pigments in ancient glass beads by means of Raman microspectroscopy, microprobe analysis and X-ray diffractometry, *Journal of Raman Spectroscopy*, 38, 113-121.
- Wen, R. and Pollard, M., 2009, Comparative study of cobalt blue pigment on Chinese blue-and-white porcelain and Islamic glazed pottery, thirteenth-seventeenth centuries, in *Scientific Research on Historical Asian Ceramics*, Archetype, London, pp. 24-32.
- Weyl, W.A., 1999, *Coloured glasses*, Society of Glass Technology, Sheffield.
- Whitehouse, D., 1971, Excavations at Sirāf, *Iran*, 9, 1-17.

## References

---

- Wilkinson, Ch.K., 1973, *Nishapur: Pottery of the Early Islamic Period*, Metropolitan Museum of Art, New York.
- Wolf, S., 2002, Estimation of the production parameters of very large medieval bricks from St. Urban, Switzerland, *Archaeometry*, 44, 1, 37-65.
- Wong, J. and Angell, C.A., 1991, *Glass: Structure by Spectroscopy*, University Microfilms International, Ann Arbor.
- Wood, N., Tite, M.S., Doherty, C. and Gilmore, B., 2007, A technological examination of ninth-tenth century ad Abbasid blue-and-white ware from Iraq, and its comparison with eighth century AD Chinese blue-and-white Sancai ware, *Archaeometry*, 49, 4, 665-684.
- Worrell, C.A. and Henshall, T., 1978, Vibrational spectroscopic studies of some lead silicate glasses, *Journal of Non-Crystalline Solids*, 29, 3, 283-299.
- Wulff, H., 1966, *The Traditional Crafts of Persia*, Cambridge, Mass.
- Yap, C.T. and Tang, S.M., 1984a, X-Ray fluorescence analysis of Chinese porcelains from K'ang Hsi to modern times using Cd-109 source, *Applied Spectroscopy*, 38, 4, 527-529.
- Yap, C.T. and Tang, S.M., 1984b, X-ray fluorescence analysis of modern and recent Chinese porcelains, *Archaeometry*, 26, 1, 78-81.
- Yap, C.T., 1986, XRF analysis of Nonya wares using an annular americium source, *Archaeometry*, 28, 2, 197-201.
- Yap, C.T., 1989, EDXRF studies on the variation in elemental concentrations of ceramic glazes, *X-Ray Spectrometry*, 18, 1, 31-34.
- Yelon, A., Saucier, A., Larocque, J.P., Smith, P.E.L. and Vandiver, P., 1992, Thermal analysis of early Neolithic pottery from Tepe Ganj Dareh, Iran, *MRS Proceedings*, 267, 591-608.
- Yousefi, E., Ghafoori, M., Lashkaripour, Gh.R. and Talebian, L., 2007, Evaluation of clay minerals in Mashhad city basin according to Atterberg limits, *The 5th Conference in Engineering Geology and Environment of Iran*, pp. 914-920. [in Persian]
- Yu, K.N. and Miao, J.M., 1996a, Non-destructive analysis of Jingdezhen blue and white porcelains, *Archaeometry*, 38, 2, 257-262.
- Yu, K.N. and Miao, J.M., 1996b, Non-destructive analysis of Jingdezhen blue and white porcelains of the Ming dynasty using EDXRF, *X-Ray Spectrometry*, 25, 6, 281-285.
- Yu, K.N. and Miao, J.M., 1999, Retrospective study of the feasibility of using EDXRF for the attribution of blue and white porcelains, *X-Ray Spectrometry*, 28, 1, 19-23.
- Yu, K.N., 2000, Attribution of antique Chinese blue-and-white porcelains using energy dispersive x-ray fluorescence EDXRF, in *Radiation in Art and Archeometry*, eds. Creagh, D.C. and Bradley, D.A., Elsevier, Amsterdam, pp. 317-346.
- Zahedi, M., Samadian, M., Tawosian, Sh., and Amidi, M., 1978, *Geological quadrangle maps of Iran no. J7: Isfahan '1:250,000'*, Ministry of Mines and Metals, Tehran Naqsheh Office Press, Tehran.

## References

---

- Zāhidīyān, K., 2001, *Deterioration Mechanisms of Yellow and Green Glazes of Haft rangi Tiles of 'Abbāsī Mosque*, M.A. Thesis, Art University of Isfahan, Dept. of Conservation and Restoration of Cultural Heritage. [in Persian]
- Zamānī, A., 1972, Ceramic art in Mind of Gunābād, *Hunar va Mardum Magazine*, 119-120, 10-24. [in Persian]
- Zamora, M.I.A., 2007, La cerámica andalusí, *Artigrama, Revista del Departamento de Historia del Arte de la Universidad de Zaragoza*, 22, 337-370.
- Zāvush, M., 1996, *Mineralogy in Ancient Iran*, Institute for Humanities and Cultural Studies, Tehran. [in Persian]
- Zucchiatti, A., Bouquillon, A., Castaing, J. and Gaborit, J.R., 2003, Elemental analysis of a group of glazed terracotta angels from the Italian renaissance as a tool for reconstruction of a complex conservation history, *Archaeometry*, 45, 391-404.
- Zucchiatti, A., Cardoni, F., Prati, P., Lucarelli, F., Mandò, P.A. and Martino, G.P., 1998, PIXE analysis of pottery from the recovery of a renaissance wreck, *Nuclear Instruments and Methods in Physics Research B*, 136-138, 893-896.
- Zumarshīdī, H., 2006, Evolution of mosaic tile-working in the monuments of Iran, *Rushd-i Āmūzis-i Hunar Magazine*, 8, 4-11. [in Persian]
- Zuo, J., Xu, C., Liu, Y. and Qian, Y., 1998, Crystallite size effects on the Raman spectra of Mn<sub>3</sub>O<sub>4</sub>, *Nanostructured Materials*, 10, 8, 1331-1335.
- Zuo, J., Xu, C., Wang, Ch. and Yushi, Zh., 1999, Identification of the pigment in painted pottery from the Xishan site by Raman microscopy, *Journal of Raman Spectroscopy*, 30, 1053-1055.

## **Appendices**

**Appendices 1**

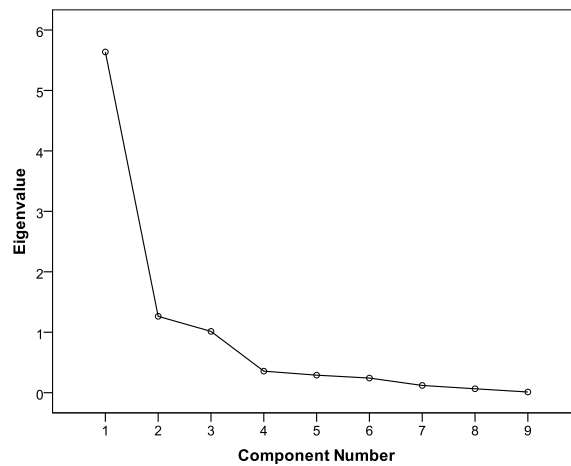
*The calculations of PCA analysis on the standardised data of major and minor elements of tiles' bodies*

KMO and Bartlett's Test of the standardised data

Kaiser-Meyer-Olkin Measure of Sampling Adequacy		0.682
Bartlett's Test of Sphericity	Approx. Chi-Square	420.810
	df	36
	Sig.	0.000

Correlation Matrix of the standardised data

	TiO <sub>2</sub>	Al <sub>2</sub> O <sub>3</sub>	Fe <sub>2</sub> O <sub>3</sub>	MnO	MgO	CaO	Na <sub>2</sub> O	K <sub>2</sub> O	P <sub>2</sub> O <sub>5</sub>
TiO <sub>2</sub>	1.000	0.821	0.817	0.608	-0.471	-0.702	-0.118	0.717	0.586
Al <sub>2</sub> O <sub>3</sub>	0.821	1.000	0.833	0.730	-0.277	-0.881	0.059	0.852	0.771
Fe <sub>2</sub> O <sub>3</sub>	0.817	0.833	1.000	0.732	-0.356	-0.798	-0.387	0.719	0.648
MnO	0.608	0.730	0.732	1.000	-0.124	-0.744	0.011	0.605	0.712
MgO	-0.471	-0.277	-0.356	-0.124	1.000	0.388	-0.099	-0.383	-0.149
CaO	-0.702	-0.881	-0.798	-0.744	0.388	1.000	-0.175	-0.882	-0.787
Na <sub>2</sub> O	-0.118	0.059	-0.387	0.011	-0.099	-0.175	1.000	0.113	0.129
K <sub>2</sub> O	0.717	0.852	0.719	0.605	-0.383	-0.882	0.113	1.000	0.707
P <sub>2</sub> O <sub>5</sub>	0.586	0.771	0.648	0.712	-0.149	-0.787	0.129	0.707	1.000



Scree plot of nine principal components shows that the maximum variability is accounted for the first two components

**Appendices 2**

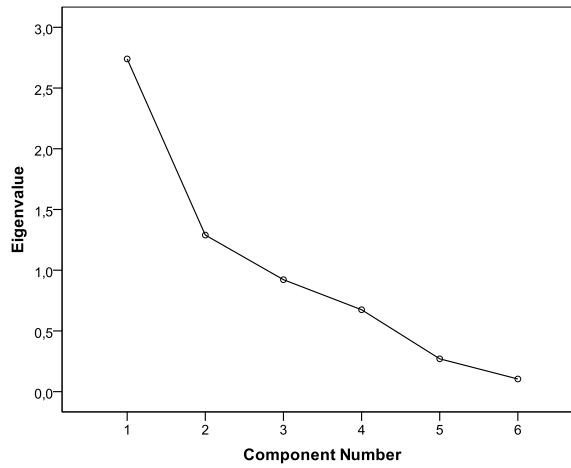
*The calculations of PCA analysis on the standardised data of trace elements of tiles' bodies*

KMO and Bartlett's Test of the standardised data

Kaiser-Meyer-Olkin Measure of Sampling Adequacy.		0.610
Bartlett's Test of Sphericity	Approx. Chi-Square	108.965
	df	15
	Sig.	0.000

Correlation matrix of the standardised data

	Co	Cr	Ni	Rb	Sr	Zr
Co	1.000	-0.048	-0.156	0.532	-0.192	0.520
Cr	-0.048	1.000	0.027	0.085	-0.229	-0.142
Ni	-0.156	0.027	1.000	-0.417	-0.099	-0.541
Rb	0.532	0.085	-0.417	1.000	-0.500	0.855
Sr	-0.192	-0.229	-0.099	-0.500	1.000	-0.352
Zr	0.520	-0.142	-0.541	0.855	-0.352	1.000



Scree plot of six principal components shows that the maximum variability is accounted for the first two components

**Appendices 3**

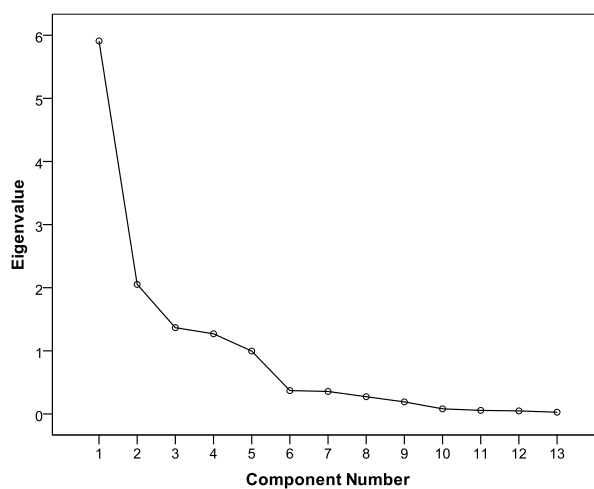
*The calculations of PCA analysis on the standardised data of trace and rare earth elements of tiles' bodies*

KMO and Bartlett's Test of the standardised data

Kaiser-Meyer-Olkin Measure of Sampling Adequacy.		0.622
Bartlett's Test of Sphericity	Approx. Chi-Square	513.944
	df	78
	Sig.	0.000

Correlation matrix of the standardised data

	Co	Cr	Ni	Rb	Sr	Zr	Ce	La	Nb	Sc	Th	V	Y
Co	1.000	-0.048	-0.156	0.532	-0.192	0.520	0.812	0.648	-0.040	0.652	0.651	0.274	0.254
Cr	-0.048	1.000	0.027	0.085	-0.229	-0.142	0.104	0.141	-0.122	-0.211	0.138	0.265	0.017
Ni	-0.156	0.027	1.000	-0.417	-0.099	-0.541	-0.436	-0.367	-0.201	0.057	-0.441	-0.072	-0.415
Rb	0.532	0.085	-0.417	1.000	-0.500	0.855	0.534	0.818	0.529	0.187	0.905	0.134	0.858
Sr	-0.192	-0.229	-0.099	-0.500	1.000	-0.352	-0.161	-0.343	-0.163	0.022	-0.449	0.079	-0.491
Zr	0.520	-0.142	-0.541	0.855	-0.352	1.000	0.616	0.723	0.527	0.235	0.795	0.096	0.843
Ce	0.812	0.104	-0.436	0.534	-0.161	0.616	1.000	0.664	0.048	0.533	0.564	0.291	0.278
La	0.648	0.141	-0.367	0.818	-0.343	0.723	0.664	1.000	0.489	0.292	0.822	0.317	0.634
Nb	-0.040	-0.122	-0.201	0.529	-0.163	0.527	0.048	0.489	1.000	-0.238	0.399	0.388	0.634
Sc	0.652	-0.211	0.057	0.187	0.022	0.235	0.533	0.292	-0.238	1.000	0.208	0.156	0.029
Th	0.651	0.138	-0.441	0.905	-0.449	0.795	0.564	0.822	0.399	0.208	1.000	0.220	0.767
V	0.274	0.265	-0.072	0.134	0.079	0.096	0.291	0.317	0.388	0.156	0.220	1.000	0.076
Y	0.254	0.017	-0.415	0.858	-0.491	0.843	0.278	0.634	0.634	0.029	0.767	0.076	1.000



Scree plot of thirteen principal components shows that the maximum variability is accounted for the first two components

**Appendices 4**

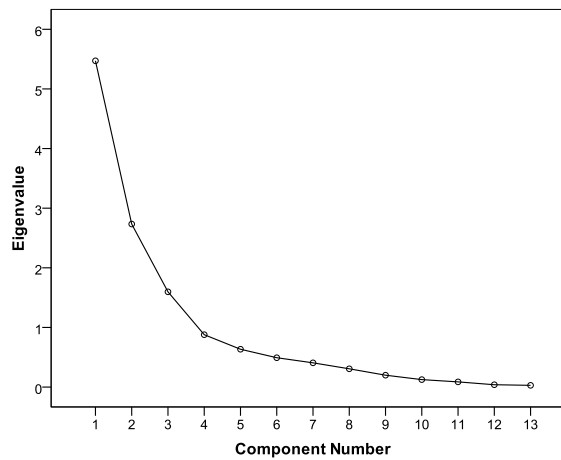
*The calculations of PCA analysis on the standardised data of trace and rare earth elements of Isfahan and Qazvin tiles' bodies*

KMO and Bartlett's Test of the standardised data

Kaiser-Meyer-Olkin Measure of Sampling Adequacy.		0.746
Bartlett's Test of Sphericity	Approx. Chi-Square	391.062
	df	78
	Sig.	0.000

Correlation matrix of the standardised data

	Ce	Co	Cr	La	Nb	Ni	Rb	Sc	Sr	Th	V	Y	Zr
Ce	1.000	0.814	-0.290	0.583	-0.369	-0.397	0.443	0.707	0.152	0.397	0.226	-0.094	0.550
Co	0.814	1.000	-0.276	0.577	-0.572	-0.237	0.441	0.750	0.093	0.660	0.314	-0.114	0.380
Cr	-0.290	-0.276	1.000	-0.290	0.015	0.801	-0.599	-0.210	-0.407	-0.449	0.138	-0.257	-0.607
La	0.583	0.577	-0.290	1.000	-0.070	-0.381	0.519	0.609	0.323	0.516	0.280	0.089	0.422
Nb	-0.369	-0.572	0.015	-0.070	1.000	-0.155	0.288	-0.276	0.360	-0.186	0.297	0.570	0.206
Ni	-0.397	-0.237	0.801	-0.381	-0.155	1.000	-0.648	-0.163	-0.591	-0.440	0.116	-0.362	-0.702
Rb	0.443	0.441	-0.599	0.519	0.288	-0.648	1.000	0.452	0.497	0.704	0.360	0.509	0.718
Sc	0.707	0.750	-0.210	0.609	-0.276	-0.163	0.452	1.000	0.081	0.483	0.427	0.055	0.376
Sr	0.152	0.093	-0.407	0.323	0.360	-0.591	0.497	0.081	1.000	0.288	0.016	0.276	0.338
Th	0.397	0.660	-0.449	0.516	-0.186	-0.440	0.704	0.483	0.288	1.000	0.241	0.368	0.564
V	0.226	0.314	0.138	0.280	0.297	0.116	0.360	0.427	0.016	0.241	1.000	0.191	0.131
Y	-0.094	-0.114	-0.257	0.089	0.570	-0.362	0.509	0.055	0.276	0.368	0.191	1.000	0.650
Zr	0.550	0.380	-0.607	0.422	0.206	-0.702	0.718	0.376	0.338	0.564	0.131	0.650	1.000



Scree plot of thirteen principal components shows that the maximum variability is accounted for the first two components

**Appendices 5**

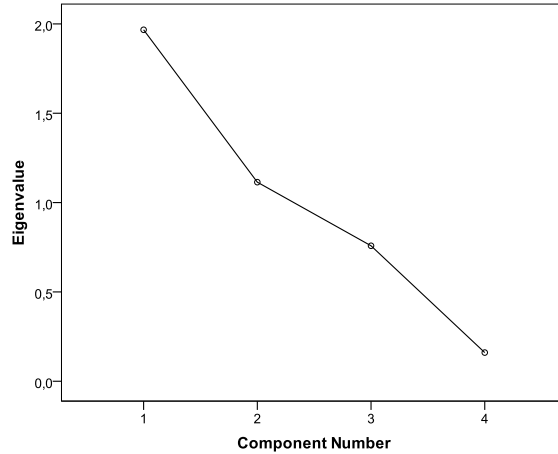
*The calculations of PCA analysis on the standardised data of SiO<sub>2</sub>, Quartz, Amorphous, and alkali contents of tiles' bodies*

KMO and Bartlett's Test of the standardised data

Kaiser-Meyer-Olkin Measure of Sampling Adequacy.		0.508
Bartlett's Test of Sphericity	Approx. Chi-Square	40.749
	df	6
	Sig.	0.000

Correlation matrix of the standardised data

	SiO <sub>2</sub>	Alkalis	Quartz	Amorphous
SiO <sub>2</sub>	1.000	-0.826	0.185	-0.010
Alkalis	-0.826	1.000	-0.261	0.151
Quartz	0.185	-0.261	1.000	-0.219
Amorphous	-0.010	0.151	-0.219	1.000



Scree plot of four principal components shows that the maximum variability is accounted for the first two components

**Appendices 6**

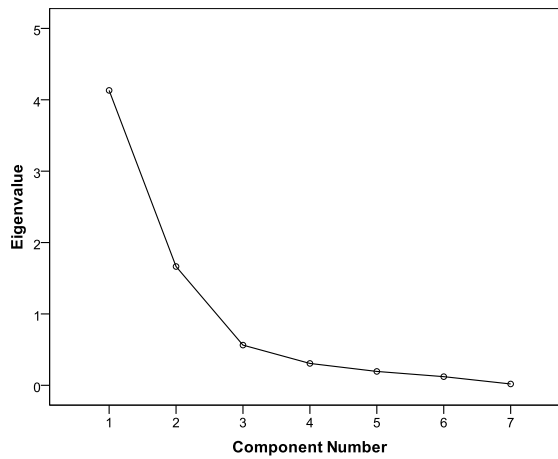
*The calculations of PCA analysis on the standardised data of EDS microanalyses on the coloured glazes*

KMO and Bartlett's Test of the standardised data

Kaiser-Meyer-Olkin Measure of Sampling Adequacy.		0.668
Bartlett's Test of Sphericity	Approx. Chi-Square	164.867
	df	21
	Sig.	0.000

Correlation matrix of the standardised data

	Na <sub>2</sub> O	MgO	Al <sub>2</sub> O <sub>3</sub>	SiO <sub>2</sub>	K <sub>2</sub> O	CaO	PbO
Na <sub>2</sub> O	1.000	0.521	-0.112	0.662	0.507	0.217	-0.643
MgO	0.521	1.000	0.574	0.537	0.423	0.736	-0.782
Al <sub>2</sub> O <sub>3</sub>	-0.112	0.574	1.000	-0.095	0.118	0.687	-0.368
SiO <sub>2</sub>	0.662	0.537	-0.095	1.000	0.723	0.397	-0.861
K <sub>2</sub> O	0.507	0.423	0.118	0.723	1.000	0.414	-0.762
CaO	0.217	0.736	0.687	0.397	0.414	1.000	-0.678
PbO	-0.643	-0.782	-0.368	-0.861	-0.762	-0.678	1.000



Scree plot of seven principal components shows that the maximum variability is accounted for the first two components